How does leukemia disrupt hematopoiesis?

Thesis submitted for the degree of Doctor of Philosophy in Medical Sciences at the University of Oxford

Weatherall Institute of Molecular Medicine

Alexander William Thomas

Green Templeton College

2018

Declaration

I, Alexander William Thomas, declare that the work presented in this thesis is my own unless where explicitly stated.

Acknowledgements

When we reach the end of any journey, we often think about the people who led us there. My parents, to whom I owe so much of my success, never doubted my abilities and always did their best to support me. I am forever grateful to them for this gift.

I would like to begin by thanking my supervisor, Professor Claus Nerlov, and my co-supervisor, Professor Thomas Milne, for showing me by example what it means to be a good scientist. I would also like to extend my gratitude to all the members of my laboratory, both past and present, who throughout my studies have provided me with continual respect and guidance. I would like to thank my college, Green Templeton, for giving me a place to call home during my time at Oxford, and Bloodwise, for entrusting me with this challenging, yet highly rewarding project.

My family and friends have been an unwavering source of encouragement, particularly my parents, Neil and Sharon, my sister, Katie, my grandparents, Stella and Derek, and my parents-in-law, Ana and Manuel. I am thankful to you all for keeping me going, especially during the moments when I doubted myself the most.

Lastly, I would like to thank my wife, Katie, whom I met at the very beginning of my studies. You taught me how to find happiness amidst the madness, encouraging me to dream bigger and do better. You have inspired me since the moment I met you, and I look forward to a lifetime of love and happiness together.

Abstract

Acute myeloid leukemia (AML) is an aggressive hematological malignancy which, if left untreated, results in complete bone marrow (BM) failure characterised by anemia, neutropenia and thrombocytopenia. Although the symptoms of AML can occur at low levels of disease burden, their manifestation is often attributed to a loss of functioning hematopoietic cells via physical displacement. Evidence now suggests, however, that leukemic populations are capable of directly interfering with supportive BM niches and neighbouring hematopoietic cells. This therefore proposes that mechanisms unrelated to displacement may play a role in hematopoietic disruption during AML.

A clinically accurate, kinetically tractable model of AML was generated through the transplantation of mutant *Cebpa* leukemic cells into recipient mice. At the onset of disease, committed BM erythroid progenitors were impaired immunophenotypically and functionally, and was an effect also observed hierarchically upstream in erythroid-forming *Gata1*-EGFP+ progenitors. In contrast, committed myeloid progenitors were expanded as a result of leukemic cell-expressed FLT3L and CCL6. Moreover, HSCs displayed no long-term defects in multi-lineage reconstitution once removed from the leukemic environment. Of note, sinusoidal BM vascular endothelial cells (VECs), demarcated by their expression of VCAM1, were reduced in frequency during leukemic development, whereas arteriolar VECs were expanded. Lastly, aged mice were capable of supporting leukemogenesis, which was accompanied by significant immunophenotypic and transcriptional changes to BM niches. Collectively, the findings presented in this study shed new light on the global immunophenotypic, functional and transcriptional changes that occur across several distinct BM populations during leukemia and ageing.

Table of contents

Abbreviations..... 8

1. Introduction

1.1. Hematopoiesis…….. 11
1.1.1. Murine hematopoietic stem cells…….. 11
1.1.1.1. Measuring HSC functionality *in vivo*…… 13
1.1.2. Mature hematopoietic populations…….. 13
1.1.3. Organising the hematopoietic hierarchy …… 14
1.1.4. RNA-sequencing and hematopoiesis……. 18
1.1.4.1. Bulk RNA-seq using SMART-seq2…… 18
1.1.4.2. Single cell RNA-seq…….. 19
1.1.4.3. RNA-seq analysis workflow…… 20
1.1.4.4. RNA-seq as a tool for studying hematopoiesis…… 21
1.2. Regulation of hematopoiesis via the BM niche…… 24
1.2.1. Niche related secreted factors……. 24
1.2.2. Hematopoietic BM niche cells……. 25
1.2.2.1. Mesenchymal stem cells……. 26
1.2.2.2. Osteoblasts……... 28
1.2.2.3. Vascular endothelial cells…… 29
1.2.2.4. Sympathetic nervous system……. 31
1.2.2.5. Adipocytes……. 32
1.2.2.6. Megakaryocytes……... 32
1.3. Acute myeloid leukemia……. 34
1.3.1. Presentation and aetiology……. 35
1.3.2. The leukemic initiating cell and leukemogenesis……. 35
1.3.3. Current treatment and outcomes……... 39
1.3.4. CEBPA and AML…….. 40
1.4. Leukemic cell interactions in the BM……. 42
1.4.1. HSPC disruption during leukemia…… 42
1.4.2. The niche as an initiator of hematological disorders…… 43
1.4.3. Malignant cell-mediated niche remodeling…… 45
1.4.4. Therapeutically targeting the niche during malignancy…… 48
1.5. Ageing hematopoiesis and the niche…… 49
1.5.1. Aged murine hematopoiesis……. 50
1.5.2. The aged murine hematopoietic niche……... 51
1.6. Concluding remarks…… 52
1.7. Aims……. 53

2. Materials and Methods

2.1. Laboratory materials and methods……... 56
2.1.1. Tissue dissection and preparation…….. 56
2.1.2. Flow cytometry antibody staining and analysis…… 56
2.1.3. Niche cell isolation……. 61
2.1.3.1. CBM niche cell isolation……. 61
2.1.3.2. BL niche cell isolation……. 62
2.1.4. *In vitro* culture of LICs…….. 62
2.1.5. Functional assays……. 63

2.1.6. Hydrodynamic injection plasmid preparation…… 64
2.1.7. Bulk RNA-seq sample preparation and sequencing…… 68
2.1.7.1. Sample collection…… 68
2.1.7.2. First-strand synthesis…….. 69
2.1.7.3. Pre-amplification…….. 70
2.1.7.4. Magnetic purification…… 71
2.1.7.5. Tagmentation and library construction…… 71
2.1.7.6. Library magnetic purification…….. 73
2.1.7.7. Sample pooling…… 73
2.1.8. scRNA-seq sample preparation…….. 73
2.1.9. Pharmacological inhibitors……... 74
2.1.10. BM serum collection and cytokine array…… 75
2.1.11. Red cell lysis and peripheral blood preparation…… 75
2.1.12. Blood smear and cytospin images…….. 75
2.2. Animal materials and methods…….. 76
2.2.1. Animals……... 76
2.2.2. Hydrodynamic injection…… 76
2.2.2.1. Krebs-Ringer modified buffer…… 76
2.2.2.2. Final working buffer…… 77
2.2.2.3. Injection procedure…….. 78
2.2.3. K/L mutant *Cebpa* LIC generation…… 78
2.2.4. Intravenous tail vein injection…….. 79
2.2.5. Drug administration…….. 79
2.3. Computational materials and methods…… 79
2.3.1. Bulk RNA-seq data analysis…… 79
2.3.1.1. Sample demultiplexing, alignment and feature counting… 79
2.3.1.2. Normalisation, principal component analysis and RPKM.. 80
2.3.1.3. Supervised heatmaps…….. 80
2.3.1.4. Statistical and post-hoc analyses…….. 80
2.3.2. scRNA-seq data analysis…… 82
2.3.2.1. Demultiplexing and alignment…… 82
2.3.2.2. Filtering, merging and normalising data…… 82
2.3.2.3. Additional filtering steps…….. 83
2.3.2.4. Linear dimensional reduction…… 83
2.3.2.5. Non-linear dimensional reduction…….. 84
2.3.2.6. Quality checking scRNA-seq datasets…….. 84
2.3.2.7. Regressing hematopoietic populations…… 85
2.3.2.8. Differential gene expression analysis, heatmaps and gene expression plots…….. 85
2.3.2.9. Isolation and analysis of vascular endothelial cells……. 96
2.3.2.10. Canonical correction analysis of young and aged VECs… 101

3. The immunophenotypic and functional consequences of leukemia on endogenous hematopoiesis and the BM niche
3.1. Introduction and aims…….. 105
3.2. The generation of a murine AML transplantation model…… 106
3.2.1. Leukemic recipients experienced white blood cell infiltration, anemia and loss of morphological heterogeneity…… 108
3.2.2. Leukemic recipients experienced splenomegaly…… 111

3.2.3. LICs lost their engraftment potential after *in vitro* culture…… 112
3.3. Immunophenotypic frequency of endogenous BM HSCs, MPPs and myeloerythroid progenitors during leukemia…… 114
3.3.1. Immunophenotypic frequency of endogenous BM HSCs and MPPs during leukemia…….. 116
3.3.2. Immunophenotypic frequency of endogenous BM myeloerythroid progenitors during leukemia…… 119
3.3.3. Immunophenotypic frequency of endogenous splenic HSCs during leukemia…….. 120
3.3.4. Immunophenotypic frequency of *Gata1*-EGFP expressing BM pGM progenitors after exposure to leukemia……. 122
3.4. Functional consequences of leukemic development on endogenous BM hematopoietic stem and progenitor cells……. 123
3.4.1. Long-term functionality of endogenous BM HSCs after exposure to leukemia……. 124
3.4.2. Peripheral blood reconstitution of myeloid, B and T cells from leukemia-exposed BM HSCs……. 126
3.4.3. Analysis of donor-derived BM HSC and myeloerythroid progenitor reconstitution……. 128
3.4.4. *In vitro* functionality of endogenous BM LK progenitors during leukemia……. 129
3.5. Immunophenotypic analysis of CBM and BL niches during leukemia…. 131
3.6. Summary and discussion…… 133
3.7. Conclusions…….. 137

4. Transcriptionally profiling endogenous hematopoietic and BM niche populations during leukemia and steady state
4.1. Introduction and aims…….. 140
4.2. Bulk RNA-seq of endogenous BM HSPCs during leukemic development…… 141
4.2.1. Data quality check……. 141
4.2.2. PCA of HSPC populations during leukemia…….. 143
4.2.3. Heatmap quality check using known HSPC genes…….. 145
4.2.4. Differential gene expression analysis of endogenous BM HSPCs during leukemia……. 147
4.2.5. Process network enrichment analysis of endogenous BM HSPCs during leukemia…… 149
4.3. Bulk RNA-seq of CBM VECs and LepR+ PV cells during leukemia…… 156
4.3.1. Data quality check……. 156
4.3.2. PCA of niche populations during leukemia…… 158
4.3.3. Heatmap quality check using known niche genes…… 160
4.3.4. Differential gene expression analysis of niche cells during leukemia……. 161
4.3.5. Process network enrichment analysis of CBM VECs and LepR+ PV cells during leukemia…….. 163
4.3.6. CBM VECs upregulated cell surface receptors and secreted factors during leukemia…… 166
4.4. Droplet-based scRNA-seq of unfractionated, non-hematopoietic BM cells…… 170

4.4.1. scRNA-seq of non-hematopoietic cells revealed significant cellular heterogeneity…… 170
4.4.2. BM VECs comprised five transcriptionally distinct populations…. 174
4.4.3. Integrative analyses of scRNA-seq and bulk RNA-seq datasets… 177
4.4.4. VCAM1 demarcated a population of VECs that were immunophenotypically depleted during leukemia……. 178
4.4.5. Differential gene expression analysis comparing *Vcam1* negative and positive VECs……. 182
4.4.6. *Vcam1* positive VECs expressed a transcriptional profile consistent with sinusoidal endothelial cells…… 184
4.5. Summary and discussion …….. 186
4.6. Conclusions…….. 191

5. Transcriptionally profiling leukemic cell populations and investigating their functional impact on normal hematopoiesis and the BM niche
5.1. Introduction and aims ……. 194
5.2. Bulk RNA-seq of LIC and blast populations during leukemia…… 195
5.2.1. Data quality check……. 196
5.2.2. PCA of LIC, blasts and healthy GMPs…… 197
5.2.3. Heatmap of known LIC and blast cell markers…….. 200
5.2.4. Differential gene expression analysis of LICs and blasts during leukemia……. 200
5.2.5. Process network enrichment analysis of LICs and blasts during leukemia……. 202
5.2.6. Pathway analysis of LICs and blasts during leukemia…… 209
5.3. Investigation of the impact of leukemic cell derived secreted factors on normal hematopoiesis and the niche…… 214
5.3.1. FLT3L and CCL6 over-expression in wild type mice caused myeloid progenitors to expand in frequency……. 215
5.3.2. Secreted factor over-expression had limited impact on mature cell types…… 217
5.3.3. Secreted factor over-expression had no impact on CBM niche cell frequencies…… 220
5.3.4. Protein expression analysis of leukemic BM serum…… 222
5.4. Combined FLT3L and CCL6 over-expression during leukemia…….. 224
5.5. Combined CCR1 and FLT3 inhibition during AML relapse…….. 227
5.5.1. Generating an AML relapse model …… 227
5.5.2. Inhibiting CCR1 and FLT3 during AML remission…… 230
5.6. Summary and discussion…… 232
5.7. Conclusions ……. 238

6. Investigating the relationship between leukemia and the aged BM niche
6.1. Introduction and aims…….. 241
6.2. Investigating the ability of leukemic cells to engraft in aged mice …….. 242
6.3. Bulk RNA-seq of the CBM and BL niche cells during ageing…… 243
6.3.1. Data quality check …… 244
6.3.2. PCA of aged and young niche cell populations…… 245
6.3.3. Heatmap of known niche cell markers…… 247

6.3.4. Differential gene expression analysis of aged BM niche populations…… 248
6.3.5. Shared process network enrichment analysis of aged niche populations…… 249
6.3.6. Aged and leukemic CBM VECs were transcriptionally and immunophenotypically alike…… 251
6.3.7. OBs were immunophenotypically and transcriptionally perturbed during ageing…… 259
6.3.8. Aged niche cells expressed a common gene signature…… 266
6.3.9. Inhibiting TGF-β receptor 1 in leukemia transplanted aged mice… 270
6.4. scRNA-seq of unfractionated non-hematopoietic BM cells from aged mice…… 271
6.4.1. Niche cell heterogeneity during ageing…… 272
6.4.2. Vascular endothelial cell heterogeneity during ageing…… 275
6.4.3. *Vcam1* did not identify a discrete sub-population of VECs during ageing…… 277
6.5. Summary and discussion…… 282
6.6. Conclusions…… 288

7. Final discussion
7.1. Key findings…… 291
7.2. Final discussion…… 291
7.3. Technical limitations…… 296
7.3.1. Murine AML transplantation model…… 296
7.3.2. RNA-sequencing…… 297
7.3.3. Hydrodynamic injections…… 297
7.3.4. Pharmacological inhibitors…… 298
7.4. Future directions…… 298
7.4.1. Delineating the molecular drivers of impaired erythropoiesis during leukemia…… 298
7.4.2. Establishing the functional impact of enhanced myelopoiesis during leukemia…… 299
7.4.3. Imaging studies…… 299

Bibliography…… 300

Abbreviations

7AAD	7-aminoactinomycin D
ALCAM	Activated leukocyte cell adhesion molecule
AML	Acute myeloid leukemia
BL	Bone lining
BM	Bone marrow
CAR	CXCL12-abundant reticular cells
CBM	Central bone marrow
CEBPA	CCAAT/enhancer binding protein alpha
CFUE	Colony forming unit erythrocytes progenitor
CMP	Common myeloid progenitor
CXCL12	C-X-C motif chemokine 12
DEG	Differentially expressed gene
FACS	Fluorescence-activated cell sorting
FDR	False discovery rate
FLT3	FMS-like tyrosine kinase 3
G-CSF	Granulocyte colony-stimulating factor
GFP	Green fluorescent protein
GMP	Granulocyte macrophage progenitor
GSEA	Gene set enrichment analysis
HGB	Hemoglobin
HSC	Hematopoietic stem cell
HSPC	Hematopoietic stem and progenitor cells
KITL	Kit ligand
LepR	Leptin receptor
LIC	Leukemic initiating cell
LK	Lineage-cKit+
LMPP	Lymphoid-primed multipotent progenitor
LogFC	Log fold change
Log2FC	Log_2 fold change
LSK	Lineage- Sca1+ cKit+
LT-HSC	Long-term hematopoietic stem cell
MEP	Megakaryocyte-erythroid progenitor
MkP	Megakaryocyte progenitor
MPP	Multipotent progenitor
NK	Natural Killer cell
OB	Osteoblast
PαS MSCs	PDGFRα MSCs
PC	Principal component

PCA	Principal component analysis
pCFUE	Pre-colony forming unit erythrocyte progenitors
PDGFRα	Plate derived growth factor alpha
PECAM1	Platelet Endothelial Cell Adhesion Molecule 1
pGM	Pre-granulocyte-macrophage progenitor
pMegE	Pre-megakaryocyte-erythrocytes progenitor
PV	Perivascular
RNA-seq	RNA-sequencing
RPKM	Reads per kilobase of transcript per million mapped reads
SCA1	Stem cell antigen 1
SCF	Stem cell factor
scRNA-seq	Single cell RNA-sequencing
SD	Standard deviation
TGF-β1	Transforming growth factor beta 1
THPO	Thrombopoietin
tSNE	t-stochastic neighbour embedding
UMI	Unique molecular identifier
VCAM1	Vascular adhesion molecule 1
VEC	Vascular endothelial cell
WBC	White blood cell

Chapter 1

Introduction

1.1. Hematopoiesis

Hematopoiesis is the tightly regulated, lifelong process of blood cell production, which occurs in the bone marrow (BM) of adult organisms. The cells that comprise the hematopoietic system are hierarchically organised into approximately 10 lineages, each of which has distinct physiological roles such as wound healing, innate/adaptive immunity and oxygen delivery (Orkin and Zon, 2008). Hematopoietic stem cells (HSCs) reside at the apex of the hierarchy, and can both self-renew to maintain a constant stem cell pool, as well as differentiate to produce increasingly committed progenitors. These then proceed to terminally differentiate into four broad categories of cell types including erythrocytes, lymphocytes, granulocytes or platelets.

The mouse serves as an important model system for studying hematopoiesis due to both its homology with the human system, and the convenience by which genetic technologies can be utilised to manipulate molecular processes. Murine models were extensively used throughout this thesis, and therefore the literature will be reviewed in the context of the mouse.

1.1.1. Murine hematopoietic stem cells

HSCs are a rare, multipotent BM cell type that possess the unique ability to both self-renew in order to maintain the stem-cell pool, as well as differentiate to generate downstream progeny. In order to achieve this, the majority of HSCs exist in a quiescent state, enabling them to persist for extended periods of time whilst minimising damage caused by cellular replication and stress (Cheng et al., 2000; Mohrin et al., 2010; Li et al., 2011; Cheshier et al., 1999).

The existence of a repopulating BM cell type was initially proposed in 1951 after it was demonstrated that shielding of the spleen was sufficient to enable

hematopoietic recovery after irradiation (Jacobsen et al., 1951). This was complemented shortly after by the observation that healthy BM cells can rescue lethally irradiated mice (Ford et al., 1956). Several successive publications between 1961 and 1964 by Till, McCulloch and Siminovitch later recognised the clonal repopulating capacity of BM by measuring colony forming spleen units after transplantation into irradiated mice (Becker et al., 1963; Siminovitch et al., 1964; Till et al., 1964a; Till et al., 1964b; McCulloch et al., 1964). Collectively, these studies paved the way for research into hematopoiesis, which over the years has undergone significant advancement and refinement.

The invention of fluorescence-activated cell sorting (FACS) technology revolutionised the hematopoietic research field by facilitating the purification of hematopoietic populations based on immunophenotypic cell-surface markers. A seminal publication from 1988 was the first to utilise this technology to prospectively isolate an enriched Lineage-SCA1+ $Thy1^{lo}$ BM HSC fraction, which contains all BM stem cell activity capable of multi-lineage reconstitution (Spangrude et al., 1988; Uchida and Weissman, 1992). A subsequent study discovered that HSCs express KIT, which led to the now widely adopted Lineage-SCA1+KIT+ (LSK) permutation of primitive stem-cell markers (Okada et al., 1991; Morrison and Weissman, 1994). A plethora of HSC enrichment strategies have since been established including LSK CD34- FLT3- (Christensen and Weissman, 2001), the Hoechst-effluxing side population (Goodell et al., 1996), LSK CD34- (Osawa et al., 1996), SLAM markers (LSK CD150+ CD48-) (Kiel et al., 2005) and LSK CD34- CD150+ FLT3- CD11a- (Fathman et al., 2014).

1.1.1.1. Measuring HSC functionality *in vivo*

The current gold standard assay for measuring long term (LT)-HSC functionality is through the use of *in vivo* transplantation assays. HSCs transplanted into lethally irradiated mice will stably engraft after 16 weeks, giving rise to all differentiated hematopoietic lineages. Due to their self-renewal capacity, "true" HSCs also have the ability to reconstitute secondary irradiated recipients. This assay is therefore widely used to understand whether certain immunophenotypic and genetic markers can prospectively isolate LT-HSCs, and to also study the effects of different conditions on HSC functionality. In order to discriminate between transplanted and recipient hematopoietic populations after transplantation, donor cells are often derived from a C57BL/6 congenic mouse strain, which are then transplanted into an irradiated wildtype C57BL/6 recipient. The C57BL/6 congenic mouse strain carries the pan leukocyte marker *Ptprc*^{a}, also known as CD45.1, whereas wildtype C57BL/6 mice express *Ptprc*^{b}, also known as CD45.2. By FACS, these two markers can be distinguished using a combination of CD45.1- and CD45.2- directed antibodies.

1.1.2. Mature hematopoietic populations

The process of hematopoietic differentiation results in the generation of several distinct cellular populations, each of which carry out different physiological roles. Erythrocytes are anuclear cells enriched for the iron-containing molecule hemoglobin (HGB). The principal role of erythrocytes is the delivery of oxygen throughout the body via an extensive network of blood vessels. In mice, mature erythrocytes express TER119 and have a life-span of approximately 40 days. Much like erythrocytes, platelets are also anuclear. However, these cells are derived from megakaryocytes and instead play a critical role in blood clotting processes.

Lymphocytes are long-lived cell populations that make up the adaptive immune system and include natural killer (NK; NK1.1+) cells, T cells (CD4+ CD8+) and B cells (CD19+). In contrast, granulocytes are short-lived white blood cells that make up the innate immune system and include neutrophils, basophils, mast cells and eosinophils. Mature granulocytes express both CD11b and GR-1, whereas monocytes, the macrophage precursor cell type, express CD11b but not GR-1.

1.1.3. Organising the hematopoietic hierarchy

The hierarchical organisation of murine hematopoietic cells has historically been constructed based on a combination of *in vivo* and *in vitro* assays that measure self-renewal capacity, long-term reconstitution and differentiation potential.

LT-HSCs exist at the apex of the BM hematopoietic hierarchy, giving rise to multipotent progenitors (MPPs) followed by increasingly lineage restricted progenitors with limited to no self-renewal capacity (Kondo et al., 1997; Akashi et al., 2000; Christensen and Weissman, 2001; Kiel et al., 2005). Early models of hematopoiesis proposed that the first lineage bifurcation occurs after the generation of two progenitor subsets that express KIT but lack SCA1 and Lineage marker expression (Lineage-SCA1-KIT+; LK). These are the common myeloid progenitors (CMPs; Lineage-KIT+ CD34+ CD16/32-, Akashi et al., 2000) and common lymphoid progenitors (CLPs; Lineage-KIT+ CD34- CD16/32-, Kondo et al., 1997). CMPs were believed to contain all myeloid, megakaryocyte and erythroid potential via the generation of either megakaryocyte-erythroid progenitors (MEPs) or granulocyte-macrophage progenitors (GMPs) (Akashi et al., 2000; Arinobu et al., 2007; Karsunky et al., 2008). CLPs, on the other hand, exclusively generate T, B and NK cell types (Kondo et al., 1997).

This model was later revised after the discovery of the lymphoid-primed multipotent progenitor (LMPP), a cell type that expresses FMS-like tyrosine kinase 3 (FLT3) and can be found within the LSK compartment. LMPPs are committed towards the lympho-myeloid lineages and lack the ability to generate erythroid and megakaryocytic progeny (Adolfsson et al., 2001; Adolfsson et al., 2005). The LMPP is now widely accepted, with a comparable cell type having been identified in humans (Goardon et al., 2011; Karamitros et al., 2017).

The organisation of intermediate myeloerythroid progenitor populations was evaluated during a landmark publication by Pronk and colleagues in 2007. This study demonstrated that the differential expression of Endoglin (Eng/CD105), lymphocytic activation molecule (Slamf1/CD150) and integrin alpha 2b (Itgab2/CD41) was sufficient to prospectively isolate myeloid progenitor populations with restricted lineage potentials. These include pre-megakaryocyte-erythrocyte progenitors (pMegE), megakaryocyte progenitors (MkPs), pre-colony forming unit erythrocyte progenitors (pCFUE), colony forming unit erythrocyte progenitors (CFUE), pre-granulocyte-macrophage progenitors (pGM) and GMPs. A further redefinition came after the discovery of two molecularly distinct pGM subsets defined by their differential expression of the genes *Flt3* and *Gata1* (Drissen et al., 2016). Using an enhanced green fluorescent protein (EGFP) *Gata1* transgenic mouse model, it was demonstrated that *Gata1*-EGFP+ pGMs give rise to mast cells, eosinophils, megakaryocytes and erythrocytes, whereas *Gata1*-EGFP- pGMs generate monocytes and neutrophils. As a result, there are now believed to be two transcriptionally and functionally distinct myeloid progenitor subsets that arise from separate ancestors.

Using single cell transplantation assays, it has been demonstrated that lineage commitment occurs at even the most primitive stages of hematopoiesis. Numerous studies have identified lymphoid-, myeloid- and platelet-biased HSCs, the existence of which are further supported by studies of unperturbed hematopoiesis (Müller-Sieburg et al., 2002; Dykstra et al., 2007; Challen et al., 2010; Sanjuan-Pla et al., 2013; Carrelha et al., 2018; Sun et al., 2014; Busch et al., 2015; Sawai et al., 2016; Pei et al., 2017; Rodriguez-Fraticelli et al., 2018). Lineage commitment and priming have also been identified in several distinct MPP populations. MPP2 cells, demarcated by their expression of LSK CD48+ CD150+ FLT3-, preferentially give rise to platelets, erythrocytes and GMPs. MPP3s labelled by LSK CD150- CD48+ FLT3-, on the other hand, produce GMPs but show no capacity to generate platelets. Lastly, MPP4 cells expressing LSK CD150- CD48+ $FLT3^{hi}$ are biased towards lymphoid output, but can also produce myeloid progeny (Pietras et al., 2015). Figure 1.1.3.a. outlines the hematopoietic hierarchy taking into consideration these findings.

1.1.3.a

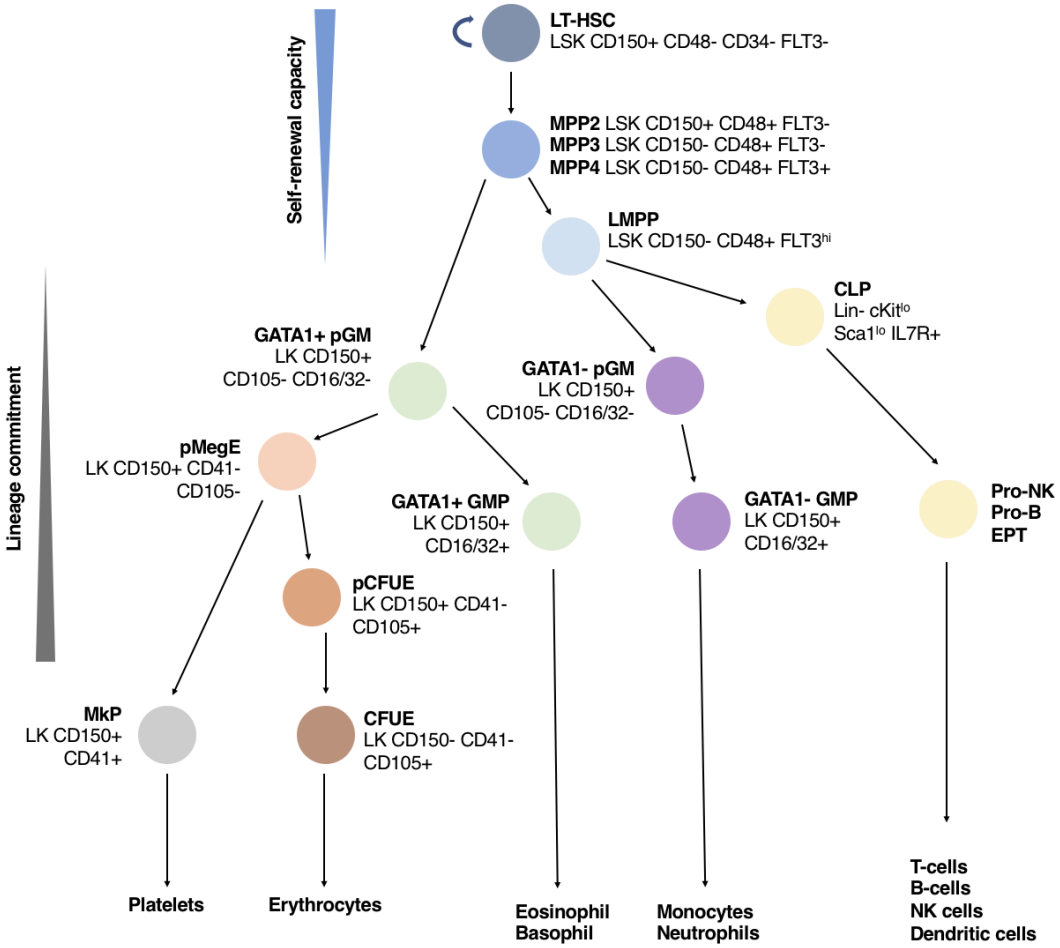


Figure 1.1.3.a. The murine hematopoietic hierarchy

Self-renewing LT-HSCs reside at the apex of the BM hematopoietic hierarchy and differentiate giving rise to MPPs. Individual MPP populations then generate both myeloerythroid and lympho-myeloid progeny. GATA1+ pGMs differentiate to produce megakaryocyte, erythroid and eosinophil/basophil progeny. LMPPs, on the other hand, generate GATA1- pGMs which are responsible for producing monocytes and neutrophils. CLPs differentiate into T, B and NK cell types via Pro-NK, Pro-B and EPT cell types. HSCs maintain the greatest self-renewal capacity which subsequently declines through each step of differentiation. Progenitors eventually become lineage restricted, losing their capacity to generate different cell types.

1.1.4. RNA-sequencing and hematopoiesis

Transcription represents the first intracellular step towards the production of a functional protein. This process relies on the conversion of deoxyribonucleic acid (DNA) into either poly-adenylated messenger ribonucleic acid (mRNA) or non-coding RNA. After additional processing, mRNA molecules are then used as a template for the generation of proteins via translation. Whilst the presence of mRNA within a cell does not necessarily ensure a functional end product, the quantification of these molecules is often used as a proxy for inferring protein expression. RNA-sequencing (RNA-seq) is a method used to determine the global RNA abundance of a cell, or population of cells, using high-throughput sequencing technologies.

1.1.4.1. Bulk RNA-seq using SMART-seq2

Although numerous methods exist for isolating and quantifying cellular RNA, the SMART-seq2 protocol provides a highly sensitive approach for preparing global cellular transcripts compatible with Illumina sequencing platforms such as the HiSeq4000 (Picelli et al., 2013).

For population based or bulk RNA-seq experiments, this technique first requires the isolation of poly-adenylated mRNA from several hundred lysed cells. To achieve this, cell populations are collected into a solution containing oligo-dT, RNase inhibitor and free deoxyribose nucleoside triphosphate (dNTPs) molecules. Following lysis, poly-adenylated mRNA molecules are hybridized with oligo-dT sequences, after which a reverse transcription (RT) reaction is used to generate single-stranded complementary DNA (cDNA). Using a template-switching oligonucleotide (TSO) and ISPCR primers, cDNA sequences are converted to double stranded DNA (dsDNA) which is subsequently amplified using a polymerase chain reaction (PCR). dsDNA is

tagmented using a transposome enzyme, which generates shorter, 200-500bp sequences and also adds P5 and P7 Illumina adapter sequences to each end of the transcript. dsDNA sequences are then labelled with unique index sequences before being pooled into libraries. Lastly, sequencing is carried out to determine the nucleotide composition and abundance of each dsDNA fragment present in the library. An outline of the SMART-seq2 sample preparation work-flow is outlined in figure 1.1.4.1.a.

1.1.4.2. Single cell RNA-seq

Earlier SMART-seq2 protocols required large quantities of input mRNA taken from multiple cells of the same population. However, significant advances in sample handling and preparation now permit the transcriptional analysis of just a single cell, also termed single cell RNA-seq (scRNA-seq) (Picelli et al., 2014). This has been improved upon further in recent years by the use of FACS index sorting (Jaitin et al., 2014), as well as the development of fluidics-based platforms such as Drop-Seq and InDrop (Macosko et al., 2015; Klein et al., 2015).

Unlike traditional scRNA-seq approaches, fluidics-based systems such as those offered commercially by 10X Genomics, partition cells into individual droplets containing RT reagents, lysis buffer and a gel-bead (Zheng et al., 2017). The surface of the gel-bead is coated with thousands of single stranded sequences, each of which begin with an Illumina P5 adapter sequence followed by a 16bp barcode, 10bp mRNA-specific unique molecular identifier (UMI) and poly-dT sequence. Individual poly-adenylated mRNA molecules are hybridized to oligo-dT sequences present on the surface of the bead, after which an RT reaction generates a single cDNA strand. Following integration of the gel bead sequence, droplets are lysed and barcoded

cDNA is processed together. Using a switching oligonucleotide and PCR primers, cDNA is converted into dsDNA, amplified by PCR and fragmented using a transposome enzyme. In doing so, unique indices are added to the ends of each transcript, enabling the sample to be pooled, sequenced and analysed.

There are several distinct advantages of using fluidics-based approaches for RNA-seq, including the ability to label several thousand cells in parallel. As a result, the amount of processing time required per cell is reduced, enabling for significantly higher throughput at much lower cost. However, due to the need for gel bead-assisted barcoding, current scRNA-seq droplet-based approaches also present with several disadvantages, including 3' biased sequencing and low-gene coverage. Figure 1.1.4.2.b illustrates the droplet-based scRNA-seq sample preparation work flow.

1.1.4.3. RNA-seq analysis workflow

After sequencing, DNA reads are sorted based on their unique indices, and are assessed for quality using one of several available software packages. Following this, sequences are computationally aligned to a reference genome, and the number of uniquely mapped reads are then counted. The number of mapped reads per gene is used to infer whether certain transcriptional events are over- or under-represented during different conditions or by distinct cell populations. This is commonly referred to as differential gene expression.

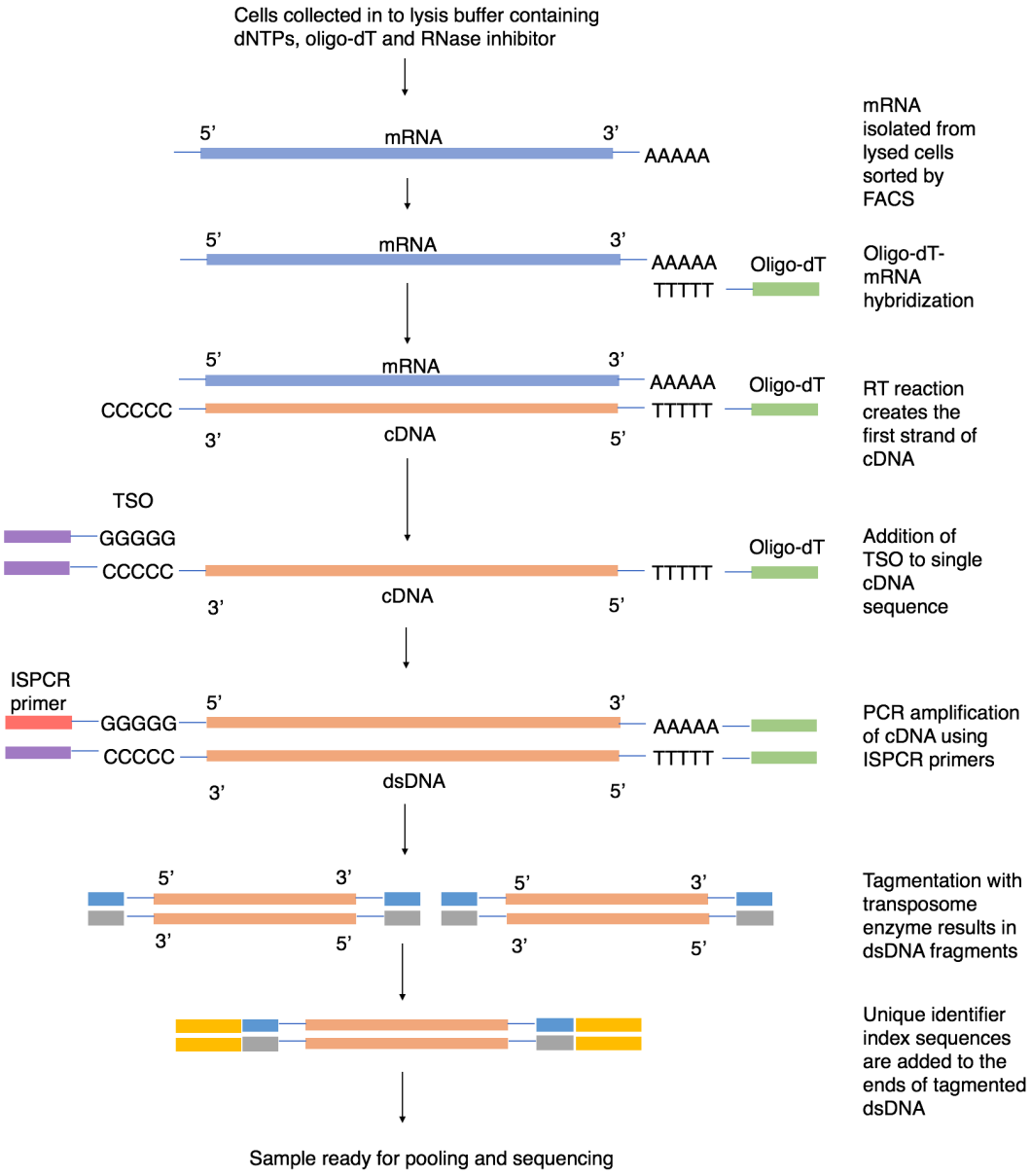
There are numerous computational packages available that can interpret the output generated by RNA-seq experiments. DESeq2, for example, models gene expression using a negative binomial statistical test, and is commonly used to determine differentially expressed genes (DEGs) from both bulk and scRNA-seq

experiments (Love et al., 2014). Online platforms such as Metacore (Thomson Reuters, www.portal.genego.com) and iPathwayGuide (Advaita Bioinformatics, www.advaitabio.com) are often used as post-hoc analysis tools. These platforms use a combination of hypergeometric statistical modelling and impact analysis to infer the enrichment of network processes or molecular pathways during different conditions, or between different cell populations (Draghici et al., 2007; Tarca et al., 2009; Khatri et al., 2007).

1.1.4.4. RNA-seq as a tool for studying hematopoiesis

Numerous groups have now utilised both bulk RNA-seq and scRNA-seq techniques to enhance our understanding of the hematopoietic hierarchy. A landmark publication by the Amit group utilised a combination of scRNA-seq and indexed FACS sorting (MARS-seq) to show that the BM myeloerythroid progenitor compartment contains significant cellular heterogeneity that can be defined by differing states of transcriptional activity (Paul et al., 2015). This was complimented further by studies investigating the transcriptomes of several thousand single LT-HSCs, progenitors and unfractionated BM cells (Nestorowa et al. 2016; Giladi et al., 2018). Importantly, scRNA-seq can be used to profile cells not based on their surface-markers, but rather by their gene expression profiles. This has revolutionised the hematopoietic research field by demonstrating that hematopoietic stem and progenitor cells (HSPCs) do not necessarily exist as discretely identifiable, homogenous populations but instead as a continuum of cell types that are constantly being replenished.

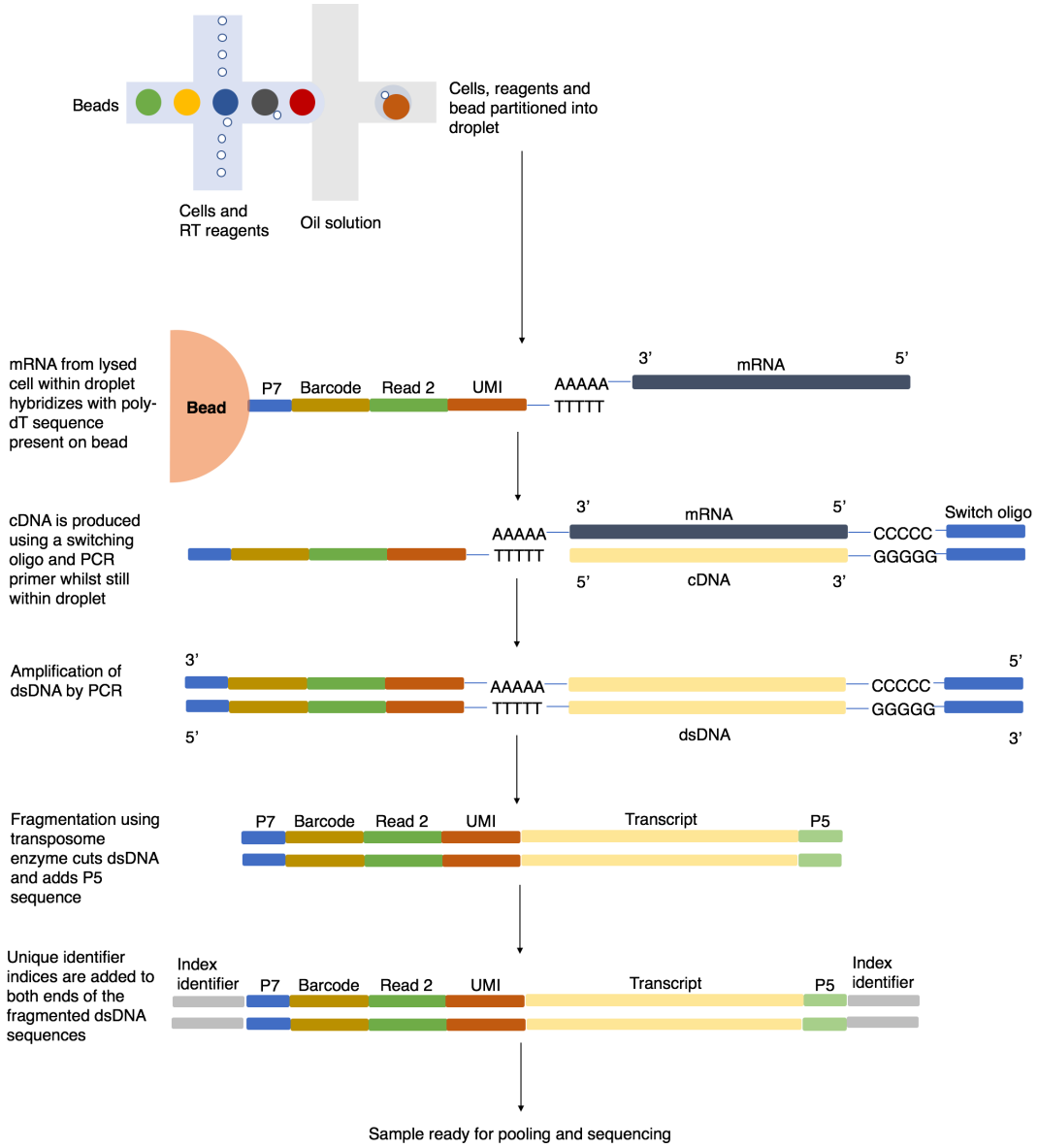
1.1.4.1.a



SMART-seq2 sample preparation

1.1.4.1.a. mRNA is isolated from lysed cells in a solution containing dNTPs, oligo-dT and RNase inhibitor. mRNA is then hybridized to oligo-dT and used to create a single cDNA strand. A TSO and ISPCR primers are used to generate dsDNA, which is then amplified by PCR. Amplified dsDNA is tagmented and indexed using unique identifier sequences. Indexed samples are pooled and sequenced. Image adapted from Picelli et al., 2013 and Picelli et al., 2014.

1.1.4.2.a



Droplet-based scRNA-seq sample workflow

1.1.4.2.a. The formation of droplets containing cells, beads and RT reagents is achieved using 10X Genomics proprietary fluidics technology. Beads express thousands of nucleotide sequences that contain a P7 index adapter sequence, 16bp barcode sequence, read 2, 10bp UMI sequence and poly-dT tail. Each of these sequences contains the same barcode, but has thousands of UMI combinations. Whilst within the droplet, cells are lysed and mRNA molecules hybridize to the bead expressed poly-dT sequence. An RT reaction using a switching oligo and PCR

primers enables the formation of a single cDNA sequence. Droplets are then emulsified, and a PCR reaction is carried out to amplify the resulting dsDNA. Fragmentation using a transposome enzyme cuts dsDNA into small fragments whilst simultaneously adding a P5 adapter sequence to the end of the transcript. Lastly, unique index identifier sequences are added to both the P7 and P5 adapter sequences at each end of the amplified dsDNA sequence. Image adapted from Zheng et al., 2017 and 10X Genomics (www.10xgenomics.com).

1.2. Regulation of hematopoiesis via the BM niche

The bone is comprised of several anatomically distinct regions. These include the epiphysis, metaphysis and diaphysis. A membrane of connective tissue, also known as the periosteum, surrounds the hard, outer cortical bone surface. Within this is the trabecular bone, followed by the endosteal surface, which encases the central BM (CBM) cavity. At steady state, HSPCs share the CBM cavity with numerous other hematopoietic and non-hematopoietic cell types, including megakaryocytes, OBs, adipocytes, endothelial cells, mesenchymal stem cells (MSCs) and perivascular cells. These cells communicate and physiologically support one another through the secretion of soluble factors and expression of cell surface receptors.

The hematopoietic niche was first conceptualised in 1978, whereby it was theorised that the maintenance of HSC self-renewal is controlled by specific BM stromal populations (Schofield, 1978). Since then, substantial research efforts have led to the discovery of multiple HSPC supportive cell types, secreted factors and cell surface expressed receptors.

1.2.1. Niche related secreted factors

BM niche populations support hematopoiesis using both direct cell-cell adhesion and via the expression of secreted factors such as cytokines and chemokines. Cytokines

are a family of small (~5-20kDa) soluble proteins that function in an autocrine, paracrine or endocrine fashion, to bind cell surface receptors and initiate intracellular signalling pathways. Chemokines are a subset of the cytokine family of proteins that induce directed chemotaxis through the creation of expression gradients. These are sensed by surface receptors on distal cell types, which migrate in response. Together, cytokines and chemokines are responsible for controlling important BM processes such as HSC self-renewal, lineage commitment, differentiation and homing.

Stem cell factor (SCF/KITL) is a cytokine that plays a critical role in maintaining homeostatic BM processes, such as HSC self-renewal (Ema et al., 2000). SCF, also known as Kit ligand, exists as both a soluble and transmembrane factor that functions by binding the KIT receptor expressed on both HSCs and progenitors.

C-X-C motif chemokine 12 (CXCL12) is a widely reported BM chemokine that is responsible for the homing and retention of HSCs within the BM (Sugiyama et al., 2006). CXCL12 acts via the receptor C-X-C chemokine receptor type 4 (CXCR4), and in doing so plays a key role throughout the BM niche as an essential factor required for maintaining both HSCs and B cell precursor cells (Nagasawa et al., 1996; Nagasawa et al., 1994).

1.2.2. Hematopoietic BM niche cells

There are believed to be two major BM niche compartments, the bone lining (BL) or endosteal niche, and the CBM or sinusoidal niche. Each consist of different cell types that utilise varying combinations of cytokines and chemokines to influence hematopoietic processes.

1.2.2.1. Mesenchymal stem cells

MSCs are a self-renewing, non-hematopoietic, multipotent cell type responsible for the generation of osteogenic, adipogenic and chondrogenic progeny (Bianco et al., 2008; Friedenstein et al., 1970; Horwitz et al., 2005; Pittenger et al., 1999). Numerous cell types in the BM have been proposed to exhibit MSC features with either tri- or bi- lineage potential. Furthermore, several cell surface and transgenic markers have been assessed for their ability to prospectively isolate MSCs, including platelet-derived growth factor receptor alpha (PDGFRα) (Morikawa et al., 2009), Nestin (Méndez-Ferrer et al., 2010), NG2 (Kunisaki et al., 2013), Leptin receptor (LepR) (Ding and Morrison, 2013; Ding et al., 2012; Zhou et al., 2014) and CXCL12 (Omatsu et al., 2010).

PDGFRα (PαS) MSCs reside within the perivascular (PV) space of the BM, associating closely with arterioles located proximal to the endosteal surface (Morikawa et al., 2009). These cells express high levels of CXCL12 and angiopoietin-1, both of which are important for maintaining hematopoiesis.

PV cells marked by *Nestin*-GFP in the BM convey a population of MSCs with self-renewal capacity and multi-lineage potential (Méndez-Ferrer et al., 2010). Much like PαS MSCs, *Nestin*-GFP labelled cells share a similar microanatomical BM location and also express CXCL12, in addition to a plethora of other important niche related factors (Pinho et al., 2013). Imaging studies have shown that *Nestin*-GFP cells closely associate with sympathetic nerve fibres, which are capable of transmitting circadian-regulated signals to the HSC niche (Méndez-Ferrer et al., 2010; Méndez-Ferrer et al., 2008; Katayama et al., 2006). Based on reporter brightness and morphology, *Nestin* expressing MSCs can be divided into two distinct subsets. *Nestin*-GFP^{bright} cells are a rare population that exist in close association

with arterioles and have been demonstrated to also express NG2. Depletion studies show that NG2-derived CXCL12, but not SCF, is important for maintaining HSC homing and quiescence (Kunisaki et al., 2013; Asada et al., 2017). *Nestin*-GFP^{dim} cells, on the other hand, are a more abundant, reticular shaped cell type present next to sinusoids (Kunisaki et al., 2013).

The use of a *Cxcl12*-GFP transgenic mouse model led to the discovery of CXCL12-abundant reticular (CAR) cells, a BM mesenchymal progenitor population capable of generating adipo-osteogenic progeny. CAR cells are a major source of SCF and CXCL12, two important factors required for normal hematopoietic function (Omatsu et al., 2010). It has formerly been demonstrated that the majority of HSCs, early B lymphoid cells and plasma cells in the BM reside in close proximity to CAR cells, again advocating that this is an indispensable niche for normal hematopoietic function (Sugiyama et al., 2006; Tokoyoda et al., 2004).

Using an *Scf*-GFP mouse model, it has been demonstrated that non-hematopoietic LepR expressing PV cells constitute a major population of multipotent MSCs which act as an important source of BM derived CXCL12 and SCF (Ding and Morrison, 2013; Ding et al., 2012; Zhou et al., 2014). Conditional deletion of *Scf* using a *Lepr*-Cre mouse model leads to the depletion of quiescent HSCs, whereas deletion of *Cxcl12* with the same model causes major HSC mobilisation to the spleen (Ding et al., 2012; Oguro et al., 2013; Ding and Morrison, 2013). Furthermore, deletion of SCF from rare *Nestin* expressing periarteriolar cells did not influence HSC frequency, despite previously being considered an important niche cell type (Ding et al., 2012). Collectively, these findings imply that LepR expressing PV cells are important for both the maintenance and retention of HSCs within the BM via the expression of CXCL12

and SCF. Moreover, these studies also strongly propose that the most quiescent BM HSC subtypes exist sinusoidally, and not in proximity to the endosteum.

1.2.2.2. Osteoblasts

Osteoblasts (OBs) are osteocyte precursor cells that reside along the inner endosteal surface of the bone and together with osteoclasts are responsible for bone remodelling processes. OBs can be prospectively isolated by FACS using the cell-surface marker activated leukocyte cell adhesion molecule (ALCAM; Nakamura et al., 2010), or through the use of a transgenic *Col2.3*-GFP mouse model (Xin et al., 2014).

The osteoblastic niche was first proposed after early immunofluorescence and BM fractionation studies found that primitive HSPCs reside in close proximity to the bone surface (Lambertsen and Weiss, 1984; Gong, 1978; Lord et al., 1975; Nilsson et al., 2001; Haylock et al., 2007). Increasing OB frequency via the administration of parathyroid hormone was later demonstrated to increase the frequency of HSCs (Calvi et al., 2003; Zhang et al., 2003a), whilst depletion resulted in the opposing effect (Visnjic et al., 2004).

Initially it was believed that HSCs interacted with OBs through the homophilic adhesion molecule N-Cadherin (Zhang et al. 2003). However this was subsequently refuted following the discovery that HSCs do not express N-cadherin, nor does the depletion of this molecule lead to perturbed hematopoiesis (Kiel et al., 2009).

In vivo and *ex vivo* three-dimensional imaging studies found that, upon transplantation into irradiated recipients, LSK CD150+ CD48- HSCs rapidly homed in close proximity to OBs. However, the same cells transplanted into non-irradiated mice were located further away from the endosteum, suggesting that the effects of

irradiation may dictate the efficiency of HSPC homing (Lo Celso et al., 2009). In addition to maintaining HSCs, OBs are also responsible for early lymphoid progenitor commitment and maturation (Zhu et al., 2007; Ding and Morrison, 2013; Greenbaum et al., 2013).

OBs fulfil their purported role as niche cells through the expression of cell-surface receptors and secreted factors such CXCL12, vascular cell adhesion molecule 1 (VCAM1), Thrombopoietin (THPO) and osteopontin. Genetic manipulation of these factors has been demonstrated to perturb normal hematopoiesis (Yoshihara et al., 2007; Nilsson et al., 2005; Stier et al., 2005; Jiang et al., 2009). Moreover, co-culture experiments suggest that ALCAM positive OBs dramatically enhance the long-term repopulating capacity of HSCs, once again suggesting the OBs and their predecessor cell types are important components of the hematopoietic niche (Nakamura et al., 2010).

1.2.2.3. Vascular endothelial cells

Vascular endothelial cells (VECs) exist throughout the BM cavity and line the surface of arterioles, sinusoids and lymphatic vessels. There are a spectrum of cell-surface markers and genetic mouse models that can be used to prospectively isolate BM VECs including Platelet Endothelial Cell Adhesion Molecule 1 (PECAM1/CD31), VE-Cadherin, Tie2 and CD105.

Anatomically, arterioles are located near the endosteal BL surface, whereas sinusoids are connected directly to the central sinus. VECs contribute to the BM niche by expressing numerous cell-surface receptors and secreted factors. E-selectin is an endothelial-specific adhesion molecule that is essential for HSC proliferation (Winkler et al., 2012). When deleted using a *Sele*$^{-/-}$ mouse model, HSCs become increasingly

quiescent. Interestingly, NOTCH and JAGGED1 expression by endothelial cells is sufficient to maintain HSC self-renewal (Butler et al., 2010; Poulos et al., 2013), yet the co-activation of mitogen-activated protein kinases and the mTOR signalling pathway is responsible for instructing lineage differentiation (Kobayashi et al., 2010). Prior to this, it was demonstrated that HSCs home to perivascular, CXCL12 expressing domains within the calvarium (Sipkins et al., 2005). Moreover, the genetic ablation of SCF in endothelial cells using a *Tie2*-Cre mouse model was later shown to result in both a depletion of HSCs from the BM, and an impairment in their capacity to reconstitute after transplantation (Ding et al., 2012). When taken together, these findings imply that endothelial cells play differential roles in regulating hematopoiesis, which appears to depend on the type of cell surface and secreted factors produced.

Despite having been extensively studied, the exact vascular niche for active and quiescent HSCs still remains widely disputed. Early imaging studies demonstrate that HSCs defined by SLAM markers reside in close proximity to BM sinusoidal vasculature (Kiel et al., 2005; Kiel et al., 2007). This is in agreement with recent findings suggesting that LT-HSCs labelled by *Ctnaal1* and *Hoxb5* reside exclusively along perisinusoidal niches (Acar et al., 2015; Chen et al., 2016). However, this is in contrast to several previous studies that suggest arterioles are the major niche for quiescent HSCs. For example, Kunisaki et al., (2013) demonstrated using whole-mount confocal imaging that LSK CD150+ CD48- CD41- HSCs are located next to small arterioles at the endosteal surface. Moreover, arterioles express high levels of SCA1 (Hooper et al., 2009), are less permeable than sinusoids, and express low levels of reactive oxygen species (ROS). Together, these attributes are believed to contribute towards the retention and quiescence of HSCs at the arteriole surface (Itkin et al., 2016; Spence et al., 2014). Sinusoids, on the other hand, express high

levels of ROS and are significantly more permeable. As a result, sinusoidal endothelium is believed to act as a site for hematopoietic cell egress from the BM (Itkin et al., 2016).

1.2.2.4. Sympathetic nervous system

The bone contains a network of autonomic nerve fibres that function to regulate bone formation, hematopoiesis and malignancy (Hanoun et al., 2015). A role for the nervous system in controlling hematopoiesis was initially evidenced after an investigation into the effects of UDP-galactose ceramide galactosyltransferase (*Cgt*) deficiency in mice. It was demonstrated that depletion of *Cgt* caused aberrant nerve conduction and minimal HSPC egress following granulocyte colony-stimulating factor (G-CSF) administration. It was concluded that G-CSF acts on adrenergic neurons causing them to inhibit OB function thereby reducing CXCL12 concentration and causing a release of HSPCs from the bone (Katayama et al., 2006). The expression of CXCL12 was later demonstrated to be influenced by photic cues that activate sympathetic nerves causing them to influence HSPC egress (Méndez-Ferrer et al., 2008).

Sympathetic nerves closely associate with *Nestin*-GFP MSCs through β3 adrenergic receptor signalling (Méndez-Ferrer et al., 2010). Nonmyelinating Schwann cells ensheath autonomic nerve fibres in the BM, and are also responsible for the localised production of TGF-β1. Loss of these cells by denervation leads to a significant depletion in HSC frequency, highlighting the importance of this cell type in maintaining hematopoiesis (Yamazaki et al., 2011).

1.2.2.5. Adipocytes

Adipocytes are specialised cell types responsible for storing energy as fat, and whose presence within the BM is negatively correlated with HSPC number and hematopoietic activity (Naveiras et al., 2009). Both genetic ablation and pharmacological inhibition of adipocytes accelerates BM engraftment following transplantation or chemotherapy (Naveiras et al., 2009, Zhu et al., 2012). This was further confirmed after an evaluation of the effects of adipogenic progenitor subsets on the reconstitution capacity of HSCs (Ambrosi et al., 2017).

Adipocytes promote myelopoiesis at the expense of lymphopoiesis via the expression of Arginase, NOS2 and IL-1 (Kennedy et al., 2015). In contrast to this, it has also been proposed that a subset of adipogenic progenitors appear to express SCF, suggesting a possible role in HSC maintenance (Zhou et al., 2017).

1.2.2.6. Megakaryocytes

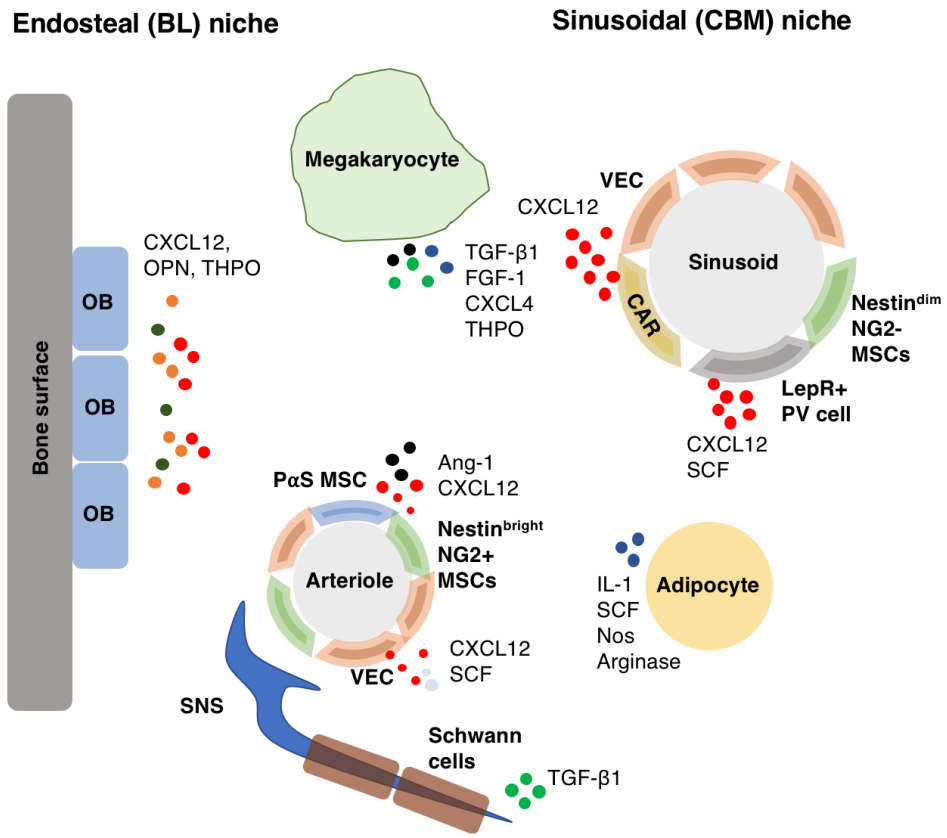
Megakaryocytes are a hematopoietic population of cells responsible for generating platelets and mediating the post-injury coagulation process. Murine megakaryocytes can be identified using the immunophenotypic markers Lineage-KIT+ CD150+ CD41+ (Nakorn et al., 2003). Despite being hematopoietic by nature, megakaryocytes have recently emerged as dichotomous regulators of HSC maintenance. Various imaging studies have shown that these platelet producing cells closely associate with sinusoidal vasculature (Junt et al., 2007) and are also adjacent to HSCs (Bruns et al., 2014; Heazlewood et al., 2013). Platelet factor-4 (PF-4) is a chemokine (also known as CXCL4) that is released by megakaryocytes at the same time as platelets. This secreted factor plays an important role in maintaining HSC quiescence via the inhibition of activating IL-8 (Dudek et al., 2003). The depletion of

megakaryocytes using a *Pf4*-Cre;iDTR mouse model leads to increased BM HSC frequency and reduced cellular quiescence (Bruns et al., 2014; Zhao et al., 2014). A contrasting study however found that the depletion of megakaryocytes using a *Pf4*-Cre;Mos-iCsp3 mouse model did not lead to an increase in HSCs, but did disrupt quiescence and repopulation potential (Nakamura-Ishizu et al., 2015).

Megakaryocytes also secrete other important hematopoietic maintenance factors such as transforming growth factor beta 1 (TGF-β1) (Zhao et al., 2014) and THPO (Nakamura-Ishizu et al., 2015). Mice depleted of megakaryocytes present with significantly lower levels of TGF-β1 and THPO. As a result, HSCs become activated and subsequently egress into the circulation, an effect that can be attenuated after re-expression (Zhao et al., 2014; Nakamura-Ishizu et al., 2015).

Interestingly, under stress conditions such as chemotherapy and irradiation, megakaryocytes have been demonstrated to play an important role in aiding the hematopoietic and niche cell recovery process. During irradiation, megakaryocytes migrate to the endosteum via THPO signalling, and repair OBs through the expression of growth factors (Olsen et al., 2013). Moreover, the secretion of fibroblast growth factor (FGF-1) by megakaryocytes after chemotherapy accelerates the proliferation of HSCs (Zhao et al., 2014). Taken together, these findings suggest that megakaryocytes carry out important roles both at steady state, and during stress conditions. Figure 1.2.2.a graphically depicts the niche composition as described in this section.

1.2.2.a



The hematopoietic niche

1.2.2.a. The BM contains niches which serve to support HSPCs through the expression of secreted factors and cell-surface expressed receptors. The niche is believed to be comprised of two areas, the endosteal or BL niche, and the sinusoidal or CBM niche. Both areas contain different cell types including OBs, arteriolar vasculature, sinusoidal vasculature, sympathetic nerves, adipocytes and megakaryocytes.

1.3. Acute myeloid leukemia

Acute myeloid leukemia (AML) is an aggressive cancer of the white blood cells, characterised by the abnormal proliferation and differentiation arrest of a clonal population of myeloid stem cells (De Kouchkovsky and Abdul-Hay, 2016). Whilst the

presentation of AML is generally uniform, the underlying disease is highly heterogenous and can differ by morphology, immunophenotype, cytogenetic profile and genetic mutations. As a result of this variability, therapeutic success is limited and long-term survival is difficult to achieve.

1.3.1. Presentation and aetiology

If left untreated, the accelerated and uncontrolled expansion of AML cells results in eventual hematopoietic BM failure. However, even at the earliest stages of leukemia patients can suffer from severe side effects including bleeding (caused by thrombocytopenia), infections (caused by neutropenia) and fatigue (caused by anemia) (Estey and Döhner, 2006). Secondary organ infiltration can also occur leading to the enlargement of the spleen (splenomegaly) and liver (hepatomegaly).

The current AML incidence rate is approximately 2-3 cases out of 100,000 persons per year, which increases to 12-15 cases per 100,000 persons per year for persons aged 60 and over (Burnett et al., 2011). For the majority of cases, there is no direct cause. However, there are several known environmental factors and conditions that increase a person's likelihood of developing AML. These include smoking, Downs syndrome, exposure to radiation, prior chemotherapy treatment (therapy-related AML) or progression from a pre-existing myeloid malignancy (secondary-AML).

1.3.2. The leukemic initiating cell and leukemogenesis

The leukemic initiating cell (LIC) is a self-renewing cell type that possesses stem-cell like properties (Dick, 2008). LICs give rise to immature myeloid blasts during AML,

which is analogous to the hierarchical organisation of functioning HSPCs (Bonnet and Dick, 1997).

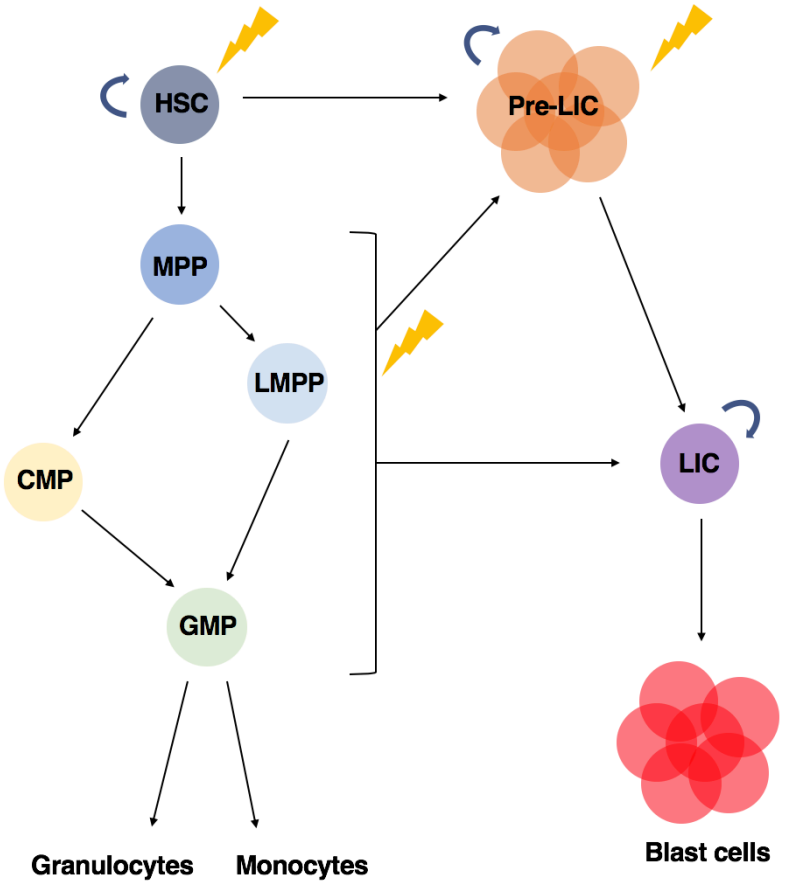
The transformation from normal to malignant is believed to occur through the step-wise acquisition of genetic and epigenetic changes. The “two-hit” model of leukemogenesis proposes a conceptual, yet likely over simplified, framework to define the various mutations present in AML (Gilliland and Griffin, 2002). These mutations can be broadly divided into two classes: Class I mutations, that result in the activation of signalling pathways responsible for uncontrolled proliferation (i.e. *FLT3*, *KRAS, NRAS*, *TP53*, *JAK2* and *KIT*) and class II mutations, also known as initiating mutations, that play a role in impairing normal hematopoietic differentiation (i.e. *CEBPA*, *NPM1*, *MLL*, *PU1, RARA*) (Kelly and Gilliland, 2002; Moore, 2005). More recently, a third class of genes that encode for epigenetic regulators has also emerged. These include *DNMT3A*, *IDH1*, *IDH2*, *TET2*, *ASXL1* and *EZH2* (Shen et al., 2011).

Due to their inherent longevity and self-renewal capacity, HSCs are believed to have a greater probability of acquiring successive mutations that result in malignant transformation, caused by both intrinsic and extrinsic stresses (Welch et al., 2012). Transformation of HSCs leads to the generation of a pre-LIC pool, where additional mutations eventually result in the creation of the LIC. Understanding the cell of origin in AML is critical for correctly assigning patients to prognostic groups. This was evident after it was discovered that MLL-AF9 transformed HSCs are more likely to induce a leukemia when compared to transformed GMPs, and are also less responsive to chemotherapy (Krivtsov et al., 2013). Earlier studies demonstrated that human AML LICs express CD34+ CD38-, an immunophenotype consistent with what is expressed by human repopulating HSCs. (Bonnet and Dick, 1997). However, a

lack of LIC activity within the human progenitor compartment was shown to be a consequence of Fc-mediated clearance of CD38+ cells. When experimentally factored in, the majority of LIC activity was actually shown to exist within the progenitor compartment (Taussig et al., 2008). This is in line with earlier findings that demonstrate murine CMPs transformed by the MLL-AF9 fusion protein become self-renewing and possess leukemogenic properties (Cozzio et al., 2003).

Although still not completely understood, it remains likely that malignant transformation can occur both at the stem and progenitor level. However, due to the inherent lack of self-renewal capacity possessed by progenitors, it is critical that this ability is invoked during transformation in order for a leukemia to propagate effectively. Figure 1.3.2.a depicts a proposed hierarchy for leukemic transformation based on the information discussed within this section.

1.3.2.a



Leukemic transformation model

1.3.2.a. Mutations arising in the HSC compartment result in the formation of a proliferative pre-LIC population. Secondary mutations then lead to the generation of the LIC clone, a self-renewing, committed progenitor-like cell defined by its ability to recapitulate a leukemic state after transplantation. LICs differentiate to produce blast cells, which are unable to differentiate but instead extensively proliferate. Mutations can also occur in progenitor cells, however since these cells lack self-renewal capacity, the mutation must invoke this ability.

1.3.3. Current treatment and outcomes

The prognosis of AML is variable and depends on clinical features, such as age of onset and comorbidities, as well as genetic features including the existence of large structural chromosomal abnormalities (cytogenetics) and/or molecular aberrations (genetic mutations).

Cytogenetic profiling provided the first genetic basis for AML prognostication, and is considered the single-strongest predictor of clinical remission and overall survival. Advances in next-generation sequencing have further enhanced the classification of AML by including the evaluation of genetic mutations. This is particularly relevant for patients that present with intermediate risk cytogenetic profiles that would otherwise be considered to have good overall prognosis (Patel et al., 2012; Papaemmanuil et al., 2016).

Despite significant advances in our understanding of AML, treatment options have remained largely unchanged for the past 30-40 years. Upon diagnosis, patients first undergo high-dose induction chemotherapy consisting of cytarabine and anthracycline, and, although effective, these drugs are non-specific and therefore impact both leukemic and non-leukemic BM cells. As a result, patients often experience periods of acute toxicity associated with BM failure and pancytopenia. The aim of chemotherapy is to induce remission, which is defined clinically as a BM blast frequency of <5%. In order to circumvent relapse, which is often the case after only a single round of chemotherapy, patients undergo multiple rounds of consolidation therapy to eradicate any residual malignant cells. The exact regime given after induction therapy depends on which prognostic group a patient is assigned (Yates et al., 1973; Grimwade et al, 2010; Döhner et al., 2010). An alternative to consolidation chemotherapy is the transplantation of hematopoietic

stem cells from a human leukocyte antigen-matched donor. This approach can be an effective way to avoid relapse, however there are also significant side effects that can incur, including graft versus host disease and severe infections. As a result, this option is normally reserved for younger patients (Cornelissen et al., 2007).

Current outcomes for AML are poor, with patients younger than 60 experiencing a long-term disease free-survival rate of ~40%, reducing further to ~10% for individuals >60 years of age (Shah et al., 2013; Appelbaum et al., 2006; Bloomfield et al., 1998). Relapse is a major challenge in AML that on average occurs two years post-remission and is significantly more frequent in elderly patients (Röllig et al., 2011; Burnett et al., 2011). The recurrence of AML after treatment is believed to be driven by a quiescent subset of LICs that evade traditional chemotherapy and are capable of re-emerging post-treatment (Kreso and Dick, 2014; Saito et al., 2010).

1.3.4. CEBPA and AML

The CCAAT/enhancer binding protein alpha (*Cebpa*) gene encodes for C/EBPα, a basic leucine zipper transcription factor (TF) that plays a critical role in hematopoietic cell fate and lineage commitment. Physiologically, *Cebpa* is an intronless gene that encodes for both a 42-kD (p42) and 30-kD (p30) DNA-binding protein, achieved by the presence of two distinct AUG translational start sites. Germ-line and conditional deletion of *Cebpa* during adulthood has been demonstrated to cause a block in neutrophil differentiation at the CMP stage, with this TF being considered an inducer of terminal differentiation (Zhang et al., 1997; Zhang et al., 2004a; Nerlov, 2007). Myeloid priming via C/EBPα has been identified in LT-HSCs, evidenced through chromatin studies, scRNA-seq and transgenic mouse models (Hasemann et al., 2014; Paul et al., 2015; Olsson et al., 2016; Wölfler et al., 2010). Moreover, in both

humans and mouse, C/EBPα fulfils it myelopoietic role by binding enhancers and promoters which subsequently activate myeloid-specific gene expression programs (Friedman, 2007; Ma et al., 2014; Federzoni et al., 2014).

Given the critical role that C/EBPα plays in myelopoiesis, and the fact that its expression can be found in cells as primitive as HSCs, it is unsurprising that *CEBPA* mutations are present in ~9% of de novo AML cases (Pabst et al., 2001; Snaddon et al., 2003). Notably, the deletion of *Cebpa* from HSCs results in what could be perceived as a premalignant expansion of HSCs (Zhang et al., 2004a). Clinically however, *CEBPA* null mutations rarely occur. Instead, mutations are divided into two categories: N-terminal mutations that block the translation of the p42 isoform, and C-terminal mutations that generate in-frame insertions and deletions within the basic-leucine zipper DNA binding domain (Leroy et al., 2005; Nerlov, 2004). The majority of *CEBPA* AML patients (>90%) present with bi-allelic mutations, harbouring an N-terminal mutation on one allele, and a C-terminal mutation on the other. The overwhelming frequency at which this type of mutation occurs in *CEBPA* AML signifies its leukemogenic importance over other genotypic combinations. Moreover, this also indicates that specific allelic mutations carry out distinct, yet collaborative roles during this subtype of leukemia, supported by the finding that complete *Cebpa* deletion in mice does not lead to leukemia (Zhang et al., 2004a, Heath et al., 2004).

The concept of collaborating *CEBPA* mutations was first evaluated using a bi-allelic mutant murine model which incorporates both a common C-terminus (K313KK, or K) and N-terminus mutations (Lp30, or L) (Bereshchenko et al., 2009; Kirtstetter et al., 2008). Commonly referred to as the K/L AML model, it was demonstrated that the transplantation of K/L fetal liver cells into irradiated mice results in the expansion of a premalignant HSC pool which then generates a

committed myeloid progenitor-like LIC population. K/L LICs express KIT but not SCA1, and give rise to a differentiated tumour cell fraction that lacks KIT but expresses CD11b (myeloid blasts). The transplantation of KIT+ K/L LICs is sufficient to recapitulate a leukemia, whereas the SCA1 positive and CD11b expressing myeloid blasts are not (Bereshchenko et al., 2009). Importantly, this study demonstrates that leukemic cells do not exist as a homogenous pool of cells, but are instead hierarchically organised.

1.4. Leukemic cell interactions in the BM

Interactions between leukemic cells, endogenous hematopoietic cells and the BM niche are considered highly important for the development and maintenance of hematological malignancies. Changes to the niche are sufficient to cause the formation of myeloid malignancies. Moreover, leukemic cells are capable of directly interacting with both endogenous HSPCs and the niche, leading to the disruption of normal cellular function in the BM.

1.4.1. HSPC disruption during leukemia

Studies from the 1970's demonstrate that leukemic cell conditioned media is capable of suppressing normal hematopoiesis (Broxmeyer et al., 1978, Miller et al., 1976). However, it is still often believed that the physical crowding of AML cells within the BM results in the displacement of normal HSPCs. This assumption was challenged during a study carried out in 2013 by the Taussig group, who proposed that BM failure experienced by AML patients is driven by interactions between leukemic and non-leukemic cell populations (Miraki-Moud et al., 2013). Using xenograft transplantation models, it was shown that the frequency of HSCs at the early- and mid-stages of

AML remain stable, despite a decrease in the number of progenitors. Furthermore, it was also demonstrated that HSCs, once removed from their immediate leukemic environment, remain functionally normal. This implies that leukemic cells do not have the capacity to intrinsically reprogram HSCs, but can directly supress hematopoietic output when in contact (Miraki-Moud et al., 2013). A later study complemented this by suggesting that there is no correlation between the BM blast infiltration experienced by AML patients and levels of cytopenia (Rauch et al., 2016).

Taken together, these findings indicate that the frequency of leukemic cells present in the BM does not necessarily correlate with an immediate decline in immunophenotypic HSPCs, therefore questioning whether displacement during AML truly plays a pivotal role in driving BM failure. Instead, these studies propose that symptoms are created by the direct molecular interaction between leukemic and hematopoietic cell types in the BM.

1.4.2. The niche as an initiator of hematological disorders

In addition to being pivotal for normal hematopoiesis, the BM niche has also been implicated as a driver of myeloid malignancies. The concept of the niche as an initiator of disease was first demonstrated by Rupec et al., (2005) using an IκBα-deficient mouse model. Ubiquitous depletion of IκBα causes a severe hematological disorder characterised by hypergranulopoiesis and constitutive Jagged1 expression in hepatocytes. Myeloid-cell specific depletion of IκBα however does not lead to a myeloproliferative disease, suggesting that stromal-changes are required in order to drive the formation of a malignancy (Rupec et al., 2005). Shortly following this, two seminal publications released in 2007 demonstrated that genetic changes to the BM niche were capable of driving the formation of myeloid malignancies (Walkley et al.,

2007a; Walkley et al., 2007b). The deletion of Retinoblastoma (*Rb*) from the hematopoietic compartment was shown to cause a significant myeloproliferative disorder. *Rb*-deficient myeloid cells transplanted into *Rb*-deficient, but not wildtype mice, were capable of initiating myeloproliferation (Walkley et al., 2007b). This implies that malignant myeloid cells rely heavily on a reprogrammed niche in order to sustain themselves during disease. Moreover, the same author demonstrated that widespread deletion of retinoic acid receptor gamma (*Rarγ*) leads to an age-related myeloproliferative neoplasm (MPN). The transplantation of wildtype hematopoietic cells into a *Rarγ*-deficient mice, but not the transplantation of *Rarγ*-deficient hematopoietic cells into wildtype mice, results in the development of an MPN-like disease (Walkley et al., 2007a). This was later complemented by a study that revealed the effects of depleting mind bomb 1 (*Mib1*), an E3-ligase and Notch ligand regulator, from the stroma. The stromal deletion of *Mib1* led to the onset of an MPN, which could be rescued by introducing an active intracellular domain of NOTCH1 in the *Mib1*-null background (Kim et al., 2008). Collectively, these studies demonstrate that changes to the niche are sufficient, and in some cases indispensable, for the formation and maintenance of hematological malignancies.

Using cell-type specific Cre mouse models, it was revealed that osteoprogenitor cells deficient in Dicer1, an RNase III endonuclease essential for micro RNA biogenesis, develop a myelodysplastic disease with random progression to AML (Raaijmakers et al. 2010). A subsequent study showed that osteoblast-specific expression of an activating mutation of β-catenin could cause altered differentiation potential of myeloid and lymphoid progenitors. The observed changes in hematopoietic composition were sufficient to cause an AML, driven by aberrant expression of Jagged1 and reversed by pharmacological and genetic manipulation

(Kode et al., 2014). Together, these findings propose that once mutated, the osteoblastic niche can drive leukemogenesis through the abnormal expression of important hematopoietic cell-surface molecules.

In addition to osteolineage cells, VECs have also been implicated as initiators of hematological malignancy. VEC-specific deletion of the downstream Notch signalling effector *Rbpj*, leads to an aggressive MPN (Wang et al., 2014). Interestingly, the loss of this molecule results in increasing levels of miR-155, an effect that drives up the expression of several cytokines including G-CSF and TNFα, thus creating a pro-inflammatory environment within which malignant cells are believed to thrive.

1.4.3. Malignant cell-mediated niche remodelling

Malignant cell-mediated niche remodelling has been reported in numerous hematological disorders including primary myelofibrosis, myelodysplastic syndrome (MDS), chronic myeloid leukemia (CML) and AML. Advances in imaging technologies and xenotransplantation assays have uncovered important insights into the behaviour of AML cells and their interactions with BM niches.

A landmark publication by Sipkins et al., (2005) revealed that circulating leukemic cells engraft around a specific subset of vasculature, demarcated by the expression of CXCL12. Moreover, it was shown that the niches occupied by leukemic cells are the same as those required by functioning HSPCs, suggesting that malignant cells are capable of "hi-jacking" physiologically important microdomains in order to survive and outcompete normal cells (Sipkins et al., 2005). A later study by Colmone et al., utilised the same imaging technique to demonstrate that upon homing to vascular niches, leukemic cells produce excessive levels of SCF (Colmone et al.,

2008). Transplanted, human CD34+ HSPCs were then shown to mobilize towards SCF expressing “hot spots” in the BM, preventing their movement into the periphery and ultimately decreasing their immunophenotypic frequency.

A recent discovery by the Lo Celso group demonstrated that MLL-AF9 leukemic blasts were capable of degrading endosteal endothelial cells and OBs. This phenomenon was subsequently shown to be spatiotemporally correlated with HSC loss (Duarte et al., 2018). Moreover, leukemic cells located in the endosteal region were revealed to express several pro-inflammatory and anti-angiogenic factors. Collectively, these findings suggest that leukemic cells actively remodel the niche within which they reside in order to disrupt normal hematopoiesis and promote malignant cell growth.

Niche remodelling has also been evidenced in mesenchymal cell types. MSCs taken from MDS (MDS-MSCs) patients lack a normal differentiation program and aberrantly express numerous niche-related secreted factors such as CDH2, VEGFA and LIF (Medyouf et al., 2014). Interestingly, exposing healthy MSCs to malignant MDS cells results in the adoption of an MDS-MSC molecular profile, suggesting that the effect of remodelling is self-perpetuating and can be passed on to adjacent, otherwise healthy cells.

Studies investigating the contribution of the niche in CML have found that leukemic cell derived G-CSF results in decreased CXCL12 expression by the BM niche. This creates a negative gradient of expression in the BM and subsequently impairs normal HSC function (Zhang et al., 2012). The transplantation of CML cells can also induce the niche-mediated expression of placental growth factor (PlGF). This leads to angiogenesis and the promotion of CML proliferation and metabolism. Treatment with an anti-PlGF antibody is sufficient to prolong the survival of CML-

transplanted mice, even in mice insensitive to traditional imatinib treatment (Schmidt et al., 2011).

MPN- and AML-mediated neuropathy can dramatically change the BM microenvironment (Arranz et al. 2014; Hanoun et al., 2014). Interestingly, denervation of sympathetic nerve fibres during a $Jak2^{V617}$ mouse model of MPN was shown to result in a reduction of *Nestin*-GFP MSCs. This reduction is not driven by differentiation, but instead as a result of mutant IL-1β producing HSCs, which trigger Schwann cell death and a subsequent decline in CXCL12 expression. The loss of CXCL12 promotes the expansion of mutant HSCs and subsequently sustains malignant cell growth (Arranz et al., 2014). Conversely, AML induced neuropathy disrupts *Nestin*-GFP MSC quiescence and promotes osteoblastic differentiation at the expense of HSC-maintaining NG2+ niche cells. The abnormal expansion of *Nestin*-GFP MSCs is also coupled with a downregulation of important HSPC retention factors such as CXCL12 (Hanoun et al., 2014).

Of note, it was recently demonstrated that AML blasts release exosomes that slow MSC-OB differentiation. In doing so, the expression of important niche related factors such as CXCL12 and KITL are decreased, reducing this niche's capacity to maintain normal HSPCs. Moreover, exosomes are capable of increasing factors that have been demonstrated to support leukemogenesis such as IL-6, CCL3 and DKK1 (Kumar et al., 2018).

Collectively, these studies provide strong evidence to suggest that in both mice and humans, malignant cells from a range of hematological disorders are capable of interfering with functioning HSPCs through direct remodelling of the niche. Understanding this process is therefore critical for the development of novel therapies

that are capable of uncoupling the molecular interactions between the niche and malignant cell types.

1.4.4. Therapeutically targeting the niche during malignancy

Having established that niche remodelling plays a pivotal role in the maintenance of numerous hematological malignancies, the disruption of these interactions and subsequent normalisation of the niche may offer a novel approach for therapeutic intervention during AML. Moreover, given that niche reprogramming occurs across a range of myeloid malignancies, a distinct advantage of this type of therapeutic intervention is its applicability and specificity to a wide spectrum of hematological conditions. A significant challenge faced by clinicians when treating AML is relapse, which occurs when the repopulating portion of a leukemia usurps traditional chemotherapy and remains in the BM even after multiple rounds of treatment. Preclinical patient and murine studies investigating the blockade of CXCR4, VCAM1 and CD44 have uncovered novel approaches for uncoupling the bond between repopulating LICs and their niche.

The expression of CXCR4 by LICs is often described as one of the primary mechanisms utilised by leukemic cells to evade chemotherapy. Treatment of AML with the CXCR4 inhibitor AMD3100, results in enhanced overall survival via the chemosensitisation of leukemic cells (Nervi et al., 2008; Zeng et al., 2009). This effect is mediated by the mobilisation of leukemic cells into the periphery, which subsequently leads to enhanced cellular eradication (Weisberg et al., 2012). AMD3100, commercially known as Plerixafor, is clinically used to mobilise HSCs into the periphery of patients. The use of this drug has also been established as a safe

adjunct to chemotherapy, and is beneficial for cases of relapsed AML (Uy et al., 2012).

CD44, also known as hyaluronic acid, is utilised by leukemic cells during engraftment (Jin et al., 2006; Krause et al., 2006). Blockage of this receptor was shown to attenuate the onset of leukemia, implicating this axis as an important therapeutic target. An approved antibody that targets CD44, also known as Bivatuzumab, was tested in combination with chemotherapy in aged AML relapsed patients. Unfortunately, however, blockade of CD44 did not improve overall survival in this study (Ossenkoppele et al., 2012). This effect is unsurprising given that chemoresistant LICs are unlikely to resemble their therapy-prone counterparts, and therefore likely rely on a different mechanism of action. Despite this, clinical trials investigating the effectiveness of Bivatuzumab during AML are still on-going.

The VCAM1-VLA4 axis has been demonstrated to promote chemoresistance through interactions between leukemic cells and MSCs (Jacamo et al., 2014). Interestingly however, heightened expression of VLA-4 by leukemic cells is associated with lower rates of relapse (Walter et al., 2010). This phenomenon likely explains why the blockage of this axis using both a monoclonal antibody and small-molecule inhibitor in a xenograft AML model results in greater overall survival (Hsieh et al., 2013; Layani-Bazar et al., 2014). Taken together, these studies provide promising evidence that targeting the niche is a viable therapeutic option for overcoming hematological disorders, both at their initial diagnosis and after relapse.

1.5. Ageing hematopoiesis and the niche

Ageing of the mammalian hematopoietic system results in the functional decline of several important physiological processes. These include a decline in the generation

of T lymphoid cells, B lymphoid cells and erythrocytes, which subsequently leads to the onset of age-related anemia and a decreased ability to fight infections (Berliner et al., 2013; Frasca et al., 2008; Kuranda et al., 2011; Plowden et al., 2004; Akbar et al., 2005). Clinically, however, the most important hematopoietic dysfunction during ageing is the dramatically increased incidence of hematological malignancies.

1.5.1. Aged murine hematopoiesis

There are significantly more phenotypic HSCs present in aged mice compared to young, however this is not accompanied by enhanced cellular functionality (Morrison et al., 1996; Dykstra et al., 2011; Rossi et al., 2005; Sudo et al., 2000; Harrison et al., 1982). The transplantation of HSCs from young mice into primary recipients results in a predominantly lineage-balanced output. However, continued transplantation of these cells eventually leads to a myeloid-skewed output, which is complemented by the presence of more myeloid-biased $CD150^{high}$ HSCs over-expressing a myeloid lineage-associated gene profile (Beerman et al., 2010; Rossi et al., 2005; Pang et al., 2011). Taken together, these findings suggest that myeloid lineage output during ageing is highly intrinsic and largely due to the superior self-renewal capacity of myeloid-biased HSCs.

Further down the hierarchy, committed progenitors have also been demonstrated to be both immunophenotypically and functionally perturbed during ageing. This extends to a decrease in CLP frequency and an increase in GMP frequency (Rossi et al., 2005). Collectively, these findings highlight the importance of cell-intrinsic pathways in determining lineage output during ageing. Moreover, alterations in lineage composition underlie age-related ailments that may explain why

elderly individuals are more likely to suffer from myeloid malignancies versus lymphoid.

An important contributor of secondary AML is clonal hematopoiesis (CH). This is the process by which a single hematopoietic population (or clone) with one or more somatic mutations expands (Bowman et al., 2018). The process of CH is strongly correlated with ageing, and is believed to be a precursor to MDS, and the eventual progression to AML. However, the development of these conditions as a result of CH is not a certainty, suggesting that mutational ordering, cell of origin and extrinsic pressures likely play a role in dictating leukemogenic transformation.

1.5.2. The aged murine hematopoietic niche

As alluded to in the previous sections of this introduction, the BM niche plays a fundamental role in maintaining normal and malignant hematopoietic cell types. It has been proposed that the BM niche may also be responsible for the immunophenotypic and functional changes that occur within the hematopoietic hierarchy during ageing.

During ageing, the BM is occupied by a greater proportion of adipocytes and fewer osteocytes, both of which originate from a common ancestor, the MSC. Age-related changes to MSCs include defects in differentiation that ultimately drive adipogenesis at the expense of osteogenesis (Singh et al., 2016; Justesen et al., 2001). Interestingly, culturing total mouse BM with adipocyte-conditioned medium results in the expansion of myeloid cells at the expense of B- and T- cells. This is believed to occur via the expression of the secreted factors IL-1, NOS2 and arginase (Kennedy et al., 2015). Given this, adipocytic expansion during ageing may account for why hematopoiesis is skewed in favour of myeloid output. Moreover, one might hypothesise that promotion of myelopoiesis at the expense of other lineage outputs

during ageing is ultimately responsible for the heightened incidence of myeloid malignancies. Indeed, obesity is associated with an increased risk of developing leukemia and relapse (Larsson and Wolk, 2008; Orgel et al., 2014).

VECs from aged mice are significantly perturbed compared to those found in young mice. There are fewer CD31^{hi} Endomucin^{hi} expressing VECs coupled with less NG2+ PV cells (Kusumbe et al., 2014; Kusumbe et al., 2016). As a consequence, SCF production is significantly reduced in the aged BM leading to changes in hematopoietic function.

Parabiotic pairing experiments uncovered that young systemic factors are sufficient to rejuvenate damaged muscle tissue (Conboy et al., 2005). This also extends to the hematopoietic system, where the transplantation of aged HSCs into a young microenvironment attenuates myeloid-skewing and restores T-cell output (Ergen et al., 2012; Rossi et al., 2005). Taken together, these findings suggest that extrinsic factors found exclusively during ageing are insufficient to maintain widespread cellular function. Moreover, this also indicates that the presence of a "normal" milieu may be adequate to restore normal cellular function.

1.6 Concluding remarks

The role that leukemic cells play in disrupting normal hematopoiesis is often attributed to the physical displacement of functioning HSPCs. Whilst this may be true at the terminal stages of AML, there is now mounting evidence to suggest that malignant cell populations are capable of both seeking out, and reprogramming, specific BM niches at the very onset of disease. Moreover, given that the symptoms of AML can occur at even the earliest stages of disease development (Estey and

Döhner, 2006), this suggests that mechanisms unrelated to physical displacement play a role in disrupting normal hematopoiesis during leukemia.

Despite several former studies having established that normal HSPCs are disrupted by the presence of malignant cell populations, the question still remained as to how this occurs and through what mechanism. Therefore, the central theme of this study was to assess the relationship between leukemic cells, individual endogenous HSPC populations and the BM niche, using a combination of immunophenotypic, functional and transcriptional assays. In doing so, the overall aim was to uncover how endogenous BM populations changed over the course of leukemic development, and attempt to elucidate the primary drivers of HSPC disruption. We also hoped to identify novel therapeutic targets in the form of receptors and secreted factors that were responsible for enabling leukemic growth at the expense of normal hematopoiesis, in addition to delineating the relationship between ageing and AML incidence.

1.7 Aims

Chapter 3

1. Create a murine model of AML that enables the simultaneous analysis of endogenous hematopoiesis, the niche and leukemic cell populations.
2. Establish which HSPC populations are immunophenotypically and functionally perturbed during the development of leukemia.

Chapter 4

3. Investigate the transcriptional profiles of endogenous HSPCs and the BM niche during leukemic development using bulk RNA-seq.
4. Delineate the composition of the BM niche using scRNA-seq.

Chapter 5

5. Identify candidate molecules that are responsible for the changes to normal cellular function during leukemia and investigate their therapeutic relevance using pharmacological inhibitors.

Chapter 6

6. Assess the aged hematopoietic niche and determine whether changes to this compartment correlate with enhanced leukemic susceptibility.

Chapter 2

Materials and methods

2.1. Laboratory materials and methods

2.1.1. Tissue dissection and preparation

For all experiments where hematopoietic and leukemic cell populations were used, the following steps were carried out to isolate tissue samples. Mice were euthanized using CO_2, and confirmation of death was achieved by cervical dislocation as per schedule 1 of the Home Office licensing requirements. Mice were placed under a sterile containment hood and sprayed with 70% ethanol solution until doused. Using sterile equipment, tibia, femur and cristae bones were dissected from mice and placed in 5mL of filtered phosphate buffered saline (PBS)/5% fetal calf serum (FCS) with 1X Penicillin-Streptomycin. Bones were then crushed in an autoclaved pestle and mortar. The BM solution was passed through a 50μm filter, centrifuged (5 minutes, 500g, 4°C) and resuspended in PBS/5% FCS. This was then repeated again on the remaining material to ensure maximum recovery of cells. A sample of the cells was then counted using a Sysmex KX-21N Automated Hematology Analyser or via a hemocytometer prior to subsequent use for assays. Splenic tissue was dissected from euthanised mice, weighed, imaged and crushed using a syringe plunger and 50μm filter. PBS/5% FCS was then used to create a single cell suspension by passing liquid through filter containing crushed spleen.

2.1.2. Flow cytometry antibody staining and analysis

Samples were first centrifuged (5 minutes, 500g, 4°C) then resuspended in purified anti-mouse CD16/32 at 4°C for 20 minutes to prevent non-specific antibody binding. For the staining of myeloerythroid progenitor populations, samples were blocked in a cocktail of anti-CD16/32 conjugated to PE-Cy7. Following this, an equal volume of 2X concentrated antibody cocktail was added to the cell solution and incubated at

4°C for an additional 20 minutes. Cells were then washed in PBS/5% FCS, centrifuged (5 minutes, 500g, 4°C) and resuspended in PBS/5% FCS unless otherwise stated. Prior to analysis/sorting, the viability dye 7-aminoactinomycin D (7AAD) (Sigma Aldrich, cat no. A9400) was added to each sample. DAPI was used as a viability staining dye when analysing mature BM cell types.

Stained cells were analysed on a BD LSRFortessa or sorted using a BD FACSAriaII/III. Single stained compensation beads were used for every experiment, in addition to fluorescence minus one controls. For experiments requiring cell sorting, purity was determined prior to commencing, proceeding only if above 95%. A complete list of antibodies used can be found in table 2.1.2.a.

Flow cytometric analysis was carried out using FlowJo (v10.4.2). For all cytometry analyses, cells were first gated on forward scatter (FSC) vs side scatter (SSC), followed by a FSC-H vs FSC-W singlets gate, and finally exclusion of dead cells (7AAD+). To calculate a populations frequency as a % of singlets, the number of events within any given population gate was divided by the number of events inside the singlets gate and multiplied by 100. For calculating donor-derived frequency, the number of events per population gate was divided by the total number of donor (CD45.1/2+) events, and multiplied by 100.

2.1.2.a. Antibodies used for flow cytometry analysis and sorting

Antibody	**Conjugate**	**Dilution**	**Clone**	**Catalogue no.**	**Supplier**	**Application**
NK1.1	BV650	1/50	PK136	108735	BioLegend	Peripheral blood staining
TER119	BV650	1/50	TER-119	116235	BioLegend	Mature cell staining
Ly6a	BV605	1/150	D7	108133	BioLegend	Niche cell staining
Streptavidin	BV421	1/200	-	405226	BioLegend	Secondary staining
CD105	Biotinylated	1/100	MJ7/18	13-1051-82	eBioscience	BM staining
CD135 (Flt3)	Biotinylated	1/100	A2F10	13-1351-82	eBioscience	BM staining
LepR	Biotinyated	1/100	-	BAF497	R&D Systems	Niche cell staining
ALCAM	Biotinyated	1/100	-	BAF1172	R&D Systems	Niche cell staining
CD45.2	APC ef780	1/25	104	47-0454-82	eBioscience	Allotype discrimination
KIT	APC ef780	1/1200	2B8	47-1171-82	eBioscience	BM staining
CD11b	APC	1/400	M1/70	17-0112-83	eBioscience	Peripheral blood staining
PDGFRa	APC	1/50	APA5	17-1401-81	eBioscience	Niche cell staining
CD150	APC	1/100	TC15-12F12.2	115910	BioLegend	BM staining
F4/80	APC	1/200	BM8	17-4801-80	eBioscience	Mature cell staining
CD45	AF700	1/100	30-F11	56-0451-82	eBioscience	Niche cell staining
CD45.2	AF700	1/200	104	56-0454-82	eBioscience	Allotype discrimination
CD45.1	AF700	1/100	A20	110724	BioLegend	Allotype discrimination
Ly6G	Pacific Orange	1/100	RB6-8C5	RM3030	ThermoFisher	Mature cell staining
CD45.2	Pacific Blue	1/100	104	109819	Biolegend	Allotype discrimination
SCA1	Pacific Blue	1/150	E13-161.7	122520	BioLegend	BM staining

2.1.2.a. Antibodies used for flow cytometry analysis and sorting

Antibody	Conjugate	Dilution	Clone	Catalogue no.	Supplier	Application
CD16/32	Unconjugated	1/50	93	14-0161-81	eBioscience	Fc receptor block
CD31	PeCy7	1/1600	390	25-0311-82	eBioscience	Niche cell staining
CD19	PeCy7	1/400	eBio1D3	25-0193-82	eBioscience	Peripheral blood/mature cell staining
CD16/32	PeCy7	1/150	93	25-0161-82	eBioscience	BM staining
CD4	PeCy5	1/800	RM4-5	100514	BioLegend	Lineage staining
CD8a	PeCy5	1/800	53-6.7	100716	BioLegend	Lineage staining
CD5	PeCy5	1/600	53-7.3	100610	BioLegend	Lineage staining
Ly6G	PeCy5	1/200	RB6-8C5	108410	BioLegend	Lineage staining
CD11b	PeCy5	1/400	M1/70	101210	BioLegend	Lineage staining
B220	PeCy5	1/200	RA3-6B2	103210	BioLegend	Lineage staining
TER119	PeCy5	1/600	TER-119	116210	BioLegend	Lineage staining
Streptavidin	PE-CF594	1/200	-	562318	BD Horizon	Secondary staining
CD11b	PE	1/200	M1/70	15-0112-82	eBioscience	BM staining
CD4	PE	1/800	GK1.5	12-0041-85	eBioscience	Peripheral blood staining
CD8a	PE	1/200	53-6.7	12-0081-85	eBioscience	Peripheral blood staining
CD41	PE	1/300	eBioMWRes30	12-0411-83	eBioscience	BM staining
CD48	PE	1/400	HM48-1	12-0481-81	Biolegend	BM staining
VCAM1	PE	1/100	429	105713	Biolegend	Niche cell staining
SiglecF	PE	1/200	1RNM44N	12-1702-82	eBioscience	Mature cell staining

2.1.2.a. Antibodies used for flow cytometry analysis and sorting

Antibody	**Conjugate**	**Dilution**	**Clone**	**Catalogue no.**	**Supplier**	**Application**
CD45.2	FITC	1/50	104	11-0454-85	eBioscience	Allotype discrimination
CD71	FITC	1/200	RI7217	113805	BioLegend	Mature cell staining
SCA1	BV786	1/200	D7	563991	BD Horizon	BM staining

2.1.3. Niche cell isolation

Adapted versions of the protocols described by Semerad et al., 2005; Nakamura et al., 2010 and Morikawa et al., 2009 were used to isolate BL (endosteal) and CBM (sinusoidal) niche populations.

2.1.3.1. CBM niche cell isolation

Dissected bones were crushed twice in a pestle and mortar containing 5mL PBS/5% FCS buffer, aspirated and passed through a 50μm mesh filter into a fresh 15mL Falcon. After crushing, remaining bone fragments were kept for isolating bone lining niche cells (section 2.1.3.2). The filtered BM solution was counted using a Sysmex KX-21N Automated Hematology Analyser, centrifuged (5 minutes, 500g, 4°C) and resuspended in 5mL Dulbecco modified eagle medium (DMEM) containing 10% FCS, 200U/mL DNaseI (Stemcell Technology, cat no. 07900) and 10mg of collagenase type IV (Worthington Biochemical, cat no. LS004188) for 20 minutes at 37°C on a rotating plate. After incubation, cells were washed with PBS/5% FCS and centrifuged (5 minutes, 500g, 4°C). The pellet was resuspended in 5mL of ammonium chloride solution (StemCell Technology, cat no. 07850) for 10 minutes at room temperature. The lysis reaction was neutralised using 5mL of PBS/5% FCS, centrifuged (5 minutes, 500g, 4°C), resuspended in 5mL PBS/5% FCS and counted. Depletion of the CD45+ cell fraction was carried out in order to improve the central BM niche cell recovery. Cells were resuspended in 90μL PBS/5% FCS and 10μL anti-CD45 microbeads (Miltenyi, cat no. 130-052-301) per $10x10^6$ cells. The solution was gently agitated every 5 minutes and incubated for a total of 20 minutes at 4°C. During this time, LS columns (Miltenyi, cat no. 130-042-401) were set up on a magnetic stand and equilibrated with 10mL PBS/5% FCS. The cell solution was then

washed with PBS/5% FCS, centrifuged (5 minutes, 500g, 4°C) and resuspended in 2mL PBS/5% FCS. Once completely clear of any remaining solution, the LS column was loaded with the cell suspension and collected in a fresh 15mL Falcon tube. Cells were centrifuged (5 minutes, 500g, 4°C), counted and stained for FACS using the antibodies outlined in table 2.1.2.a.

2.1.3.2. BL niche cell isolation

Bone from section 2.1.3.1 was minced into smaller fragments using scissors. Bone fragments were then resuspended in 5mL of PBS/5% FCS and centrifuged (5 minutes, 500g, 4°C). Bone fragments were resuspended in 5mL DMEM containing 10% FCS, 200U/mL DNaseI (Stemcell Technology, cat no. 07900) and 15mg of collagenase type I (Worthington Biochemical, cat no. LS004197) for 45 minutes at 37°C on a rotating plate. Digested bone fragments were allowed to settle and the top layer was aspirated, passed through a 70μm mesh filter into a 50mL Falcon tube and stored at 4°C. Collagenase treatment was repeated once more on the remaining bone material to ensure maximum niche cell recovery. The resulting cell solution was washed with 10mL PBS/5% FCS and centrifuged (5 minutes, 500g, 4°C). Cells were then stained for FACS using the antibodies outlined in table 2.1.2.a.

2.1.4. *In vitro* culture of LICs

Frozen LICs were thawed, washed in PBS/5% FCS and centrifuged (500g, 5 minutes, 4°C). Cells were then resuspended in Iscove's modified Dulbecco's media (IMDM) containing HSPC supportive factors (see table 2.1.4.2.a) and counted using a haemocytometer. Cells were plated at a density of 75,000 viable cells/mL in 1.5cm tissue culture dishes (Corning, cat no. CLS430599) and incubated for 0, 24 or 48

hours at 37°C with 5% CO_2. After each time point, cells were washed in PBS/5% FCS, centrifuged (500g, 5 minutes, 4°C) and counted. Total cultured cells were then transplanted into sub-lethally irradiated (520 rads, single dose) CD45.1/2 recipient mice as per the protocol described in section 2.2.4 of this chapter.

2.1.4.a. – HSPC supportive factors for LIC culture

Component	Stock concentration	Final concentration
mIL-3	10ng/μL	10ng/mL
mIL-6	10ng/μL	10ng/mL
SCF	50ng/μL	50ng/mL
Penicilin-Streptomycin	100X	1X
β-ME	100X	1X
BSA	-	0.5%

2.1.5. Functional assays

To assess LT reconstitution and functionality of HSCs, mice were transplanted with leukemia for a period of either 2 or 3 weeks. BM cells were dissected after these time points and stained. 100 CD45.1/2+ LSK CD150+ CD48- HSCs were sorted into chilled Eppendorf tubes containing 200μL PBS/5% FCS using a BD FACSAriaII. Helper cells (250,000 CD45.1 total BM) were added to the solution of sorted HSCs, which were then transplanted into lethally irradiated (1000 rads, split dose) 8-week-old C57BL/6 female mice (Envigo, Huntingdon) as described in section 2.2.4.

To assess progenitor functionality, mice were transplanted for a period of 2 or 3 weeks, euthanized and their BM dissected. Myeloid and erythroid progenitor function was assessed by sorting 500 or 1000 Lineage-KIT+CD45.1/2+ directly into 100μL chilled IMDM, respectively. Cells were then transferred into either 0.9mL CFU-GM (StemCell Technologies, cat no. 3534) or BFU-E (StemCell Technologies, cat no. 3436) MethoCult solutions, plated into 1mL sterile culture dishes, incubated at

37°C with 5% CO_2 and manually counted after 14 days. Additional SCF was added to each BFU-E culture at a total concentration of 100ng/mL.

2.1.6. Hydrodynamic injection plasmid preparation

All plasmids used for hydrodynamic injections were purchased from Origene on a pCMV6-Entry vector backbone (figure 2.1.6.f and table 2.1.6.a) and expanded in the laboratory. Details of plasmids can be found in table 2.1.6.b. Lyophilised plasmid DNA was dissolved in TE at a concentration of 100ng/μL and left to shake for 5 minutes at 1500RPM. Competent Stbl3 E.Coli bacterial cells (ThermoFisher, cat no. C737303) were thawed and incubated with 10ng of dissolved plasmid DNA on ice for 20 minutes. The mixture was heat shocked at 42°C for 2 minutes after which the solution was placed back on ice for 5 minutes. A 1mL volume of liquid broth was added and cells were incubated for 1 hour at 37°C on an Eppendorf shaker set to 1050 RPM. Cells were centrifuged for 1 minute at 10,000 RPM, the supernatant discarded and the remaining pellet resuspended in 100μL of liquid broth. The solution was spread using glass beads on kanamycin treated (15μg/mL) agar plates and left to incubate over night at 37°C. Single colonies were selected from each of the agar plates and added to conical flasks containing 200mL of liquid broth with 15μg/mL kanamycin. Flasks were left to incubate at 37°C overnight on an Infors shaking unit set to 220 RPM. Overnight expanded bacteria were harvested by centrifugation (6000 RPM, 15 minutes, 4°C) and plasmid DNA extracted using a Qiagen Plasmid Maxi Kit (Qiagen, cat no. 12162). The resulting cell pellet was resuspended in 10mL of buffer P1 followed by 10mL of buffer P2. The mixture was then gently inverted 4-6 times and incubated for 5 minutes. The resulting blue solution was added to 10mL of pre-chilled buffer P3, gently inverted 4-6 times and incubated on ice for 20 minutes

until turning colourless. The solution was centrifuged (6000 RPM, 30 minutes, 4°C), supernatant aspirated and the pellet centrifuged (13,000 RPM, 15 minutes, 4°C). During this time, Qiagen columns were equilibrated using 2X 30mL buffer QC, allowing the solution to pass completely through the columns. The supernatant was added to the columns followed by 2X 30mL of QC buffer. A fresh 50mL Falcon tube was placed below the column and the DNA was eluted using 15mL of QF buffer. Plasmid DNA was precipitated by adding 10.5mL of 70% isopropanol, mixing and centrifuging (11500 RPM, 30 minutes, 4°C). The supernatant was carefully decanted and the remaining pellet washed with 5mL of room temperature 70% ethanol solution. This was then centrifuged (11500 RPM, 15 minutes, 4°C), the supernatant decanted and the pellet left to dry for 5-10 minutes. The dry pellet was resuspended in TE buffer and the DNA concentration measured using the NanoDrop (see table 2.1.6.c).

Plasmid DNA (1μg) was quality checked using the restriction enzyme NcoI. This restriction enzyme was selected for its ability to cut each plasmid at least 3-4 times, outside of the target cDNA sequence. Table 2.1.6.d describes the DNA/restriction enzyme mixtures that were used to incubate plasmid DNA prior to quality checking. Plasmid DNA was digested for 1 hour at 37°C on an Eppendorf shaker. Both digested and non-digested plasmid DNA were run on a 1% agarose gel for 1 hour. Table 2.1.6.e describes the expected fragment size following restriction enzyme digestion and location on the agarose gel image shown in figure 2.1.6.g.

2.1.6.a – pCMV6-Entry vector components

Sequence	Description
CMV promoter	Constitutive eukaryotic promoter sequence
T7 promoter	Constitutive prokaryotic promoter sequence
cDNA insert	Position of cDNA sequence
Myc-DDK	C-terminal tag sequence facilitating detection and purification
PolyA signal	Termination sequence
ColE1	Colicin E1sequence
Kan/Neo	Kanomycin/neomycin resistance sequences
SV40 origin	Mammalian origin of replication sequence
F1 origin	Phage derived origin of replication

2.1.6.b – Plasmid DNA descriptions

Plasmid	Tag	Vector	Catalogue number	Supplier
Ccl3	Myk-DDK	pCMV6-Entry	MR225554	Origene
Ccl6	Myk-DDK	pCMV6-Entry	MR200502	Origene
Ccl9	Myk-DDK	pCMV6-Entry	MR223660	Origene
Ccl17	Myk-DDK	pCMV6-Entry	MR200247	Origene
Cxcl10	Myk-DDK	pCMV6-Entry	MR200291	Origene
Cxcl12	Myk-DDK	pCMV6-Entry	MR227145	Origene
Flt3l	Myk-DDK	pCMV6-Entry	MR227308	Origene
Il18	Myk-DDK	pCMV6-Entry	MR226935	Origene
Tnfsf12	Myk-DDK	pCMV6-Entry	MR224787	Origene
Empty	Myk-DDK	pCMV6-Entry	PS100001	Origene

2.1.6.c – Final plasmid DNA concentrations

Plasmid	Concentration (μg/uL)
Ccl3	1.59
Ccl6	1.21
Ccl9	1.27
Ccl17	1.67
Cxcl10	1.34
Cxcl12	1.15
Flt3l	1.32
Il18	1.66
Tnfsf12	1.93
Empty	0.99

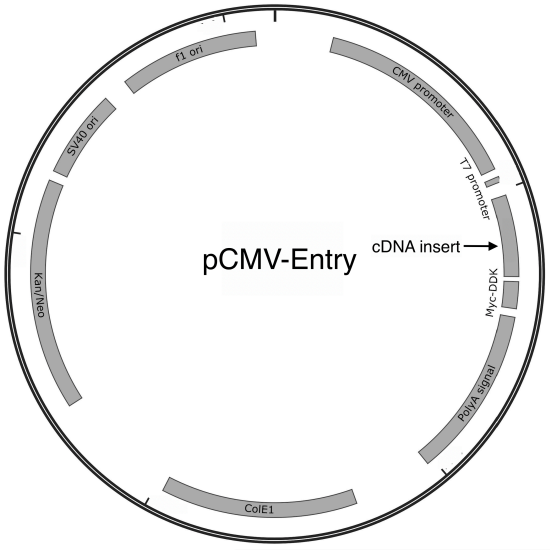
2.1.6.d – Restriction enzyme reaction mixture

Component	Volume (μL)
NcoI	0.5
NEBuffer 2.1	2
Plasmid	0.5
Water	17

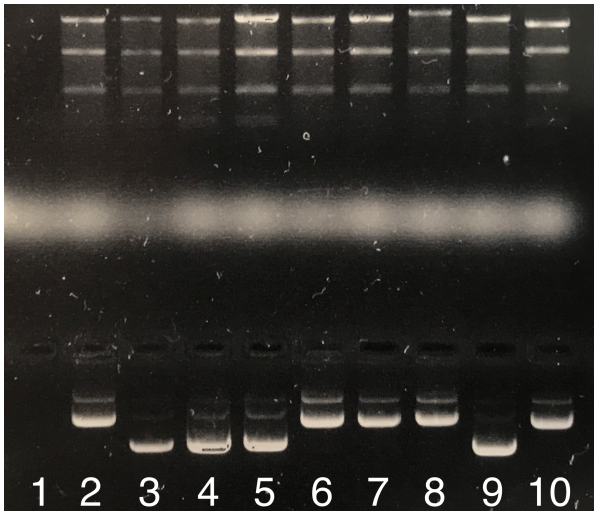
2.1.6.e – Plasmid DNA band size and gel location

Plasmid	Lane number	Non-digested estimated size (bp)	Estimated digested band size (bp)
Water	1	-	-
Ccl17	2	5160	2922, 703, 1535
Ccl9	3	5247	3009, 703,1535
Il18	4	5457	309,2910,703,1535
Tnfsf12	5	5628	309,3081,703,1535
Cxcl10	6	5175	2937, 703, 1535
Ccl6	7	5229	2991, 703, 1535
Flt3l	8	5577	3339,703,1535
Ccl3	9	5157	2919,703,1535
Cxcl12	10	5160	309,2613,703,1535

2.1.6.f – pCMV6-Entry vector



2.1.6.g – Plasmid DNA was incubated with the restriction enzyme NcoI. The top panel of bands illustrates digested plasmid and the bottom panel illustrates non-digested plasmid. Information on lanes 1-10 can be found in table 2.1.6.e



Digested fragments

Non-digested fragments

2.1.7. Bulk RNA-seq sample preparation and sequencing

2.1.7.1. Sample collection

An adapted version of the low-cell number SMART-seq2 protocol described by Picelli et al., (2013) and Picelli et al., (2014) was used for processing bulk RNA-seq samples. For all bulk RNA-seq experiments, 100 cells/biological replicate were isolated by FACS directly into thin-walled PCR tubes containing 4μl of lysis buffer with dNTPs and oligo-dT as detailed in tables 2.1.7.1.a and 2.1.7.1.b. Immediately after sorting, samples were vortexed, centrifuged (700g, 10s, room temperature), and placed at -80°C for a maximum of 4 weeks before being further processed.

2.1.7.1.a – SMART-seq2 lysis buffer

Component	Stock concentration	Volume	Supplier	Cat no.
Triton X-100	0.4%	19μl	Sigma Aldrich	T9284

RNase inhibitor	40 U μl-1	1μl	Clontech	2313A

2.1.7.1.b – Complete SMART-seq2 buffer

Component	**Stock concentration**	**Volume**	**Supplier**	**Cat no.**
Lysis buffer	-	2μl	Sigma Aldrich	-
dNTPs	10μM	1μl	Clontech	2313A
Oligo-dT	10μM	1μl	Biomer	-

2.1.7.2. First-strand synthesis

Upon thawing, samples were heated for 3 minutes at 72°C, centrifuged (700g, 10s, room temperature) and placed on ice to allow for oligo-dT hybridization. 5.6μl of RT-mix was added to each sample, the contents and volumes of which are detailed in table 2.1.7.2.a. After addition of the RT-mix, samples were centrifuged (700g, 10s, room temperature) and the reaction incubated in a thermal cycler with heated lid using the RT program detailed in table 2.1.7.2.b.

2.1.7.2.a – RT mix

Component	**Stock concentration**	**Volume/sample**	**Supplier**	**Cat no.**
SuperScript II reverse transcriptase	200 U μl-1	0.25μl	Invitrogen	18064-014
SuperScript II first-strand buffer	5X	2μl	Invitrogen	18064-014
DTT	100mM	0.5μl	Invitrogen	18064-014
Betaine	5M	2μl	Sigma	61962
MgCl2	1M	0.1μl	Sigma	M8266
Template switching oligo (TSO)	100μM	0.1μl	Exiqon	-
RNase inhibior	40 U μl-1	0.25μl	Clontech	2313A
Water (RT-PCR grade)	-	0.4μl	Ambion	AM9935

2.1.7.2.b – RT program

Cycle	Temperature (°C)	Time	Purpose
1	42	90 min	RT and template switching
2-11	50	2 min	Unfolding of RNA secondary structures
	42	2 min	Completion/continuation of RT and template switching
12	70	15 min	Enzyme inactivation
13	4	Hold	Storage

2.1.7.3. Pre-amplification

Following RT incubation, 15μl of PCR mix (table 2.1.7.3.a) was added to each of the first-strand synthesis reaction products. Samples were centrifuged (700g, 10s, room temperature) and the reaction incubated within a thermal cycler (with heated lid) using the PCR amplification program detailed in table 2.1.7.3.b.

2.1.7.3.a – PCR mix

Component	Stock concentration	Volume/sample	Supplier	Cat no.
KAPA HiFi HS Ready Mix	2X	12.5μl	KAPA Biosystems	KK2601
ISPCR primers	10μM	0.125μl	Biomer	-
Water (RT-PCR grade)	-	2.375μl	Ambion	AM9935

2.1.7.3.b – PCR amplification program

Cycle	Denature	Anneal	Extend	Hold
1	98°C, 3 min	-	-	-
2-16	98°C, 20 s	67°C, 15 s	72°C, 6 min	-
17	-	-	72°C, 5 min	-
18	-	-	-	4°C

2.1.7.4. Magnetic purification

Prior to purification, Agencourt Ampure XP magnetic beads (Beckman Coulter, cat no. A63882) were equilibrated to room temperature for 30 minutes and vortexed. Samples containing amplified cDNA from the previous step were transferred to a V-bottom assay plate (Axygen, cat no. P-96-450V-C-S) and diluted with 8μl of RT-PCR grade water. 25μl of Ampure XP beads were added to each of the diluted cDNA samples, which were mixed by pipetting and incubated for 8 minutes at room temperature to allow for sufficient cDNA binding. Following this, the plate was transferred to a magnetic stand (Ambion, cat no. AM10027) and incubated for an additional 5 minutes. Whilst still on the magnetic stand, the supernatant was aspirated and discarded, and each of the samples was washed twice with 200μl of 80% ethanol solution. The remaining pellet was left to air dry for 5 minutes, following which 17.5μl of elution buffer (Qiagen, cat no. 19086) was added to each sample. The plate was then removed from the magnetic stand, the samples mixed by pipetting and allowed to incubate for 2 minutes. Samples were placed back on the magnetic stand and the subsequent supernatant aspirated and stored in fresh thin-walled PCR tubes, ensuring minimal magnetic bead carry over. After purification, all samples were quality checked using a Agilent high-sensitivity DNA chip (Agilent Technologies, cat no. 5067-4626) and an Agilent 2100 Bioanalyser (Agilent Technologies, cat no. G2938C). cDNA concentration was determined using a Qubit dsDNA HS kit (Invitrogen, cat. no. Q32851) and a Qubit fluorometer (Invitrogen, cat no. Q32866).

2.1.7.5. Tagmentation and library construction

Tagmentation and indexing was performed using the Nextera XT DNA sample preparation kit (Illumina, Cat. FC-131-1096). Purified cDNA was diluted to 0.3-

0.75ng/sample in a total volume of 5μL nuclease-free water. The tagmentation reaction mixture was set up on ice. A detailed component list and volumes used can be found in table 2.1.7.5.a. After addition of the tagmentation reaction mixture to the diluted cDNA, samples were incubated in a thermal cycler with a heated lid using the tagmentation program described in table 2.1.7.5.b. Following tagmentation, 5μl of neutralisation buffer was added to each sample and mixed by pipetting to strip the Tn5 transposase from the tagmented DNA. Samples were incubated for 5 minutes at room temperature to ensure complete neutralisation. A PCR was carried out using the reagents described in table 2.1.7.5.c and the program shown in table 2.1.7.5.d. Each sample was assigned an index to allow for the demultiplexing after sequencing.

2.1.7.5.a – Tagmentation reaction mix

Component	**Volume**
Tagment DNA buffer	10μl
Amplicon tagment mix	5μl
DNA	5μl

2.1.7.5.b – Tagmentation program

Cycle	**Temperature**	**Time**
1	55°C	5 min
2	4°C	Hold

2.1.7.5.c – Amplification of adapter ligated fragments

Component	**Volume (μl)**
DNA	25
Nextera PCR master mix	15
Index 1 primers (N7)	5
Index 2 primers (N5)	5
Total volume	50

2.1.7.5.d – Adapter ligated fragment PCR program

Cycle	Denature	Anneal	Extend	Hold
1	–	–	72 °C, 3 min	–
2	95 °C, 30 s	–	–	–
3–14	95 °C, 10 s	55 °C, 30 s	72 °C, 30 s	–
15	–	–	72 °C, 5 min	–
16	–	–	–	4 °C

2.1.7.6. Library magnetic purification

Following the amplification of the indexed samples, the purification step described in section 2.1.7.4 was repeated with exception to the final resuspension step. After being washed in ethanol, samples were instead resuspended in elution buffer (Qiagen, cat no. 19086) before being placed back on the magnetic stand. The supernatant was then collected in fresh thin-walled PCR tubes.

2.1.7.7. Sample pooling

In order to pool samples, it was necessary to first measure sample cDNA fragment size and concentration as previously described in section 2.1.7.5. A library was generated for sequencing that had equimolar representation of each sample, totalling a molar concentration of 10nM. Pools were quality checked on the Bioanalyser.

2.1.8. scRNA-seq sample preparation

BL and CBM niche cells for droplet based scRNA-seq were prepared separately, as described in section 2.1.3. A total of 5300 BL and 5300 CBM niche cells were FACS isolated based on their expression of 7AAD- CD45- TER119-, into 0.04% bovine serum albumin solution. Library preparation was performed following the Chromium Single Cell 3' Reagents Kit v2 users guide (CG00052, Rev C). Quantification of cDNA was done using the Qubit dsDNA HS kit (Invitrogen, cat. no. Q32851) and a Qubit

fluorometer (Invitrogen, cat no. Q32866). Fragment sizes were determined using an Agilent high-sensitivity DNA chip (Agilent Technologies, cat no. 5067-4626) and an Agilent 2100 Bioanalyser (Agilent Technologies, cat no. G2938C). After pooling, library quantification was determined using the KAPA qPCR platform (Kapa Biosystems KK4824).

2.1.9. Pharmacological inhibitors

Table 2.1.9.a outlines the vehicle solutions, dosing, catalogue numbers and in vivo delivery routes used to investigate the effects of inhibitors during this study.

2.1.9.a. Inhibitor vehicle solutions, delivery routes, dosing, and catalogue number/suppliers

Inhibitor	**Company**	**Catalogue**	**Vehicle**	**Delivery route**	**Dose (mg/kg)**	**Target**
SB525334	MedChem Express	HY-12043	100% corn oil	Oral gavage	30	TGFBR1
J113863	Tocris	2595	2.5% ethanol, 97.5% saline solution	I.P	10	CCR1
Quizartinib	MedChem Express	HY-13001	22% (2-Hydroxypropyl)-β-cyclodextrin	Oral gavage	10	FLT3
Doxorubicin	MedChem Express	HY-15142A	10% water, 90% PBS	I.P	3	Topoisomerase II
Cytarabine	MedChem Express	HY-13605	10% water, 90% PBS	I.P	100	Antimetabolite Inhibitor

2.1.10. BM serum collection and cytokine array

BM serum was collected from mice by washing BM cells in PBS, centrifuging (500g, 5 minutes, 4°C) and aspirating the supernatant. BM serum was stored at -80°C for a maximum of 1 month before use. We then used the Proteome Profiler XL Cytokine Array (R&D Systems, cat no. ARY028), as per the manufacturers protocol.

2.1.11. Red cell lysis and peripheral blood preparation

For analysing peripheral white blood cells after transplantation of either leukemic cells or HSCs, between 50-100µL of blood was first collected in EDTA-treated Microvette tubes (Sarstedt). Samples were resuspended in 9mL of lysis buffer containing ammonium chloride (150mM) and potassium bicarbonate (10mM) for 3 minutes at room temperature. 1mL of 10X PBS was added to stop the lysis reaction and samples were centrifuged (500g, 5 minutes, 4°C). Following lysis, cells were blocked and stained prior to analysis.

2.1.12. Blood smear and BM cytospin images

To produce blood smear images, 1µL of freshly isolated blood was pipetted onto a microscope slide, and spread using another slide. Smeared blood samples were allowed to air dry overnight. Cytospin images were generated by counting 50,000 viable cells into a maximum volume of 200µL filtered 5% FCS/ PBS media. Cells were loaded into a slide funnel attached to a microscope slide. Once loaded, cells were spun at 1000RPM for 10 minutes, after which slides were air dried overnight. Both blood smears and cytospin samples were stained in Giemsa and May Grünwald solutions following protocols provided by Sigma Aldrich.

2.2. Animal materials and methods

2.2.1. Animals

All animals were bred and maintained in accordance with UK Home Office regulations and with the approval of the University of Oxford Ethical Committee. All experiments were performed under project licenses. To generate heterozygous CD45.1/2 recipients, wild-type C57BL/6 CD45.1 mice were bred with wild-type C57BL/6 CD45.2 mice (Envigo, Huntingdon). C57BL/6 CD45.1/2 *Gata1*-EGFP mice were produced by breeding CD45.1 *Gata1*-GFP mice with C57BL/6 CD45.2 mice. CD45.1 *Gata1*-GFP mice were generated as described by Drissen et al., 2016.

2.2.2. Hydrodynamic injection

2.2.2.1. Krebs-Ringer modified buffer

Krebs-Ringer modified buffer was used as the vehicle solution for all hydrodynamic injections. Table 2.2.2.1.a describes the stock solutions, and Table 2.2.2.1.b displays the volumes required from each stock solution to generate the buffer. The solution was buffered to a pH of 7.4, passed through a 0.2μm vacuum filter and stored at room temperature for up to one month.

2.2.2.1.a – Krebs-Ringer modified buffer components

Component	Formula weight (g/mol)	Required mass (g)	Volume of water to add (mL)	Stock concentration
NaCl	58.4	146	500	5mM
KCl	74.6	37.3	500	1mM
MgSO4	120.4	6	500	100mM
K2HPO4	172.4	8.7	500	100mM
Glucose	180.2	9	500	100mM
HEPES	238.3	11.9	500	100mM
CaCl2	111	5.5	500	100mM

2.2.2.1.b – Krebs-Ringer modified buffer (pH 7.4)

Component	Stock concentration	Final concentration	Volume added (mL)
NaCl	5mM	135mM	12.5
KCl	1mM	5mM	2.5
MgSO4	100mM	1mM	5
K2HPO4	100mM	0.4mM	2
Glucose	100mM	5.5mM	27.5
HEPES	100mM	20mM	100
CaCl2	100mM	1mM	5
			344.5 MilliQ

2.2.2.2. Final working buffer

The final working hydrodynamic injection buffer was generated each time the injection procedure was performed. To do this, a fresh 1% w/v BSA solution was created by dissolving 0.5g of BSA into a Falcon containing 50mL of MilliQ water. After complete dissolution, the 1% BSA solution was passed through a 0.2μm syringe filter and diluted to a final concentration of 0.05% in Krebs-Ringer modified buffer. This was stored on ice and used as the vehicle for all subsequent hydrodynamic injections. Prior to beginning the procedure, mice were weighed to determine total injection volume. The equation in figure 2.2.2.2.a was used to determine the appropriate injection volume for each mouse (Kim and Ahituv, 2013). A volume of plasmid solution that equated to 1μg of total DNA material was then added to the injection solution.

2.2.2.2.a – Equation for determining appropriate hydrodynamic injection volume

$$Total\ volume\ (mL) = \frac{mouse\ weight\ (g)}{10 g/mL} + 0.1mL\ delivery\ solution$$

2.2.2.3. Injection procedure

Prior to injecting, mice were warmed for 20-25 minutes at 37°C to ensure optimal tail vein dilation, following which a 2.5mL Terumo syringe was filled with the appropriate volume of the plasmid solution using a blunt end needle. The syringe was evacuated of any bubbles by gentle inversion followed by the attachment of a 27½ gauge needle. IsoFlo (Zoetis) was loaded into an anaesthesia machine and the pump turned on, allowing the chamber to fill up. Mice were then individually placed into the anaesthesia chamber, left for 2-3 minutes and monitored for consciousness by pinching the foot and assessing reflex. After losing consciousness, mice were transferred to a face-mask where they were rapidly injected (4-7 seconds) via the tail vein with the complete plasmid solution. Mice were taken off the facemask and transferred to a hot-blanket to recover prior to placing them back in their respective cages. An empty pCMV6-entry vector was used as a negative control for all hydrodynamic injections, injected at an equivalent concentration and in a weight-appropriate volume.

2.2.3. K/L mutant *Cebpa* LIC generation

125,000 CD45.2+ E14.5 K/L mutant *Cebpa* fetal liver cells were transplanted into lethally irradiated CD45.1/2+ heterozygous recipients with 50,000 BM helper cells. Upon developing leukemia, mice were culled, their tibia's and femur's dissected and crushed using a pestle and mortar. cKit enrichment was then carried out on the leukemic CBM. LICs used during this present study represent the cKit+ cell fraction from the BM of these transplanted mice (Bereschchenko et al., 2009).

2.2.4. Intravenous tail vein injection

Mice transplanted with LICs were irradiated with a single dose of 520rads, 4 hours prior to being intravenously injected. HSC transplantations were done into lethally irradiated recipients, whereby mice received two doses of 520rads, 4 hours apart. Prior to injection, mice were warmed for 15-20 minutes at 25-30°C. All samples for injection were kept on ice for the duration of the procedure. Mice were restrained and injected whilst conscious with a maximum volume of 200µL using a Terumo 29U insulin syringe, unless otherwise stated. Control mice for LIC transplantations were sub-lethally irradiated and time-matched, but not transplanted.

2.2.5. Drug administration

For administration of drugs via I.P route, a 25 gauge needle was used with a maximum injection volume of 2mL, as per the project license. For oral gavage, disposable flexible needles were used to avoid irritation over a prolonged period of dosing. A maximum oral gavage dosing volume of 100µL/10g was used, as per the project license.

2.3. Computational materials and methods

2.3.1. Bulk RNA-seq data analysis

2.3.1.1. Sample demultiplexing, alignment and feature counting

Bulk RNA-seq samples were sequenced on an Illumina HiSeq4000 (50bp single end reads) and demultiplexed by the Wellcome Trust for Human Genetics, University of Oxford. FASTQ files were inspected using FastQC (v0.10.1; Andrews, 2010) followed by Nextera adapter sequence removal using TrimGalore! with a stringency setting of 3 (v0.4.1; Krueger, 2012). Reads were aligned to the mm9 transcriptome using STAR

(v2.4.2a; Dobin et al., 2013). Unique reads were counted using featureCounts (v1.4.5-p1, Liao et al., 2014) and the UCSC mm9 annotation file. All output files were quality assessed using MultiQC (v0.7, Ewels et al., 2016).

2.3.1.2. Normalisation, principal component analysis and RPKM

For all bulk RNA-seq samples, read counts were imported into R Studio and normalized using the rlogTransformation function in DESeq2 (v1.14.1; Love et al., 2014) with the blind setting set to true. This function log transforms data and normalises gene expression with respect to library size. Principal component analysis (PCA) was carried out on rlogTransformed data for all genes and the quality of each sample was inspected by plotting library size, number of genes detected and percentage mapping against PC1 and PC2 values. PCA was also carried out on the top 500 variable genes to assess unsupervised sample clustering. Reads per Kilobase of transcript per Million mapped reads (RPKM) values were generated using the EdgeR::rpkm function (v2.16.5; Robinson et al., 2010).

2.3.1.3. Supervised heatmaps

Euclidean distance and Wards clustering methods were used to cluster samples according to their expression of known gene sets. Log(RPKM+1) expression values were used as input.

2.3.1.4. Statistical and post-hoc analyses

Differential gene expression analysis was carried out using DESeq2 (v1.14.1; Love et al., 2014). For all datasets, a local fit method was used, and DEGs with an adjusted $p \leq 0.05$ were used for all post-hoc analyses. Gene set enrichment analysis (GSEA)

(v3.0; Subramanian et al., 2005) was used to determine enriched functions. DEGs were ranked by log_2 fold change (Log2FC) and imported into the GSEAPreranked tool. Gene sets for GSEA were taken from either the literature where stated, or from the Molecular Signatures Database (www.software.broadinstitute.org/gsea/msigdb/index.jsp).

Metacore v6.35 (Thomson Reuters, www.portal.genego.com) was used to determine enriched process networks. Ranked DEGs (adjusted $p \leq 0.05$) were used as input for Metacore, which models functionally enriched ontology based on a hypergeometric distribution model. After calculating a *p*-value for all terms within a given ontology, each term is then tested as a separate hypothesis which results in the generation of a q-value. This subsequently provides an estimate of false discovery rate (FDR). All Metacore output displayed in this study have both a $p \leq 0.05$ and FDR$\leq$0.05.

For pathway analysis, the iPathwayGuide platform (Advaita Bioinformatics, www.advaitabio.com) was used. DEGs with an adjusted $p \leq 0.05$ and log2FC$\geq$0.5, $\leq$-0.5 were imported into iPathwayguide. This tool uses impact analysis to infer molecular pathway enrichment (Draghici et al., 2007; Tarca et al., 2009; Khatri et al., 2007), and in doing so generates two probabilities, pORA and pAcc. The first, pORA, is based on a hypergeometric distribution that calculates the likelihood of observing a list of DEGs in a given pathway that is greater than, or equal to, observing one by chance. The second, pAcc, is calculated based on the amount of total accumulation of DEGs measured in a given pathway. The two probabilities are then combined to generate a single *p*-value using Fishers method.

2.3.2. scRNA-seq data analysis

CBM and BL niche cells were FACS isolated and processed from young (~2 months) and aged (~22-24 months) mice separately using the 10X Genomics droplet based sampler. Alignment, quality checking, filtering and analysis of UMI-based scRNA-seq datasets discussed in chapters 4 and 6 was achieved using the following steps.

2.3.2.1. Demultiplexing and alignment

Sequencing of UMI based cDNA libraries from young and aged unfractionated niche cells was carried out using the Illumina HiSeq4000 platform (75bp paired end reads). Sample demultiplexing was completed by the Wellcome Trust Centre for Human Genetics, University of Oxford, and FASTQ files were aligned to the mm10 reference genome using CellRanger (v2.0.0; 10X Genomics). Biological replicates from the same conditions were aggregated using the CellRanger::Aggregate function. This function normalises the number of mapped reads per cell across libraries from different biological samples.

2.3.2.2. Filtering, merging and normalising data

Filtered gene-cell matrices of aggregated CBM and BL samples were imported into R Studio using the Seurat::Read10X function (v2.3.0; Satija et al., 2015). Two separate Seurat objects were created for BL and CBM datasets using the Seurat::CreateSeuratObject function. CBM and BL Seurat objects were then merged using Seurat::MergeSeurat and an initial pre-filtering step was performed whereby cells expressing fewer than 50 genes, and genes expressed in fewer than 3 cells were regressed from the dataset. The merged data was normalised by the total

expression of genes for each cell, multiplied by a scale factor of 10,000, and log-transformed.

2.3.2.3. Additional filtering steps

Mitochondrial gene expression is associated with cells undergoing stress and cell death, and can produce uninteresting sources of gene-variance in scRNA-seq datasets (Ilicic et al., 2016). The percentage of mitochondrial gene expression for each cell was therefore calculated by dividing the expression of mitochondrial genes from each cell (total expression of genes containing the suffix '*Mt-*') by the total expression of all genes. Violin plots displaying total number of genes, UMIs and percentage mitochondrial gene expression for young and aged datasets can be found in figures 2.3.2.3.a and 2.3.2.3.b. Both datasets were filtered using the Seurat::FilterCells function by removing cells that express >5% mitochondrial gene expression and cells with >50 or <6000 expressed genes.

2.3.2.4. Linear dimensional reduction

Highly variable genes were identified using the Seurat::FindVariableGenes function. This calculates the average expression and dispersion for each gene, places these genes into bins, and then calculates a z-score for dispersion within each bin. Data were scaled and linear dimensional reduction was carried out using the Seurat::RunPCA function on variable genes. The appropriate number of PCs to use for clustering in both young and aged datasets was determined using an elbow plot that depicts standard deviation on the Y-axis and PC number on the X-axis (figures 2.3.2.4.a and 2.3.2.4.b).

2.3.2.5. Non-linear dimensional reduction

Based on the elbow plots in figures 2.3.2.4.a and 2.3.2.4.b, non-linear dimensional reduction was carried out on the first 15 PCs for both young and aged niche cell datasets, with a resolution of 0.5 using the Seurat::FindClusters function. tSNE was then run to visualise the datasets in two-dimensional space, identifying a total of 15 (figure 2.3.2.5.a) and 11 clusters (figure 2.3.2.5.b) for young and aged niche datasets, respectively. The Seurat::BuildClusterTree function was used to generate phylogenetic trees constructed in PCA space.

2.3.2.6. Quality checking scRNA-seq datasets

The number of genes and UMIs per cell was visualised on tSNE plots (figures 2.3.2.6.a and 2.3.2.6.b). A central cluster of cells in both aged and young datasets expressed significantly higher levels of genes and UMIs compared to others. The Seurat::AddModuleScore function was used to carry out cell cycle analysis. S/G2M genes were taken from Kowalczyk et al., (2015). This analysis revealed that the central cluster of cells, in addition to displaying high numbers of genes and UMIs, was also highly proliferative (figures 2.3.2.6.c and 2.3.2.6.d).

To ensure that these cells were non-hematopoietic, the expression of the pan-hematopoietic marker *Ptprc* was visualised using the Seurat::FeaturePlot function in young and aged datasets (figures 2.3.2.6.e and 2.3.2.6.f). Very few cells expressed *Ptprc*, suggesting at first that these were non-hematopoietic. However, upon visualising the expression of the erythroid marker *Tfrc* using the Seurat::FeaturePlot function (figures 2.3.2.6.g and 2.3.2.6.h), it was discovered that the highly proliferative central cluster identified in both young and aged datasets overlapped with this marker expression. Based on this analysis, and in conjunction with evidence

from the literature, we concluded that these cells were likely late erythroid progenitors that expressed *Tfrc* but lacked *Ptprc* expression (Dai et al., 2000; Chen et al., 2009; Chao et al., 2015).

2.3.2.7. Regressing hematopoietic populations

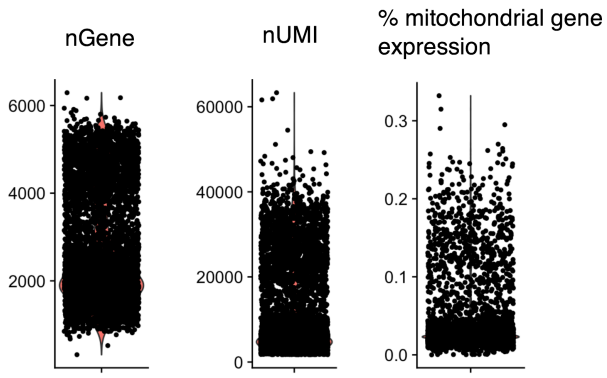
Using the Seurat::SubsetData function, all erythroid progenitor clusters were filtered and a new Seurat object was created. Sections 2.3.2.2 - 2.3.2.4 of this chapter were then repeated. Figures 2.3.2.7.a and 2.3.2.7.b depict the violin plots of genes, UMIs and mitochondrial gene expression per cell from both young and aged datasets, and figures 2.3.2.7.c and 2.3.2.7.d display the elbow plots for selecting an appropriate PC number. Non-linear dimensional reduction was carried out on young and aged datasets using the first 20 and 10 PCs, respectively, with a resolution of 0.2. tSNE was then run to visualise data, identifying a total of 11 clusters for young and 6 clusters for aged niche cells (figures 2.3.2.7.e and 2.3.2.7.f). The number of genes and UMIs per cell after filtering was visualised on separate tSNE plots (figures 2.3.2.7.g and 2.3.2.7.h). There was a uniform distribution of genes and UMIs for all cell types after filtering erythroid progenitors in both young and aged niche cells.

2.3.2.8. Differential gene expression analysis, heatmaps and gene expression plots

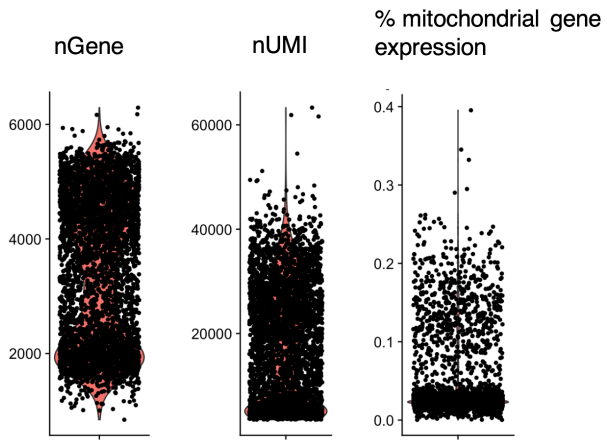
Differential gene expression analysis was carried out using a negative binomial statistical test (Di, 2015). DEGs with an adjusted $p \leq 0.05$ and LogFC$\geq$0.25 were returned and used for subsequent analyses. The top DEGs per cluster were isolated and plotted on a heatmap using the Seurat::DoHeatMap function. Expression of *Pdgfra*, *Lepr* and *Pecam1*, markers of PαS MSCs, LepR+ PV cells and VECs,

respectively, were visualised using the Seurat::FeaturePlot function (see Chapter 4, figure 4.4.1.c and Chapter 6, figure 6.4.1.c).

2.3.2.3.a



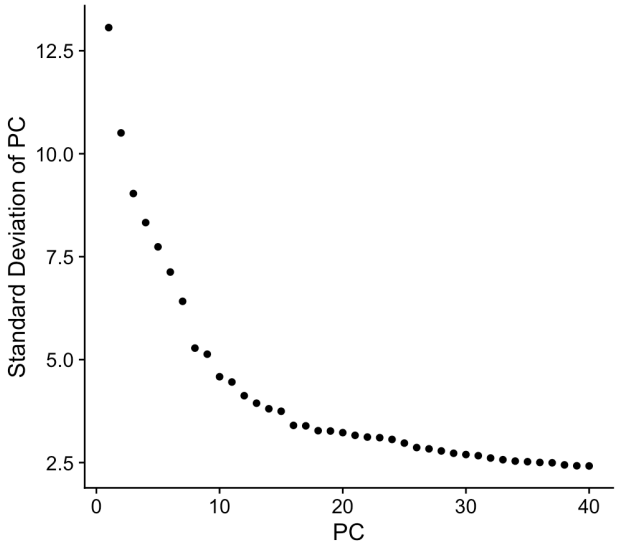
2.3.2.3.b



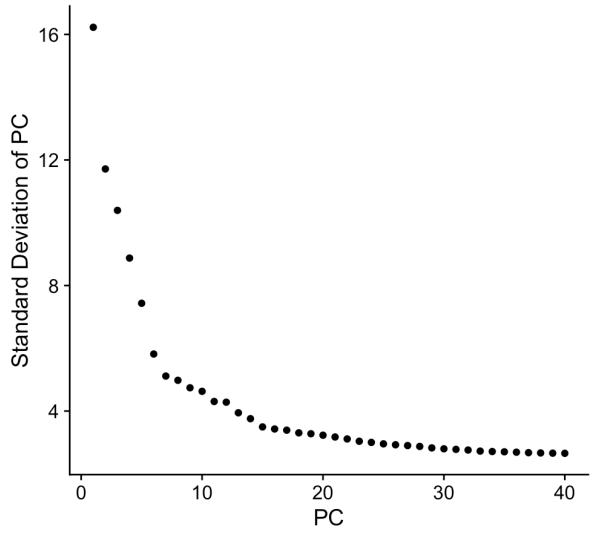
Additional filtering steps

Number of genes (nGene), UMIs and mitochondrial gene expression per cell in young (**2.3.2.3.a**) and aged (**2.3.2.3.b**) niche cells.

2.3.2.4.a



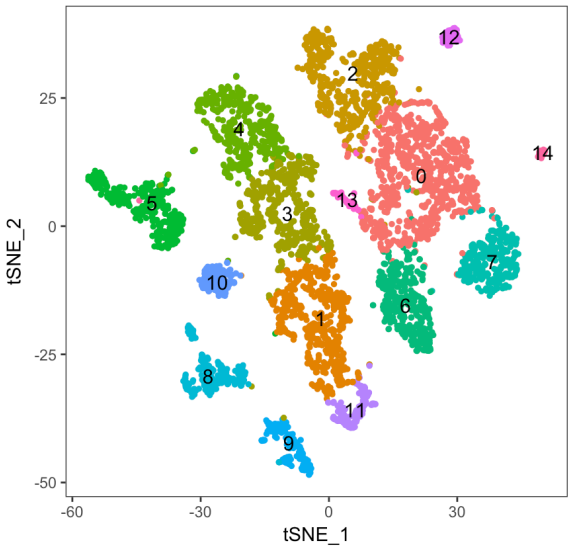
2.3.2.4.b



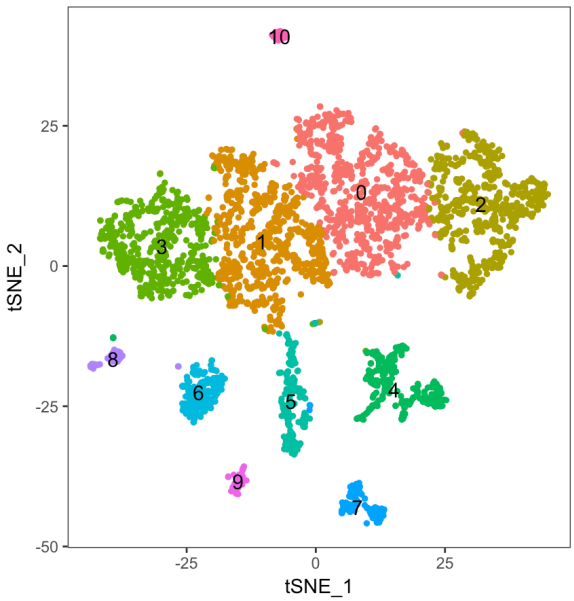
Linear dimensional reduction

Elbow plot depicting standard deviation of principal components 1-40 from young (**2.3.2.4.a**) and aged (**2.3.2.4.b**) datasets

2.3.2.5.a



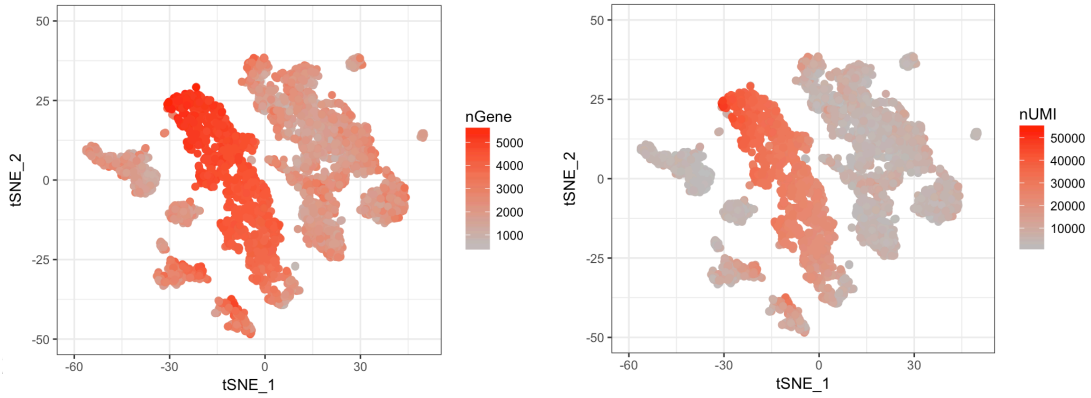
2.3.2.5.b



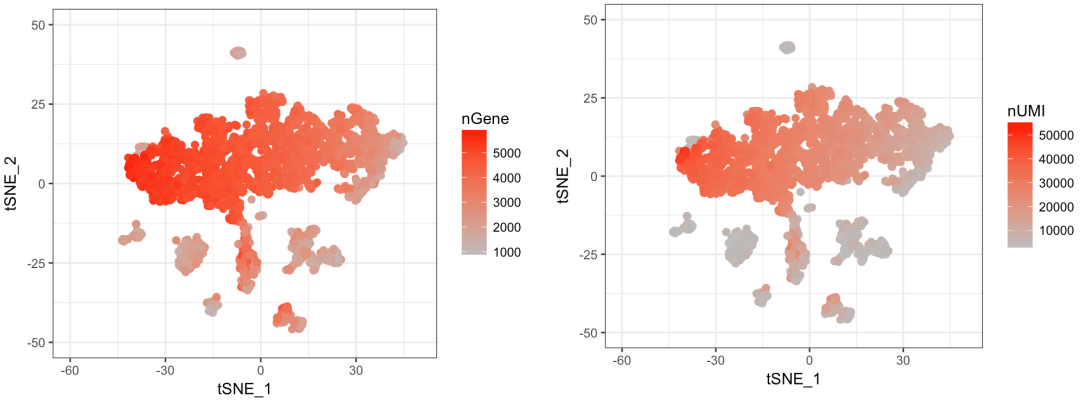
Non-linear dimensional reduction

tSNE plot of non-hematopoietic cell populations prior to quality checking. A total of 15 clusters were identified in young (**2.3.2.5.a**) and 11 clusters in aged (**2.3.2.5.b**) niche cell datasets.

2.3.2.6.a



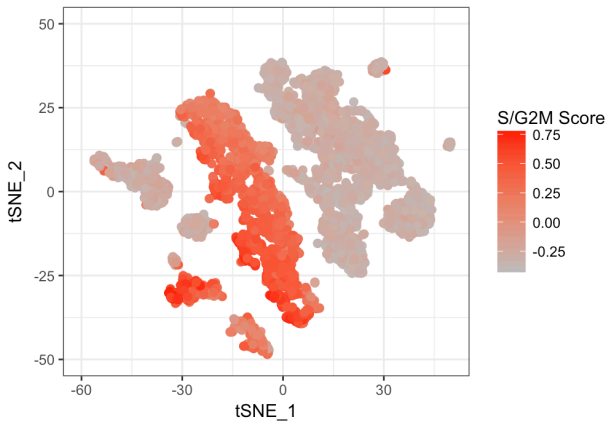
2.3.2.6.b



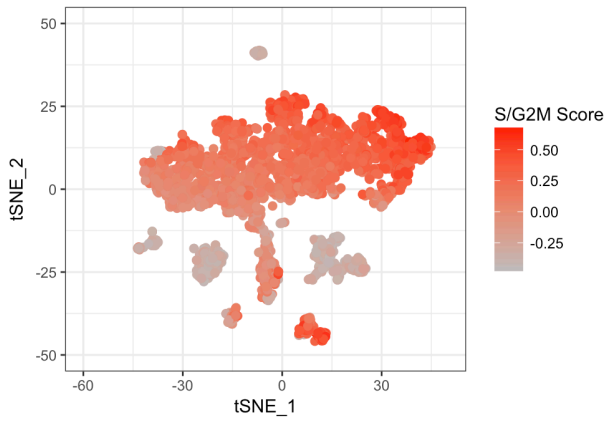
Quality checking scRNA-seq datasets

tSNE plots displaying the number of genes and UMIs per cell from young (**2.3.2.6.a**) and aged (**2.3.2.6.b**) datasets.

2.3.2.6.c



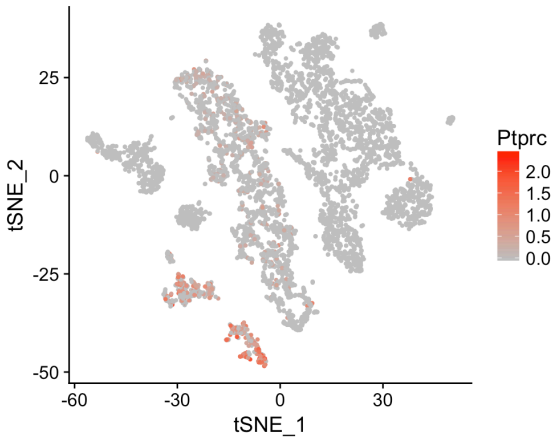
2.3.2.6.d



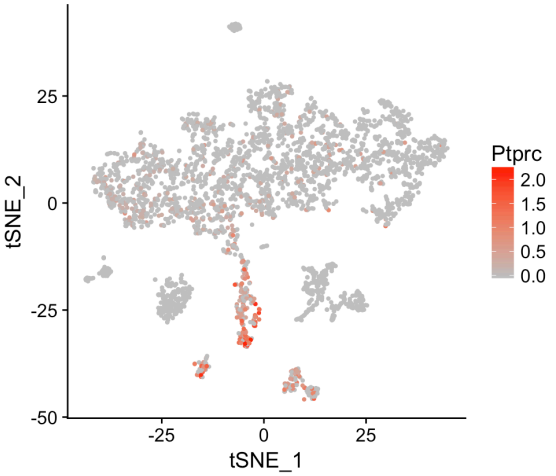
Quality checking scRNA-seq datasets

tSNE plots visualising the expression of S/G2M gene scores in all cells from young (**2.3.2.6.c**) and aged (**2.3.2.6.d**) niche datasets

2.3.2.6.e



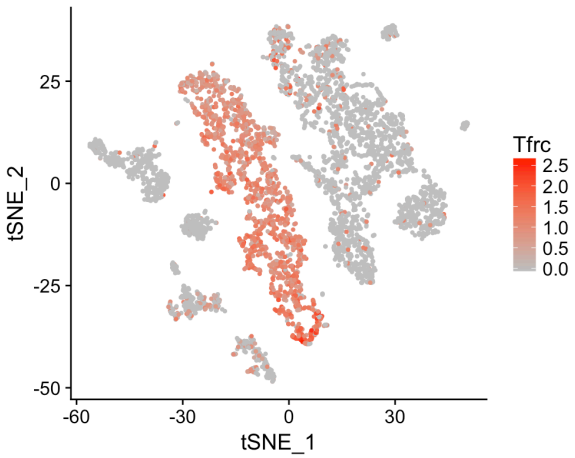
2.3.2.6.f



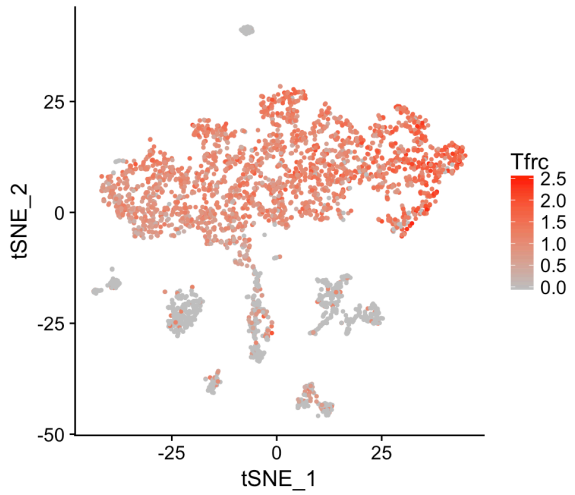
Quality checking scRNA-seq datasets

tSNE plots visualising the normalised expression of *Ptprc* in young (**2.3.2.6.e**) and aged (**2.3.2.6.f**) niche datasets.

2.3.2.6.g



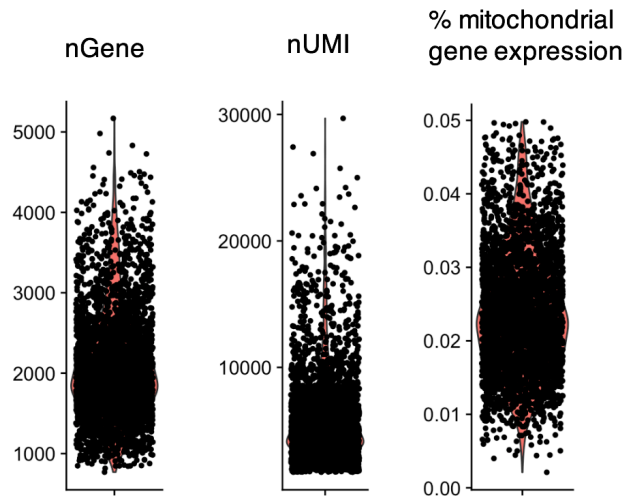
2.3.2.6.h



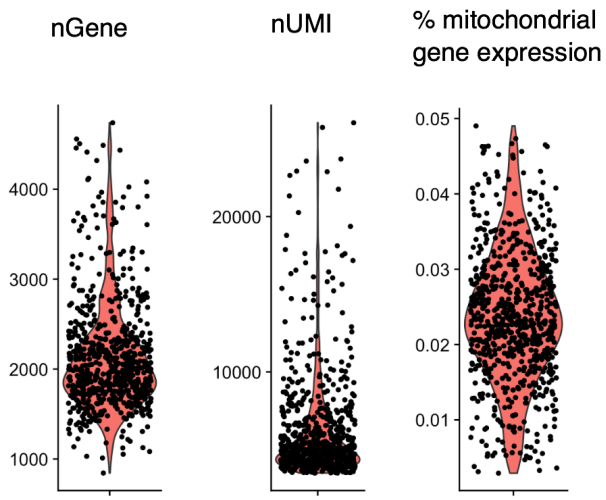
Quality checking scRNA-seq datasets

tSNE plots visualising the normalised expression of *Trfc* in young (**2.3.2.6.g**) and aged (**2.3.2.6.h**) niche datasets.

2.3.2.7.a



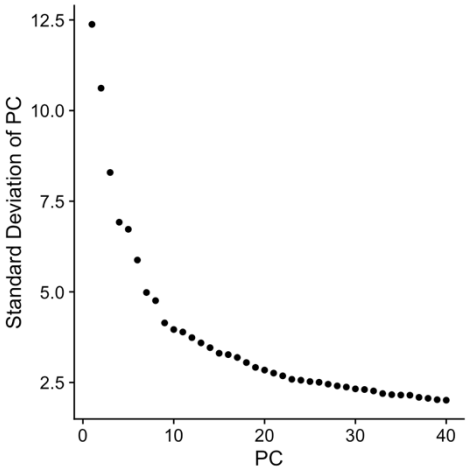
2.3.2.7.b



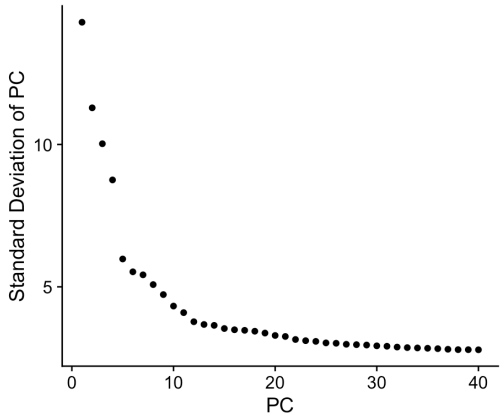
Regressing hematopoietic populations

Number of genes (nGene), UMIs and mitochondrial gene expression per cell from erythroid progenitor filtered datasets in young (**2.3.2.7.a**) and aged (**2.3.2.7.b**) conditions.

2.3.2.7.c



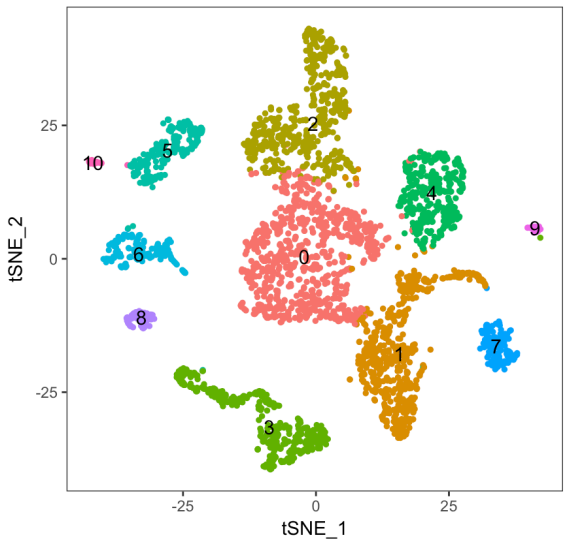
2.3.2.7.d



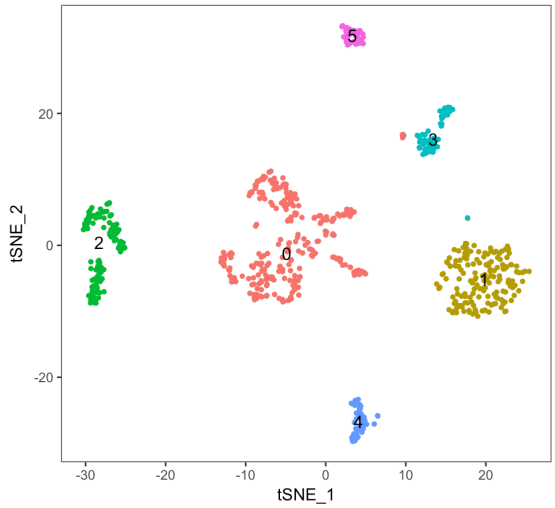
Regressing hematopoietic populations

Elbow plots for determining appropriate PC number after erythroid progenitor filtering in young (**2.3.2.7.c**) and aged (**2.3.2.7.d**) niche datasets.

2.3.2.7.e



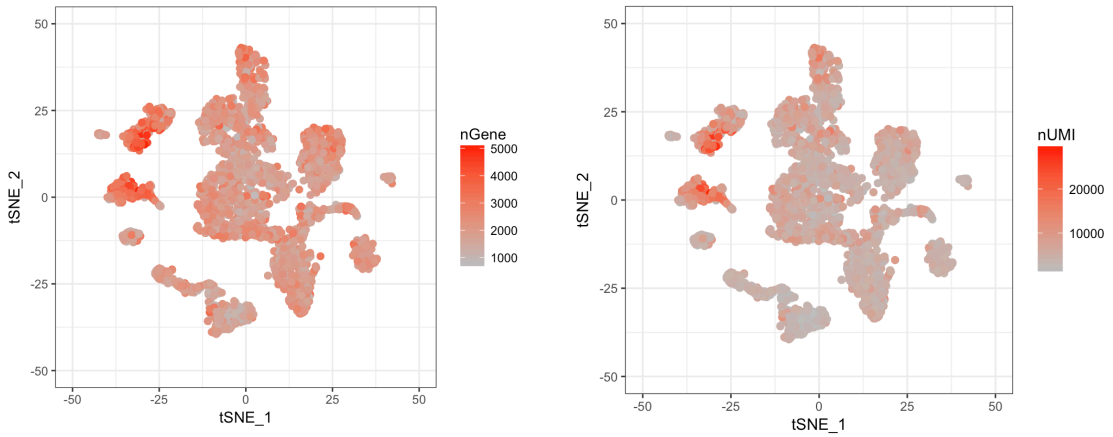
2.3.2.7.f



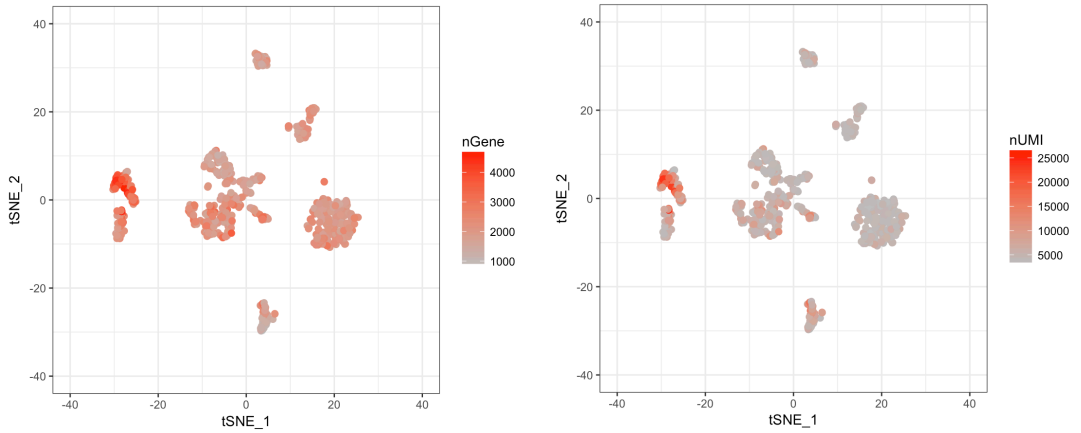
Regressing hematopoietic populations

Final tSNE plot of non-hematopoietic populations after filtering in young (**2.3.2.7.e**) and aged (**2.3.2.7.f**) niche datasets.

2.3.2.7.g



2.3.2.7.h



Regressing hematopoietic populations

tSNE plots displaying the number of genes and UMIs per cell from erythroid-progenitor filtered dataset in young (**2.3.2.7.g**) and aged (**2.3.2.7.h**) conditions.

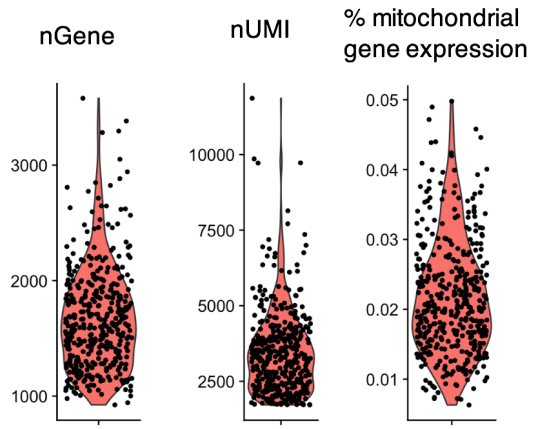
2.3.2.9. Isolation and analysis of vascular endothelial cells

The Seurat::SubsetData function was used to isolate cluster 3 from the young and aged scRNA-seq datasets displayed in 2.3.2.7.e and 2.3.2.7.f, after which, parts 2.3.2.2 - 2.3.2.4 of this chapter were repeated. Figures 2.3.2.9.a and 2.3.2.9.b depict

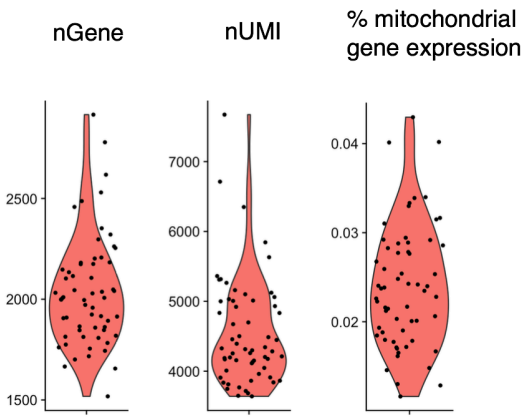
a violin plots of genes, UMIs and mitochondrial gene expression per cell for young and aged cluster 3, respectively. Figure 2.3.2.9.c and 2.3.2.9.d display elbow plots for selecting an appropriate number of PCs. Non-linear dimensional reduction of young VECs was carried with the first 10 PCs using a resolution of 1. Due to the low number of VECs in our aged dataset, non-linear dimensional reduction was instead carried out on the first 5 PCs, changing perplexity to 10 and using a resolution of 1. tSNE was then run on both datasets, identifying a total of 5 clusters in young, and 2 clusters in aged VECs (figures 2.3.2.9.e and 2.3.2.9.f). Differential gene expression analysis using a negative binomial statistical test was carried out to identify cluster-specific genes. DEGs that had an adjusted $p \leq 0.05$ and LogFC$\geq$0.25 were returned.

A negative binomial statistical test was also used to identify genes differentially expressed between *Vcam1* negative and positive clusters with the same parameters. The top 10 DEGs per cluster were isolated and plotted on a heatmap using the Seurat::DoHeatMap function. The Seurat::FeaturePlot was used to visualise cluster-specific genes. Scatterplots comparing healthy VEC subpopulation gene markers and differentially expressed genes in VECs during leukemia were generated to observe whether certain clusters were transcriptionally up- or down-regulated during leukemia. Genes that were expressed in both healthy VEC sub-populations and differentially expressed by VECs at weeks 3 and 4 post-transplantation were identified and visualised using ggplot2.

2.3.2.9.a



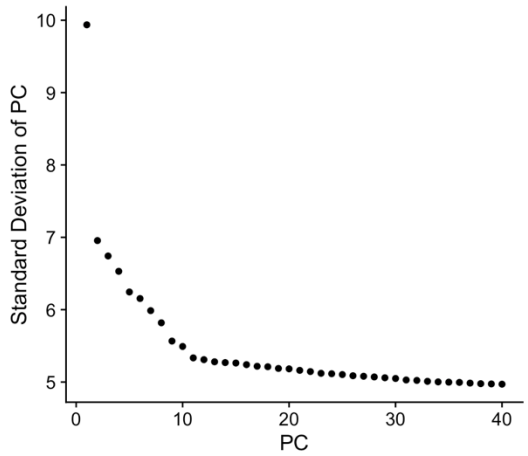
2.3.2.9.b



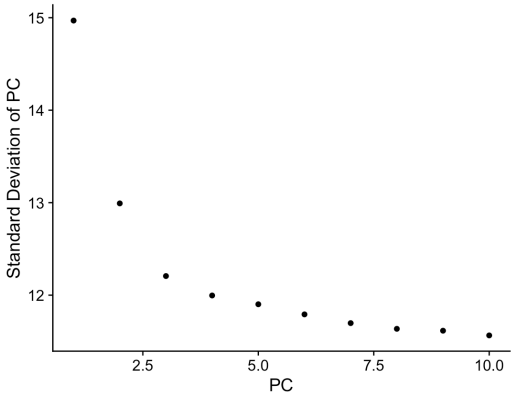
Isolation and analysis of vascular endothelial cells

Number of genes (nGene), UMIs and mitochondrial gene expression per cell from young (**2.3.2.9.a**) and aged (**2.3.2.9.b**) VEC cluster 3 (isolated from total tSNE plots in figures 2.3.2.7.e and 2.3.2.7.f).

2.3.2.9.c



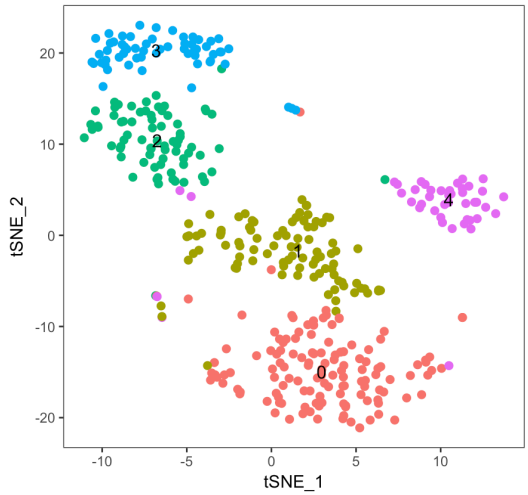
2.3.2.9.d



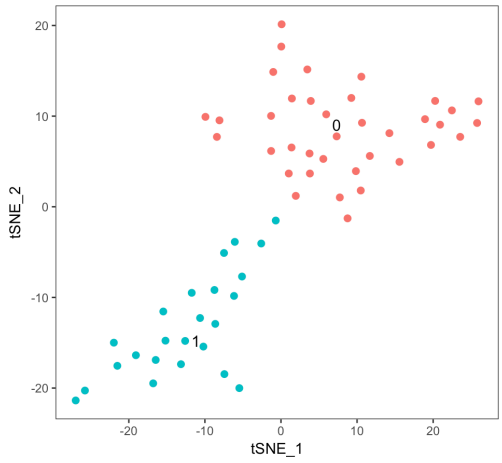
Isolation and analysis of vascular endothelial cells

Elbow plots for determining appropriate PC number in VECs from young (**2.3.2.9.c**) and aged (**2.3.2.9.d**) niche datasets.

2.3.2.9.e



2.3.2.9.f



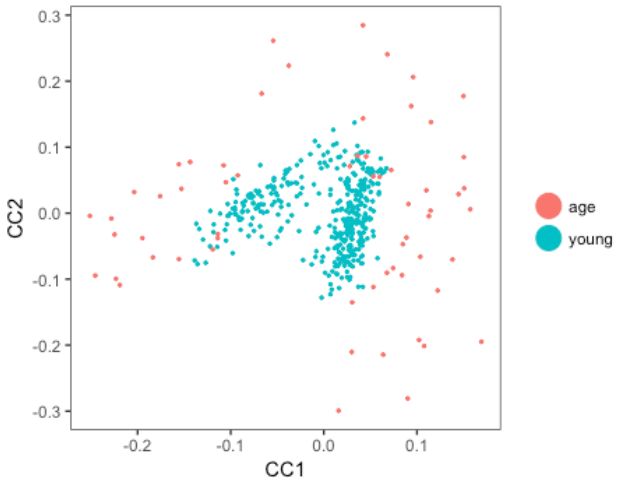
Isolation and analysis of vascular endothelial cells

tSNE plot of *Pecam1* expressing VECs isolated from young (**2.3.2.9.e**) and aged (**2.3.2.9.f**) niche datasets.

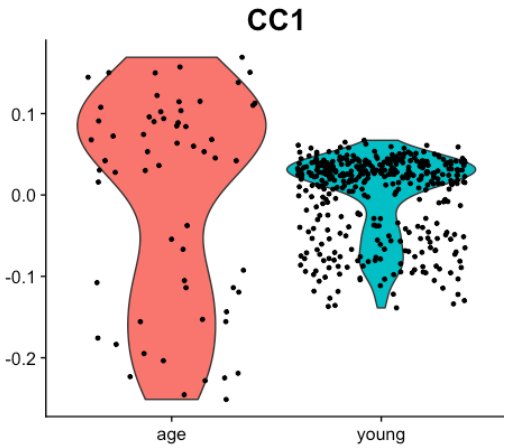
2.3.2.10. Canonical correlation analysis of young and aged VECs

Canonical correlation analysis (CCA) was carried out on VECs isolated from young and aged single cell datasets. VECs were isolated from datasets following the steps described between 2.3.2.2 and 2.3.2.9 of this chapter. After isolation, CCA was run using the Seurat::RunCCA function on the top 1000 variable genes from both young and aged datasets. Figure 2.3.2.10.a illustrates CC1 and CC2 co-ordinates for each cell, and figure 2.3.2.10.b depicts violin plots of CC1 values from all aged and young VECs. A CC dimensional cut off value of 20 was used, based on figure 2.3.2.10.c, and the Seurat::AllignSubspace function was then ran to align cells based on their CC expression value. As depicted in figure 2.3.2.10.d, after alignment, cells shared similar CC values. The Seurat::FindClusters function was then run on the first 20 aligned CC dimensions with a resolution of 0.2.

2.3.2.10.a



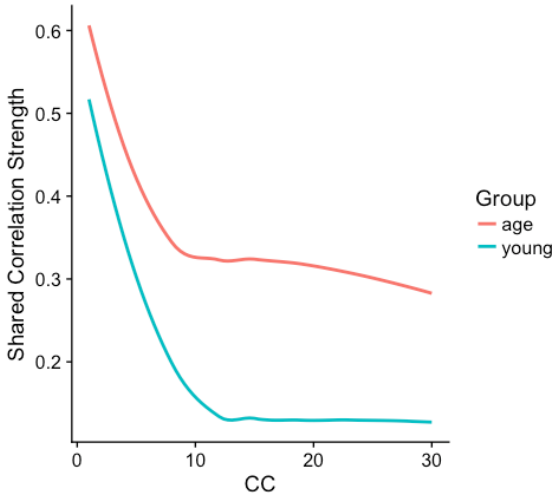
2.3.2.10.b



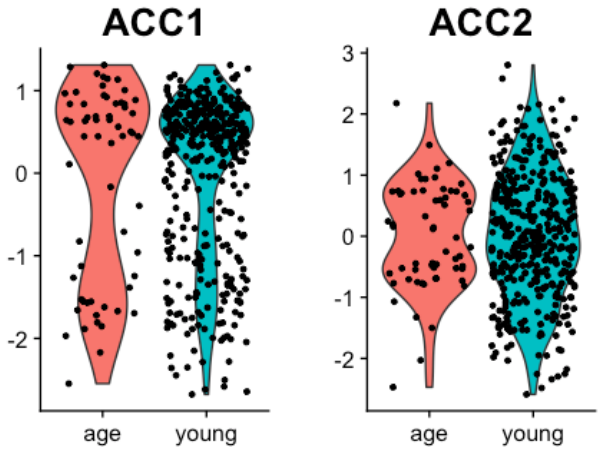
Canonical correlation analysis of young and aged VECs

2.3.2.10.a. CC1 and CC2 values for young and aged VECs after running the Seurat::RunCCA function. **2.3.2.10.b.** Violin plot depicting CC1 values for individual cells in young and aged VECs.

2.3.2.10.c



2.3.2.10.d



Canonical correlation analysis of young and aged VECs

2.3.2.10.c. Shared correlation plot for CC dimensions 1-30 from young and aged VECs before alignment. A cut off of 20 was selected for running the Seurat::AlignSubspace function. **2.3.2.10.d.** Aligned CC1 and CC2 values for individual cells after running CCA alignment.

Chapter 3

The immunophenotypic and functional consequences of leukemia on endogenous hematopoiesis and the BM niche

3.1. Introduction and aims

Hematopoietic failure during AML is predicated on the assumption that malignant cell crowding within the BM causes functioning HSPCs to become physically displaced. There is now, however, evidence to suggest that leukemic cells impair normal hematopoiesis through both direct and indirect mechanisms, suggesting that processes unrelated to displacement are at play during leukemogenesis.

Studies carried out in the 1970's demonstrated that the co-culture of leukemic and non-leukemic cells resulted in impaired hematopoietic function and output (Broxymeyer et al., 1978; Miller et al., 1976). These findings were amongst the first to demonstrate that both leukemia-derived secreted factors and direct cell-cell contact was sufficient to disrupt normal hematopoiesis. More recently, AML xenograft studies revealed that normal HSC differentiation becomes impeded during leukemogenesis (Miraki-Moud et al., 2013). Moreover, the lack of correlation between clinical BM blast burden and cytopenia onset suggests that functioning HSPCs remain in the BM regardless of leukemic infiltration (Rauch et al., 2016). Collectively, these findings imply that molecular interactions between leukemic and non-leukemic BM cells precede hematopoietic failure, and thus likely contribute towards BM failure, and the inevitable onset of symptoms.

BM niches are essential for normal hematopoiesis, and are also heavily relied upon by leukemic cells. This was highlighted by Sipkins et al., (2005), who demonstrated that leukemic cells seek out important endothelial-derived ligands in order to migrate into the BM. This was later complemented by the discovery that malignant cells also express high levels of SCF, which leads to the sequestration and impairment of normal HSPCs (Colmone et al., 2008). Taken together, these findings indicate that interactions between leukemic and BM niche populations might also

precede hematopoietic failure, and may therefore also play both an important role in disease progression and hematopoietic disruption.

Despite this wealth of information, it is yet to be established exactly which cell populations in the hematopoietic hierarchy are perturbed during leukemogenesis, at what point during leukemic development this occurs, and whether this leads to reduced cellular functionality. Therefore, in order to study the effects of a progressing leukemia on both hematopoietic and non-hematopoietic populations in the BM, the following aims were proposed:

1. Develop a robust, kinetically tractable model of AML that allows for the simultaneous analysis of leukemic and non-leukemic cell types.
2. Assess the immunophenotypic composition of endogenous HSPCs during different stages of leukemia development.
3. Investigate the functional changes to endogenous HSCs during different stages of leukemia using long term *in vivo* transplantation assays.
4. Explore the changes in progenitor functionality using *in vitro* colony forming assays.
5. Assess the immunophenotypic composition of the CBM and BL niche cells at the different stages of leukemia.

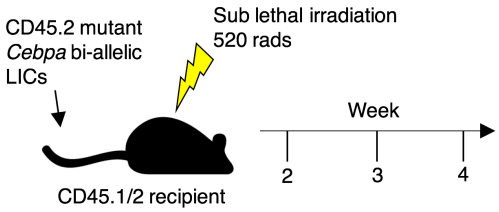
3.2. The generation of a murine AML transplantation model

To assess the impact of leukemic development on endogenous BM hematopoiesis, a transplantation model was developed that used LICs derived from K/L *Cebpa* mutant fetal-liver transplanted mice (Bereshchenko et al., 2009). A total of 25,000 K/L mutant *Cebpa* KIT enriched CD45.2+ LICs were transplanted intravenously into sub-lethally irradiated (520 rads) CD45.1/2+ recipient mice (figure 3.2.a). After 2, 3

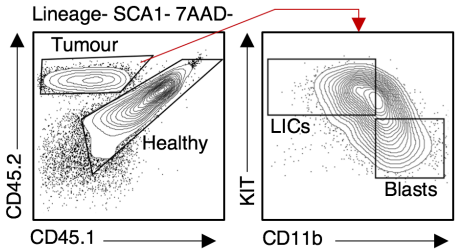
and 4 weeks post-transplantation, recipient mice were euthanized and assessed for BM and spleen leukemic burden. The differential CD45 allotype between leukemic (CD45.2) and recipient (CD45.1/2) cell populations was leveraged during flow cytometric analyses in order to discriminate malignant from normal (figure 3.2.b, left panel). Moreover, the cell surface markers KIT and CD11b, as previously described by Bereshchenko et al., (2009) and Kirstetter et al., (2008), were used to define LICs and blasts, respectively (figure 3.2.b, right panel).

After 2 weeks, total leukemic burden represented only a fraction of total singlets in the BM (10±8%) and spleen (29±17%) (figure 3.2.c). Of note, the difference in BM and spleen leukemic burden at this time point was approximately 3 fold, suggesting that the spleen was likely the primary site of LIC infiltration following transplantation (figure 3.2.d). By week 3, leukemic burden exceeded the endogenous cell frequency in both the BM and spleen, accounting for 72±23% and 83±7% of live singlets, respectively. There was also a 1.3 and 1.4 fold reduction in the proportion of LICs as a percentage of the total tumour burden in both the BM and spleen at week 3, respectively. This reduction in LIC frequency paralleled the emergence of CD11b+ blasts, which exhibited a continued expansion into the final time point of this model. After 4 weeks, leukemic cells comprised 93±1.5% and 84±5.3% of live singlets in the BM and spleen, respectively.

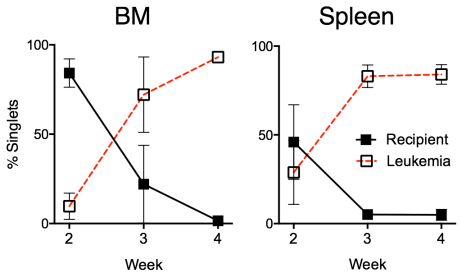
3.2.a



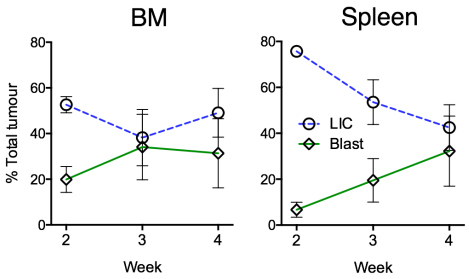
3.2.b



3.2.c



3.2.d



The generation of a murine AML transplantation model

3.2.a. Graphical depiction of the leukemia transplantation model. Briefly, 25,000 KIT enriched mutant bi-allelic *Cebpa* LICs (CD45.2) were transplanted into sub-lethally irradiated recipients (CD45.1/2). After 2, 3 and 4 weeks post-transplantation, various analyses were performed on the bones, spleen and blood of euthanized mice. **3.2.b.** Flow cytometry gating strategy used to determine leukemic burden and LIC/blast frequencies. **3.2.c.** Total leukemic burden in the BM and spleen during disease as a % of total singlets. Mean±SD, N=6 from two experiments. **3.2.d.** Frequency of LICs and blasts over the time course of leukemic development. Mean±SD, N=6 from two experiments.

3.2.1. Leukemic recipients experienced white blood cell infiltration, anemia and loss of morphological heterogeneity

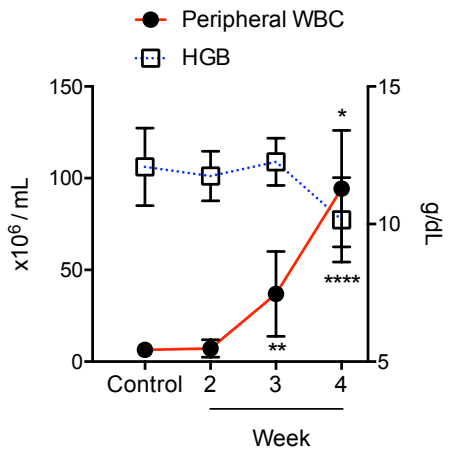
Peripheral white blood cell (WBC) count is measured clinically in order to evaluate patient status before, during and after chemotherapy treatment. Therefore, the WBC count was measured in non-transplanted, sub-lethally irradiated control mice as well

as leukemia-transplanted mice at weeks 2, 3 and 4 (figure 3.2.1.a, left Y-axis). Control and week 2 transplanted mice exhibited a statistically comparable peripheral WBC count (7.2±4.9x10^6/mL vs. 6.4±4.7x10^6/mL, $p>0.05$), which reflected the low level of total tumour burden and CD11b+ AML blast frequency in the BM and spleen at this time point (figures 3.2.1.a, 3.2.c and 3.2.d). Peripheral WBC increased significantly after 3 weeks (37±19x10^6/mL, $p\leq0.005$), and continued to rise in week 4 (94±34x10^6/mL, $p\leq0.0001$).

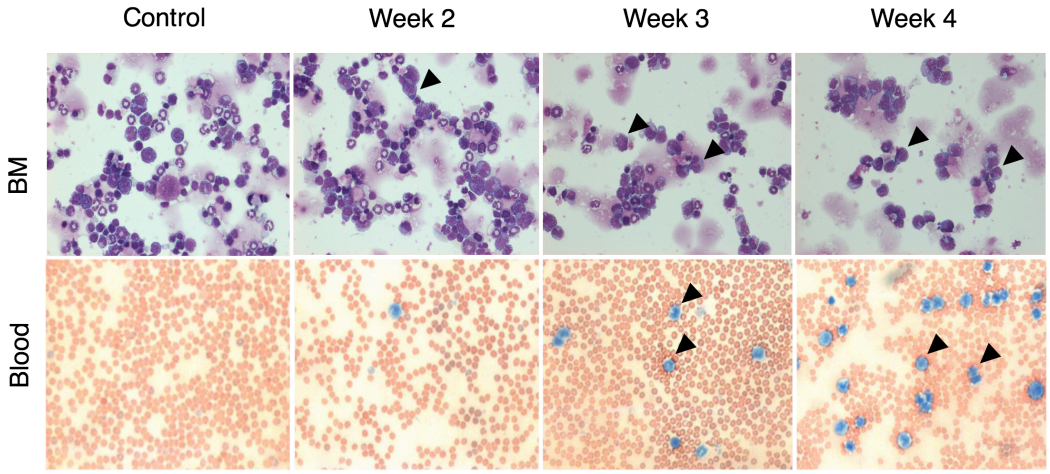
Erythrocytes contain hemoglobin (HGB), which is measured clinically to infer anemic onset in AML patients. The levels of HGB were measured at each time point of leukemic development, and are illustrated in figure 3.2.1.a, right Y-axis. HGB levels in the first 2 weeks remained comparable to control (11.7±0.9g/dL vs. 12±1.3g/dL, $p>0.05$), which also continued into week 3 (12±0.9g/dL vs. 12±1.3g/dL, $p>0.05$). After 4 weeks, recipients began experiencing a statistically significant decline in HGB levels when compared to control (10±1.6g/dL vs. 12±1.3g/dL, $p\leq0.05$), equating clinically to anemia. The time taken to reach this symptoms onset likely reflects the >40 day life span of terminally differentiated mouse erythrocytes, but also implied that BM erythroid progenitor populations were being actively disrupted relatively early on in leukemic development.

Morphologically, there was a time-dependent increase in peripheral blast infiltration, as illustrated in 3.2.1.b, top panel. This was also accompanied by a progressive loss of normal BM heterogeneity and visible increase blast infiltration, confirming the observations made in figures 3.2.1.b and 3.2.c.

3.2.1.a



3.2.1.b



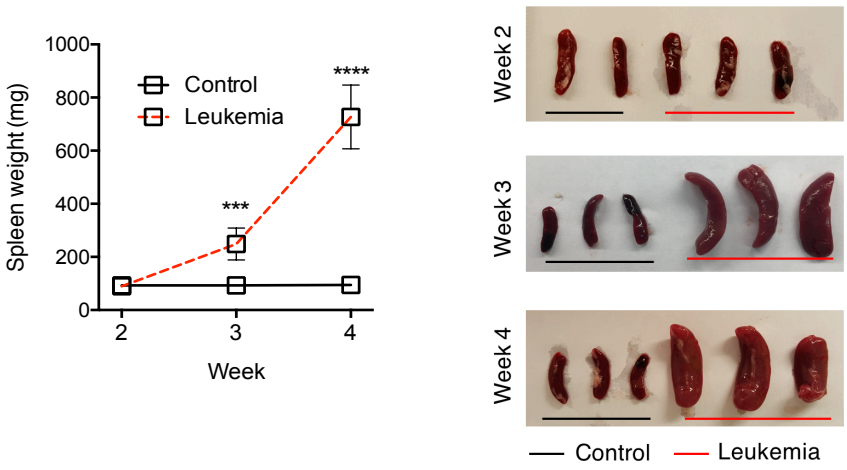
Leukemic recipients experienced white blood cell infiltration, anemia and loss of morphological heterogeneity

3.2.1.a. Peripheral WBC counts and HGB levels. A two-tailed unpaired *t*-test was used to determine significance, comparing leukemia-transplanted mice to non-transplanted control mice (*$p \leq 0.05$,**$p \leq 0.005$, ****$p \leq 0.0001$). Mean±SD, N=6-9 from two experiments. **3.2.1.b.** Cytospin and blood smear images from control and leukemic recipients (black arrows indicate blast cells).

3.2.2. Leukemic recipients experienced splenomegaly

Splenomegaly is a common side effect experienced by AML patients, and is caused by leukemic blast infiltration in the spleen. Leukemia transplanted recipients did not experience splenomegaly after 2 weeks, exhibiting comparable spleen weights to control mice (92±19mg vs 90±18mg, $p>0.05$). By week 3, leukemic mice presented with a statistically significant increase in spleen weight when compared to controls (93±12mg vs. 249±67mg, $p\leq0.001$), evidenced also as a visible increase in size (figure 3.2.2.b, middle panel). After 4 weeks, leukemic spleens continued to increase in weight (95±12mg vs. 727±118mg, $p\leq0.0001$) and size (figure 3.2.2.b, bottom panel). The point at which splenomegaly occurred, coincided with the emergence of CD11b+ leukemic blasts within both the BM, spleen (figure 3.2.d) and periphery (figure 3.2.1.a).

3.2.2.a **3.2.2.b**



Leukemic recipients experienced splenomegaly

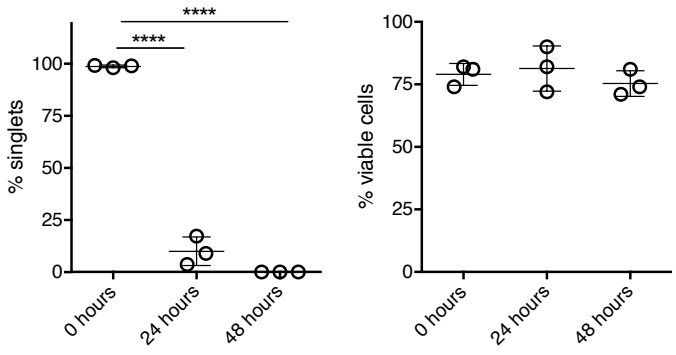
3.2.2.a. Spleen weight (mg) over the time course of the disease. A two-tailed unpaired *t*-test was used to determine significance, comparing leukemia-transplanted mice to time-matched, non-transplanted, sub-lethally irradiated control mice (***$p \leq 0.001$, ****$p \leq 0.0001$). Mean±SD, N=6 from two experiments. **3.2.2.b.** Spleen images from mice at different time points of disease progression. Red lines identify spleens from leukemic mice, black lines define non-transplanted control mice.

3.2.3. LICs lost their engraftment potential after *in vitro* culture

The leukemogenic capacity of LICs was assessed by culturing LICs in liquid media containing the HSPC supportive factors IL-3, IL-6 and SCF (Ogawa et al., 1997; Holyoake et al., 1996) for 0, 24 or 48 hours. Following culture, LICs were transplanted into sub-lethally irradiated (520 rads) mice and leukemic engraftment was measured 4 weeks post-transplantation. Figures 3.2.3.a and 3.2.3.b depict leukemic engraftment as a percentage of live singlets, and cellular viability as a percentage of total cells, respectively.

Culturing LICs in HSPC supportive media for 24 hours resulted in significantly lower levels of leukemic engraftment when compared to 0 hour control (10±9% vs. 98.7±0.6%, $p \leq 0.0001$), and despite cells remaining viable (81±9% vs. 79±4% vs, $p > 0.05$). Leukemogenecity decreased further after 48 hours (0.008±0.003% vs. 98.7±0.6%, $p \leq 0.0001$), again despite normal levels of viability (75±5% vs. 79±4%, $p > 0.05$). Collectively, these findings suggested that the factors normally supportive of HSPCs were unable to maintain the leukemogenicity of LICs in this model.

3.2.3.a **3.2.3.b**



LICs lost their engraftment potential after *in vitro* culture

3.2.3.a. Recipient BM leukemic burden as a % of total BM singlets after four weeks post-transplantation of *in vitro* cultured LICs. LICs were cultured in IL-3, IL-6 and SCF for 0, 24 or 48 hours and were transplanted into sub-lethally irradiated mice. **3.2.3.b.** Viability of cultured cells as a % of total cell number, determined using trypan blue solution. Mean±SD, N=3 from one experiment. A two-tailed unpaired *t*-test was used to determine significance, comparing 24h and 48h time points to 0h controls ($^{****}p \leq 0.0001$).

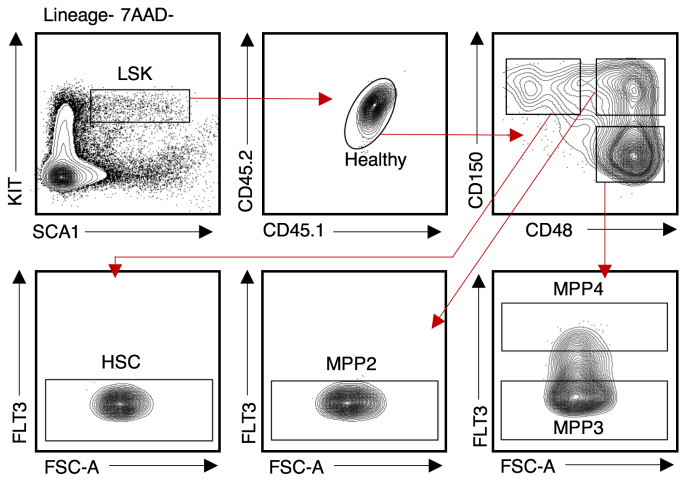
3.3. Immunophenotypic frequency of endogenous BM HSCs, MPPs and myeloerythroid progenitors during leukemia

Given that the symptoms of AML, i.e. anemia, thrombocytopenia, neutropenia, are driven by a lack of normal BM HSPCs, the immunophenotypic frequency of these cell types during leukemic development was assessed. The frequency of BM HSCs, MPPs and myeloerythroid progenitors were determined at weeks 2, 3 and 4 post-transplantation, and were compared to time-matched, non-transplanted, sub-lethally irradiated control mice. Table 3.3.a outlines the immunophenotypic definitions used to discriminate HSC, MPP and myeloerythroid progenitors, and figures 3.3.b and 3.3.c illustrate the flow cytometry gating strategies used.

3.3.a

Cell Type	*Cell surface marker*	*Citation*
HSC	LSK CD150+CD48-FLT3-	Wilson et al., 2008
MPP2	LSK CD150+ CD48+ FLT3-	Wilson et al., 2008
MPP3	LSK CD150-CD48+FLT3-	Wilson et al., 2008
MPP4	LSK CD150-CD48+FLT3^{hi}	Wilson et al., 2008
MkP	LK CD150+ CD41+	Pronk et al., 2007
pMegE	LK CD41- CD16/32- CD150+ CD105-	Pronk et al., 2007
pCFUE	LK CD41- CD16/32- CD105+ CD150+	Pronk et al., 2007
CFUE	LK CD41- CD16/32- CD150- CD105+	Pronk et al., 2007
pGM	LK CD41- CD16/32- CD150- CD150-	Pronk et al., 2007
GMP	LK CD41-CD150- CD16/32+	Pronk et al., 2007

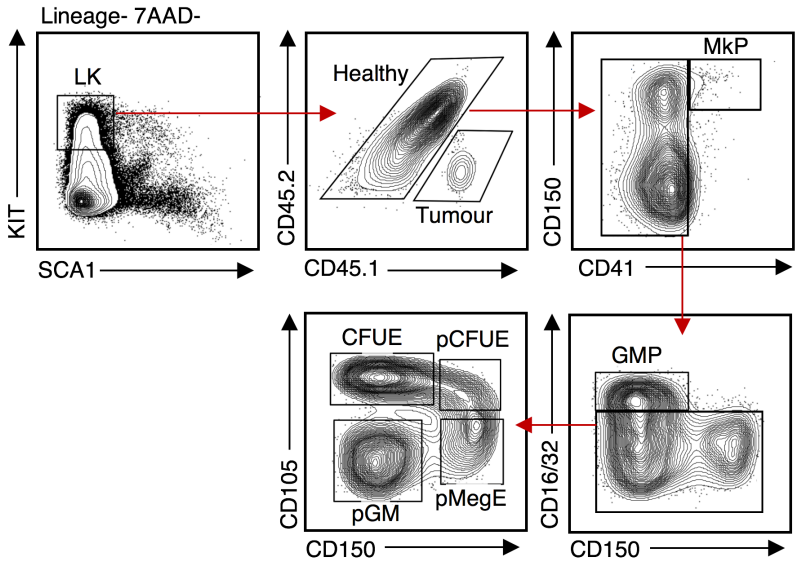
3.3.b



Immunophenotypic frequency of endogenous BM HSCs, MPPs and myeloerythroid progenitors during leukemia

3.3.a. Table outlining the immunophenotypic definitions used to discriminate BM HSC, MPP and myeloerythroid progenitors. **3.3.b.** BM HSC and MPP gating strategies used for flow cytometry analyses. This strategy enabled for the identification of healthy vs. leukemic (CD45.1/2 vs. CD45.2), HSC, MPP2, MPP3 and MPP4 populations.

3.3.c



Immunophenotypic frequency of endogenous BM HSCs, MPPs and myeloerythroid progenitors during leukemia

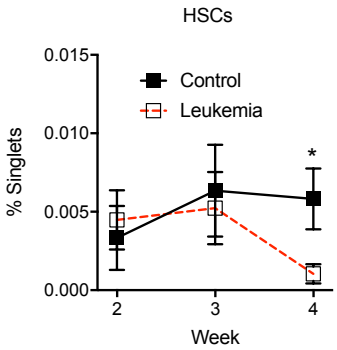
3.3.c. BM myeloerythroid progenitor gating strategies used for flow cytometry analyses. This strategy enabled for the identification of healthy vs. leukemic (CD45.1 vs. CD45.2), MkP, GMP, pGM, pCFUE, CFUE and pMegE progenitors.

3.3.1. Immunophenotypic frequency of endogenous BM HSCs and MPPs during leukemia

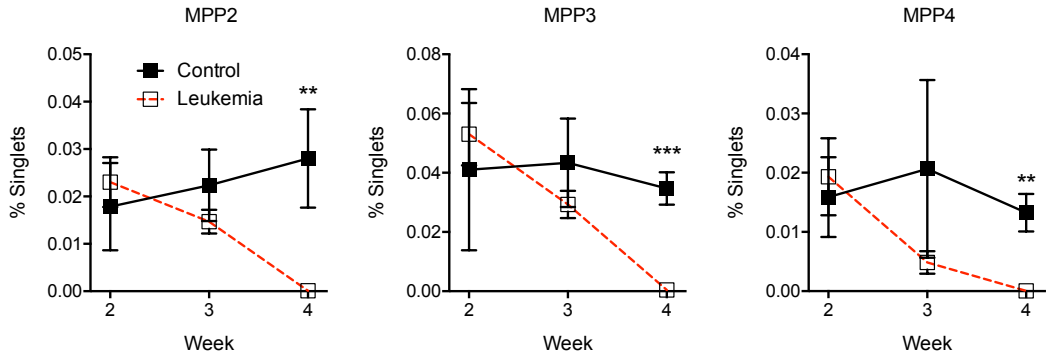
Figures 3.3.1.a and 3.3.1.b illustrate the frequencies of endogenous HSC and MPP populations during leukemic development. As a percentage of live singlets, the frequency of endogenous HSCs after 2 weeks of leukemic development remained comparable to controls (0.004±0.002% vs. 0.003±0.002%, $p>0.05$). This was also true of MPP2 (0.023±0.005% vs. 0.018±0.009%, $p>0.05$), MPP3 (0.053±0.01% vs. 0.041±0.03%, $p>0.05$) and MPP4 (0.019±0.007% vs. 0.016±0.007%, $p>0.05$) populations.

Remarkably, HSC (0.005±0.002% vs. 0.006±0.003%, $p>0.05$), MPP2 (0.015±0.003% vs. 0.02±0.008%, $p>0.05$) and MPP3 (0.029±0.005% vs. 0.043±0.015%, $p>0.05$) were further maintained in frequency after 3 weeks of this model, despite the leukemic burden exceeding >50% of total BM singlets (figure 3.2.c). Although not statistically significant, MPP4 frequency at week 3 was marginally reduced in two out of the three mice analysed (0.005±0.002% vs. 0.02±0.015%, $p>0.05$). By the final time point, the frequencies of HSC (0.001±0.0006% vs. 0.006±0.002%, $p\leq0.05$), MPP2 (0.0001±0% vs. 0.028±0.01%, $p\leq0.01$), MPP3 (0.0004±0.0004% vs. 0.035±0.006%, $p\leq0.001$) and MPP4 (0±0% vs. 0.013±0.003%, $p\leq0.01$) were significantly below that of controls.

3.3.1.a



3.3.1.b



Immunophenotypic frequency of endogenous BM HSCs and MPPs during leukemia

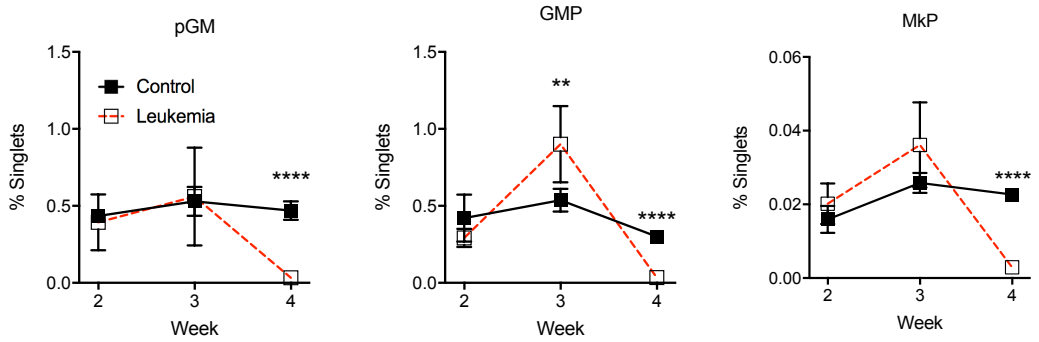
3.3.1.a. Endogenous HSC frequency as a % of BM singlets at weeks 2, 3 and 4 of leukemic development. Mean±SD, N=3-6 from two experiments. **3.3.1.b.** Endogenous MPP2, MPP3 and MPP4 frequency as a % of BM singlets at weeks 2, 3 and 4 of leukemic development. Mean±SD, N=3 from one experiment. A two-tailed unpaired *t*-test was used to determine significance, comparing leukemia-transplanted mice to time-match, non-transplanted, sub-lethally irradiated control mice (*$p \leq 0.05$, **$p \leq 0.01$, ***$p \leq 0.001$).

3.3.2. Immunophenotypic frequency of endogenous BM myeloerythroid progenitors during leukemia

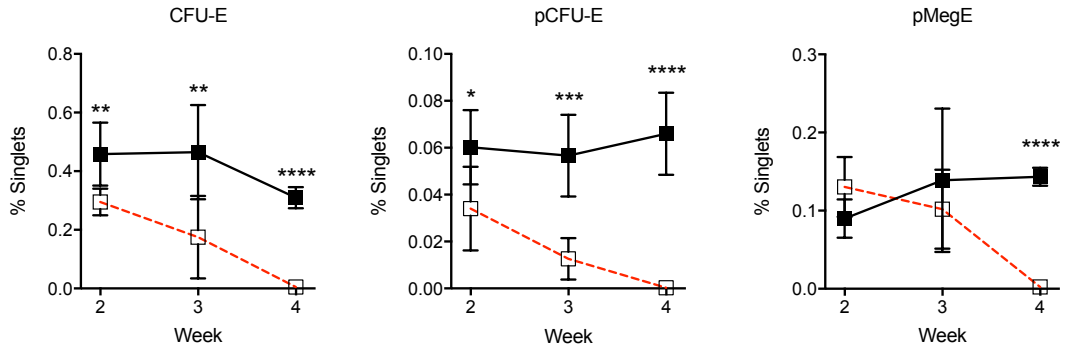
Figures 3.3.2.a and 3.3.2.b depict the frequencies of endogenous BM myeloid and erythroid progenitors as a percentage of BM singlets at weeks 2, 3 and 4 of leukemic development. The pGM (0.39±0.18%, vs. 0.44±0.04, $p>0.05$) and GMP (0.29±0.06% vs. 0.42±0.15%, $p>0.05$) myeloid progenitor populations remained comparable to controls after 2 weeks. In contrast, the frequencies of pCFUE (0.03±0.02% vs. 0.06±0.16%, $p\leq0.05$) and CFUE (0.3±0.045% vs. 0.46±0.1%, $p\leq0.05$) were significantly decreased. MkP (0.020±0.014% vs. 0.016±0.009%, $p>0.05$) and pMegE (0.13±0.04% vs. 0.09±0.02%, $p>0.05$) remained normal.

By week 3, the frequency of GMPs increased significantly (0.90±0.25% vs. 0.54±0.07%, $p\leq0.01$), whereas the CFUE (0.18±0.14% vs. 0.47±0.16%, $p\leq0.01$) and pCFUE (0.013±0.009% vs. 0.057±0.017%, $p\leq0.001$) continued to decline. After 4 weeks, the BM was devoid of endogenous myeloerythroid progenitor populations.

3.3.2.a **3.3.2.c**



3.3.2.b



Immunophenotypic frequency of endogenous BM myeloerythroid progenitors during leukemia

3.3.2.a. Endogenous pGM, GMP, **3.3.2.b.** CFUE, pCFUE, pMegE and **3.3.2.c** MkP frequencies as a % of BM singlets. Mean±SD, N=3-6 from two experiments. A two-tailed unpaired *t*-test was used to determine significance comparing leukemia-transplanted mice to non-transplanted, time-matched, sub-lethally irradiated control mice (*$p \leq 0.05$, **$p \leq 0.01$, ***$p \leq 0.001$, ****$p \leq 0.0001$).

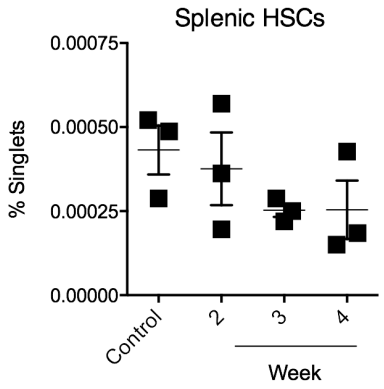
3.3.3. Immunophenotypic frequency of endogenous splenic HSCs during leukemia

HSC frequency was depleted only at the terminal stages of leukemic development (figure 3.3.1.a), implying that these cells remained largely unaffected despite a rapidly expanding leukemia. Splenic extramedullary hematopoiesis occurs when the

BM becomes unable to support normal cellular function, and is a common feature amongst hematological disorders. Therefore, to evaluate whether HSCs left the BM during leukemic development, the frequency of SLAM HSCs within the spleen of non-transplanted and transplanted mice at weeks 2, 3 and 4 was assessed.

In non-transplanted control mice, the frequency of HSCs as a percentage of live singlets in the spleen was ~10-fold less than in the BM (0.0004±0.0001% vs. 0.006±0.003%; figures 3.3.1.a and 3.3.3.a). The frequency of splenic HSCs remained statistically comparable (p>0.05) throughout leukemic development, which suggested that the spleen did not act as an extramedullary site for hematopoiesis at any point during this model.

3.3.3.a



Immunophenotypic frequency of endogenous splenic HSCs during leukemia

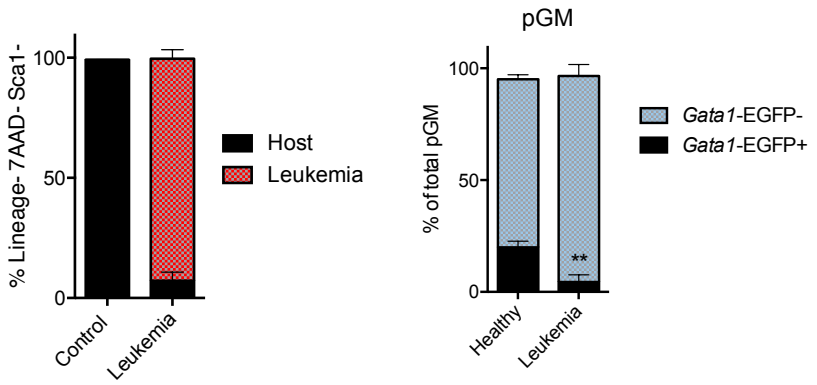
3.3.3.a. Frequency of endogenous splenic HSCs as a % of splenic singlets from recipients transplanted with leukemia for 2, 3 and 4 weeks. Mean±SD, N=3 from one experiment. A two-tailed unpaired *t*-test was used to determine significance, comparing leukemia-transplanted mice at each time point to non-transplanted, sub-lethally irradiated control mice.

3.3.4. Immunophenotypic frequency of *Gata1*-EGFP expressing BM pGM progenitors after exposure to leukemia

Gata1 expression defines a subpopulation of pGM progenitors that are committed towards generating erythrocytes, basophils, mast cells and eosinophils (Drissen et al., 2016, see Chapter 1, figure 1.1.3.a). There was a consistent decrease in the frequency of endogenous BM pCFUE and CFUE erythroid progenitors populations throughout leukemic development (figure 3.3.2.b). Therefore, to determine if this effect was also measurable in upstream progenitors, the proportional change in *Gata1* expressing pGMs was assessed during leukemia. To achieve this, a cohort of CD45.1/2+ *Gata1*-EGFP mice were sub-lethally irradiated (520 rads) and transplanted with 25,000 KIT+ LICs. After three weeks, mice were euthanized and the proportion of *Gata1*-EGFP expressing BM pGMs was studied by flow cytometry.

In non-transplanted, time-matched, sub-lethally irradiated control mice, 19±2.8% of total pGM progenitors were identified as *Gata1*-EGFP+ (figure 3.3.4.b), which was consistent with previous reports (Drissen et al., 2016). As illustrated in figure 3.3.4.b, *Gata1*-EGFP+ endogenous BM pGMs after 3 weeks of leukemia were significantly reduced in proportion when compared to control (4.5±3.2% vs. 19±2.8%, $p \leq 0.01$). These findings therefore suggested that the erythroid immunophenotype observed during leukemic development was likely preceded by the impairment of hierarchically upstream erythroid committed pGMs. Furthermore, the expansive GMP immunophenotype that was observed (figure 3.3.2.a) may also be explained by the higher proportion of neutrophil and monocyte committed *Gata1*-EGFP- pGMs.

3.3.4.a **3.3.4.b**



Immunophenotypic frequency of *Gata1*-EGFP expressing BM pGM progenitors after exposure to leukemia

3.3.4.a. Frequency of leukemic burden as a % of BM singlets after 3 weeks post-transplantation of LICs into *Gata1*-EGFP recipients. **3.3.4.b.** Proportion of *Gata1*-EGFP expressing as a % of total pGMs in control and leukemic recipients. Mean±SD, N=3 from one experiment. A two-tailed unpaired *t*-test was used to determine significance, comparing leukemia transplanted mice, to non-transplanted, time-matched, sub-lethally irradiated control mice (**$p \leq 0.01$).

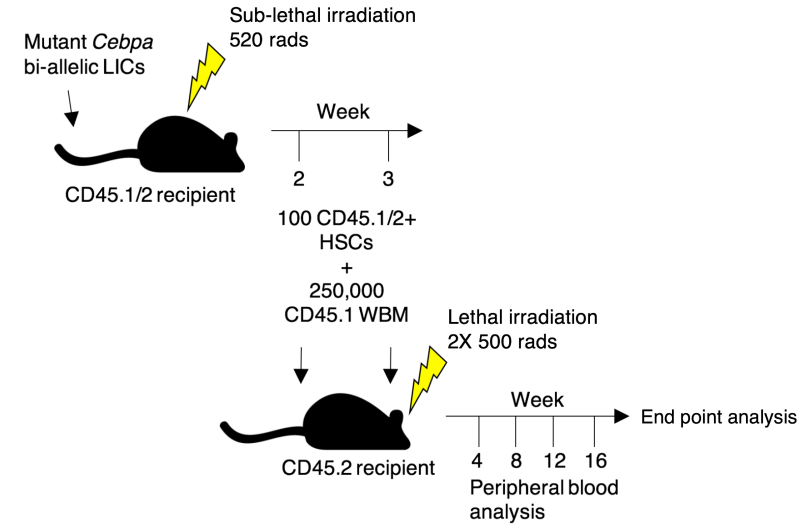
3.4. Functional consequences of leukemic development on endogenous BM hematopoietic stem and progenitor cells

Immunophenotypically, endogenous BM HSPCs were differentially affected by leukemic development (*i.e.* GMPs expanded, erythroid progenitors declined). Therefore, to understand whether leukemic cells induced functional changes to normal hematopoietic populations, endogenous HSCs and LK progenitors were FACS isolated from leukemia-transplanted and non-transplanted control mice at weeks 2 and 3, and were used for both *in vitro* and *in vivo* functionality assays. These assays were not completed in mice transplanted for 4 weeks due to insufficient cell number.

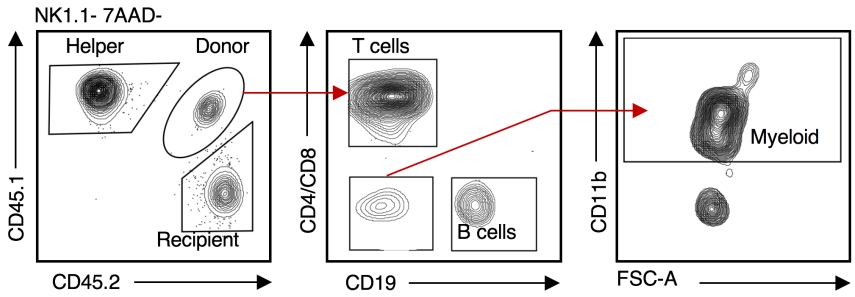
3.4.1. Long-term functionality of endogenous BM HSCs after exposure to leukemia

To study whether leukemic development functionally impaired endogenous HSCs, 100 CD45.1/2+ HSCs were FACS isolated from either leukemia-transplanted or non-transplanted, time-matched,sub-lethally irradiated control mice after 2 and 3 weeks. Isolated HSCs were then transplanted into lethally-irradiated recipients (1000 rads) with 250,000 helper BM cells (figure 3.4.1.a). Mature myeloid, B and T cell peripheral blood reconstitution (figure 3.4.1.b) was assessed at 4-week intervals for a total of 16 weeks. After the final peripheral blood readout, recipients were euthanized and analysed for donor HSC and myeloerythroid BM reconstitution. Recipients that exhibited <1% peripheral blood engraftment after 16 weeks were excluded from subsequent analyses. Population frequencies in all analyses are expressed as a percentage of donor-derived (CD45.1/2+) cells.

3.4.1.a



3.4.1.b



Long-term functionality of endogenous BM HSCs after exposure to different stages of leukemia

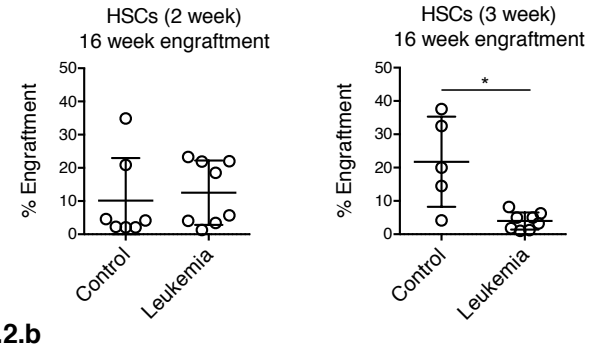
3.4.1.a. Graphical depiction of experimental approach for evaluating long term HSC functionality after exposure to leukemia. HSCs were FACS isolated from leukemia transplanted and non-transplanted, sub-lethally irradiated, time matched controls. Isolated HSCs were transplanted into lethally-irradiated CD45.2 recipients. At 4 week intervals, mice were bled and donor-derived T, B and myeloid cell reconstitution was assessed. After 16 weeks, mice were culled, and donor-derived BM HSC and myeloerythroid engraftment was assessed. **3.4.1.b.** Flow cytometry gating strategy used to define the peripheral blood donor reconstitution of myeloid (CD11b+), B (CD19+) and T cells (CD4/CD8+).

3.4.2. Peripheral blood reconstitution of myeloid, B and T cells from leukemia-exposed BM HSCs

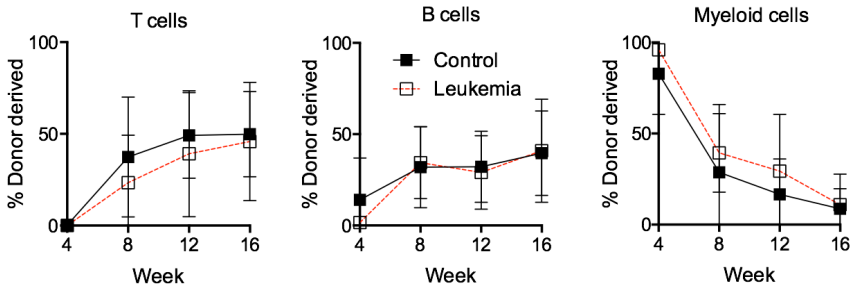
As seen in figure 3.4.2.a left panel, HSCs exposed to leukemia for a 2 week period shared a statistically comparable 16 week peripheral blood engraftment level to controls (10.1±14.4% vs. 12.5±8.7%, $p>0.05$). There were also no significant, long term defects in mature myeloid, B or T cell reconstitution (figure 3.4.2.b). The long-term 16 week engraftment of HSCs isolated from mice after 3 weeks of leukemia (figure 3.4.2.a, right panel) was significantly lower than controls (4±2.7% vs. 21.8±9.1%, $p\leq0.05$). This however did not translate into any statistically significant ($p>0.05$) changes in mature myeloid, B or T cell reconstitution (figure 3.4.2.c).

When taken together, these findings implied that once removed from the leukemic microenvironment, HSCs were not impaired in their capacity to generate mature cell types after transplantation.

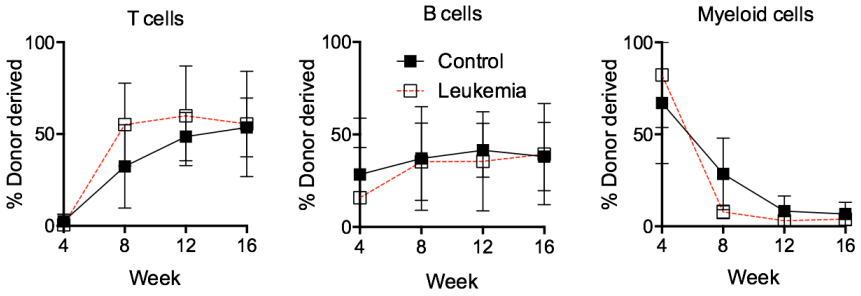
3.4.2.a



3.4.2.b



3.4.2.c



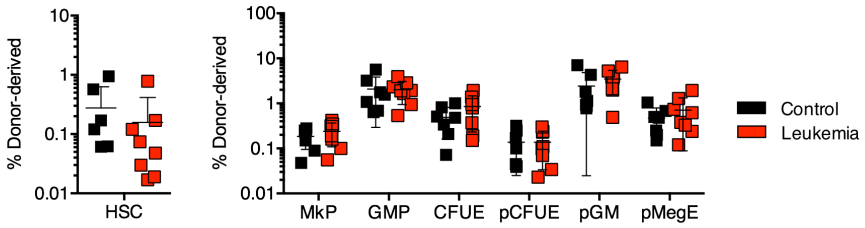
Peripheral blood reconstitution of myeloid, B and T cells from leukemia-exposed BM HSCs

3.4.2.a. 16 week peripheral blood engraftment as a % of singlets for HSCs exposed to leukemia for 2 or 3 weeks. Peripheral blood reconstitution as a % of total donor cell (CD45.1/2+) frequency for T, B and myeloid cells from 2 (**3.4.2.b**) or 3 (**3.4.2.c**) week exposed HSCs. Mean±SD, N=5-8 from two experiments. A Mann-Whitney statistical test was used to determine significance, comparing leukemia-transplanted mice to time-matched, non-transplanted, sub-lethally irradiated mice (*$p \leq 0.05$).

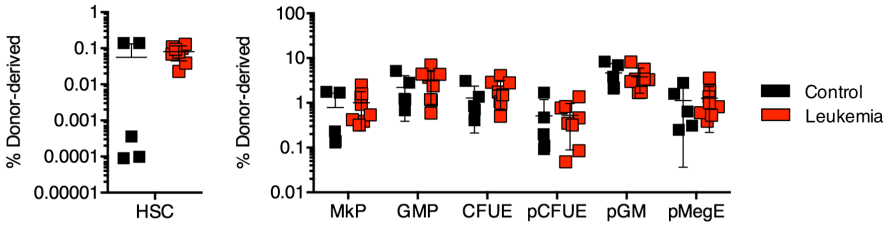
3.4.3. Analysis of donor-derived BM HSC and myeloerythroid progenitor reconstitution

Mice transplanted with HSCs exposed to leukemia for 2 and 3 weeks of leukemic development (see section 3.4.2) were euthanized after 16 weeks and analysed for BM donor-derived (CD45.1/2+) HSC and myeloerythroid progenitor reconstitution. In line with the findings from figures 3.4.2.b and 3.4.2.c, there were no statistically significant differences (p>0.05) identified between mice that were transplanted and control mice (figures 3.4.3.a and 3.4.3.b). This further confirmed that HSCs remained functionally intact once removed from the leukemic microenvironment, and were capable of reconstituting normally.

3.4.3.a



3.4.3.b



Analysis of donor-derived BM HSC and myeloerythroid progenitor reconstitution

Frequency of donor-derived (CD45.1/2+) BM HSC and myeloerythroid progenitor engraftment from recipients transplanted with HSCs exposed to leukemia for 2 (**3.4.3.a**) or 3 (**3.4.3.b**) weeks. Mean±SD, N=5-8 from two experiments. A Mann-Whitney statistical test was used to determine statistical significance, comparing

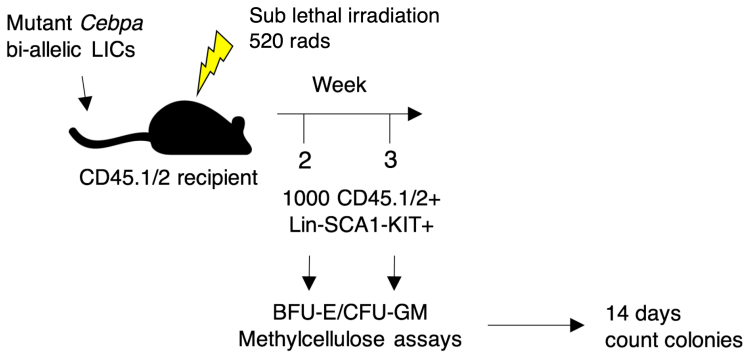
leukemia-transplanted mice to time-matched, non-transplanted, sub-lethally irradiated control mice.

3.4.4. *In vitro* functionality of endogenous BM LK progenitors during leukemia

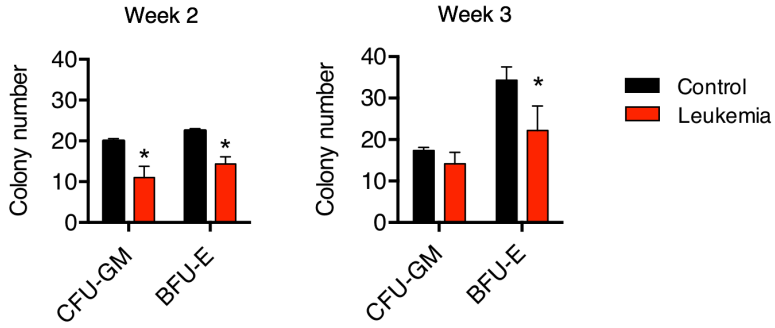
Methylcellulose-based clonogenic assays are a useful *in vitro* tool for studying the functionality of hematopoietic cell populations under different conditions. Therefore, 1000 CD45.1/2+ BM LK cells were FACS isolated from either leukemia-transplanted or non-transplanted mice after 2 and 3 weeks, and plated into myeloid (CFU-GM; M3534) and erythroid (BFU-E; M3436) methylcellulose colony forming media. BFU-E assays were supplemented with 100ng/mL SCF to promote erythroid colony formation. Colonies were manually counted under a microscope after 14 days (figure 3.4.4.a).

As seen in figure 3.4.4.b, CD45.1/2+ LK progenitors isolated from mice 2 weeks after leukemic transplantation showed signs of reduced CFU-GM (11±2.7 colonies vs. 20±1 colonies, $p \leq 0.05$) and BFU-E (14.3±1.8 colonies vs. 22.5±0.86 colonies, $p \leq 0.05$) colony forming ability when compared to time-matched, non-transplanted, sub-lethally irradiated controls. After 3 weeks, LK progenitors still lacked the ability to generate erythroid-colonies (22.2±6 colonies vs. 34.3±3.2 colonies, $p \leq 0.05$), but showed no sign of impaired myeloid colony forming ability (14.2±2.8 colonies vs. 17.3±0.76 colonies, $p > 0.05$). Collectively, this implied that erythroid progenitors became functionally impaired throughout leukemic development, which was consistent with the immunophenotypic observations made in figure 3.3.2.b.

3.4.4.a



3.4.4.b



***In vitro* functionality of endogenous BM LK progenitors during leukemia**

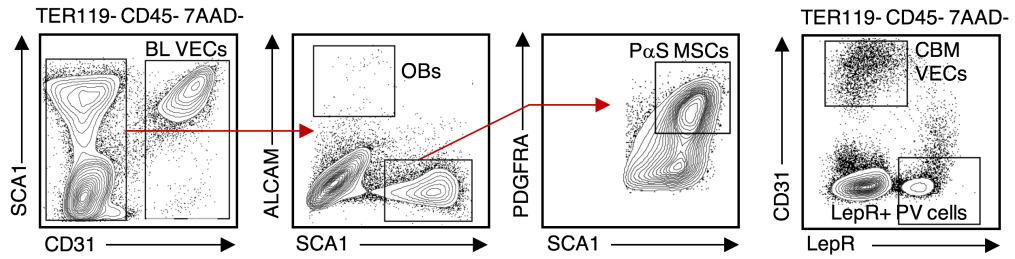
3.4.4.a. Endogenous LK progenitors were FACS isolated from leukemic mice after 2 and 3 weeks post-transplantation and cultured in either erythroid (BFU-E; 1000 cells) or myeloid (CFU-GM; 1000 cells) supportive Methylcellulose media. After 14 days, colonies were manually counted. **3.4.4.b.** Number of colonies generated by endogenous BM LK progenitors after 2 (left) or 3 (right) weeks exposure to leukemia. Mean±SD, N=3 from one experiment. A two-tailed unpaired *t*-test was used to determine statistical significance, comparing leukemia-transplanted mice to time-match, non-transplanted mice (*$p \leq 0.05$).

3.5. Immunophenotypic analysis of CBM and BL niches during leukemia

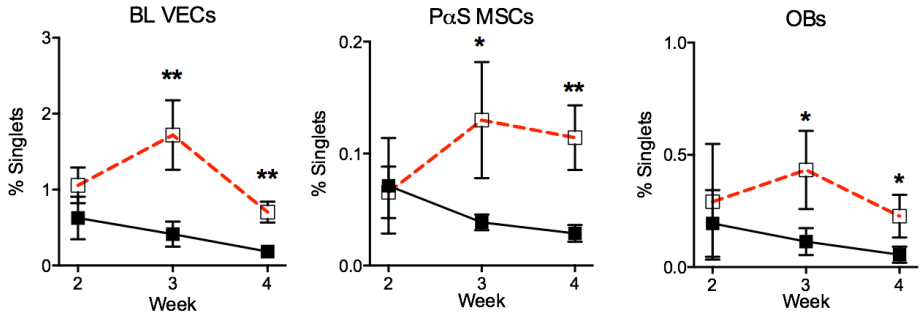
The immunophenotypic frequency of CBM (sinusoidal) and the BL (endosteal) niche cells from leukemia-transplanted and non-transplanted, time-matched, sub-lethally irradiated control mice were investigated after 2, 3 and 4 weeks. BL niche cells that were analysed included BL VECs (CD45- TER119- CD31+), PαS MSCs (CD45- TER119- CD31- ALCAM- SCA1+ PDGFRA+) and OBs (CD45- TER119- CD31- ALCAM+ SCA1-; figure 3.5.a). CBM niche cells that were analysed included CBM VECs (CD45- TER119- CD31+) and LepR+ PV cells (CD45- TER119- LepR+; figure 3.5.b).

As a percentage of BM singlets, CBM VECs were significantly reduced in frequency after 2 weeks when compared to non-transplanted, time-matched, sub-lethally irradiated control mice (0.023±0.01% vs. 0.047±0.008%, $p \leq 0.05$). This downward trend continued into week 3 (0.017±0.003% vs. 0.05±0.01%, $p \leq 0.01$) and week 4 (0.004±0.001% vs. 0.024±0.003%, $p \leq 0.001$). LepR+ PV cells remained unchanged in frequency at week 2 (0.06±0.03% vs. 0.04±0.004%, $p > 0.05$), but appeared to undergo a significant expansion by week 3 (0.16±0.05% vs. 0.04±0.02, $p \leq 0.05$), returning to a comparable frequency again by week 4 (0.05±0.005 vs. 0.05±.0.01%, $p > 0.05$). BL VECs, PαS MSCs and OBs remained at a statistically comparable frequency at week 2, yet appeared to expand significantly at week 3, which continued in all cell types into week 4 (figure 3.5.c).

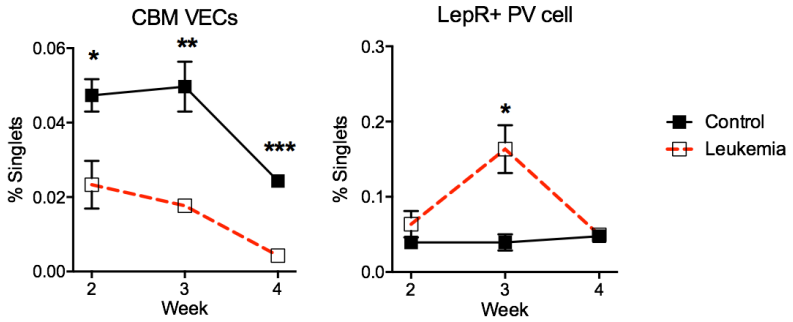
3.5.a **3.5.b**



3.5.c



3.5.d



Immunophenotypic analysis of CBM and BL niches during leukemia

Flow cytometry gating strategies for BL (**3.5.a**) and CBM (**3.5.b**) niche populations. Analysis of BL VECs, OBs and PαS MSCs (**3.5.c**) or CBM VECs and LepR+ PV cells (**3.5.d)** during leukemic development. Mean±SD, N=3 from one experiment. Frequencies are represented as a % of BM singlets. A two-tailed unpaired *t*-test was used to determine statistical significance, comparing leukemia-transplanted mice to time-matched, non-transplanted, sub-lethally irradiated control mice (*$p \leq 0.05$, **$p \leq 0.01$, ***$p \leq 0.001$).

3.6. Summary and discussion

The transplantation model described in this chapter (figure 3.2.a) provided a robust and clinically relevant means for studying the different stages of leukemic development. The kinetics, despite being rapid, remained predictable, enabling for the step-wise analysis of leukemic cells, the endogenous hematopoietic compartment and the BM niche.

Leukemic recipients at the early stages of disease development exhibited low levels of BM and spleen tumour engraftment (figure 3.2.c), with no signs of splenomegaly, WBC infiltration or anemia (figures 3.2.1.a and 3.2.2.a). In contrast to recent work completed by Duarte et al., (2018), AML spleen engraftment in the present model was considerably higher than the BM (figure 3.2.c). This suggested that leukemic cells may have been preferentially engrafted within the spleen rather than the BM, either because the spleen provided a permissive niche within which the leukemic cells were able to thrive, or simply because it was the first location that the LICs came into contact with after transplantation. By week 3, blast cells began emerging in the BM, which was also seen in the periphery and spleen (figures 3.2.d, 3.2.1.a and 3.2.2). By the final stages of the disease, mice began exhibiting outward signs of ill health such as weight loss, pale paw pads and hunching. Interestingly, the inability of LICs to retain their leukemogenecity after *in vitro* culture in HSPC supportive media (figure 3.2.3.a) suggested that these cells required a highly specific milieu of secreted factors that were only available *in vivo*. Indeed, a study completed by Kumar et al., (2018) suggested that AML secreted exosomes reduce the expression of important HSPC supportive niche factors such as CXCL12 and KITL. As a result, it was discovered that this lead to a reduction in the frequency of normal hematopoietic BM cells, but not leukemic cells. When considered alongside the data

presented here, this suggests that the factors required for leukemogenesis may differ from those utilised by normal, functioning HSPCs.

The frequency of endogenous HSC, MPP and myeloerythroid progenitor populations during leukemic development exhibited striking differences. HSC, MPP and myeloid progenitor cell populations remained at a constant frequency during both the early and intermediate stages of disease (figures 3.3.1 and 3.3.2.a). Furthermore, HSCs did not migrate to the spleen to undergo extra medullary hematopoiesis (figure 3.3.3.a), unlike in other hematological conditions such as myelofibrosis (Wang et al., 2012). GMPs did however increase in frequency at week 3 (figure 3.3.2.a), the same time point at which myeloid blasts began emerging in the BM, spleen and periphery. The immunophenotypic expansion of these cells could be an indirect consequence of a myeloid promoting environment created by leukemic cells. Indeed, it has previously been shown that patients with different solid tumours exhibit a similar increase in circulating GMPs and myeloid-biased HSPCs as a result of aberrantly expressed GM-CSF and IL-6 (Wu et al., 2014). In contrast to this, erythroid progenitors became immunophenotypically depleted at a time point where leukemic cells occupied only a fraction of the total cells in the BM (figure 3.3.2.b). These findings were in line with a proportional decrease in *Gata1*-EGFP+ pGMs (figure 3.3.4.b), suggesting that upstream populations responsible for generating erythroid cells were also perturbed in this model of leukemia. The immediate decline in erythroid progenitor frequency preceded the decrease in peripheral HGB levels (figure 3.2.1.a) and was therefore observed only at the terminal stages of the disease. The decline in erythroid progenitor frequency despite the maintenance of other BM cell types suggested that leukemic cells either outcompeted erythroid progenitors within their own niche, or that there were direct negative cellular interactions that

occurred between leukemic cells and erythroid progenitors. Previous work by Boyd et al., (2017) highlighted that the disruption of BM adipocytes during leukemia led to impaired endogenous myeloerythroid progenitor maturation. However, in contrast to this report, the present study did not demonstrate that myeloid progenitors were affected equally to erythroid progenitors.

LT-HSC functionality was not compromised after exposure to leukemia for 2 or 3 weeks. These findings were in agreement with what has formerly been demonstrated (Miraki-Moud et al., 2013), and suggested that the removal of HSCs from their immediate leukemic environment was sufficient to mitigate any persistent functional defects in progenitor output. In contrast to this, progenitors were functionally impaired (figure 3.4.4.b) and were unable to efficiently generate erythroid colonies at both the early- and mid-stage of this AML model. This reflected both a sustained lack of intrinsic functionality, as well a reduction in the absolute number of erythroid colony forming cell types. Myeloid colony forming capacity on the other hand was not impacted, suggesting that the leukemic BM environment may have been supportive of myelopoiesis at the expense of erythropoiesis. A technical limitation faced during these functional assays was the necessity to sub-lethally irradiated recipient mice prior to leukemia transplantation. As a result, HSC engraftment was significantly impaired, even in non-leukemia transplanted control mice. Defects in donor chimerism after total body irradiation have previously been reported, and were not reversible by increasing cell number or after serial transplantation (Chua et al., 2012). To overcome this, a leukemia transplantation model that does not require sub-lethal irradiation would need to be created.

Niche cells were immunophenotypically perturbed throughout leukemic development. BL VECs, PαS MSCs and OBs were consistently increased in frequency, but only after 3 (and therefore 4) weeks post-transplantation (figure 3.5.1.c). This was also the same time point at which myeloid blasts began emerging, suggesting that niche cells may have become conditioned in support of leukemogenesis. In contrast to this, CBM VECs were consistently decreased in frequency, even after only 2 weeks (figure 3.5.1.d). Recent work by Passaro et al., (2017) and Kumar et al., (2018) highlighted that remodelling of the BM niche contributes greatly towards AML disease progression and chemotherapy drug resistance. However, the increase in BL VECs and decrease in CBM VECs observed during this present study, directly contradicts recent findings by Duarte et al., (2018), who report that endosteal VECs, but not sinusoidal, were reduced in frequency during AML. Furthermore, it was also demonstrated that OBs were decreased in frequency, which was again in direct contrast to what was observed during this present study, as well as others (Boyd et al., 2017). There are however a number of experimental disparities that may account for these differences. For example, Duarte et al., used an MLL-AF9 model of leukemia, and transplanted these cells into non-irradiated mice. It is therefore unlikely that this malignant cell, although also considered a myeloid leukemia, relies on the same interactions within the BM to survive and propagate.

3.7. Conclusions

1. **A robust, kinetically tractable model of AML that accurately mimics the human disease was developed**

The transplantation of 25,000 bi-allelic mutant *Cebpa* cells into sub-lethally irradiated mice generated a kinetically tractable model of AML. Symptoms experienced by mice during this model mimicked those found in patients, and included splenomegaly, anemia and significant white cell infiltration.

2. **The frequencies of specific endogenous BM HSPC populations during leukemic development were confirmed**

Using a transplantation model of AML, it was demonstrated that BM HSCs, MPPs, myeloid progenitors and MkPs during the early- and mid-stages of AML model remained immunophenotypically unperturbed, whereas erythroid progenitors were not. By week 3, GMP myeloid progenitors expanded in frequency, whereas erythroid progenitors continued to decline. The decline in committed erythroid progeny was also evident as a proportional decrease in erythroid producing *Gata1*-EGFP+ pGMs. Collectively, these findings suggested that prior to complete hematopoietic failure, leukemic cells were capable of selectively depleting erythroid cells whilst simultaneously expanding myeloid progenitors.

3. **The functionality of endogenous HSCs and progenitors during the development of a leukemia were evaluated**

LT-HSC functionality remained unchanged at both the early- and mid-stages of leukemic development, a finding that is consistent with the literature and was also in line with the frequencies of donor reconstituted BM HSCs and myeloerythroid

progenitors. In contrast, endogenous LK progenitors were unable to efficiently generate erythroid colonies once removed from the leukemic environment. This suggested that progenitor populations were differentially impaired during AML.

4. **The immunophenotypic frequency of niche cells during the development of AML were investigated**

CBM and BL niche cell populations were immunophenotypically perturbed during the development of leukemia. CBM VECs were significantly depleted at the onset of disease whereas BL VECs, PαS MSCs, LepR+ PV cells and OBs were increased in frequency after 3 weeks. Collectively, this suggested that leukemic cells were capable of physiologically altering important niche cells.

Chapter 4

Transcriptionally profiling endogenous hematopoietic and BM niche populations during leukemia and steady state

4.1. Introduction and aims

As evidenced in the previous chapter, endogenous BM HSC and MPP populations remained immunophenotypically unperturbed during the majority of leukemic development, whereas myeloerythroid progenitors were not. Moreover, the functionally of HSCs remained normal after being removed from the leukemic microenvironment, despite erythroid progenitors exhibiting a sustained intrinsic impairment in colony forming ability. Collectively, these findings suggested that prior to complete hematopoietic failure, leukemic cells were responsible for either directly, or indirectly impairing normal progenitor function within the BM, which ultimately caused the onset of symptoms commonly associated with AML. It was also observed that important BM niches were differentially perturbed in frequency throughout AML, which is in agreement with a mounting body of evidence that suggests the reprogramming of the BM niche as an essential component for leukemogenesis (Arranz et al., 2014; Boyd et al., 2017; Duarte et al., 2018; Kumar et al., 2018; Colmone et al., 2008; Lim et al., 2016).

Despite this, however, very little is currently known about the changes to global gene expression that occur within both BM niche populations and endogenous HSPCs during the different stages of leukemic development. Therefore, the AML transplantation model described in chapter 3 (figure 3.2.a) was utilised to address the following aims:

1. Transcriptionally profile endogenous BM HSPCs exposed to leukemia using bulk RNA-seq, and determine the significantly enriched process networks
2. Transcriptionally profile CBM niches during leukemia using bulk RNA-seq, and determine whether these populations become molecularly reprogrammed by the presence of leukemic cells.

3. Investigate the heterogeneity of the BM niche using droplet-based scRNA-seq, and use an integrated analysis to understand whether significant niche remodeling occurs during leukemia.

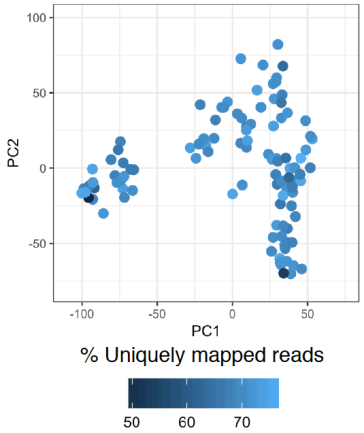
4.2. Bulk RNA-seq of endogenous BM HSPCs during leukemic development

Endogenous HSC, MPP2, MPP3, MPP4, pCFUE, CFUE, pGM, pMegE and GMP cell populations were isolated by FACS for bulk RNA-seq analysis from mice at weeks 2 and 3 of leukemic development, and from time-matched, non-transplanted, sub-lethally irradiated control mice (see Chapter 3, figures 3.3.a and 3.3.b). Samples were processed using the SMART-seq2 protocol (see Materials and methods, section 2.1.7). Due to insufficient cell numbers, BM HSPC populations at the week 4 time point of leukemic development were not isolated.

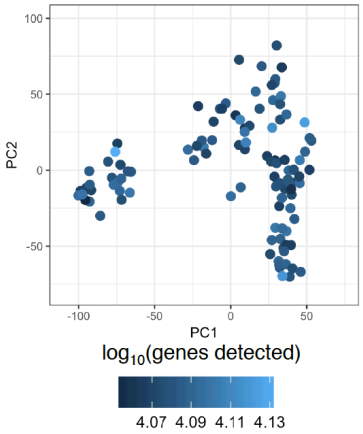
4.2.1. Data quality check

Prior to analysis, sequenced BM HSPC samples were validated for read mapping percentage, total read library size and total number of unique genes detected per sample. These values were plotted against their principal component (PC)1 and PC2 values. Values for library size and total number of genes detected are displayed as $\log_{10}$ values. As seen in figure 4.2.1.a, all sequenced HSPC samples aligned to the mm9 reference genome with ~50-70% mapping efficiency. The library sizes and number of detected genes for each sample was consistent (figures 4.2.1.b and 4.2.1.c).

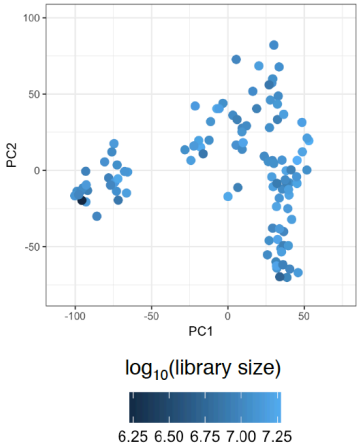
4.2.1.a



4.2.1.b



4.2.1.c



RNA-seq data quality check

4.2.1.a. Percentage of mapped reads per HSPC sample. **4.2.1.b.** Log_{10} number of genes detected per HSPC sample. **4.2.1.c.** Log_{10} library size per HSPC sample. Samples are plotted against their PC1 and PC2 values determined from total genes.

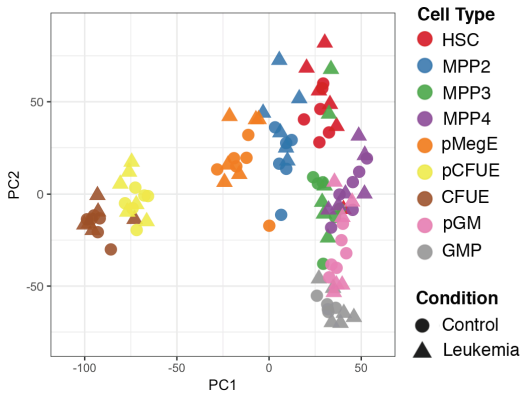
4.2.2. PCA of HSPC populations during leukemia

Principal component analysis (PCA) was carried out on all genes from HSPC samples to assess unsupervised clustering based on total gene variance.

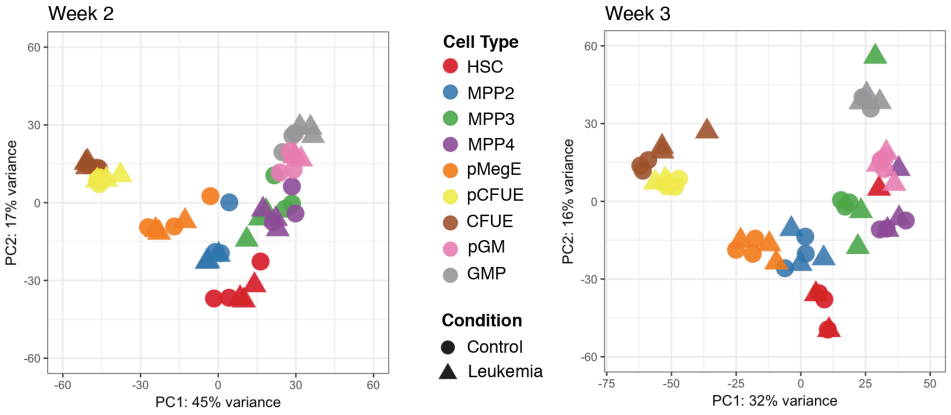
As seen in figure 4.2.2.a, Y-axis (PC2) variation appeared to define cellular maturity (*i.e.* Multipotent HSC to committed progenitor), whereas X-axis variation (PC1) defined cellular commitment/bias (*i.e.* erythroid or myeloid). HSCs were located at the apex of the hierarchy, and were closely associated with the MPP2, MPP3 and MPP4 populations. Myeloid-biased MPP3 and lymphoid-biased MPP4 (Pietras et al., 2015) cell types preferentially clustered near pGM and GMP myeloid progenitor populations, whereas erythroid-biased MPP2 (Pietras et al., 2015) cells were in closer proximity to the pMegE, pCFUE and CFUE progenitors.

PCA was also performed based on the top 500 variable genes from HSPC samples at weeks 2 and 3 separately (figure 4.2.2.b). At week 2, all cells clustered appropriately, following an inverted pattern consistent with what was observed in figure 4.2.2.a. At week 3, a single HSC and MPP3 sample clustered in closer proximity to the myeloid lineage branch. Based on both analyses, it was concluded that the populations isolated and sequenced, accurately represented the assumed cellular identities.

4.2.2.a



4.2.2.b



PCA of HSPC populations during leukemia

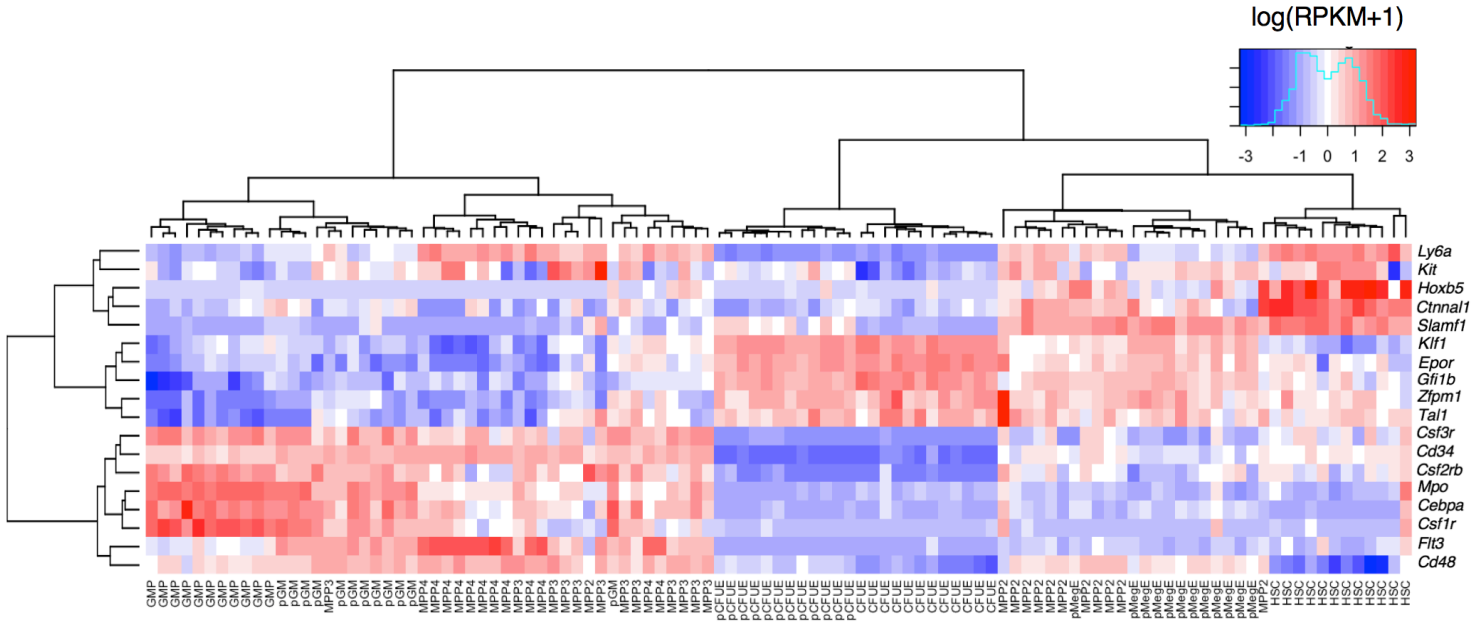
4.2.2.a. PCA of all HSPC samples on total genes from control and leukemic conditions. **4.2.2.b.** PCA on top 500 variable genes from HSPC samples divided by time point.

4.2.3. Heatmap quality check using known HSPC genes

To further ensure that the sequenced BM HSPC samples accurately represented the expected cell types, supervised clustering using Euclidean distance and Wards methods was performed on all samples using known HSC, MPP, erythroid and myeloid progenitor genes (figure 4.2.3.a).

Myeloid-biased MPPs (MPP3, MPP4) and committed myeloid progenitors (pGM, GMPs) clustered together based on their expression of the myeloid genes *Csf3r*, *Cd34*, *Csf2rb*, *Mpo*, *Cebpa*, *Csf1r* (Pronk et al., 2007), but were separated based on their differential expression of *Ly6a* and *Kit*. CFUE and pCFUE erythroid progenitors clustered together based on their expression of the erythroid genes *Klf1*, *Epo*r, *Gfi1b*, *Zfpm1* and *Tal1* (Pronk et al., 2007), and were also more closely positioned near erythroid-biased MPP2 cells and pMegE progenitors. MPP2 and pMegE cells also clustered together based on their expression of erythroid genes, however MPP2 cells expressed several myeloid genes, in addition to *Ly6a*, likely due to their capacity for generating myeloid cells during stress conditions (Pietras et al., 2015). HSCs clustered together based on their expression of the genes *Ly6a*, *Kit*, *Hoxb5*, *Ctnnal1* and *Slamf1* (Chen et al., 2016; Oguro et al., 2013; Acar et al., 2015), but lacked *Cd48* and remained in close proximity to MPP2 and pMegE cell types. In conclusion, isolated HSPCs samples clustered as expected based on known, previously published genes.

4.2.3.a



Heatmap quality check using known HSPC genes

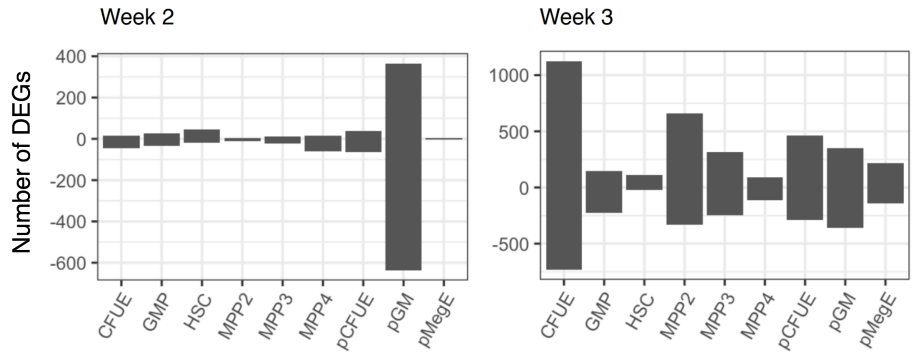
4.2.3.a. Endogenous HSPC samples were clustered using Euclidean distance and Wards method on previously published genes that identify HSC, MPP and myeloerythroid progenitor populations. Expression values are scaled, log(RPKM+1).

4.2.4. Differential gene expression analysis of endogenous BM HSPCs during leukemia

Differential gene expression analysis was carried out on individual BM HSPC populations at weeks 2 and 3 post-transplantation, comparing individual leukemic exposed endogenous HSPC populations to non-leukemia exposed, time-matched, sub-lethally irradiated controls. For each population at each time point, a list of DEGs was generated. Genes that were upregulated in leukemic exposed cell populations display a positive Log2FC value, whereas genes down regulated are expressed as a negative Log2FC value.

Figures 4.2.4.a and 4.2.4.b depict the number of up- and down-DEGs with an adjusted $p \leq 0.05$ from each HSPC cell type analysed at weeks 2 and 3 post-transplantation. After 2 weeks, pGM progenitors expressed 1001 DEGs, a number that far exceeded any other cell type at this time point (figure 4.2.4.a). By week 3, however, several cell types exhibited significant changes to global gene expression, including MPP2 (992 DEGs), pCFUE (753 DEGs), CFUE (1855 DEGs) and pGM (710 DEGs). At both time points, HSCs exhibited very few transcriptional changes, which also reflected their lack of immunophenotypic and functional impairment during this model of leukemia (see Chapter 3, figures 3.3.1.a and 3.4.2.b, 3.4.2.c).

4.2.4.a **4.2.4.b**



Differential gene expression analysis of endogenous BM HSPCs during leukemia

Number of DEGs with an adjusted $p \leq 0.05$ from BM HSPC populations after 2 (**4.2.4.a**) and 3 (**4.2.4.b**.) weeks post-leukemia transplantation. DESeq2 was used to determine DEGs, where each population was compared to a time-matched, non-leukemia transplanted control population.

4.2.5. Process network enrichment analysis of endogenous BM HSPCs during leukemia

Metacore is a computational tool that calculates functionally enriched gene ontology (also known as process networks) using a hypergeometric statistical test and a list of DEGs and their Log2FC values. This analysis tool was used to investigate enriched process networks from endogenous BM HSPCs exposed to leukemia for 2 and 3 weeks. DEGs with an adjusted $p \leq 0.05$ were used as input for this analysis. All process networks shown have a $p \leq 0.05$ and FDR$\leq$0.05.

After 2 weeks, very few HSPC populations exhibited significant transcriptional changes (figure 4.2.4.a). As a result, not all HSPC populations enriched for process networks based on the significance criteria cut off used ($p \leq 0.05$, FDR$\leq$0.05). Enriched process networks at week 2 post-transplantation can be found in table 4.2.5.a. HSCs at this time point were enriched for translation and mitosis processes, and was an effect driven predominantly by the expression of ribosomal genes. In general, protein synthesis is lower in HSCs than most other hematopoietic cell types *in vivo*, where a heightened level is associated with an increased risk of leukemogenesis (Signer et al., 2014). pGMs exhibited a significant number of enriched process networks, ranging from cell cycle, cell adhesion, inflammation, proliferation and signal transduction. Taken together, these data suggested that pGMs were highly transcriptionally active at the very earliest stage of this model. This also coincided with differences in progenitor functionality (see Chapter 3, figure 3.4.4.b), as well as differential immunophenotypic changes to *Gata1*-EGFP expressing pGMs and committed erythroid progenitors (see Chapter 3, figures 3.3.4.b and 3.3.2.b). This therefore implied that prior to the expansion of GMPs and decline in erythroid progenitors, pGMs may have become lineage become primed.

After 3 weeks (figure 4.2.5.b), process network enrichment was again only observed in a limited number of HSPC populations. MPP2, MPP3 and MPP4 cells enriched for processes related to cell cycle, transcription and protein synthesis. Of note, despite being almost completely devoid in frequency by the week 3 time point of this model, pCFUE and CFUE progenitors were highly enriched for cell cycle, DNA damage and protein synthesis processes. This likely reflected an emergency proliferative response to being immunophenotypically depleted. The number of total enriched processes in pGMs decreased at this time point of the model, however these cells remained enriched for protein synthesis and cell cycle-related processes. GMPs, on the other hand, enriched for a high number of inflammatory, cell cycle and signal transduction processes, including the neutrophil activation pathway, IL-6 and TREM-1 signalling. This was in line with the significant immunophenotypic expansion of these cells at an equivalent time point (see Chapter 3, figure 3.3.2.a).

When considered together, these findings demonstrated that endogenous HSPCs during leukemia became altered at the gene expression level, with the majority of changes occurring at the mid-time point of this AML model, and within cell types that also displayed functional and immunophenotypic impairment.

4.2.5.a.

Cell Type	*Process Network*	*-log(p-value)*
HSC	Translation_Elongation-Termination	6.99
	Translation_Translation initiation	6.85
	Cell cycle_Mitosis	3.31
pMegE	Inflammation_IL-4 signalling	2.60
	Inflammation_Jak-STAT Pathway	2.19
CFUE	Signal transduction_Leptin signalling	3.86
pGM	Transcription_Chromatin modification	7.21
	Translation_Regulation of initiation	6.53

Protein folding_ER and cytoplasm	5.71
DNA damage_Checkpoint	5.59
Reproduction_Male sex differentiation	5.02
Protein folding_Protein folding nucleus	4.96
Development_EMT_Regulation of epithelial-to-mesenchymal transition	4.95
Cytoskeleton_Regulation of cytoskeleton rearrangement	4.51
Proteolysis_Ubiquitin-proteasomal proteolysis	4.37
Signal transduction_WNT signalling	4.33
Cytoskeleton_Actin filaments	3.94
Signal Transduction_TGF-beta, GDF and Activin signalling	3.57
Apoptosis_Apoptotic mitochondria	3.53
Inflammation_MIF signalling	3.30
Cell cycle_G1-S Growth factor regulation	3.24
Inflammation_TREM1 signalling	3.10
Cell cycle_Mitosis	3.04
Protein folding_Response to unfolded proteins	2.92
Cell cycle_G2-M	2.89
Immune response_TCR signalling	2.84
Cell cycle_G1-S	2.84
Cytoskeleton_Intermediate filaments	2.79
Cardiac development_Role of NADPH oxidase and ROS	2.71
Inflammation_IL-2 signalling	2.65
Immune response_IL-5 signalling	2.65
Reproduction_Spermatogenesis, motility and copulation	2.60
Cell cycle_Meiosis	2.57
Development_Hedgehog signalling	2.56
Signal transduction_ESR2 pathway	2.50
Anti-Apoptosis mediated by external signals via MAPK and JAK/STAT	2.34
Signal Transduction_BMP and GDF signalling	2.33
Signal transduction_Androgen receptor signalling cross-talk	2.27
Cell adhesion_Amyloid proteins	2.22
Proliferation_Positive regulation cell proliferation	2.17
Protein folding_Folding in normal condition	2.09
Cytoskeleton_Spindle microtubules	2.05
Cell adhesion_Integrin-mediated cell-matrix adhesion	2.05
Signal transduction_ESR1-nuclear pathway	2.00

	Translation_Translation initiation	1.92
	Reproduction_FSH-beta signalling pathway	1.90
GMP	Transport_Manganese transport	3.48
	Transport_Iron transport	3.40

Process network enrichment analysis of endogenous BM HSPCs during leukemia

4.2.5.a. Metacore analysis of significantly enriched process networks from endogenous HSC, pMegE, CFUE, pGM and GMP cell types at week 2 post-transplantation. DEGs with an adjusted $p \leq 0.05$ were used as input. All process networks shown have a $p \leq 0.05$ and FDR≤ 0.05. Enrichment is depicted as -log(*p*-value).

4.2.5.b

Cell Type	*Process Network*	*-log(p-value)*
MPP2	Cell cycle_Mitosis	10.41
	Protein folding_Folding in normal condition	5.68
	Translation_Translation in mitochondria	5.18
	Proteolysis_Ubiquitin-proteasomal proteolysis	4.84
	Cell cycle_G2-M	4.14
	Transcription_Transcription by RNA polymerase II	3.72
	Immune response_Phagosome in antigen presentation	3.72
	Cytoskeleton_Regulation of cytoskeleton rearrangement	3.70
	Cytoskeleton_Spindle microtubules	3.48
	Translation_Translation initiation	3.29
	Proteolysis_Proteolysis in cell cycle and apoptosis	3.23
	Protein folding_Protein folding nucleus	2.91
	Transcription_mRNA processing	2.85
	Cell cycle_S phase	2.81
	Cell cycle_Meiosis	2.66
	Development_Regulation of telomere length	2.62
	Translation_Elongation-Termination	2.59
	Cell cycle_G1-S	2.38
	DNA damage_DBS repair	2.30
MPP3	Protein folding_Folding in normal condition	6.45
	Proteolysis_Proteolysis in cell cycle and apoptosis	5.41
	Protein folding_Protein folding nucleus	4.74

	Cell cycle_G1-S	4.00
	Protein folding_ER and cytoplasm	3.25
	DNA damage_Checkpoint	3.07
	Cell cycle_G1-S Interleukin regulation	2.95
	Proteolysis_Ubiquitin-proteasomal proteolysis	2.90
	Protein folding_Response to unfolded proteins	2.70
	Inflammation_Neutrophil activation	2.66
	Immune response_Antigen presentation	2.62
	Transcription_Chromatin modification	2.50
	Cell cycle_G2-M	2.44
	Apoptosis_Anti-apoptosis mediated by external signals via NF-kB	2.42
MPP4	Cell cycle_G2-M	5.14
	Transcription_Chromatin modification	3.35
pMegE	Cell cycle_S phase	5.91
	DNA damage_DBS repair	4.39
	Cell cycle_Mitosis	4.26
	Cell cycle_G2-M	3.07
pCFUE	Transcription_mRNA processing	7.07
	Translation_Translation in mitochondria	6.10
	Protein folding_Folding in normal condition	4.87
	Translation_Translation initiation	4.84
	Cell cycle_S phase	4.13
	Cell cycle_Core	3.36
	DNA damage_DBS repair	3.32
	Translation_Elongation-Termination	3.32
	Protein folding_Protein folding nucleus	3.09
	DNA damage_Checkpoint	3.03
	DNA damage_Core	2.88
	Protein folding_ER and cytoplasm	2.58
	Proteolysis_Proteolysis in cell cycle and apoptosis	2.50
	Transcription_Transcription by RNA polymerase II	2.42
	Cell cycle_G1-S	2.32
	Cell cycle_Mitosis	2.32
CFUE	Translation_Translation in mitochondria	13.17
	Cell cycle_Mitosis	12.12
	Translation_Translation initiation	10.18
	Protein folding_Folding in normal condition	9.07
	Transcription_Transcription by RNA polymerase II	8.20
	Transcription_mRNA processing	8.11
	Proteolysis_Ubiquitin-proteasomal proteolysis	7.58

	Protein folding_Protein folding nucleus	6.29
	Immune response_Phagosome in antigen presentation	5.97
	Cell cycle_S phase	5.28
	Transcription_Chromatin modification	5.24
	Cell cycle_G2-M	5.18
	Cytoskeleton_Spindle microtubules	4.76
	Translation_Elongation-Termination	4.75
	DNA damage_DBS repair	3.81
	Cell cycle_G1-S	3.64
	Protein folding_Response to unfolded proteins	3.35
	Proteolysis_Proteolysis in cell cycle and apoptosis	3.20
	Protein folding_ER and cytoplasm	3.12
	DNA damage_Checkpoint	2.61
	Immune response_Antigen presentation	2.43
	Cytoskeleton_Regulation of cytoskeleton rearrangement	2.42
	Cell cycle_Core	2.40
	Apoptosis_Apoptotic mitochondria	2.35
	Response to hypoxia and oxidative stress	2.19
pGM	Protein folding_ER and cytoplasm	4.58
	Cell cycle_Mitosis	4.56
	Protein folding_Folding in normal condition	4.47
	Cell cycle_S phase	4.23
	Protein folding_Protein folding nucleus	4.21
	Protein folding_Response to unfolded proteins	4.15
	Cell cycle_G2-M	4.07
	Immune response_Antigen presentation	3.92
	Immune response_Phagosome in antigen presentation	3.40
	Apoptosis_Apoptotic mitochondria	2.53
GMP	Transcription_Chromatin modification	4.30
	Cytoskeleton_Actin filaments	4.05
	Inflammation_IL-2 signalling	3.70
	Cell adhesion_Integrin-mediated cell-matrix adhesion	3.69
	Signal Transduction_Cholecystokinin signalling	3.63
	Inflammation_Protein C signalling	3.56
	Signal transduction_WNT signalling	3.46
	Immune response_BCR pathway	3.33
	Cell adhesion_Cell junctions	3.26
	Inflammation_Neutrophil activation	3.15
	Immune response_Antigen presentation	3.02
	Immune response_TCR signalling	2.99

Inflammation_IgE signalling	2.75
Inflammation_MIF signalling	2.68
Inflammation_IL-6 signalling	2.63
Inflammation_TREM1 signalling	2.57
Cell adhesion_Attractive and repulsive receptors	2.46
Cell cycle_Mitosis	2.39
Signal transduction_Leptin signalling	2.36
Reproduction_FSH-beta signalling pathway	2.27
Inflammation_Histamine signalling	2.26
Immune response_Phagosome in antigen presentation	2.22
Inflammation_NK cell cytotoxicity	2.19
Immune response_T helper cell differentiation	2.18
Cell cycle_G1-S Growth factor regulation	2.11
Cell adhesion_Amyloid proteins	2.11
Inflammation_Amphoterin signalling	2.11

Process network enrichment analysis of endogenous BM HSPCs during leukemia

4.2.5.b. Metacore analysis of significantly enriched process networks from endogenous MPP2, MPP3, MPP4, pMegE, pCFUE, CFUE, pGM and GMP cell types at week 3 post-transplantation. DEGs with an adjusted $p \leq 0.05$ were used as input. All process networks shown have a $p \leq 0.05$ and FDR$\leq$0.05. Enrichment is depicted as -log(*p*-value).

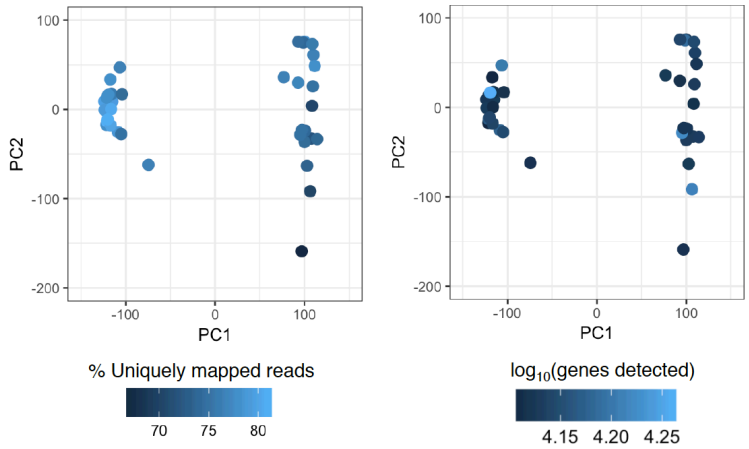
4.3. Bulk RNA-seq of CBM VECs and LepR+ PV cells during leukemia

Significant immunophenotypic changes were observed in CBM VECs and LepR+ PV cells during leukemic development (see Chapter 3, figure 3.5.d). Therefore, in order to assess how these populations changed on a gene expression level, CBM VECs and LepR+ PV cells were FACS isolated from leukemia-transplanted mice after 2, 3 and 4 weeks, and time-matched, non-transplanted, sub-lethally irradiated control mice. Isolated samples were then processed for bulk RNA-seq analysis using the SMART-seq2 protocol (see Materials and methods, section 2.1.7).

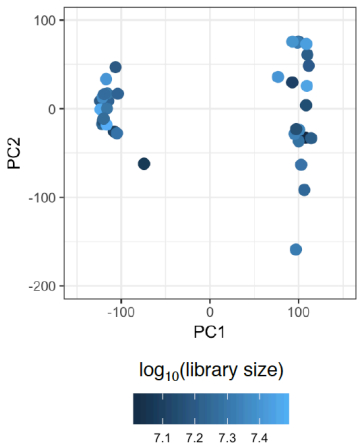
4.3.1. Data quality check

Prior to analysis, sequenced CBM niche samples were validated for read mapping percentage, library size and total number of genes detected per sample. Values for library size and total number of genes detected are displayed as $\log_{10}$ values. As seen in figure 4.3.1.a, all sequenced niche samples aligned to the mm9 reference genome with approximately 60-80% mapping efficiency. The number of uniquely detected genes and total library size for each sample was consistent (figures 4.3.1.b and 4.3.1.c) and therefore no samples were excluded on this basis.

4.3.1.a **4.3.1.b**



4.3.1.c



RNA-seq data quality check

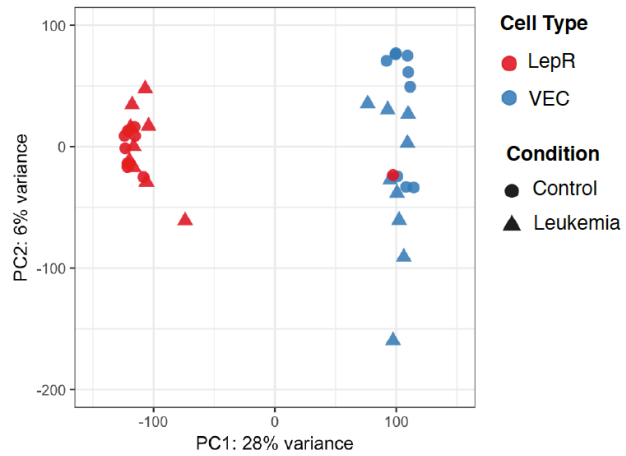
4.3.1.a. Percentage of mapped reads per niche sample. **4.3.1.b.** Log_{10} number of genes detected per niche sample. **4.3.1.c.** Log_{10} library size per niche sample. Samples are plotted against their PC1 and PC2 values determined from total genes.

4.3.2. PCA of niche populations during leukemia

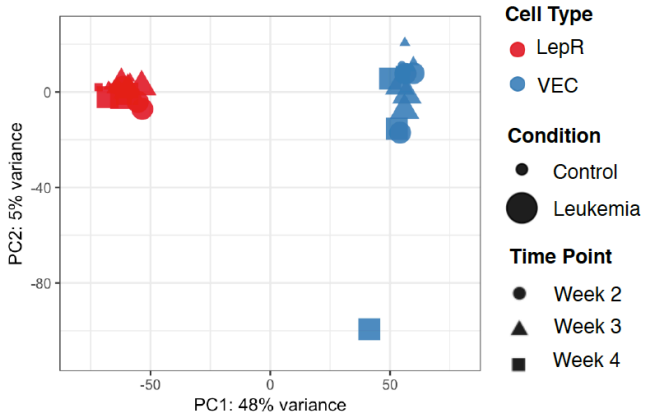
PCA was carried out on niche samples to assess unsupervised clustering based on total gene variance. As seen in figure 4.3.2.a, variance on the Y-axis (PC2) defined inter-sample differences, whereas X-axis variance (PC1) was driven by differences in cell type (*i.e.* whether a cell was a LepR+ PV or CBM VEC). A single LepR+ PV cell sample from week 4 clustered alongside CBM VECs, and was likely a result of incorrect indexing during the sample preparation step. This sample was excluded from subsequent analyses after additional confirmation steps.

Figure 4.3.2.b depicts PCA based on the top 500 variable genes excluding the outlier LepR+ PV sample. Samples displayed weaker variance on the Y-axis (PC2) after selecting for the top variable genes, but retained X-axis (PC1) variance. From this analysis it was not possible to visualise significant inter-sample variance, therefore PCA was ran again on individual cell types (figure 4.3.2.c). From this, X-axis (PC1) variance in both cell types appeared driven by sample conditioning (*i.e.* whether a cell population is derived from a control or leukemic mouse).

4.3.2.a



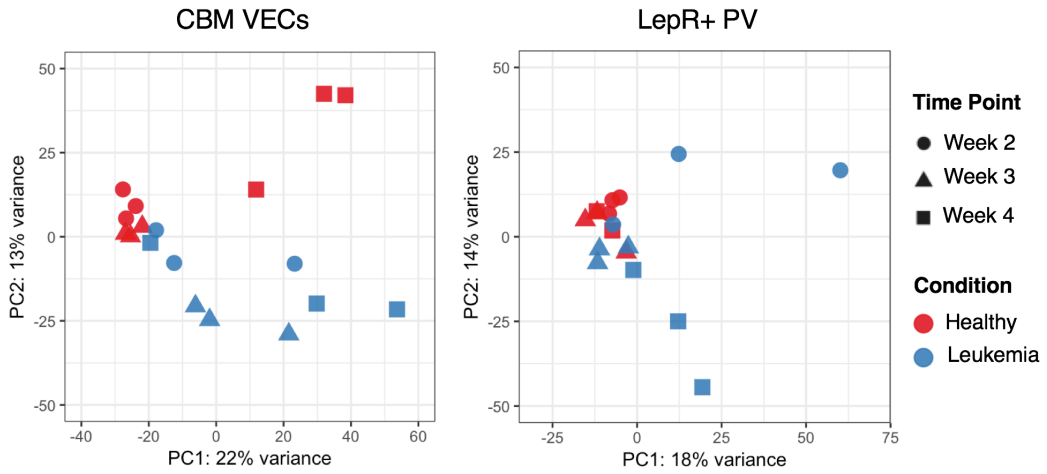
4.3.2.b



PCA of niche populations during leukemia

4.3.2.a. PCA of VEC and LepR+ PV niche populations in control and leukemic mice. PCs were calculated based on total gene. **4.3.2.b.** PCA of VEC and LepR+ PV niche populations from control and leukemic mice, separated by time point. PCs were calculated based on the top 500 variable genes.

4.3.2.c



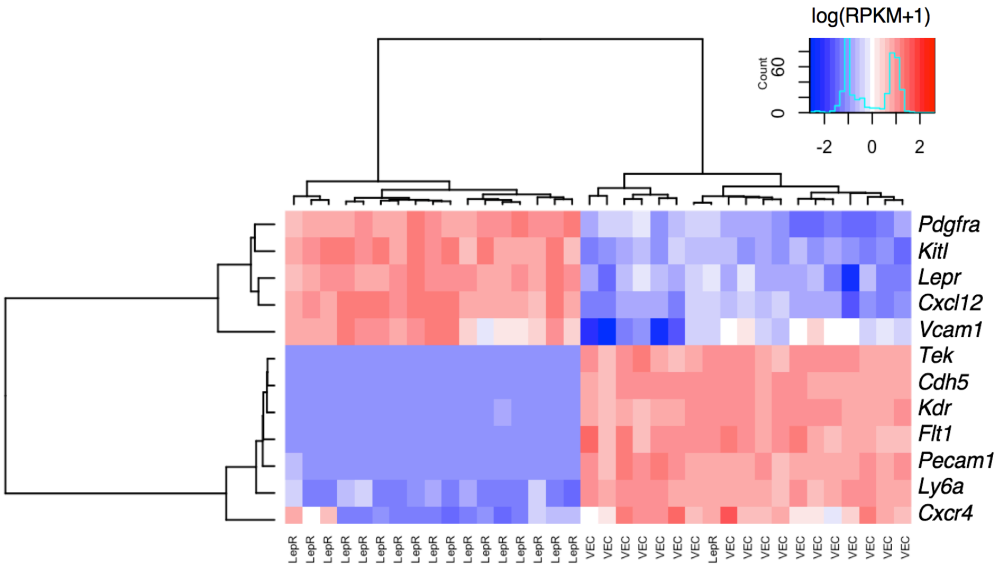
PCA of niche populations during leukemia

4.3.2.c. PCA of VEC and LepR+ PV niche populations from healthy and leukemic mice. Niche populations were plotted separately and PCs calculated based on top 500 variable genes.

4.3.3. Heatmap quality check using known niche genes

Supervised clustering of niche populations was carried out on all samples using known niche genes for VEC and LepR+ PV cell types. CBM VECs clustered together based on their expression of *Tek*, *Cdh5*, *Kdr*, *Flt1*, *Pecam1*, *Ly6a* and *Cxcr4*. In contrast, LepR+ PV cells, clustered together based on their expression of *Pdgfra*, *Kitl*, *Lepr*, *Cxcl12* and *Vcam1*. This analysis confirmed that, with the exception of one sample, the populations being used for subsequent analyses represented the cell types that were isolated by FACS.

4.3.3.a



Heatmap quality check using known niche genes

4.3.3.a. Supervised clustering of niche populations using genes that identify VEC and LepR+ PV cells. Expression values are represented as log(RPKM+1) .

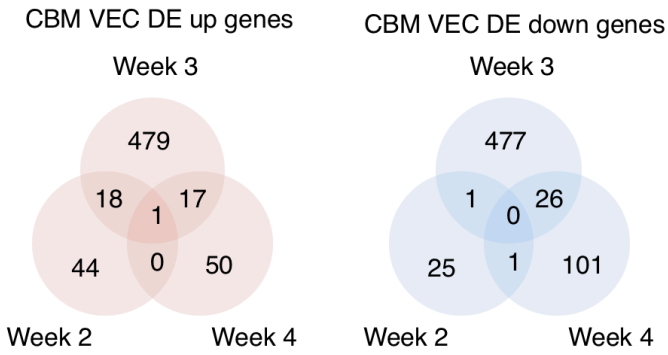
4.3.4. Differential gene expression analysis of niche cells during leukemia

Differential gene expression analysis was carried out, comparing CBM VECs and LepR+ PV cells at each time point of leukemic development, to time-matched, non-transplanted controls. Figures 4.3.4.a and 4.3.4.b summarise the numbers of up- and down-DEGs with an adjusted $p \leq 0.05$ from each population.

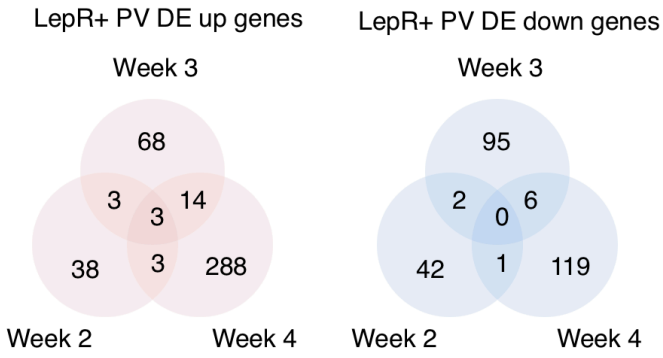
The majority of transcriptional changes within CBM VECs occurred at week 3, whereas LepR+ PV cells expressed a greater number of DEGs at week 4. Of note, both niche populations expressed few overlapping genes between time points. Leukemic CBM VECs consistently overexpressed the gene *Pgf*, but did not share any down-regulated genes. LepR+ PV cells expressed three shared up-regulated genes between time points, including *Ramp1*, *Anxa*3 and *Bhlhe41*, but shared no

down regulated genes. The lack of overlapping genes observed between time points in both populations implied that leukemogenesis may have required highly stage-dependent transcriptional events in order to successfully propagate.

4.3.4.a



4.3.4.b



Differential gene expression analysis of niche cells during leukemia

Overlapping up- and down- DEGs (adjusted $p \leq 0.05$) from VECs (**4.3.4.a**) and LepR+ PV cells (**4.3.4.b**) after 2, 3 and 4 weeks of leukemic development.

4.3.5. Process network enrichment analysis of CBM VECs and LepR+ PV cells during leukemia

Using Metacore, process network analysis was carried out on CBM VECs and LepR+ PV cells at weeks 2, 3 and 4 of leukemic development. DEGs with an adjusted $p \leq 0.05$ were used as input for this analysis. All process networks shown have a $p \leq 0.05$ and FDR$\leq$0.05.

Based on the data presented in table 4.3.5.a, it was observed that CBM VECs during leukemia consistently enriched for blood vessel morphogenesis, cytoskeleton remodelling and angiogenic process networks at weeks 2, 3 and 4. This was consistent with the immunophenotypic remodelling of CBM vasculature observed earlier (see Chapter 3, figure 3.5.d). The majority of process network enrichment in CBM VECs occurred after 3 weeks, and coincided with the major immunophenotypic and functional changes to endogenous HSPC and leukemic populations. CBM VECs also upregulated several pro-inflammatory networks including IL-6, IL-4 and the JAK-STAT pathway. Moreover, there were numerous process networks related to cell adhesion, which extended to integrin priming, leukocyte chemotaxis, cell matrix interactions and platelet aggregation.

Table 4.3.5.b outlines the significantly enriched process networks present in LepR+ PVs at weeks 3 and 4 post-transplantation. Due to the significance criteria used during this analysis ($p \leq 0.05$, FDR$\leq$0.05), there were no statistically significant enriched process networks after 2 weeks in LepR+ PV cells. At week 3 however, these cells enriched for 2 processes including cytoskeleton remodelling and bone ossification. LepR+ PV cells have osteogenic potential (Zhou et al., 2014) and therefore the enrichment of these processes correlated with the immunophenotypic change in OB frequency observed during this model (see chapter 3, figure 3.5.c). By

week 4, OBs expressed networks similar to those found in CBM VECs including adhesion, leukocyte chemotaxis, cell cycle and proliferation.

4.3.5.a

Time Point	*Process Network*	*-log(p-value)*
Week 2	Development_Blood vessel morphogenesis	2.96
	Reproduction_Spermatogenesis, motility and copulation	2.96
	Protein folding_Response to unfolded proteins	2.84
	Proteolysis_Connective tissue degradation	2.82
	Signal transduction_WNT signalling	2.81
	Inflammation_Kallikrein-kinin system	2.71
Week 3	Cell adhesion_Platelet-endothelium-leucocyte interactions	7.24
	Immune response_Phagocytosis	6.11
	Inflammation_NK cell cytotoxicity	3.86
	Reproduction_Feeding and Neurohormone signalling	3.7
	Proliferation_Positive regulation cell proliferation	3.33
	Development_EMT_Regulation of epithelial-to-mesenchymal transition	3.23
	Cytoskeleton_Actin filaments	3.01
	Cell adhesion_Integrin-mediated cell-matrix adhesion	2.86
	Development_Blood vessel morphogenesis	2.78
	Signal Transduction_TGF-beta, GDF and Activin signalling	2.66
	Cell adhesion_Cell-matrix interactions	2.61
	Cell adhesion_Leucocyte chemotaxis	2.53
	Inflammation_IL-4 signalling	2.53
	Cell adhesion_Platelet aggregation	2.52
	Cytoskeleton_Regulation of cytoskeleton rearrangement	2.44
	Inflammation_IL-6 signalling	2.38
	Inflammation_Jak-STAT Pathway	2.36
	Development_Regulation of angiogenesis	2.32
	Cell adhesion_Integrin priming	2.32
	Cytoskeleton_Intermediate filaments	2.24
Week 4	Regulation of epithelial-to-mesenchymal transition	3.19
	Cell adhesion_Platelet-endothelium-leucocyte interactions	2.85
	Proteolysis_ECM remodeling	2.72
	Proliferation_Positive regulation cell proliferation	2.68
	Development_Regulation of angiogenesis	2.66
	Signal Transduction_TGF-beta, GDF and Activin signalling	2.6

	Development_Blood vessel morphogenesis	2.58

Process network enrichment analysis of CBM VECs and LepR+ PV cells during leukemia

4.3.5.a. Metacore analysis of significantly enriched process networks from CBM VECs. DEGs with an adjusted $p \leq 0.05$ were used as input. All process networks shown have a $p \leq 0.05$ and FDR≤0.05. Enrichment is depicted as -log(*p*-value).

4.3.5.b

Time Point	*Process Network*	*-log(p-value)*
Week 3	Development_Ossification and bone remodeling	3.53
	Cytoskeleton_Actin filaments	3.14
Week 4	Development_Blood vessel morphogenesis	8.61
	Cell cycle_Mitosis	5.92
	Reproduction_Progesterone signalling	5.34
	Chemotaxis	4.86
	Cell adhesion_Cell-matrix interactions	4.31
	Cell cycle_Core	3.85
	Proliferation_Positive regulation cell proliferation	3.55
	Regulation of epithelial-to-mesenchymal transition	3.49
	Signal transduction_NOTCH signalling	3.24
	Cell adhesion_Leucocyte chemotaxis	3.06
	Cytoskeleton_Spindle microtubules	2.86
	Anti-Apoptosis mediated by external signals via PI3K/AKT	2.84
	Development_Hedgehog signalling	2.48
	Development_Melanocyte development and pigmentation	2.47

Process network enrichment analysis of CBM VECs and LepR+ PV cells during leukemia

4.3.5.b. Metacore analysis of significantly enriched process networks from LepR+ PV cells. DEGs with an adjusted $p \leq 0.05$ were used as input. All process networks shown have a $p \leq 0.05$ and FDR≤0.05. Enrichment is depicted as -log(*p*-value).

4.3.6. CBM VECs upregulated cell surface receptors and secreted factors during leukemic development

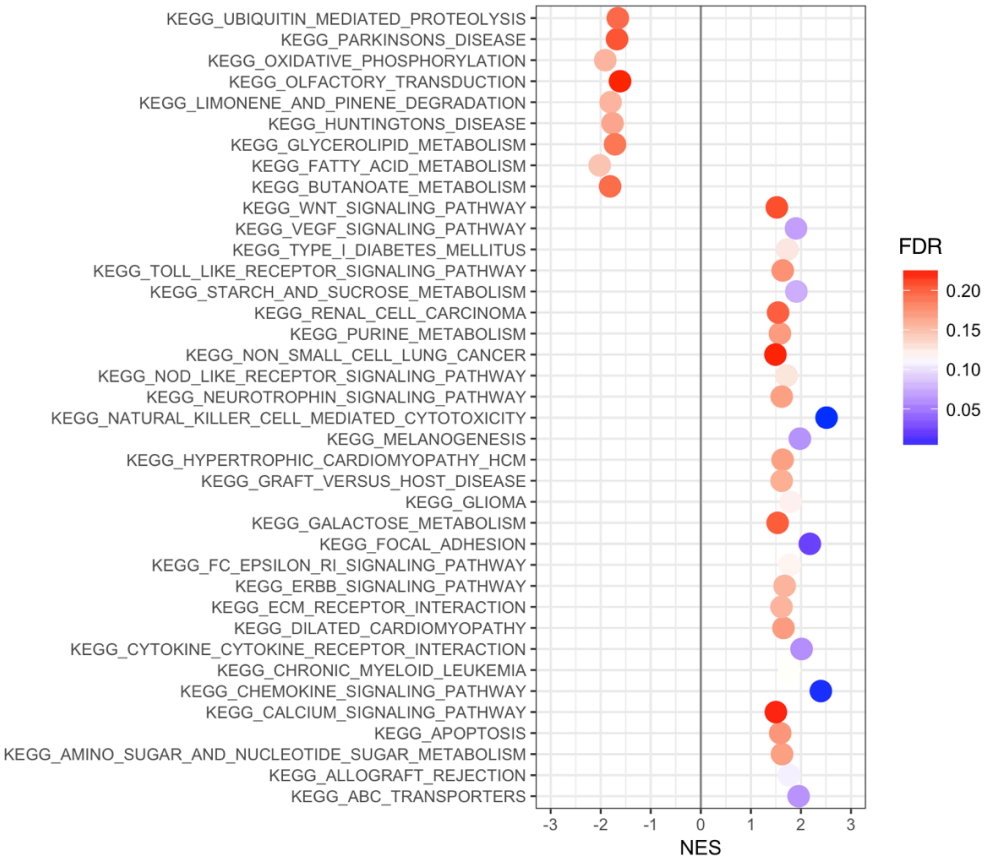
Given that CBM VECs exhibited the majority of their transcriptional changes at a time point where endogenous hematopoietic cells were also significantly perturbed, it was hypothesised that this niche population was reprogrammed by the leukemic BM environment. To verify this, GSEA was run to evaluate KEGG database gene signatures (Kanehisa and Goto, 2000) at week 3 of leukemic development in CBM VECs. Ranked DEGs with an adjusted $p \leq 0.05$ were used as input for this analysis. All gene signatures shown have a $p \leq 0.05$ and FDR$\leq$0.25. Positively enriched gene signatures have a normalised enrichment score (NES) of >0, whereas down-regulated signatures have an NES of <0.

GSEA revealed that several additional pathways were enriched in CBM VECs at the week 3 time point of this AML model. This included cytokine-cytokine receptor interactions, chemokine signalling, VEGF signalling and apoptosis (figure 4.3.6.a). The enrichment of cytokine and chemokine signalling pathways suggested that CBM VECs may have begun aberrantly expressing secreted factors and cell surface receptors in response to the leukemic environment. To investigate this further, leading edge genes from the GSEA analysis were isolated and visualised based on their RPKM expression values, which represents a normalised gene expression value, taking into consideration sequencing depth. Secreted factors identified included *Edn1, Ccl2*, *Tnf*, *Tnfsf11*, *Il12a* and *Tgfb2* (figure 4.3.6.b), and the cell-surface receptors *Cd44*, *Ldlr*, *Cd34*, *Csf3r*, *Tnfrsf9*, *Il17rb* and *Ccr1* (figure 4.3.6.c).

Taken together, these findings suggested that CBM VECs were conditioned during leukemia, which caused an over-expression of secreted factors and cell surface receptors. Moreover, enrichment of morphogenic and apoptotic molecular

pathways, in conjunction with the previous immunophenotypic observations, suggested that CBM VECs likely underwent significant physical remodelling during leukemia development.

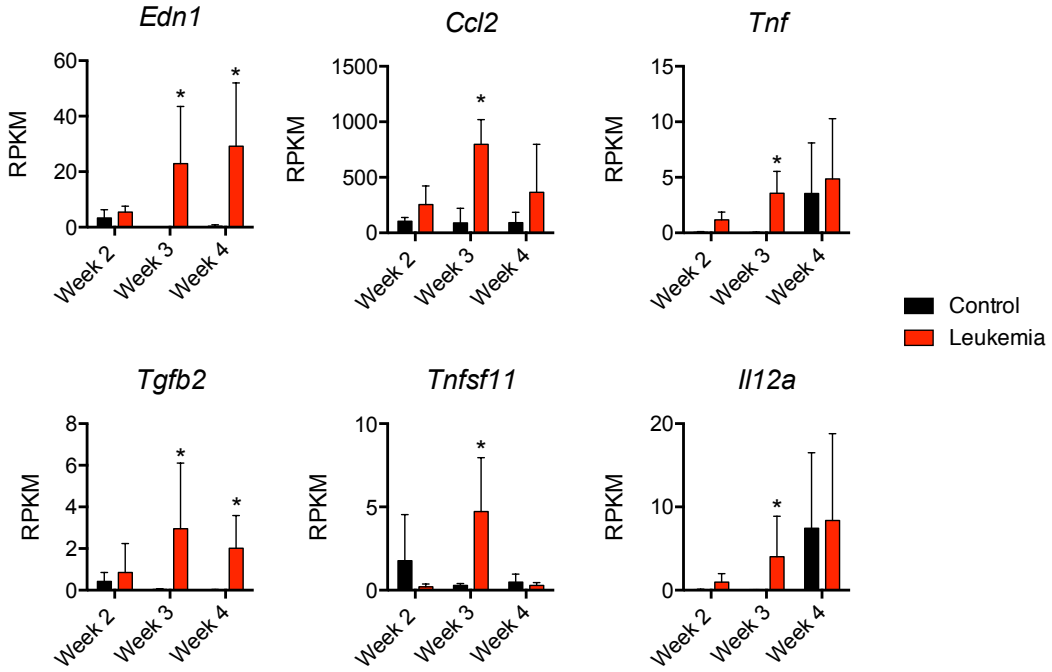
4.3.6.a



CBM VECs upregulated cell surface receptors and secreted factors during leukemic development

4.3.6.a. Preranked GSEA of KEGG gene signatures enriched in CBM VEC DEGs with an adjusted $p \leq 0.05$ after 3 weeks post-transplantation. Gene signatures shown were significantly enriched with a $p \leq 0.05$ and FDR≤0.25. Positively enriched gene signatures have a normalised enrichment score (NES) of >0, whereas down-regulated signatures have an NES of <0.

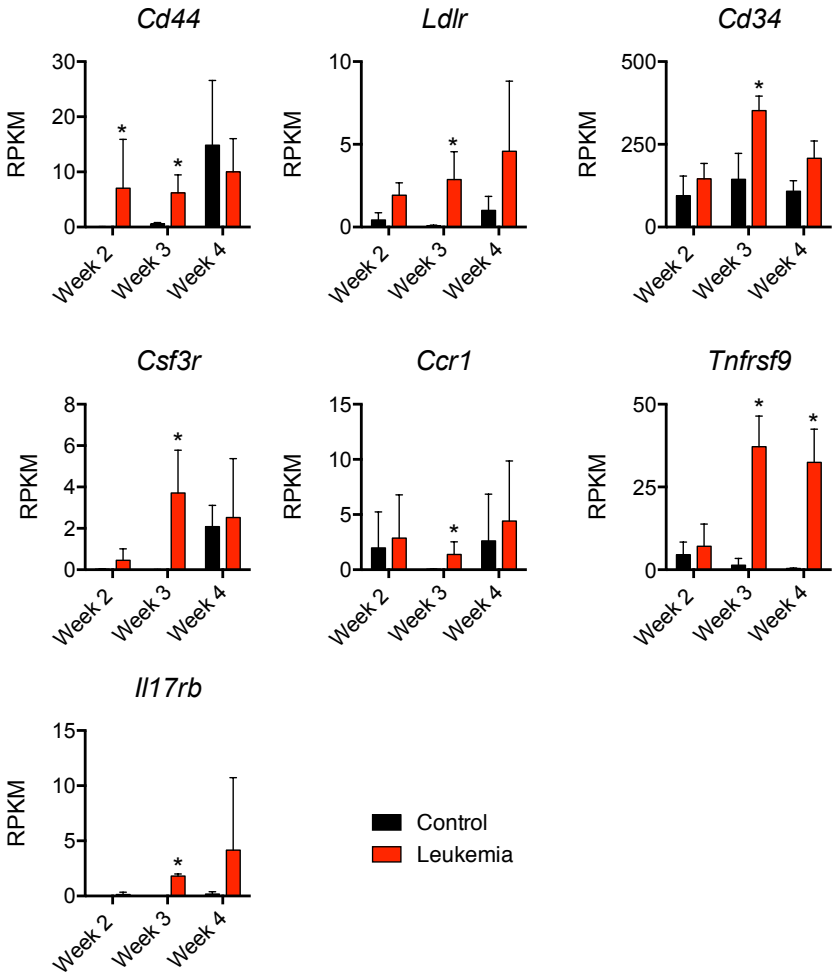
4.3.6.b



CBM VECs upregulated cell surface receptors and secreted factors during leukemic development

4.3.6.b. RPKM expression values of leading edge GSEA secreted factor genes from CBM VECs at weeks 2, 3 and 4 in leukemia-transplanted and non-leukemia transplanted, time matched controls (*adjusted $p \leq 0.05$ as determined by DESeq2). Mean±SD, N=3 from one experiment.

4.3.6.c



CBM VECs upregulated cell surface receptors and secreted factors during leukemic development

4.3.6.c. RPKM expression values of leading edge GSEA cell surface receptor genes from CBM VECs at weeks 2, 3 and 4 in leukemia-transplanted and non-leukemia transplanted, time matched controls (*adjusted $p \leq 0.05$ as determined by DESeq2). Mean±SD, N=3 from one experiment.

4.4 Droplet-based scRNA-seq of unfractionated, non-hematopoietic BM cells

Droplet-based scRNA-seq was utilised to evaluate BM niche heterogeneity at steady state. To achieve this, 5300 BL and 5300 CBM niche cells (CD45- TER119- 7AAD-) were isolated by FACS from young mice (~2 month), and used for droplet based scRNA-seq (see Materials and methods, section 2.1.8). In total, 5785 unfractionated niche cells were captured and sequenced. After computational filtering (see Materials and methods, section 2.3.2), 3342 cells remained, expressing an average of 2082 genes and 5993 unique molecular identifiers (UMIs).

4.4.1. scRNA-seq of non-hematopoietic cells revealed significant cellular heterogeneity

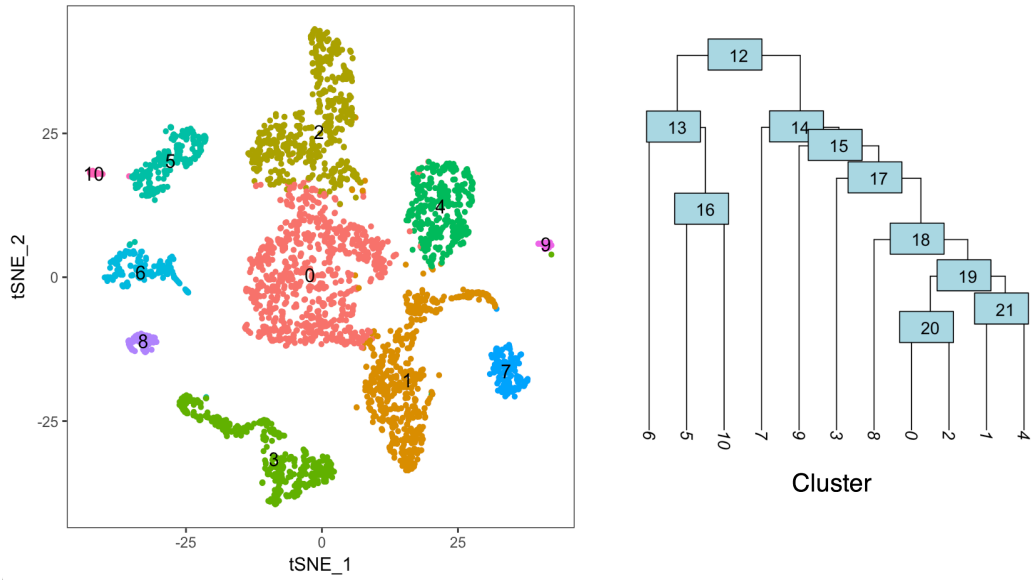
As seen in figure 4.4.1.a, there were 11 non-hematopoietic populations present in the BM of young mice. Differential gene expression analysis was carried out using a negative binomial statistical test. The top DEGs (adjusted $p \leq 0.05$, LogFC$\geq$0.25) from each cell cluster can be seen in figure 4.4.1.b as a heatmap.

LepR+ PV cells, PαS MSCs and VECs were visualised based on their expression of *Lepr*, *Pdgfra* and *Pecam1*, respectively (figures 4.4.1.c and 4.4.1.a). Cluster 1 was marked by high levels of *Tnmd*, or Tendomodulin, which is predominantly expressed by tendon and ligament tissues (Brandau et al., 2001). Cluster 2 was likely a chondrocytic progenitor population due to its expression of *Lect1*, *Prg4*, *Cytl1* and *Acan*. *Lect1* in particular is expressed by chondrocytes and plays an important role in endochondrial bone formation (Shukunami et al., 2001). Cluster 0 expressed genes that have previously been described in osteoprogenitor and MSC populations including *Spp1* and *Myoc* (Oldberg et al., 1986; Kwon et al., 2013). In contrast, cluster 8 differentially expressed genes related to muscle tissue

such as *Myf5* and *Des* (Ott et al., 1991; Lazarides et al., 1976). Despite efforts to exclude hematopoietic populations from this analysis (see Materials and methods, section 2.3.2), clusters 5, 6 and 10 expressed genes commonly found in pre-B lymphocyte and myeloid progenitor cell types, including *Cd79a*, *Vpreb3*, *Mpo*, *Fcer1g* and *Ebf1* (Mason et al., 1991; Pinkus and Pinkus, 1991; Holtschke et al., 1996; Shirasawa et al., 1993). This assumed hematopoietic identity was confirmed using phylogenetic clustering constructed based on PCA, which demonstrated that clusters 5, 6 and 10 also shared a close transcriptional relationship, separating at node 12 from other cell populations (figure 4.4.1.a, right panel).

Overall, non-hematopoietic cellular heterogeneity within the BM was extensive, and consisted of numerous cell types including muscle cells, vascular endothelium, LepR+ PV cells, MSCs and OB progenitors.

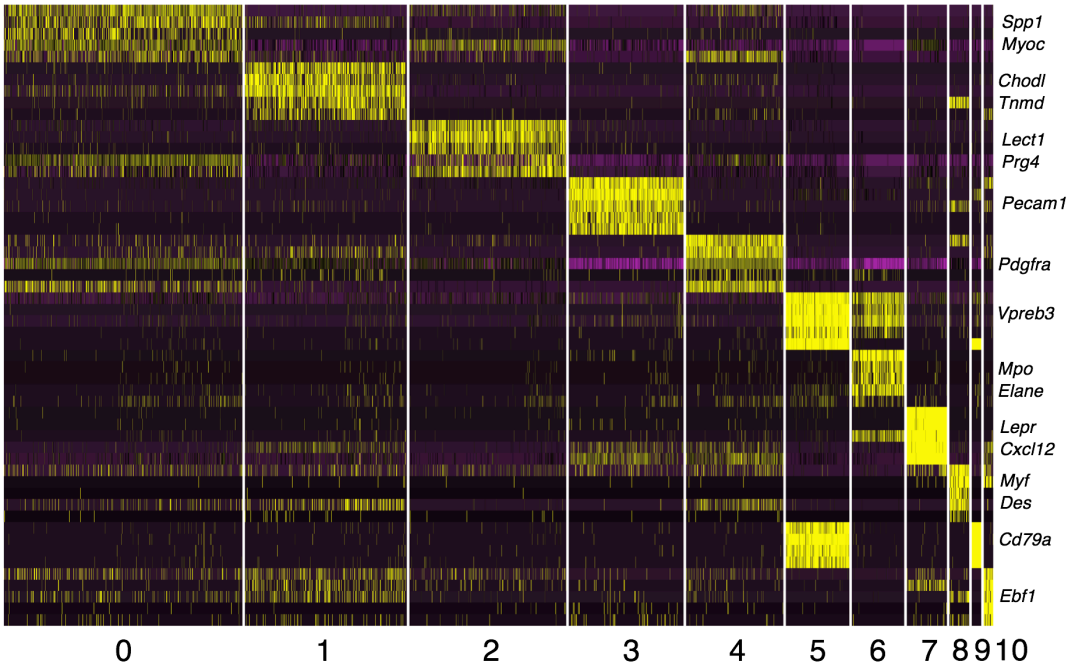
4.4.1.a



scRNA-seq of non-hematopoietic cells revealed significant cellular heterogeneity

4.4.1.a. tSNE plot displaying 3342 filtered, non-hematopoietic BL and CBM cell niche populations isolated from young (~2 month) mice. Phylogenetic tree constructed in PCA space and ordered by cluster.

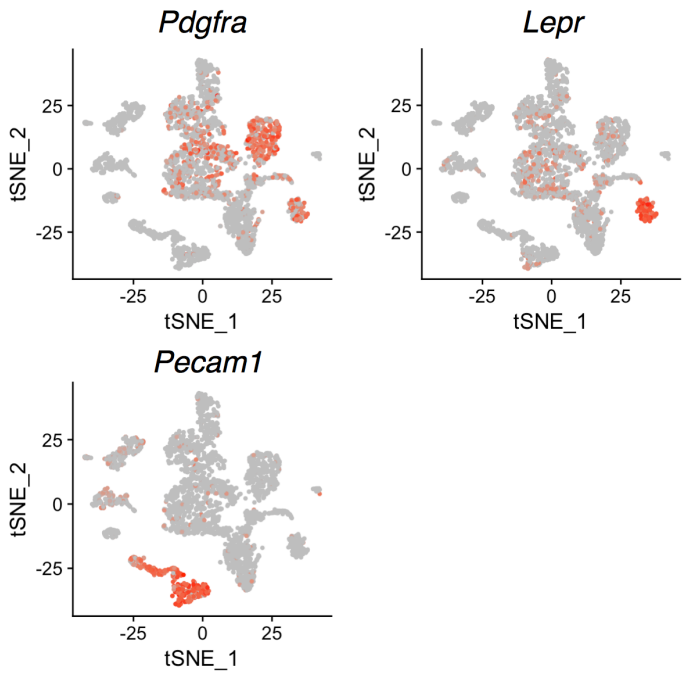
4.4.1.b



scRNA-seq of non-hematopoietic cells revealed significant cellular heterogeneity

4.4.1.b. Heatmap of top DEGs from each cell population. Differential gene expression analysis was performed using a negative-binomial statistical test (adjusted $p \leq 0.05$ and LogFC$\geq$0.25).

4.4.1.c



scRNA-seq of non-hematopoietic cells revealed significant cellular heterogeneity

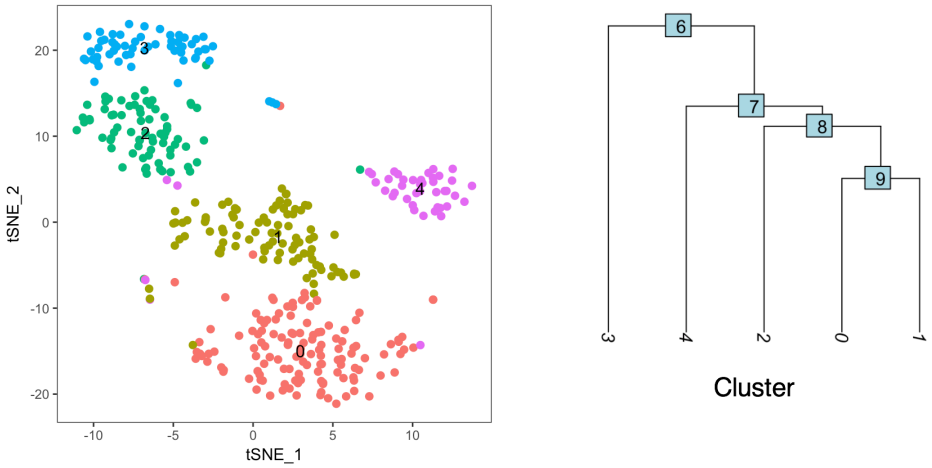
4.4.1.c. Expression of *Pdgfra*, *Lepr* and *Pecam1*, gene markers of PαS MSCs, LepR+ PV cells and VECs, respectively. Red highlights expression within specific clusters of tSNE plots.

4.4.2. BM VECs comprised five transcriptionally distinct populations

Given that VECs were differentially affected during leukemia (see Chapter 3, figures 3.5.c and 3.5.d), and also appeared to be highly heterogenous at steady state (figures 4.4.1.a and 4.4.1.c), these cells were investigated further at the single cell level. Upon being isolated and reclustered, there were 398 BM VECs in total, forming 5 clusters (figure 4.4.2.a), each of which could be labelled by distinct transcriptional markers (figure 4.4.2.b). Phylogenetic clustering also revealed that VECs clustered into two broader populations, separated at node 6 (figure 4.4.2.a, right panel).

Differential gene expression analysis using a negative binomial statistical test (adjusted $p \leq 0.05$, LogFC$\geq$0.25) revealed that VEC sub-populations 0, 1, 2, 3 and 4 could be discriminated using the genes *Timp4, Vwf*, *Ednrb*, *Vcam1* and *Fbln5* (figure 4.4.2.c). Overall, this analysis demonstrated that there was significant, previously unidentified, cellular heterogeneity between BM VECs.

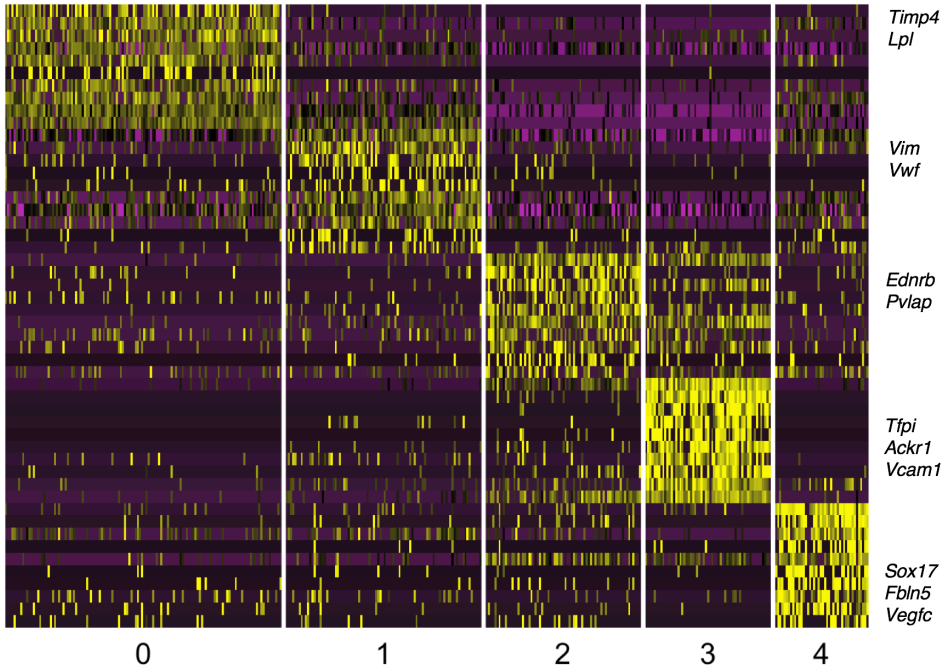
4.4.2.a



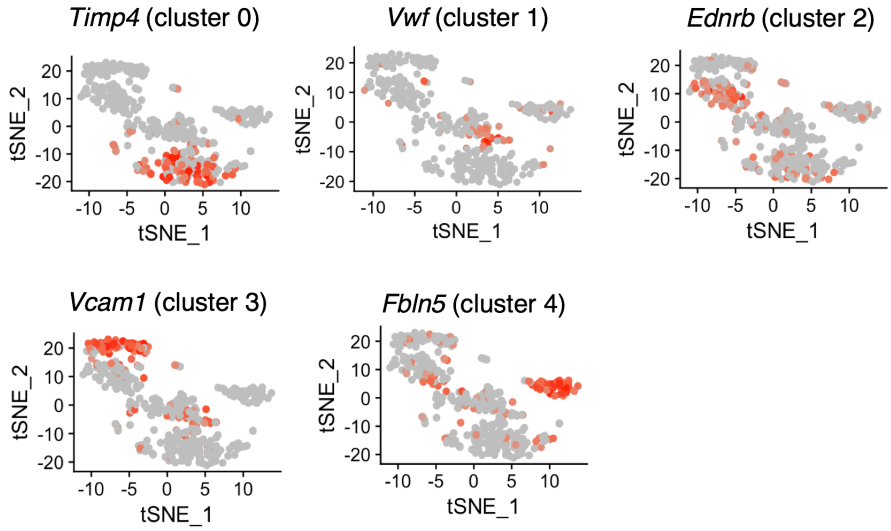
BM VECs comprised five transcriptionally distinct populations

4.4.2.a. tSNE plot of *Pecam1* expressing VECs isolated from total non-hematopoietic compartment cluster number 3. VECs clustered into 5 transcriptionally distinct sub-populations. Phylogenetic tree constructed in PCA space and ordered by cluster.

4.4.2.b



4.4.2.c



BM VECs comprised five transcriptionally distinct populations

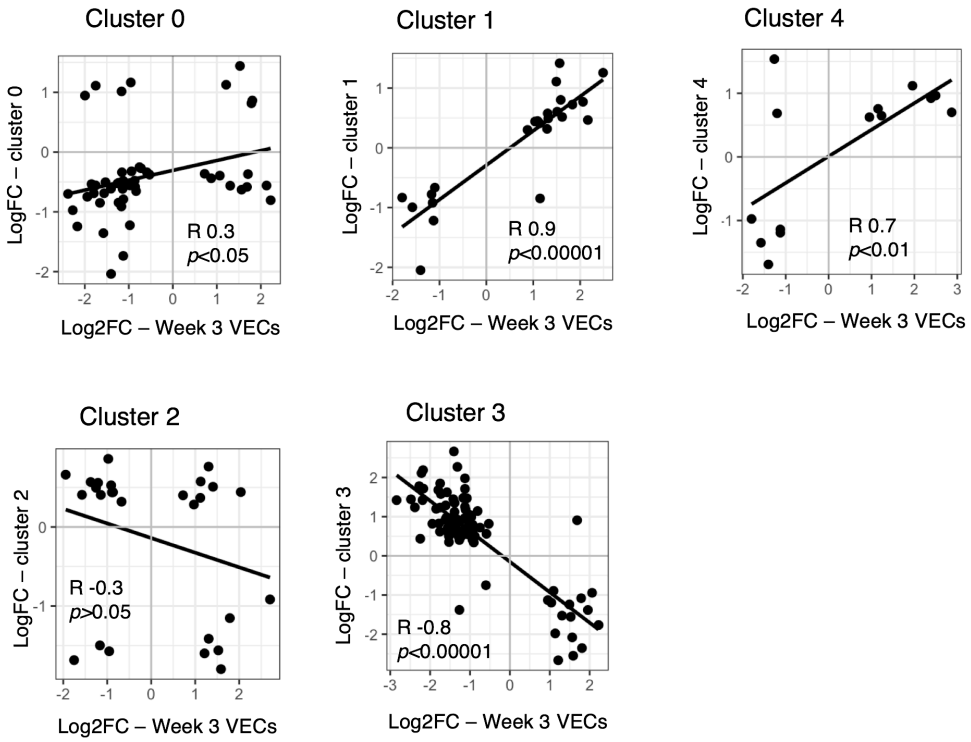
4.4.2.b. Heatmap of top DEGs from each VEC cluster. Differential gene expression analysis was done using a negative-binomial statistical test. Genes shown have an adjusted $p \leq 0.05$ and LogFC$\geq$0.25. **4.4.2.c.** Cluster specific expression of the genes *Timp4*, *Vwf*, *Ednrb*, *Vcam1* and *Fbln5*.

4.4.3. Integrative analysis of scRNA-seq and bulk RNA-seq datasets

During leukemic development, the most significant transcriptional and immunophenotypic changes to vasculature occurred at week 3 (see Chapter 3, figures 3.5.d and 4.3.4.b). Therefore, DEGs (adjusted $p \leq 0.05$) from CBM VECs exposed to leukemia for 3 weeks were correlated against DEGs (adjusted $p \leq 0.05$, LogFC$\geq$0.25) from each VEC cluster identified in figure 4.4.2.a.

For clusters 0, 1 and 4 there was a positive correlation ($p<0.05$, $R>0$) with genes expressed by leukemia exposed CBM VECs. In contrast, clusters 2 and 3 were both inversely correlated ($R<0$), which indicated that genes normally expressed by these clusters at steady state became down regulated during leukemia (figure 4.4.3.a). In particular, cluster 3 displayed a strong negative correlation (R -0.8, $p<0.00001$), which suggested that the loss of this VEC sub-population during leukemia was highly likely on a transcriptional level. Collectively, this analysis demonstrated that certain VEC sub-populations were transcriptionally down-regulated by CBM VECs during leukemia at the mid-point of disease development.

4.4.3.a



Integrative analysis of bulk and scRNA-seq datasets revealed transcriptional down regulation of certain VEC sub-populations during leukemia

4.4.3.a. Correlation analysis of DEGs with an adjusted $p \leq 0.05$ from VECs exposed to leukemia for 3 weeks (Log2FC – Week 3) against DEGs with an adjusted $p \leq 0.05$ and LogFC$\geq$0.25 expressed by VEC clusters 0, 1, 2, 3 and 4 at steady state. Pearson correlation coefficient R and *p* values are displayed for each plot.

4.4.4. VCAM1 demarcated a population of VECs that were immunophenotypically depleted during leukemia

DEGs from CBM VECs at week 3 of leukemic development negatively correlated with VEC cluster 3 at steady state (figure 4.4.3.a). Upon closer inspection of the genes that comprised this negative correlation, it was observed that *Vcam1* was transcriptionally down-regulated in CBM VECs at week 3 post-transplantation (figure

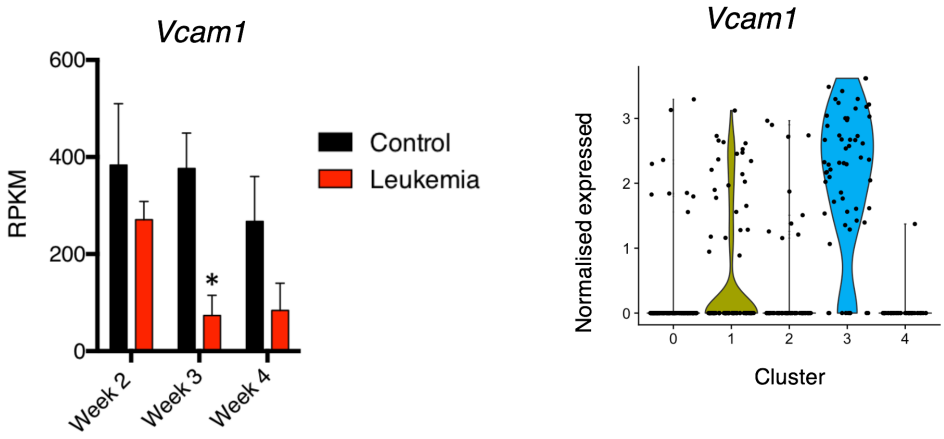
4.4.4.a). There was also a trending decrease at weeks 2 and 4, however this was not statistically significant. Given that VCAM1 is an established marker of BM endothelium (Sipkins et al., 2005), and was also capable of labelling a sub-population of VECs at steady state (figures 4.4.2.c and 4.4.4.b), it was hypothesised that this population became depleted during leukemia.

To evaluate this, the expression of VCAM1 as a percentage of CD31+ CBM and BL VECs in healthy mice was measured using flow cytometry. Based on figure 4.4.4.c, VCAM1 appeared to resolve vascular heterogeneity, but did not label discrete populations. CD31+ VECs were therefore categorised as being either VCAM1-, VCAM1^{lo} or VCAM1^{hi}. Healthy CBM VECs were comprised of 30.5±7.3% VCAM1^{hi}, 50.5±3.8% VCAM1^{lo} and 13.8±5.4% VCAM1-. In contrast, the majority (72.8±5%) of BL VECs were VCAM1- and only 20.9±4.5% and 2.8±0.3% were VCAM1^{lo} and VCAM1^{hi}, respectively (figure 4.4.4.d). Given that the majority of VCAM1^{hi} expression was confined to CBM VECs, VCAM1 appeared to act as a proxy for discriminating sinusoidal (CBM) from arteriolar (BL) VECs.

The proportion of VCAM1 expressing VECs as a percentage of CD31+ was next investigated at the 3 week time point of leukemic development (figure 4.4.4.e). This stage was chosen as it represented a time point where both CBM VECs and BL VECs were impacted immunophenotypically (see Chapter 3, figures 3.5.c and 3.5.d). VCAM1^{hi} expressing CBM VECs decreased significantly in response to leukemia (7.5±2.3% vs. 30.5±7.3%, $p \leq 0.01$), which resulted in a proportional increase of VCAM1- cells (42±7.4% vs. 13.8±5.4, $p \leq 0.01$), but caused no change to VCAM1^{lo} cells (45.7±4.6 vs. 50.5±3.8%, $p > 0.05$). BL VECs also experienced a decrease in VCAM1^{hi} expressing cells (0.96±0.3% vs. 2.8±0.3%, $p \leq 0.01$), as well as expanded VCAM1^{lo} cells (20.9±4.5% vs. 12.7±3.4%, $p \leq 0.05$). However, the starting VCAM1^{hi}

expressing population in control BL VECs represented only a fraction of total CD31+ cells. Taken together, these data strongly suggested that, in addition to being transcriptional perturbed, VCAM1 expressing VECs were also immunophenotypically remodelled during leukemia. Given that VCAM1 expressing VECs were likely sinusoidal (CBM), whereas VCAM1^{lo} and VCAM1- VECs were arteriolar (BL), these findings further validated the earlier immunophenotypic data from chapter 3, which identified a differential change in VEC frequency during leukemic development. (see Chapter 3, figures 3.5.c and 3.5.d).

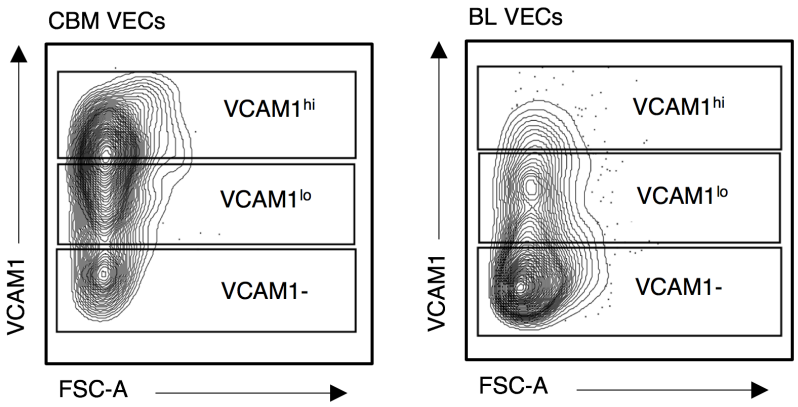
4.4.4.a **4.4.4.b**



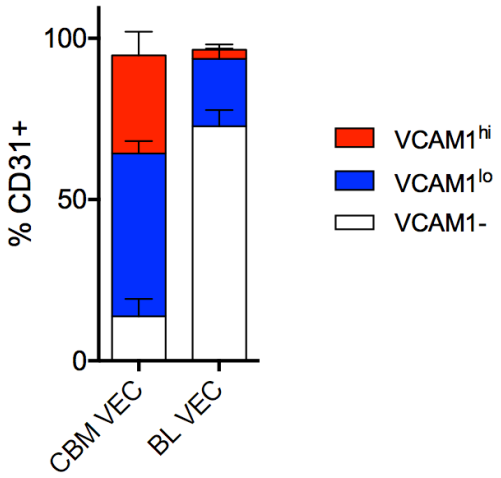
VCAM1 demarcated a population of VECs that were immunophenotypically depleted during leukemia

4.4.4.a. RPKM expression values for *Vcam1* in CBM VECs during leukemic development at weeks 2, 3 and 4 (*adjusted $p \leq 0.05$ as determined by DESeq2). Mean±SD, N=3 from one experiment. **4.4.4.b.** Normalised expression of *Vcam1* in VEC clusters 0, 1, 2, 3 and 4 at steady state.

4.4.4.c



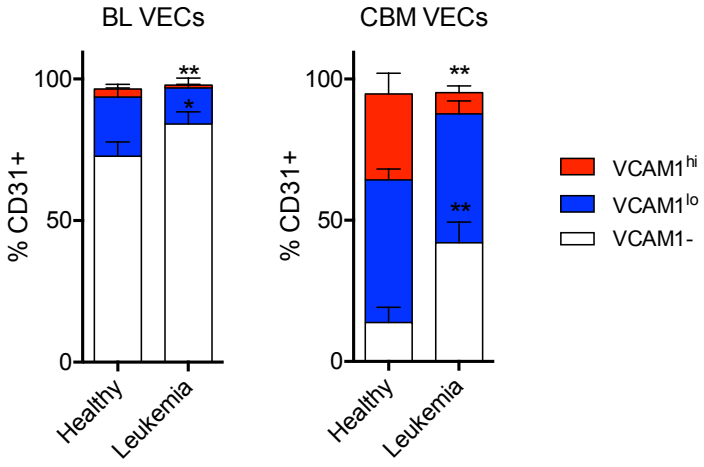
4.4.4.d



VCAM1 demarcated a population of VECs that were immunophenotypically depleted during leukemia

4.4.4.c. Flow cytometry gating strategy used to define VCAM1 expression in CD31+ CBM and BL VECs in healthy mice. Gates shown were taken from TER119- CD45- 7AAD- CD31+ cells. **4.4.4.d.** Frequency of VCAM1-, VCAM1^{lo} and VCAM1^{hi} as a percentage of total CD31+ VECs from BL and CBM niches of healthy mice. Mean±SD, N=5 from one experiment.

4.4.4.e



VCAM1 demarcated a population of VECs that were immunophenotypically depleted during leukemia

4.4.4.e. Proportion of VCAM1-, VCAM1^{lo} and VCAM1^{hi} expressing CD31+ CBM and BL VECs from 3 week leukemia-transplanted and non-leukemia transplanted control mice. Mean±SD, N=3 from one experiment. A two-tailed unpaired *t*-test was used to determine significance, comparing leukemia-transplanted to non-transplanted, time-matched, sub-lethally irradiated controls (*$p \leq 0.05$, **$p \leq 0.01$).

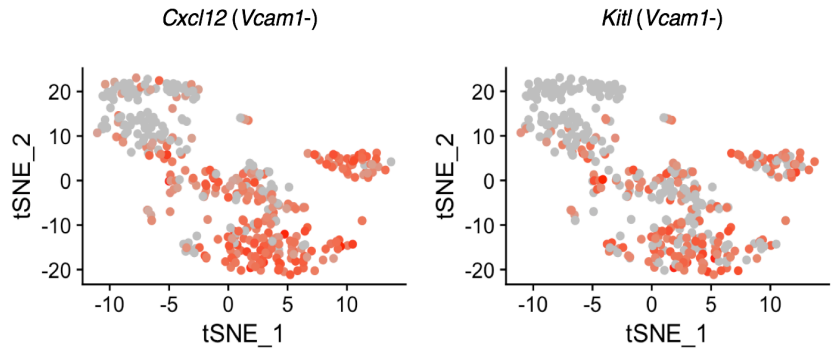
4.4.5. Differential gene expression analysis comparing *Vcam1* negative and positive VECs

During leukemia, the proportion of VCAM1^{hi} expressing VECs decreased, whereas VCAM1- VECs increased, suggesting that there was cell-specific remodelling in response to leukemic development. Therefore, to investigate these populations further, differential gene expression analysis using a negative binomial statistical test was carried out (adjusted $p \leq 0.05$, LogFC≥ 0.25), comparing *Vcam1* negative and *Vcam1* positive VEC populations.

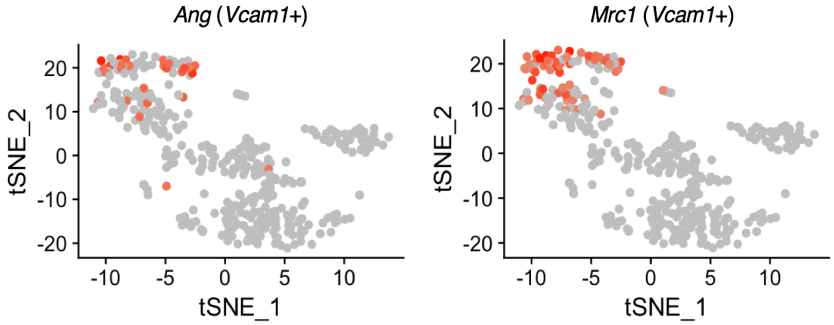
Vcam1 negative VECs expressed several important niche related factors including *Kitl* and *Cxcl12* (figure 4.4.5.a). In contrast, *Vcam1* positive VECs

expressed *Mrc1* and *Ang* (figures 4.4.5.b), the latter of which was formerly described as being responsible for maintaining HSC quiescence, and enhancing LT-HSC reconstitution capacity (Goncalves et al., 2016; Silberstein et al., 2016).

4.4.5.a



4.4.5.b



Differential gene expression analysis comparing *Vcam1* negative and positive VECs

4.4.5.a. Expression of *Cxcl12* and *Kitl* in *Vcam1*- VEC sub-populations at steady state. **4.4.5.b.** Expression of *Ang* and *Mrc1* in *Vcam1*+ VEC sub-population at steady state. Markers were identified by differential gene expression analysis comparing *Vcam1*- and *Vcam1*+ VECs with a negative binomial statistical test (adjusted $p \leq 0.05$, LogFC$\geq$0.25).

4.4.6. *Vcam1* positive VECs expressed a transcriptional profile consistent with sinusoidal endothelial cells

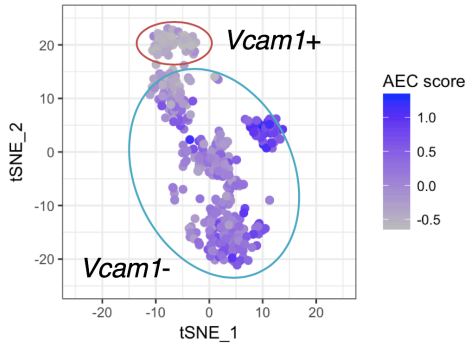
A recent publication demonstrated that arteriole endothelial cells (AECs) and sinusoidal endothelial cell (SECs) are transcriptionally distinct (Xu et al., 2018). SECs were demonstrated to express *Vcam1*, whereas AECs expressed the majority of endothelial-derived *Cxcl12* and *Kitl,* a finding that parallels what was observed during this present study (figure 4.4.5.a). Therefore, AEC- and SEC-specific gene sets were exported from Xu et al., (2018) and were used to score VECs at the single cell level using the Seurat::AddModuleScore function. AEC genes were more predominantly expressed by *Vcam1* negative VECs (figure 4.4.6.a), whereas SEC genes were expressed by *Vcam1* positive VECs (figure 4.4.6.b). Indeed, this was also confirmed using a phylogenetic tree, which demonstrated that *Vcam1* expressing VEC cluster 3 was transcriptionally separate from *Vcam1*- clusters 0, 1, 2 and 4 at node 6 (figure 4.4.2.a, right panel).

BL and CBM cells used in this analysis were isolated and processed separately before being merged computationally. Therefore, the original identities of CBM and BL VECs were plotted against the assumed distribution of SECs and AECs. As seen in figure 4.4.6.c, VECs isolated from the CBM portion of the niche localised in the SEC gene set enriched region of the tSNE plot, whereas BL VECs mainly localised in AEC gene enriched regions. Interestingly, a high proportion of BL VECs also appeared in areas enriched for SEC genes. However, this was likely due to the processing technique used to isolate VECs.

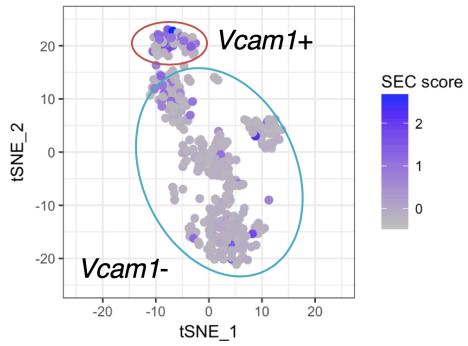
Collectively, these analyses implied that *Vcam1* negative VECs were likely arteriolar, whereas *Vcam1* positive VECs were sinusoidal. This also indicated that

AECs, also referred to as BL VECs, expanded in frequency during leukemia, an effect which may have resulted in the over-expression of important niche related factors.

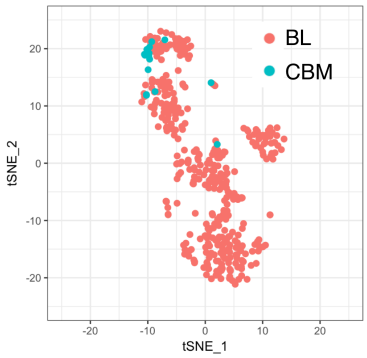
4.4.6.a



4.4.6.b



4.4.6.c



***Vcam1* positive VECs express a transcriptional profile consistent with sinusoidal endothelial cells**

4.4.6.a. Gene score of AEC-related genes in total CD31+ VECs. **4.4.6.b.** Gene score of SEC-related genes in total CD31+ VECs. **4.4.6.c.** tSNE plot labelling VECs based on their original cellular location within the BM. Gene scoring was done using the Seurat::AddModuleScore function.

4.5. Summary and discussion

The global gene expression profiles of endogenous HSPCs during leukemic development has not, to our knowledge, been formerly investigated. Therefore, the findings discussed within this chapter represent a comprehensive and novel overview of how these populations change transcriptionally in response to leukemogenesis. Early in leukemic development, significant transcriptional changes were confined to the pGM compartment (figure 4.2.4.a), which after 3 weeks extends to CFUE, pCFUE and erythroid biased MPP2 cells (figure 4.2.4.b; Pietras et al., 2015). In line with the immunophenotypic and functional observations made in chapter 3, endogenous HSCs and MPPs remained relatively unaffected transcriptionally (figure 3.4.2.c). This lack of transcriptional activity suggested that leukemic populations had limited contact with HSCs, proposing that LICs may have occupied distinct niches to those required by more primitive cell types. Indeed, LICs within the present model express an immunophenotype consistent with that of a committed myeloid progenitor, rather than an HSC (see chapter 2, figure 3.2.b; Kirstetter et al., 2008). This is also validated by numerous studies that have demonstrated the existence of distinct HSC and progenitor specific niches (Ding and Morrison, 2013; Hérault et al., 2017). If true of the present model, these findings would also explain why transcriptional changes were confined to the pGM compartment at the early stages of this disease onset.

Inflammatory and chemotactic signalling process networks were consistently enriched amongst numerous HSPC and niche populations, which strongly suggested that the microenvironment within the BM during this model was pro-inflammatory. This included the enrichment of IL-6 and IL-4 molecular processes. Moreover, GSEA of CBM VECs at the week 3 time point of this model were significantly enriched for cytokine-cytokine receptor interaction and chemokine signalling pathways (figure

4.3.6.a). Closer inspection of the genes that comprised the leading edge of this analysis revealed the overexpression several secreted molecules including *Tnf*, *Ccl2*, *Edn1* and *Tgfb2*, as well as the cell surface receptors *Ccr1* and *Tnfrsf9* (figures 4.3.6.c and 4.3.6.d). *Ccl2* was recently reported as a stromal-derived secreted factor important for AML proliferation and transmigration (Macanas-Pirard et al., 2017, Binato et al., 2015). Furthermore, the endothelial-specific over-expression of *Edn1* has formerly been demonstrated to promote chemoresistance and survival in chronic lymphocytic leukemia (Maffei et al., 2014). Both *Edn1* and *Ccl2* are over-expressed by CBM VECs after 3 and 4 weeks during this AML model, suggesting that leukemia-induced conditioning of the niche occurred after prolonged exposure. Interestingly, *Tnf* was recently reported as a potent, niche-derived negative regulator of HSCs, whose inhibition during leukemia was sufficient to partially rescue normal hematopoietic cell function (Mead et al., 2017). In this present study, however, there was no observable decrease in HSC frequency, nor defects in long-term functionality at the early- and mid-stages of leukemic development (see Chapter 3, figures 3.3.1.a and 3.4.2.c). However, TNFα was also recently reported as an effective inhibitor of erythropoiesis during ageing (Mei et al., 2018), which may account for the depletion of erythroid progenitors and eventual onset of anemia during this model of AML. Taken together, these findings strongly suggested that reprogramming of the niche played a significant role in the disruption of normal hematopoiesis, however the exact mechanism is yet to be determined.

Recent work completed by Zambetti et al., (2016) provided the first evidence for leukemic predisposition as a consequence of niche-derived inflammatory signalling. From this report, it was concluded that niche-derived secreted factors were responsible for causing genotoxic stress within HSPC populations, resulting in

leukemic susceptibility. As previously eluded to, endogenous myeloid progenitor populations in the reported model appeared to expand after prolonged exposure to the leukemic environment. It is therefore possible that pro-inflammatory secreted factors released by either the niche or leukemic cells induced myeloid progenitor expansion. Indeed, the link between enhanced myeloid output and inflammation has formerly been described through studies investigating immune system replenishment (Nagai et al., 2006) and cytokine-mediated hematopoietic lineage commitment (Rieger et al., 2009). Furthermore, an increased frequency of circulating GMPs and myeloid-biased HSPCs as a result of pro-inflammatory secreted molecules is observed in numerous solid tumour settings (Wu et al., 2014). However, in the present study, the exact consequence of such an expansive immunophenotype is yet to be established, and may be an indirect consequence of a myeloid-promoting BM microenvironment.

Transcriptionally, CBM VECs were enriched for pro-inflammatory, chemotactic and morphogenic molecular pathways, which was in line with the differential immunophenotype of BL VECs and CBM VECs observed earlier (see Chapter 3, figures 3.5.c and 3.5.d). Vascular heterogeneity within the BM has historically been investigated using imaging based approaches (Kopp et al., 2009; Chi et al., 2003). During this present study, scRNA-seq was used to demonstrate that *Pecam1* expressing VECs were highly heterogenous, and could be clustered into 5 distinct sub-populations, each possessing a unique transcriptional profile (figures 4.4.2.a and 4.4.2.b). Of note, *Vcam1* expression defined a subset of VECs that were detectable by flow cytometry, predominantly within the CBM niche (figures 4.4.2.c and 4.4.4.c). Moreover, SEC-specific genes (Xu et al., 2018) appeared to enrich within *Vcam1* positive VECs, and also in cells that were isolated from the sinusoidal

niche (figures 4.4.6.b and 4.4.6.c). Upon additional analysis, DEGs from *Vcam1* positive VECs were inversely correlated with DEGs from CBM VECs exposed to leukemia (figures 4.4.3.a and 4.4.3.b). Furthermore, VCAM1^{hi} VECs became immunophenotypically depleted in frequency during leukemia, whereas VCAM1- VECs did not. Taken together, these findings strongly suggested that VCAM1 expression could be used an accurate means for discriminating sinusoidal from arteriolar endothelium, and whose immunophenotypic frequencies during leukemia paralleled what was observed in chapter 3. Differential gene expression analysis revealed that *Vcam1* positive VECs in healthy mice transcriptionally expressed *Ang* (angiogenin), a secreted ribonuclease that plays an important role in maintaining HSC quiescence (Silberstein et al., 2016; Goncalves et al., 2016). A reduction of this factor's expression through the depletion of VCAM1^{hi} VECs may therefore explain why HSCs from leukemic mice failed to engraft to the same extent as non-transplanted controls after 3 weeks of leukemic exposure (see Chapter 3, figure 3.4.2.a).

Previous studies have demonstrated that endothelial expressed VCAM1 acts as an important BM niche for erythropoiesis (Hamamura et al., 1996), and whose loss of expression can negatively impact erythroblast differentiation (Yamashita et al., 2008). Given there was a depletion of erythroid progenitor frequency throughout the reported AML model (see Chapter 3, figure 3.3.2.b), this effect could have been due to the loss of critical niches required for BM erythropoiesis. Collectively, these studies highlight that changes to endothelial cell composition and cell-surface expression can significantly disrupt normal HSPC function, and could therefore be a contributing factor to the eventual depletion of endogenous HSPCs observed at the terminal stages of this AML model.

In addition to a loss of VCAM1^{hi} cells during leukemia, there was also a gain in VCAM1- VECs, a finding that was in agreement with the earlier observed expansion of endosteal BL VECs (see Chapter 3, figure 3.5.c). At steady state, *Vcam1* negative VECs expressed *Cxcl12* and *Kitl*, two important niche factors that are pivotal for normal HSC function and have also been identified as relevant therapeutic targets during leukemia (Ding et al., 2013; Juarez et al., 2003; Hoellenriegel et al., 2014; Kuribayashi et al., 2016). An over-expression of *Kitl* and *Cxcl12* as a result of expanded VCAM1- VECs may explain why there was an observed retention of HSCs in the BM at the mid-stage of our AML model. Moreover, given that CXCL12 expressing vasculature is considered an important homing site for leukemic cells post-transplantation (Sipkins et al., 2005), this would further suggest that VCAM1- VECs during leukemia may also act as an important site for LIC infiltration.

The interpretation of data derived from RNA-seq experiments presents as a potential limitation of this chapter. Although measuring the abundance of RNA can be used as an accurate proxy for inferring protein expression, the presence of RNA alone does not guarantee a functional end product. On several occasions, supporting experiments were carried out using flow cytometric analyses, however, in many cases this was not done. Inferences made using RNA-seq data must therefore be accompanied with an additional means of validation before drawing conclusions.

4.6. Conclusions

1. **Endogenous HSPCs were transcriptionally profiled during leukemic development**

Using bulk RNA-seq, individual HSC, MPP and myeloerythroid progenitor compartments were transcriptionally profiled during the early- and mid-stages of leukemic development. Inflammatory and chemotactic pathways were consistently enriched across the majority of HSPC populations. Transcriptional activity at the early stages of leukemic development was confined to the pGM compartment, which also reflected the deficiencies in erythroid progenitor frequency.

2. **The transcriptional profile of CBM VEC and LepR+ PV niche cells during leukemia was investigated**

Using bulk RNA-seq, the global gene expression profiles of CBM VECs and LepR+ PV cells during leukemic development was investigated. Both cell types were enriched for chemotactic and pro-inflammatory molecular processes. GSEA revealed that CBM VECs expressed numerous cell surface receptors and secreted factors after prolonged exposure to leukemia. Taken together, these findings suggested that niche cells were conditioned by leukemic populations, resulting in the expression of several potentially pro-leukemic secreted factors and cell surface receptors.

3. **The BM niche at steady state was assessed using scRNA-seq**

The transcriptional heterogeneity of BL and CBM niche cells was assessed at the single cell level using droplet-based scRNA-seq. The niche was comprised of approximately 11 distinct clusters, including OBs, MSCs, LepR+ PV cells, VECs, chondrocytes, muscle cells and osteoprogenitors.

4. BM VEC heterogeneity at steady state was investigated

At steady state, VECs were comprised of 5 sub-populations that could be demarcated by the expression of different genetic markers. *Vcam1* transcriptionally labelled a subset of VECs that were also detectable by flow cytometry. There was a negative correlation between genes that defined *Vcam1* positive VECs and those that were expressed by CBM VECs during leukemia. Of note, during leukemic development, VCAM1^{hi} VECs declined in frequency, whereas VCAM1- VECs increased. Moreover, *Vcam1* negative VECs were recently reported as being arteriolar, a finding that was in line with the immunophenotypic observations made in chapter 3 of this study. When taken together, these findings suggested that VCAM1^{hi} VECs likely represented sinusoidal CBM VECs, whose frequency during AML was perturbed, validating the immunophenotypic observations made in chapter 3.

Chapter 5

Transcriptionally profiling leukemic cell populations and investigating their functional impact on normal hematopoiesis and the BM niche

5.1. Introduction and aims

Throughout chapters 3 and 4, it was demonstrated that leukemic development caused significant immunophenotypic, transcriptional and functional changes to endogenous HSPCs prior to complete hematopoietic failure. This also included the expansion of *Cxcl12* and *Scf* expressing arteriolar (BL) VECs, and the depletion of VCAM1^{hi} sinusoidal (CBM) VECs. Taken together, these findings suggested that leukemic cells drastically conditioned the environment within which they resided, leading to the expansion of leukemic cells at the eventual expense of normal hematopoietic populations. However, the mechanism used by leukemic cells in order to achieve this has not yet been established.

Inflammatory and chemotactic molecular pathways were significantly enriched across several distinct cell populations during leukemic development, leading to the hypothesis that leukemic populations perturbed normal hematopoiesis and the niche through the release of pro-inflammatory secreted factors. In support of this, two independent analyses investigating AML patient serum samples revealed that combinations of cytokines and chemokines could predict survival as well as response to therapy (Kornblau et al., 2010; Niyongere et al., 2018). These findings therefore imply that systemically expressed secreted factors during leukemia may contribute towards disease pathogenesis. Indeed, LICs from this present study cannot recapitulate a leukemic state after prolonged *in vitro* culture in an HSPC supportive cytokine cocktail (see Chapter 3, figure 3.2.3.a). This suggested that the process of leukemogenesis itself relied extensively on a specific microenvironment before being able to propagate. Secreted factors and cell surface receptors supplied by the BM niche, as well as other hematopoietic cells, play a pivotal role in the maintenance of normal hematopoiesis. (Ding et al., 2012; Ding et al., 2013;

Silberstein et al., 2016; Méndez-Ferrer et al. 2010; Zhou et al. 2014). Moreover, the remodelling of these populations by leukemic cells has formerly been demonstrated to enhance survival, proliferation and resistance to therapy during AML (Colmone et al., 2008; Boyd et al., 2017; Kumar et al., 2018). Despite this however, very little is currently known about how the global gene expression profiles of leukemic populations change as a function of disease development, and which leukemia-derived secreted factors and cell surface receptors contribute towards disrupted hematopoiesis. To address this, the following aims were set:

1. To identify the major molecular processes that exist within LICs and blasts during leukemic development.
2. To understand if leukemic cells over-express any secreted factors capable of disrupting endogenous hematopoiesis, and remodeling the CBM niche.
3. To evaluate whether the pharmacological inhibition of leukemia-expressed cell surface receptors results in enhanced survival during AML.

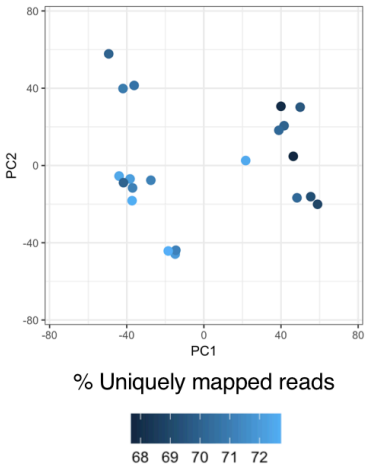
5.2. Bulk RNA-seq of LIC and blast populations during leukemia

LIC and blast cells were FACS isolated from the BM of leukemia-transplanted mice at weeks 2, 3 and 4 of leukemic development (see Chapter 3, figures 3.2.a and 3.2.b). Samples were then processed for bulk RNA-seq analysis using the SMART-seq2 protocol (see Materials and methods, section 2.1.7), after which a series of computational analyses were carried out including differential gene expression analysis, process network enrichment analysis and molecular pathway analysis.

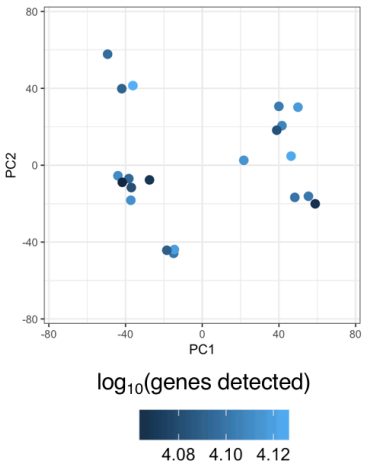
5.2.1. Data quality check

Sequenced samples were validated for read mapping percentage, library size and total number of genes detected per sample. Values for library size and total number of genes detected are displayed as $\log_{10}$ values. As seen in figure 5.2.1.a, all sequenced leukemic cell samples aligned to the mm9 reference genome with ~68-73% mapping efficiency. The library sizes and number of uniquely detected genes for each sample was consistent (figures 5.2.1.b and 5.2.1.c) and therefore no samples were excluded on this basis.

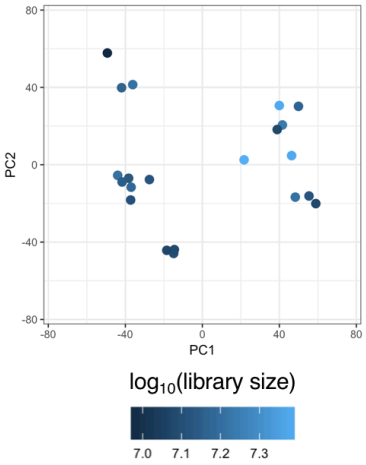
5.2.1.a



5.2.1.b



5.2.1.c



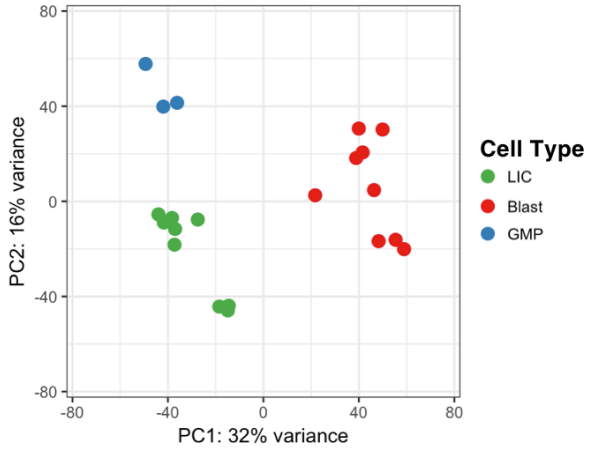
Data quality check

5.2.1.a. Percentage of mapped reads per leukemic cell sample. **5.2.1.b.** Log_{10} number of unique genes detected per leukemic cell sample. **5.2.1.c.** Log_{10} library size per leukemic cell sample.

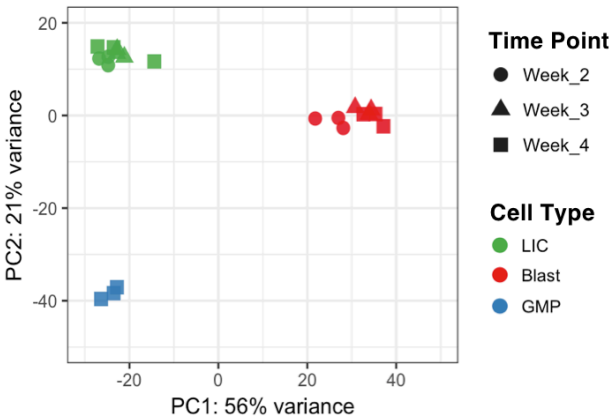
5.2.2. PCA of LIC, blasts and healthy GMPs

Principal component analysis (PCA) was carried out on LIC, blast and healthy GMP populations. As expected, cell types that were isolated based on a similar immunophenotype clustered together, but were distanced from distinct cell types (figure 5.2.2.a). Additional PCA was performed on the top 500 variable genes from each sample (figure 5.2.2.b). Of note, LICs clustered away from their direct progeny (blasts), but were also distanced from healthy GMPs. This suggested that, although being considered immunophenotypically comparable cell types (Kirstetter et al. 2008), LICs and GMPs were appreciably different on a gene expression level.

5.2.2.a



5.2.2.b



PCA of LIC, blasts and healthy GMPs

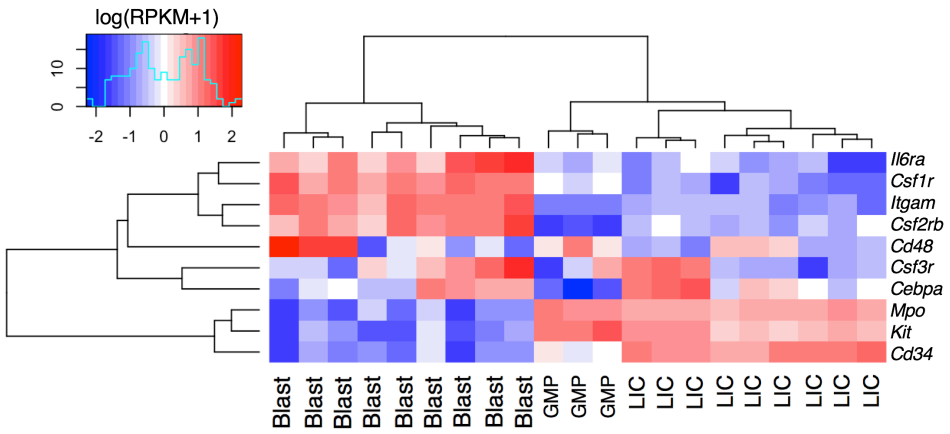
5.2.2.a. PCA of total genes for LIC, blast and healthy GMP cells types. **5.2.2.b.** PCA of top 500 variable genes for LIC, blast and healthy GMP cell types.

5.2.3. Heatmap of known LIC and blast cell markers

LICs, blasts and healthy GMPs were clustered using Wards method and Euclidean distance based on their expression of known mature myeloid and committed myeloid progenitor genes (figure 5.2.3.a).

LICs and healthy GMPs clustered together based on their expression of the cell surface markers *Kit*, *Mpo* and *Cd34* (Pronk et al., 2007). This suggested that LICs immunophenotypically resembled a committed myeloid progenitor, despite existing disparately by PCA. In contrast, blasts clustered based on their expression of the genes *Itgam* (CD11b), *Csf1r*, *Csf2rb* and *Il6ra*, validating their assumed identity as a hierarchically mature cell type.

5.2.3.a



Heatmap of known LIC and blast cell markers

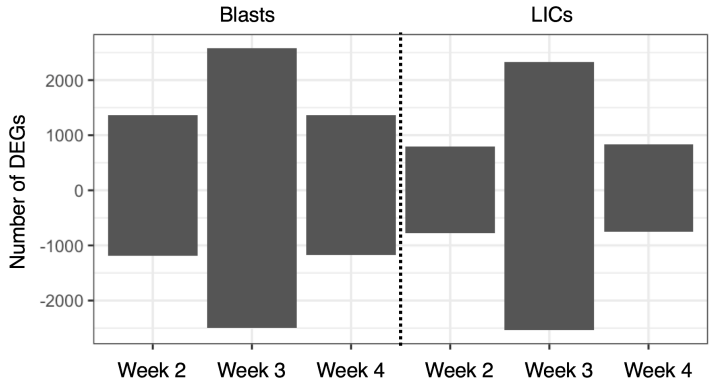
5.2.3.a. Unsupervised heatmap of LIC, blast and healthy GMP cell types clustered against myeloid progenitor genes using Euclidean distance and Wards methods. Expression values are scaled, log(RPKM+1).

5.2.4. Differential gene expression analysis of LICs and blasts during leukemia

Differential gene expression analysis was carried out using DESeq2, comparing LICs and blast populations at weeks 2, 3 and 4 of leukemic development, to healthy GMPs. Figure 5.2.4.a illustrates the number of up- and down-DEGs with an adjusted $p \leq 0.05$ from both cell populations at all time points assessed.

Both LICs and blasts expressed a consistently high number (>1000) of DEGs throughout leukemic development. The number of DEGs appeared to peak (>4000) in both cell types at week 3, returning to normal at week 4. The rise in transcriptional activity that was observed at this time point coincided with the major immunophenotypic, functional and transcriptional changes that to endogenous HSPCs and CBM VEC niche populations.

5.2.4.a



Differential gene expression analysis of LICs and blasts during leukemia

5.2.4.a. Number of DEGs with an adjusted $p \leq 0.05$ from LICs and blasts at weeks 2, 3 and 4 post-transplantation. DEGs were generated using DESeq2, by comparing LICs and blasts to healthy GMPs.

5.2.5. Process network enrichment analysis of LICs and blasts during leukemia

Process network enrichment analysis was carried out using DEGs from LICs and blasts at weeks 2, 3 and 4 post-transplantation. DEGs with an adjusted $p \leq 0.05$ were used as input for this analysis. All process networks shown have a $p \leq 0.05$ and FDR$\leq$0.05.

Table 5.2.5.a outlines the enriched process networks for LICs at weeks 2, 3 and 4 post-transplantation. LICs at week 2 enriched for two process networks, one of which included endothelial cell adhesion. This likely reflected the LICs requirement for localisation to a specific vascular niche at the early stage of this leukemia model. By week 3, LICs were enriched for numerous process networks including translation, signal transduction, inflammation, proliferation, cell cycle, adhesion and protein synthesis. These findings suggested that LICs at week 3 were highly transcriptionally active, which was also paralleled by their expansive immunophenotype and propensity to generate myeloid blasts at an equivalent time point (see Chapter 3, figures 3.2.c and 3.2.d). By week 4, LICs were enriched for fewer process networks, which may be due to slowed activity. Indeed, by this time point, leukemic cells comprised 93±1.5% and 84±5.3% of the live singlets in the BM and spleen, respectively (see chapter 3, figure 3.2.c), indicating that additional growth may not have been required.

Table 5.2.5.b outlines significantly enriched process networks for blasts at weeks 2, 3 and 4 post-transplantation. Blast cells at 2 weeks post-transplantation enriched for 66 process networks, despite making up only 19.9±5.7% of the total BM tumour population (figure 3.2.d). This included signal transduction, inflammation and cell cycle process networks, which persisted throughout weeks 3 and 4.

Taken together, these findings highlighted that both LICs and blasts were highly transcriptionally active, even at the earliest stages of leukemic development. Moreover, both cell types appeared to be enriched for numerous processes related to inflammation, consistent with what was observed transcriptionally within neighbouring niche and endogenous HSPC populations (see Chapter 4, sections 4.2.5 and 4.3.5).

5.2.5.a

Time Point	*Process network*	*-log(p-value)*
Week 2	Immune response_Phagosome in antigen presentation	4.14
	Cell adhesion_Platelet-endothelium-leucocyte interactions	3.28
Week 3	Anti-Apoptosis mediated by external signals via MAPK and JAK/STAT	1.9
	Anti-apoptosis mediated by external signals via NF-kB	1.9
	Apoptosis_Endoplasmic reticulum stress pathway	2.44
	Cell adhesion_Integrin priming	2.48
	Cell adhesion_Integrin-mediated cell-matrix adhesion	2.72
	Cell adhesion_Platelet aggregation	2.18
	Cell cycle_Core	2.85
	Cell cycle_G1-S Interleukin regulation	2.78
	Cytoskeleton_Actin filaments	2.27
	Development_Hemopoiesis, Erythropoietin pathway	3.43
	DNA damage_BER-NER repair	2.46
	Immune response_BCR pathway	2.8
	Immune response_IL-5 signalling	2.71
	Immune response_TCR signalling	2.4
	Inflammation_Amphoterin signalling	4.07
	Inflammation_IL-2 signalling	3.35
	Inflammation_NK cell cytotoxicity	1.82
	Inflammation_Protein C signalling	2.13
	Inflammation_TREM1 signalling	4.33
	Proliferation_Lymphocyte proliferation	2
	Proliferation_Positive regulation cell proliferation	2.49
	Protein folding_ER and cytoplasm	1.85
	Protein folding_Folding in normal condition	3.64
	Protein folding_Protein folding nucleus	4.32

	Protein folding_Response to unfolded proteins	3.82
	Reproduction_FSH-beta signalling pathway	2.26
	Signal transduction_Androgen receptor nuclear signalling	2.95
	Signal Transduction_Cholecystokinin signalling	2.56
	Signal transduction_ESR1-nuclear pathway	3.46
	Signal transduction_ESR2 pathway	2.45
	Translation_Regulation of initiation	4.38
	Translation_Translation in mitochondria	4.12
	Translation_Translation initiation	3.57
Week 4	Apoptosis_Endoplasmic reticulum stress pathway	3.3
	Cell adhesion_Integrin priming	3.23
	Cell adhesion_Platelet-endothelium-leucocyte interactions	2.88
	Immune response_Antigen presentation	3.16
	Immune response_Phagocytosis	4.61
	Immune response_Phagosome in antigen presentation	6.14
	Inflammation_Neutrophil activation	2.75
	Protein folding_ER and cytoplasm	2.95
	Protein folding_Folding in normal condition	2.74
	Protein folding_Response to unfolded proteins	2.91

Process network enrichment analysis of LICs and blasts during leukemia

5.2.5.a. Process networks enriched in LICs at weeks 2, 3 and 4 post-transplantation as determined using Metacore. DEGs with an adjusted $p \leq 0.05$ were used as input. All networks shown have a $p \leq 0.05$ and FDR$\leq$0.05. Enrichment is illustrated as -log(*p*-value).

5.2.5.b

Time Point	*Process network*	*-log(p-value)*
Week 2	Anti-Apoptosis mediated by external signals via MAPK and JAK/STAT	2.35
	Apoptosis_Anti-apoptosis mediated by external signals via NF-kB	3.71
	Apoptosis_Endoplasmic reticulum stress pathway	5.9
	Blood coagulation	2.17
	Cardiac development_FGF_ErbB signalling	1.69
	Cardiac development_Role of NADPH oxidase and ROS	1.73
	Cell adhesion_Amyloid proteins	3.11
	Cell adhesion_Glycoconjugates	1.92

Cell adhesion_Integrin priming	4.58
Cell adhesion_Integrin-mediated cell-matrix adhesion	9.58
Cell adhesion_Leucocyte chemotaxis	5.68
Cell adhesion_Platelet aggregation	7.69
Cell cycle_Core	2.73
Cell cycle_G1-S	2.35
Cell cycle_G1-S Growth factor regulation	2.36
Cell cycle_G1-S Interleukin regulation	3.17
Cell cycle_G2-M	3.91
Cell cycle_Mitosis	2.35
Cytoskeleton_Actin filaments	6.4
Cytoskeleton_Intermediate filaments	2.37
Cytoskeleton_Regulation of cytoskeleton rearrangement	7.41
Development_Blood vessel morphogenesis	2.13
Development_EMT_Regulation of epithelial-to-mesenchymal transition	1.87
Development_Hemopoiesis, Erythropoietin pathway	5.51
Development_Neurogenesis_Axonal guidance	2.7
Development_Regulation of angiogenesis	3.87
Development_Regulation of telomere length	2.34
DNA damage_Checkpoint	2.49
Immune response_Antigen presentation	3.01
Immune response_BCR pathway	7.64
Immune response_IL-5 signalling	3.02
Immune response_Phagocytosis	11.4
Immune response_Phagosome in antigen presentation	8.56
Immune response_TCR signalling	3.72
Immune response_Th17-derived cytokines	1.94
Inflammation_Amphoterin signalling	5.97
Inflammation_Histamine signalling	3.8
Inflammation_IFN-gamma signalling	5.1
Inflammation_IgE signalling	2.34
Inflammation_IL-2 signalling	6.1
Inflammation_IL-4 signalling	2.14
Inflammation_Inflammasome	2.25
Inflammation_Interferon signalling	5
Inflammation_Kallikrein-kinin system	4.61
Inflammation_MIF signalling	4.03
Inflammation_Neutrophil activation	6.63
Inflammation_NK cell cytotoxicity	4.04
Inflammation_Protein C signalling	3.95

	Inflammation_TREM1 signalling	2.2
	Neurophysiological process_Corticoliberin signalling	2.73
	Proliferation_Lymphocyte proliferation	4.58
Week 3	Anti-Apoptosis mediated by external signals via MAPK and JAK/STAT	2.84
	Anti-apoptosis mediated by external signals via NF-kB	7.4
	Apoptosis_Anti-Apoptosis mediated by external signals by Estrogen	1.73
	Apoptosis_Apoptosis stimulation by external signals	2.11
	Apoptosis_Apoptotic mitochondria	4.9
	Apoptosis_Apoptotic nucleus	5.42
	Apoptosis_Endoplasmic reticulum stress pathway	5.92
	Autophagy_Autophagy	1.92
	Cardiac development_Role of NADPH oxidase and ROS	2.65
	Cell adhesion_Integrin priming	4.28
	Cell adhesion_Integrin-mediated cell-matrix adhesion	9.54
	Cell adhesion_Leucocyte chemotaxis	3
	Cell adhesion_Platelet aggregation	3.63
	Cell cycle_G1-S	3.43
	Cell cycle_G1-S Growth factor regulation	4.21
	Cell cycle_G1-S Interleukin regulation	5.49
	Cell cycle_G2-M	7.32
	Cell cycle_Meiosis	1.81
	Cell cycle_Mitosis	4.96
	Cell cycle_S phase	2.87
	Cytoskeleton_Actin filaments	5.94
	Cytoskeleton_Cytoplasmic microtubules	3.68
	Cytoskeleton_Intermediate filaments	2.47
	Cytoskeleton_Regulation of cytoskeleton rearrangement	8.66
	Development_EMT_Regulation of epithelial-to-mesenchymal transition	2.47
	Development_ERK5 in cell proliferation and neuronal survival	1.67
	Development_Hemopoiesis, Erythropoietin pathway	7.46
	Development_Keratinocyte differentiation	1.61
	Development_Regulation of angiogenesis	4.14
	Development_Regulation of telomere length	2.51
	DNA damage_BER-NER repair	1.96
	DNA damage_Checkpoint	4.24
	Immune response_Antigen presentation	7.43
	Immune response_BCR pathway	9.56
	Immune response_IL-5 signalling	5.69

Immune response_Phagocytosis	12.3
Immune response_Phagosome in antigen presentation	19.5
Immune response_TCR signalling	6.19
Inflammation_Amphoterin signalling	11.6
Inflammation_Histamine signalling	2.58
Inflammation_IFN-gamma signalling	2.03
Inflammation_IgE signalling	3.44
Inflammation_IL-10 anti-inflammatory response	4.52
Inflammation_IL-12,15,18 signalling	2.1
Inflammation_IL-2 signalling	6.85
Inflammation_IL-4 signalling	3.07
Inflammation_IL-6 signalling	6.88
Inflammation_Inflammasome	2.51
Inflammation_Innate inflammatory response	2.55
Inflammation_Kallikrein-kinin system	2.03
Inflammation_MIF signalling	5.68
Inflammation_Neutrophil activation	10.2
Inflammation_NK cell cytotoxicity	3.34
Inflammation_Protein C signalling	7.03
Inflammation_TREM1 signalling	6.86
Proliferation_Lymphocyte proliferation	2.38
Proliferation_Positive regulation cell proliferation	3.28
Protein folding_ER and cytoplasm	3.58
Protein folding_Folding in normal condition	8.25
Protein folding_Protein folding nucleus	2.94
Protein folding_Response to unfolded proteins	4.52
Proteolysis_Proteolysis in cell cycle and apoptosis	3.7
Proteolysis_Ubiquitin-proteasomal proteolysis	10.7
Reproduction_Feeding and Neurohormone signalling	2.78
Reproduction_FSH-beta signalling pathway	3.71
Signal transduction_Androgen receptor nuclear signalling	2.34
Signal Transduction_BMP and GDF signalling	1.81
Signal Transduction_Cholecystokinin signalling	6.48
Signal transduction_ESR1-membrane pathway	1.81
Signal transduction_ESR1-nuclear pathway	4.16
Signal transduction_ESR2 pathway	2.01
Signal transduction_Leptin signalling	2.46
Signal transduction_NOTCH signalling	2.02
Signal Transduction_TGF-beta, GDF and Activin signalling	2.26
Signal transduction_WNT signalling	2.14

	Transcription_Chromatin modification	5.03
	Transcription_mRNA processing	4.58
	Transcription_Nuclear receptors transcriptional regulation	3.7
	Transcription_Transcription by RNA polymerase II	4.69
	Translation_Regulation of initiation	6.83
	Translation_Translation in mitochondria	2.55
	Translation_Translation initiation	6.58
Week 4	Apoptosis_Anti-Apoptosis mediated by external signals via MAPK and JAK/STAT	1.78
	Apoptosis_Anti-apoptosis mediated by external signals via NF-kB	5.96
	Apoptosis_Apoptotic nucleus	2.06
	Apoptosis_Endoplasmic reticulum stress pathway	4.59
	Cell adhesion_Integrin priming	3.91
	Cell adhesion_Integrin-mediated cell-matrix adhesion	5.16
	Cell adhesion_Leucocyte chemotaxis	3.22
	Cell adhesion_Platelet aggregation	3.61
	Cell cycle_G1-S	2.21
	Cell cycle_G1-S Growth factor regulation	2.24
	Cell cycle_G1-S Interleukin regulation	2.37
	Cell cycle_G2-M	2.47
	Cytoskeleton_Actin filaments	5.82
	Cytoskeleton_Intermediate filaments	2.12
	Cytoskeleton_Regulation of cytoskeleton rearrangement	7.22
	Development_Hemopoiesis, Erythropoietin pathway	4.48
	Development_Regulation of angiogenesis	2.49
	DNA damage_Checkpoint	3.57
	Immune response_Antigen presentation	3.15
	Immune response_BCR pathway	4.78
	Immune response_IL-5 signalling	3.09
	Immune response_Innate immune response to RNA viral infection	1.93
	Immune response_Phagocytosis	11.2
	Immune response_Phagosome in antigen presentation	9.68
	Immune response_T helper cell differentiation	1.83
	Immune response_Th17-derived cytokines	2.64
	Inflammation_Amphoterin signalling	3.65
	Inflammation_Complement system	2.18
	Inflammation_IFN-gamma signalling	3.61
	Inflammation_IL-12,15,18 signalling	1.92
	Inflammation_IL-2 signalling	2.91
	Inflammation_IL-4 signalling	2.84

Inflammation_IL-6 signalling	2.29
Inflammation_Inflammasome	2.65
Inflammation_Innate inflammatory response	3.81
Inflammation_Interferon signalling	4.3
Inflammation_Kallikrein-kinin system	2.44
Inflammation_MIF signalling	5.32
Inflammation_Neutrophil activation	3.86
Inflammation_NK cell cytotoxicity	3.87
Inflammation_Protein C signalling	2.33
Inflammation_TREM1 signalling	1.81
Neurophysiological process_Corticoliberin signalling	1.94
Proliferation_Lymphocyte proliferation	3.85
Proliferation_Negative regulation of cell proliferation	3
Proliferation_Positive regulation cell proliferation	3.01
Protein folding_ER and cytoplasm	5.15
Protein folding_Folding in normal condition	3.58
Protein folding_Response to unfolded proteins	3.47
Proteolysis_Proteolysis in cell cycle and apoptosis	2.48
Reproduction_Feeding and Neurohormone signalling	4.14
Reproduction_FSH-beta signalling pathway	1.87
Signal Transduction_Cholecystokinin signalling	2.77

Process network enrichment analysis of LICs and blasts during leukemia

5.2.5.b. Process networks enriched in blasts at weeks 2, 3 and 4 post-transplantation as determined using Metacore. DEGs with an adjusted $p \leq 0.05$ were used as input. All networks shown have a $p \leq 0.05$ and FDR$\leq$0.05. Enrichment score is illustrated as -log(*p*-value).

5.2.6. Pathway analysis of LICs and blasts during leukemia

Having established that LICs and blasts enriched for numerous process networks, upregulated KEGG pathways (Kanehisa and Goto, 2000) were next investigated. DEGs with an adjusted $p \leq 0.05$ and Log2FC$\geq$0.5 or $\leq$-0.5 from LICs and blasts throughout leukemic development were imported into iPathwayGuide (Adavaita

Bioinformatics). All enriched pathways shown in tables 5.2.6.a and 5.2.6.b have a combined Fishers $p \leq 0.05$.

This analysis revealed that numerous pathways were enriched in both LICs and blasts, including cGMP-PKG signalling, ECM-receptor interactions and focal adhesion. Having observed significant inflammatory signalling process network enrichment in both leukemic fractions (see tables 5.2.5.a and 5.2.5.b), of particular interest during this analysis was the consistent enrichment of the cytokine-cytokine receptor interaction pathway (tables 5.2.6.a and 5.2.6.b, in bold). The DEGs that comprised this pathway were investigated further in figure 5.2.6.c. From this, a number of secreted factors and cell-surface receptors were differentially expressed, including *Ccl6*, *Ccl3* and *Flt3l*.

Taken together, this analysis demonstrated that leukemic cells aberrantly over-expressed a range of pro-inflammatory secreted factors and cell surface receptors, a number of which may have been responsible for the disruption of normal hematopoiesis during leukemic development.

5.2.6.a

Time point	*Enriched Pathway*	*Fishers p-value*
Week 2	cGMP-PKG signalling pathway	0.012
	Cytokine-cytokine receptor interaction	0.013
	Calcium signalling pathway	0.022
	Pathways in cancer	0.048
Week 3	**Cytokine-cytokine receptor interaction**	0.001
	Calcium signalling pathway	0.001
	cGMP-PKG signalling pathway	0.002
	cAMP signalling pathway	0.004
	Complement and coagulation cascades	0.006
	Intestinal immune network for IgA production	0.007
	ECM-receptor interaction	0.01

	Regulation of lipolysis in adipocytes	0.011
	Vascular smooth muscle contraction	0.011
	Systemic lupus erythematosus	0.014
	Autoimmune thyroid disease	0.018
	Asthma	0.022
	Allograft rejection	0.023
	Focal adhesion	0.024
	Leukocyte transendothelial migration	0.028
	Fluid shear stress and atherosclerosis	0.032
	NF-kappa B signalling pathway	0.036
	Hepatitis B	0.044
	HIF-1 signalling pathway	0.046
	Regulation of actin cytoskeleton	0.048
	ErbB signalling pathway	0.048
Week 4	**Cytokine-cytokine receptor interaction**	0.007
	Regulation of lipolysis in adipocytes	0.009
	Autoimmune thyroid disease	0.041
	Allograft rejection	0.042
	cAMP signalling pathway	0.043
	Asthma	0.044
	Systemic lupus erythematosus	0.047

Pathway analysis of LICs and blasts during leukemia

5.2.6.a. Pathway enrichment analysis of LICs at weeks 2, 3 and 4 post-transplantation using iPathwayGuide. All pathways illustrated are significant with a combined Fishers $p \leq 0.05$. DEGs from LICs at weeks 2, 3 and 4 with an adjusted $p \leq 0.05$ and Log2FC ≥ 0.5 or ≤ -0.5 were used as input for this analysis.

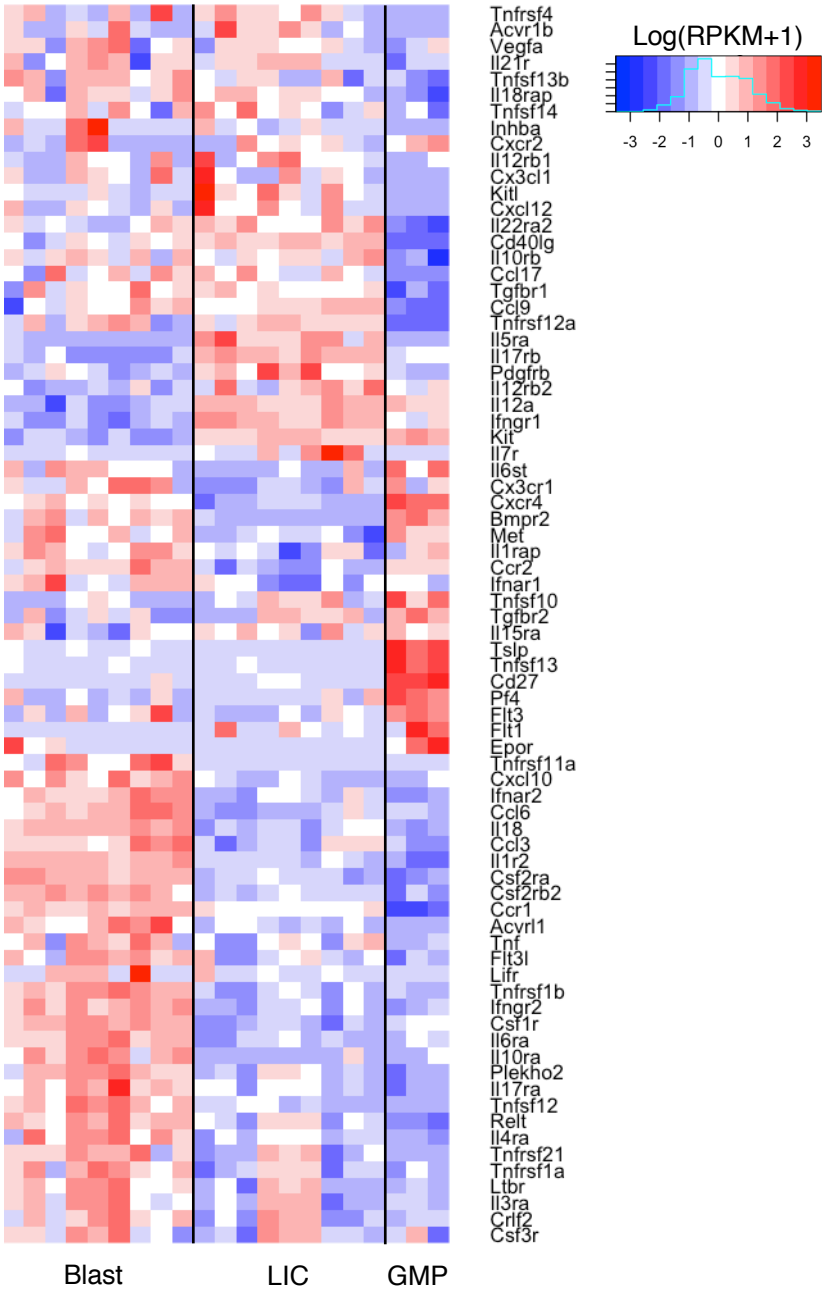
5.2.6.b

Time point	*Enriched Pathway*	*Fishers p-value*
Week 2	ECM-receptor interaction	0.008
	Calcium signalling pathway	0.013
	cGMP-PKG signalling pathway	0.033
Week 3	ECM-receptor interaction	0.003
	Focal adhesion	0.004
	Toll-like receptor signalling pathway	0.007
	Cytokine-cytokine receptor interaction	0.008
	cGMP-PKG signalling pathway	0.009
	Endocrine resistance	0.022
	Regulation of actin cytoskeleton	0.023
	Leukocyte transendothelial migration	0.024
	Chemokine signalling pathway	0.024
	Measles	0.026
	NF-kappa B signalling pathway	0.031
	Mitophagy - animal	0.044
	Calcium signalling pathway	0.044
	Complement and coagulation cascades	0.046
Week 4	ECM-receptor interaction	0.008
	Focal adhesion	0.013
	Cytokine-cytokine receptor interaction	0.014
	NOD-like receptor signalling pathway	0.028
	Chemokine signalling pathway	0.033

Pathway analysis of LICs and blasts during leukemia

5.2.6.b. Pathway enrichment analysis of blasts at weeks 2, 3 and 4 post-transplantation using iPathwayGuide. All pathways illustrated are significant with a combined Fishers $p \leq 0.05$. DEGs from blasts at weeks 2, 3 and 4 with an adjusted $p \leq 0.05$ and Log2FC ≥ 0.5 or ≤ -0.5 were used as input for this analysis.

5.2.6.c



Pathway analysis of LICs and blasts during leukemia

5.2.6.c. Heatmap depicting differentially expressed cytokine-cytokine receptor interaction pathway genes that are differentially expressed (adjusted $p \leq 0.05$) by LICs and blasts from all time points of leukemic development compared to healthy GMPs. Expression values are depicted as log(RPKM+1).

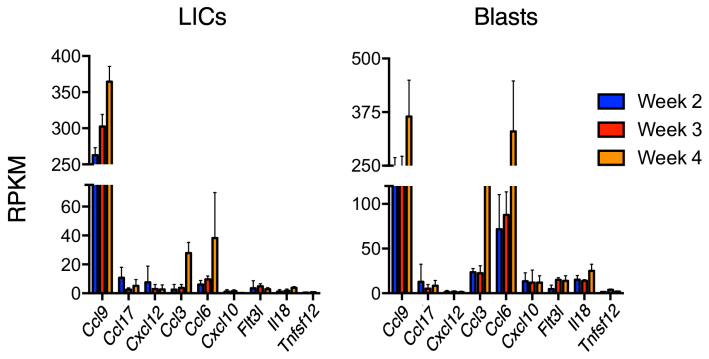
5.3. Investigation of the impact of leukemic cell-derived secreted factors on normal hematopoiesis and the niche

Leukemic cells expressed a range of secreted factors, which led to the hypothesis that the expression of these factors was sufficient to drive the endogenous myeloerythroid progenitor immunophenotype observed during leukemic development (*i.e.* expansion of GMPs and depletion of erythroid progenitors; see Chapter 3, figures 3.3.2.a and 3.3.2.b).

The hydrodynamic intravenous injection technique was leveraged in order to investigate the impact of myeloerythroid progenitor frequency after transient *in vivo* protein over-expression of leukemia-derived secreted factors. Briefly, this technique employs the rapid injection of an isotonic solution containing plasmid DNA encoding for a protein of interest (Zhang et al., 1999). Delivery via this method results in the transfection of foreign DNA into hepatocytic cells, and subsequent systemic protein over-expression for a period of 4-6 weeks.

This technique was used in the present study to over-express the 9 secreted factors identified in section 5.2.5. Mice were injected with 1µg of plasmid DNA (pCMV6-entry vector) and were incubated for a 3 day period before being euthanized. The RPKM expression values for each of the 9 factors investigated are illustrated in figure 5.3.a, and included *Ccl3*, *Ccl6*, *Ccl9*, *Ccl17*, *Cxcl10*, *Cxcl12*, *Flt3l*, *Tnfsf12* and *Il18*. The negative control for all hydrodynamic injection experiments was an empty pCMV6-entry vector, injected at an equivalent nucleic acid concentration and volume. A complete description of the hydrodynamic injection technique can be found in Materials and methods, section 2.1.6.

5.3.a



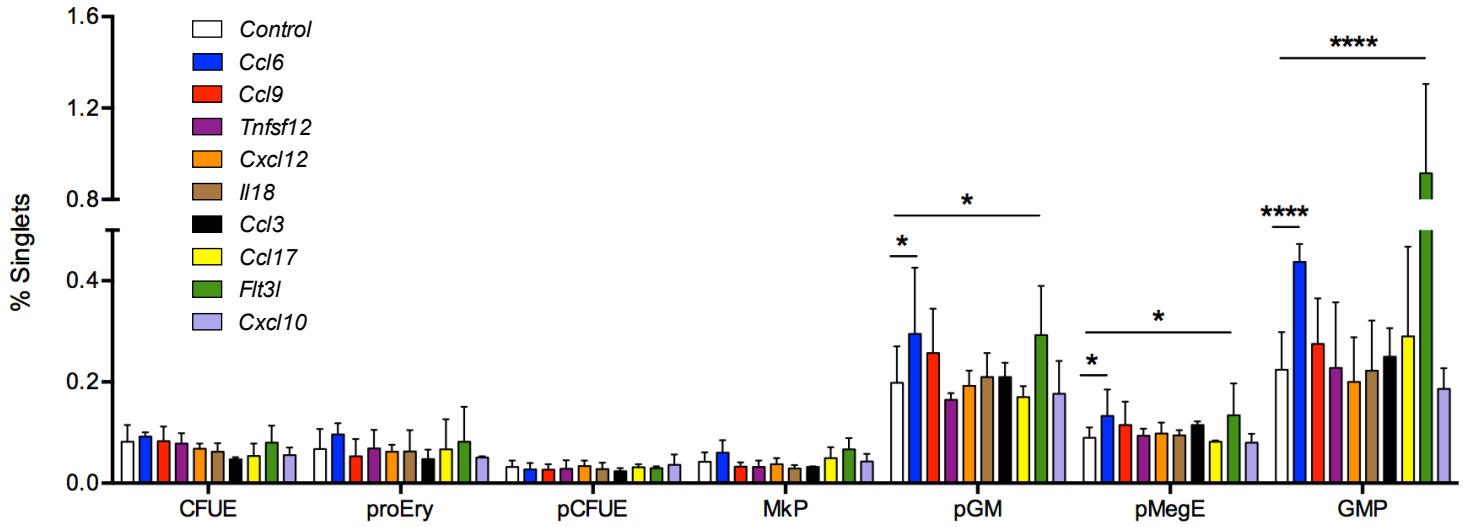
Investigation of the impact of leukemic cell-derived secreted factors on normal hematopoiesis and the niche

5.3.a. RPKM expression values for differentially expressed secreted factors from LICs and blasts at weeks 2, 3 and 4. Secreted factors originate from the pathway analysis described in section 5.2. Mean±SD, N=3 from one experiment.

5.3.1. FLT3L and CCL6 over-expression in wild type mice caused myeloid progenitors to expand in frequency

Figure 5.3.1.a depicts the frequency of myeloerythroid progenitor populations as a percentage of BM singlets in wild type mice after exposure for 3 days to each of the leukemia-derived secreted factors. Of note, the over-expression of *Ccl6* and *Flt3l* caused a statistically significant increase in pMegE (*Ccl6*; 0.133±0.05% vs. 0.089±0.02%, *Flt3l*; 0.134±0.063% vs. 0.089±0.02%, $p \leq 0.05$), pGM (*Ccl6*; 0.3±0.13% vs. 0.19±0.07, *Flt3l*; 0.29± 0.09% vs. 0.19±.07, $p \leq 0.05$) and GMP (*Ccl6*; 0.44±0.04% vs. 0.22±0.07%, $p \leq 0.05$, *Flt3l*; 0.92±0.39%, $p \leq 0.0001$) progenitor populations when compared to empty vector controls. However, these factors did not affect the frequency of committed erythroid progenitors. Taken together, these findings implied that through the expression of CCL6 and FLT3L, leukemic cells were capable of promoting endogenous myeloid progenitor expansion during disease development.

5.3.1.a



FLT3L and CCL6 over-expression in wild type mice caused myeloid progenitors to expand in frequency

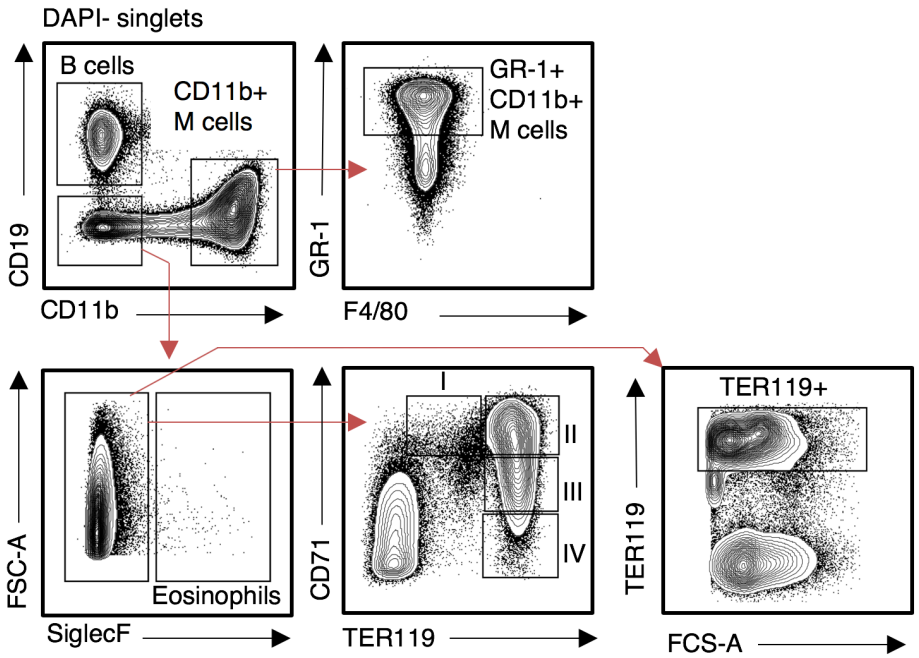
5.3.1.a. Myeloerythroid progenitor frequency as a % of BM singlets in wild type mice after the hydrodynamic injection of 9 individual, leukemic cell-derived secreted factors. Negative control was an empty pCMV6-entry vector injected at an equivalent nucleic acid concentration and volume. Mice were euthanized after 3 days of *in vivo* over-expression. Mean±SD, N=2-4±SD from two experiments. Two-tailed unpaired *t*-test was used to determine significance, comparing empty vector injected mice to secreted factor injected mice (*$p \leq 0.05$, ****$p \leq 0.0001$).

5.3.2. Secreted factor over-expression had limited impact on mature BM cell types

The frequency of B cells (CD19+), myeloid cells (CD11b+; CD11b+ GR1+), eosinophils (SiglecF+), total erythroid cells (TER119+) and erythroblasts, at the various stages of differentiation defined by CD71 and TER119 (Socolovsky et al., 2001), after hydrodynamic injection with the secreted factors described in figure 5.3.a were next assessed. This analysis was done 3 days following hydrodynamic injection, and used the flow cytometry gating strategy depicted in figure 5.3.2.a.

Figure 5.3.2.b, depicts the significant immunophenotypic changes to mature cell frequency as a percentage of live singlets after over-expression. When compared to empty vector injected control mice, there was a reduction in B cell frequency after *Ccl6* overexpression (17.4±8% vs. 24.6±5.6%, $p \leq 0.05$), an increase in CD11b+ frequency after *Tnsfsf12* overexpression (42±3.1% vs. 32.4±8.6%, $p \leq 0.05$) and an increase in stage IV erythroblast frequency after *Il18* overexpression (2.2±0.5 vs. 1.33±0.48%, $p \leq 0.05$). Despite causing significant changes to myeloid progenitor frequency, neither *Flt3l* nor *Ccl6* over-expression significantly affected mature cell population frequencies. This suggested that either the over-expression incubation period used was not sufficient to cause any significant changes to mature cell types, or that the secreted factors investigated had no physiological capacity to effect mature cell population frequency.

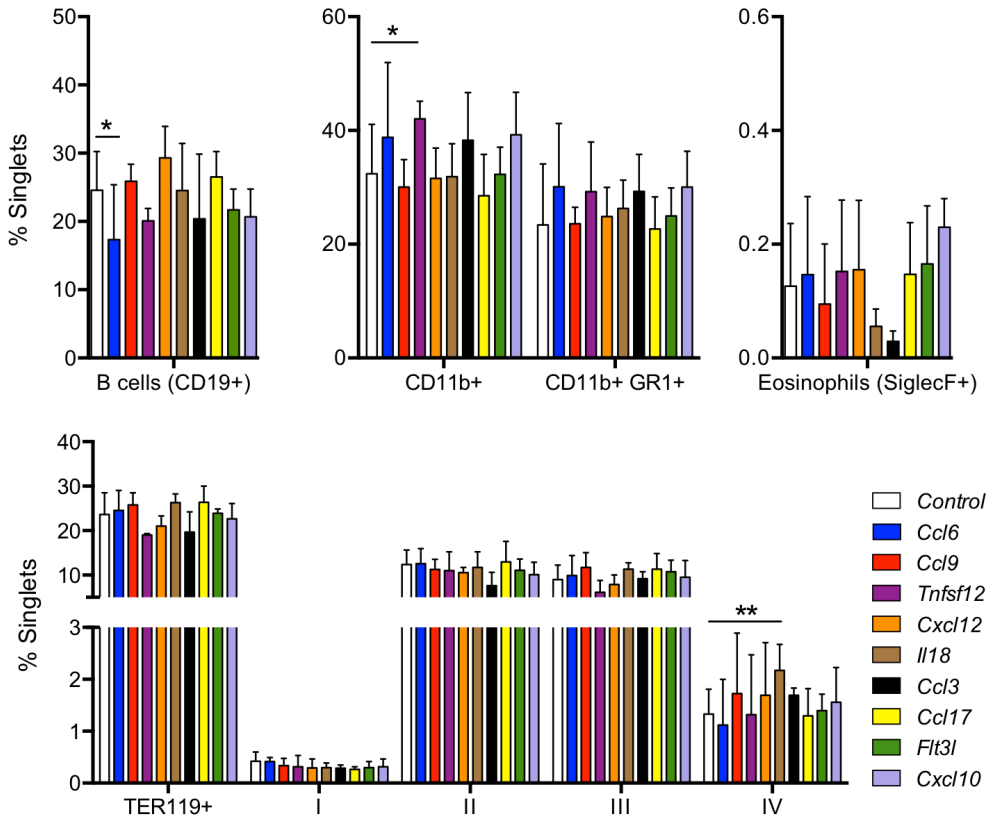
5.3.2.a



Secreted factor over-expression had limited impact on mature BM cell types

5.3.2.a. Flow cytometry gating strategy used to immunophenotypically identify mature cell types including B cells (CD19+), myeloid cells (CD11b+, CD11b+ GR-1+), eosinophils (SiglecF+), erythroblasts (I-IV) and total erythroid cells (TER119+).

5.3.2.b



Secreted factor over-expression had limited impact on mature BM cell types

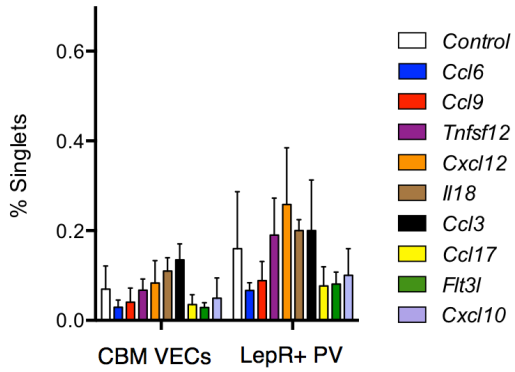
5.3.2.b. Mature cell type frequencies as a % of BM singlets in wild type mice hydrodynamically injected with 9 individual secreted factors. Mean±SD, N=2-4 from two experiments. A two-tailed unpaired *t*-test was used to determine significance, comparing empty vector injected mice to secreted factor injected mice (*$p \leq 0.05$, **$p \leq 0.01$).

5.3.3. Secreted factor over-expression had no impact on CBM niche cell frequencies

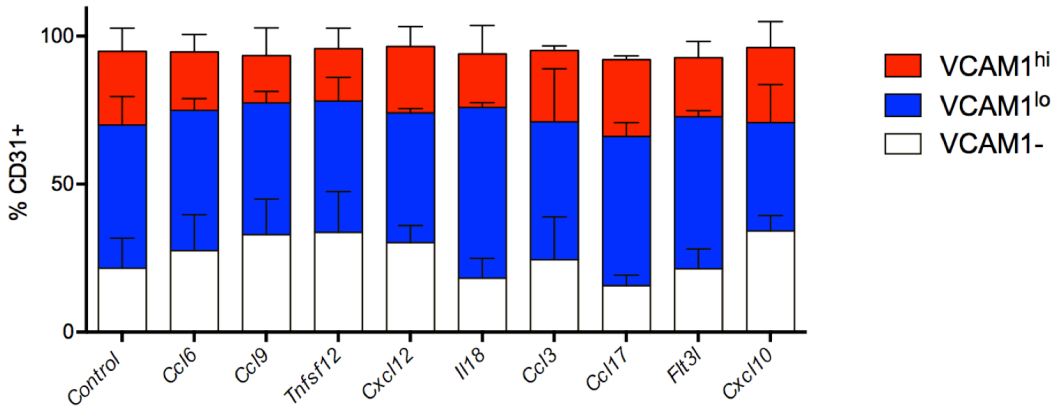
Finally, having observed significant remodelling of the niche during leukemic development (see Chapter 4, figures 4.5.c, 4.5.d), the frequency of CBM VECs and LepR+ PV cells, in addition to the proportion of VCAM1^{hi}, VCAM1^{lo} and VCAM1- CBM VECs after secreted factor over-expression was investigated.

Secreted factor over-expression in wild type mice did not cause any statistically significant immunophenotypic changes to niche cell frequency, nor change the proportion of VCAM1 expressing CBM VECs (figures 5.3.3.a and 5.3.3.b). These data therefore suggested that pro-inflammatory secreted factor over-expression was insufficient to significantly alter niche composition. This lack of effect may again be due to an insufficient incubation period, which may have limited the immunophenotypic effect.

5.3.3.a



5.3.3.b



Secreted factor over-expression had no impact on CBM niche cell frequencies

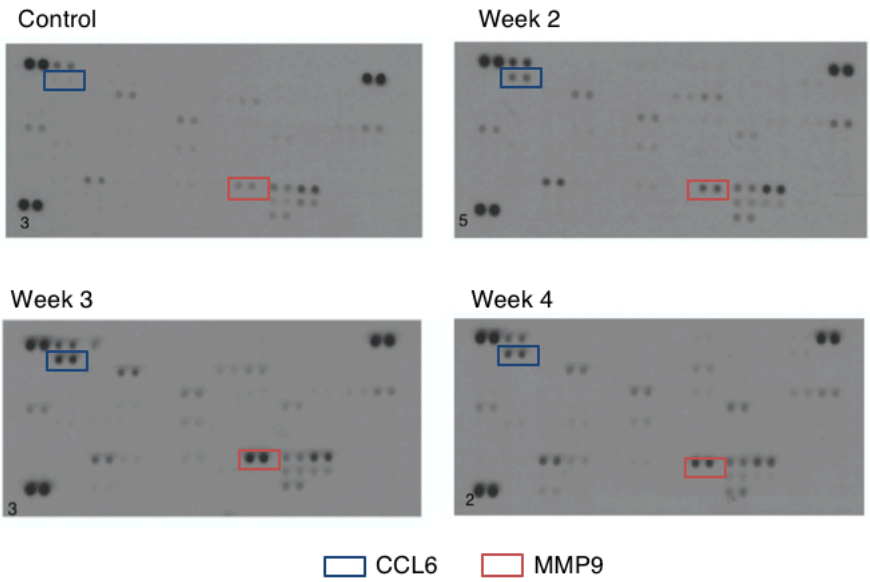
5.3.3.a. Frequencies of CBM VEC and LepR+ PV niche cells as a % of BM singlets in wild type mice, hydrodynamically injected individually with 9 secreted factors. Mean±SD, N=2-4 from two experiments. **5.3.3.b.** The proportion of VCAM1^{hi}, VCAM1^{lo} and VCAM1- CBM VECs as a % of CD31+ cells in wild type mice hydrodynamically injected with 9 different secreted factors. Mean±SD, N=2-4 from two experiments. A two-tailed unpaired *t*-test was used to determine significance, comparing empty vector injected mice to secreted factor injected mice.

5.3.4. Protein expression analysis of leukemic BM serum

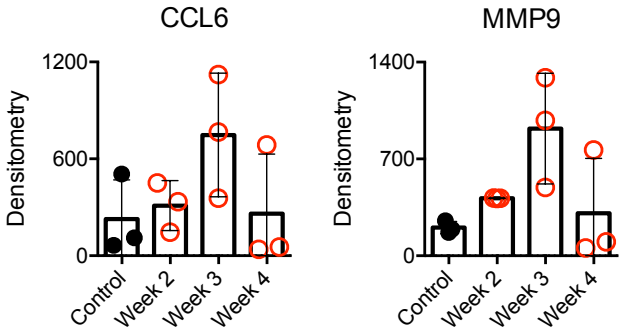
Having observed significant transcriptional upregulation of several pro-inflammatory secreted factors (figure 5.3.a), the BM protein expression level of these factors was next investigated. To achieve this, BM serum was isolated from non-transplanted, sub-lethally irradiated controls and leukemia-transplanted mice at weeks 2, 3 and 4 of leukemic development. Samples were then run on a multiplexed cytokine array (see Materials and methods, section 2.1.10).

In line with the transcriptional data presented in figure 5.3.a, CCL6 was over-expressed at the protein level in leukemic BM serum samples, in addition to MMP9 (figures 5.3.4.a and 5.3.4.b). When compared to non-transplanted recipients, the expression of these proteins (as determined by densitometry analysis) was greatest at week 3 (CCL6; 748±227 vs. 227±242, MMP9; 919±399 vs. 204±34), and decreased again by week 4 (CCL6; 260±368 vs. 227±242, MMP9; 307±396 vs. 204±34). At the gene expression level, *Mmp9* was expressed exclusively by blast cells, at a time point that correlated with protein expression (figure 5.3.4.c). In contrast, FLT3L was not detected at the protein level despite being expressed transcriptionally by both LICs and blasts. These data suggested that *Ccl6*, in addition to being transcriptionally expressed, was also detected at the protein level during leukemia.

5.3.4.a



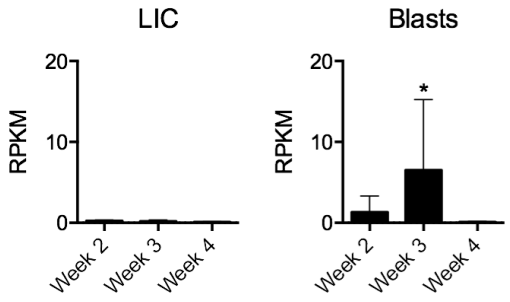
5.3.4.b



Protein expression analysis of leukemic BM serum

5.3.4.a. Cytokine protein array of BM serum taken from mice transplanted with leukemia for 2, 3 and 4 weeks. The expression of CCL6 and MMP9 are highlighted with blue and red boxes, respectively. **5.3.4.b.** Densitometry values of CCL6 and MMP9 from leukemia-transplanted and non-transplanted mice. Mean±SD, N=3 from one experiment. A two-tailed unpaired *t*-test was used to determine significance, comparing leukemia-transplanted to non-transplanted controls.

5.3.4.c



Protein expression analysis of leukemic BM serum

5.3.4.c. RPKM expression values for *Mmp9* in LIC and blast cells at weeks 2, 3 and 4 post-transplantation (*adjusted $p \leq 0.05$, determined using DESeq2 by comparing leukemic cell types to healthy GMPs). Mean±SD, N=3, from one experiment.

5.4. Combined FLT3L and CCL6 over-expression during leukemia

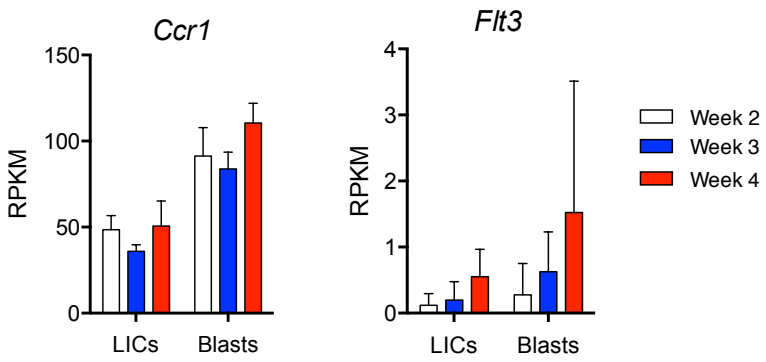
Both LICs and blasts transcriptionally expressed the receptors for CCL6 (*Ccr1*) and FLT3L (*Flt3*) throughout leukemic development. (figure 5.4.a). Therefore, in order to delineate whether leukemic cell-derived FLT3L and CCL6 acted in an autocrine signalling fashion to promote leukemogenesis, *Flt3l* and *Ccl6* were over-expressed individually, and in combination, prior to the transplantation of 25,000 KIT+ LICs into non-irradiated mice.

After 21 days post-transplantation, the peripheral blood engraftment of leukemic cells as a percentage of singlets in *Flt3l* and *Ccl6*+*Flt3l* injected mice was significantly lower compared to empty vector injected mice (*Flt3l*; 0.05±0.04% vs. 0.22±0.11%, *Ccl6*+*Flt3l*; 0.03±0.02% vs. 0.22±0.11%, $p \leq 0.05$). This was also observed after 28 days (*Flt3l*; 9.3±12.3% vs. 36.2±13.2%, *Ccl6*+*Flt3l*; 9.1±7.9% vs. 36.2±13.2%, $p \leq 0.05$), but not 33 days (*Flt3l*; 53.9±12.6% vs. 64.6±2.4%, *Ccl6*+*Flt3l*; 53.3±15.2% vs. 64.6±2.4%, $p > 0.05$) (figure 5.4.b). This effect was not evident after

over-expressing *Ccl6* alone, which suggested that *Flt3l* was the major driver of the reduced peripheral blood engraftment that we observed. After 33 days, all mice, regardless of condition, exhibited comparable levels of BM and spleen leukemic engraftment (figure 5.4.c).

Taken together, these findings suggested that the over-expression of *Ftl3l* led to reduced peripheral blood engraftment, rather than increased. Interestingly, the spleen leukemic cell engraftment in *Ccl6* and *Ccl6+Flt3l*, but not *Flt3l* over-expressing mice was significantly higher compared to controls, suggesting that *Ccl6* over-expression may have enhanced tumour metastasis to the spleen (figure 5.4.c).

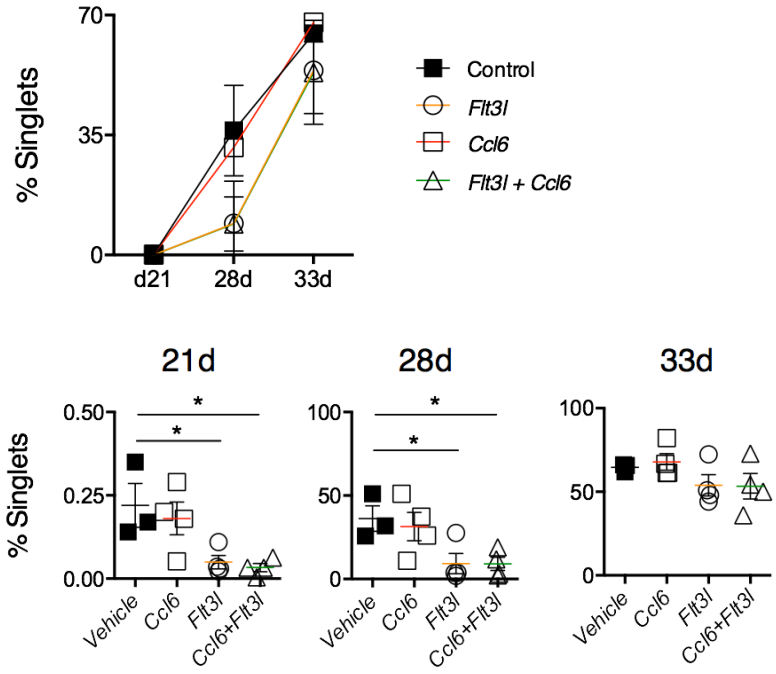
5.4.a



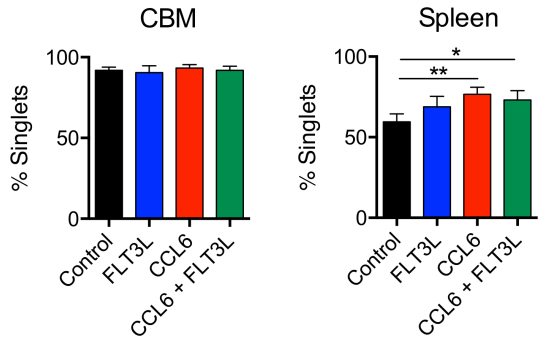
Combined FLT3L and CCL6 over-expression during leukemia

5.4.a. RPKM expression values for *Ccr1* and *Flt3* in LICs and blast cells after 2, 3 and 4 weeks of leukemic development. Mean±SD, N=3, from one experiment.

5.4.b



5.4.c



Combined FLT3L and CCL6 over-expression during leukemia

5.4.b. Engraftment of leukemic cells in the peripheral blood of mice after 21, 28 and 33 days as a % of singlets. Non-irradiated mice were first hydrodynamically injected with plasmids encoding for *Ccl6*, *Flt3l* or *Ccl6* + *Flt3l*, and then after 2 days transplanted with 25,000 KIT+ LICs. Mean±SD, N=3-4, from one experiment. **5.4.c**. CBM and spleen leukemic engraftment as a % of live singlets after 33 days post-transplantation. Mean±SD, N=3-4, from one experiment. Two-tailed unpaired *t*-test used to determine statistical significance, comparing empty vector injected mice to secreted factor injected mice (*$p \leq 0.05$, **$p \leq 0.01$).

5.5. Combined CCR1 and FLT3 inhibition during AML relapse

The over-expression of *Flt3l* and *Ccl6 in vivo* caused a significant expansion of endogenous myeloid progenitors (figure 5.3.1.a), and also transiently reduced the peripheral blood engraftment of leukemic cells (figure 5.4.b). Therefore, the impact of simultaneously inhibiting CCR1 and FLT3, the major receptors for CCL6 and FLT3L, respectively, was next investigated during leukemia. The aim of this analysis was to assess whether simultaneous inhibition of these receptors was sufficient to extend the remission period following chemotherapy treatment. Therefore, to achieve this, an AML relapse model was first established.

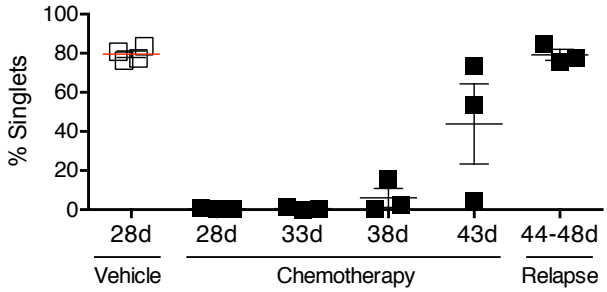
5.5.1. Generating an AML relapse model

A relapse model of leukemia was created by transplanting sub-lethally irradiated mice with 25,000 KIT+ LICs, and after 18 days treating recipients with a single, five-day chemotherapy regime. The first three days of treatment comprised a combination of cytarabine (100mg/kg) and doxorubicin (3mg/kg doxorubicin), and the last two days consisted of cytarabine (100mg/kg) alone. This protocol has formerly been shown to accurately mimic the human treatment regime (Zuber et al. 2009).

Figure 5.5.1.a illustrates the peripheral blood engraftment of CD45.2 leukemic cells as a percentage of live singlets from vehicle treated, chemotherapy treated and relapsed mice. Relapse status was considered when leukemic cell (CD45.2) peripheral blood engraftment reached >60%, after which point mice were euthanized and their BM and spleen analysed by FACS. Chemotherapy treated mice after 28 days post-transplantation exhibited a residual leukemic population in the BM (6.5±4% of live singlets), comprised predominantly of LICs, and not blasts (42.7±2.7% vs. 13.2±3%; figures 5.5.1.b and 5.5.1.c). Leukemic cells became detectable in the

peripheral blood after ~38 days (6±8.4% of singlets), and rapidly increased in frequency by day 43 (44±35% of singlets). Beyond 44-48 days, all mice experienced relapse, displaying high leukemic cell burdens in the BM (92.2±3.1% of singlets) and spleen (71.5±9.1% of singlets), in addition to significant splenomegaly (figures 5.5.1.c and 5.5.1.d).

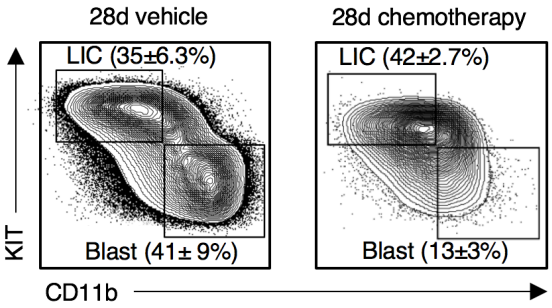
5.5.1.a



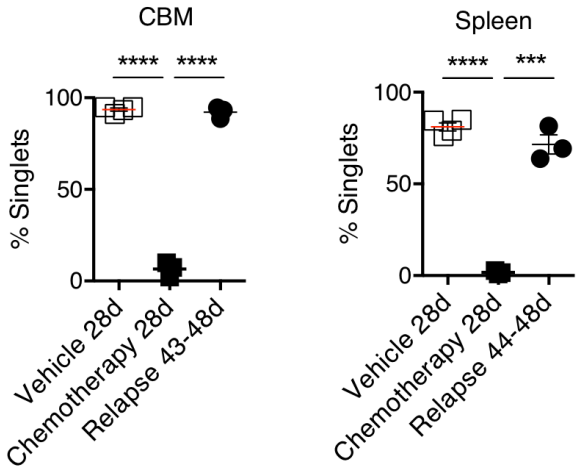
Generating an AML relapse model

5.5.1.a. Peripheral blood engraftment of either vehicle or chemotherapy treated mice as a % of live singlets. Chemotherapy consisted of 3 days combined doxorubicin (3mg/kg) and cytarabine (100mg/kg), followed by 2 days of cytarabine (100mg/kg) alone. Relapse was considered once leukemic (CD45.2) peripheral blood engraftment reached >60%. Mean±SD, N=3, from one experiment.

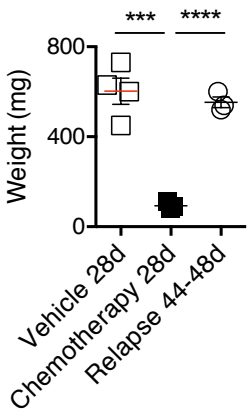
5.5.1.b



5.5.1.c



5.5.1.d



Generating an AML relapse model

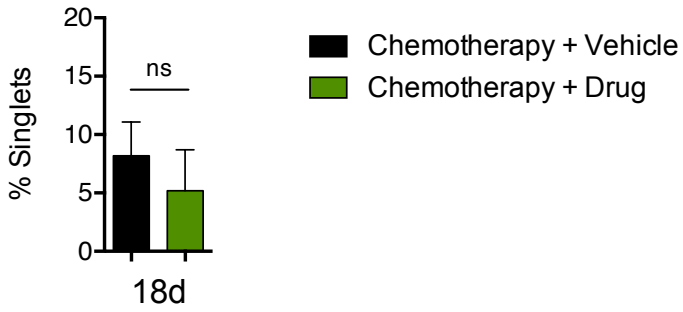
5.5.1.b. LIC and blast cell fractions from vehicle and chemotherapy treated mice after 28 days post-transplantation. Frequencies shown are a % of singlets. **5.5.1.c.** Frequency of total leukemic cells as a % of live singlets in vehicle treated, chemotherapy treated and relapsed mice. **5.5.1.d.** Spleen weight (mg) for vehicle treated, chemotherapy treated and relapsed mice. Mean±SD, N=3-4, from one experiment. Two-tailed unpaired *t*-test was used to determine significance, comparing vehicle to chemotherapy treated, and chemotherapy to relapse (***$p \leq 0.001$, ****$p \leq 0.0001$).

5.5.2. Inhibiting CCR1 and FLT3 during AML remission

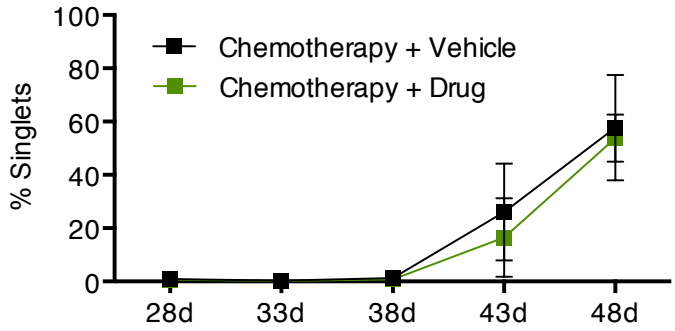
Having established a clinically relevant AML relapse model, the effectiveness of combined CCR1 and FLT3 inhibition was next assessed. To achieve this, chemotherapy-treated mice were given a combination of 10mg/kg Quizartinib (FLT3 inhibitor) and 10mg/kg J113863 (CCR1 inhibitor), or vehicle the day immediately after the final chemotherapy treatment. Peripheral blood engraftment was then tracked over a period of 48 days.

Prior to commencing chemotherapy, leukemic blood engraftment was assessed in both treatment groups, and was found to be statistically comparable as a percentage of live singlets (8.2±2.9% vs. 5.2±3.5%, $p>0.05$; figure 5.5.2.a). Treatment with both inhibitors after chemotherapy reduced leukemic peripheral blood engraftment marginally at day 43 post-transplantation (16.5±14.8% vs. 26.1±18.1%, $p>0.05$; figures 5.5.2.b and 5.5.2.c). After 48 days, all mice, regardless of treatment group, experienced relapse (figure 5.5.2.d). In conclusion, these findings suggested that after only 3 days of dosing, the combined inhibition of CCR1 and FLT3 did not improve overall survival after chemotherapy.

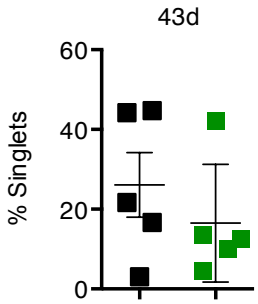
5.5.2.a



5.5.2.b



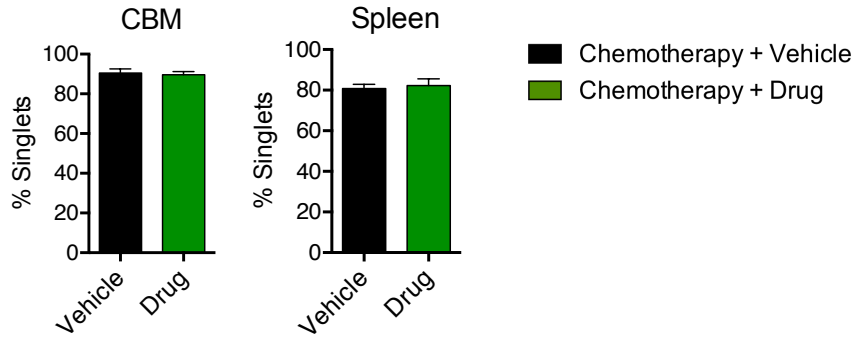
5.5.2.c



Inhibiting CCR1 and FLT3 during AML remission

5.5.2.a. Leukemic (CD45.2) peripheral blood engraftment as a % of singlets from vehicle and drug treatment groups prior to chemotherapy treatment commencement. **5.5.2.b.** Peripheral blood engraftment as a % of singlets over a 48 day period post-transplantation. Two groups are shown, chemotherapy treated alone, and chemotherapy plus CCR1 and FLT3 inhibitor treated **5.5.2.c.** Peripheral blood engraftment at day 43 post-transplantation. Mean±SD, N=5, from one experiment. Two-tailed unpaired *t*-test was used to determine significance, comparing vehicle treated and drug treated groups.

5.5.2.d



Inhibiting CCR1 and FLT3 during AML remission

5.5.2.d. CBM and spleen leukemic cell engraftment as a % of BM or splenic singlets in chemotherapy treated alone, or in combination with FLT3 and CCR1 inhibitors after 48 days. Mean±SD, N=5, from one experiment. Two-tailed unpaired *t*-test was used to determine significance, comparing vehicle treated and drug treated groups.

5.6. Summary and discussion

The global gene expression profiles of LICs and blasts were evaluated during this chapter in order to delineate through what mechanism normal hematopoiesis and the BM niche was perturbed during leukemic development. On a transcriptional level, both LICs and blasts were consistently enriched for cell cycle, cell adhesion, protein synthesis and inflammatory process networks (tables 5.2.5.a and 5.2.5.b). Subsequent pathway analysis revealed that LICs and blasts consistently upregulated the cytokine-cytokine receptor interaction pathway (tables 5.2.6.a and 5.2.6.b), leading to the discovery that both leukemic fractions over-expressed a plethora of chemokines, cytokines and growth factors (figures 5.2.5.c and 5.3.a). Indeed, different combinations of chemokines and cytokines have formerly been described as having both prognostic and diagnostic power in human MDS, AML and CMML (Kornblau et al., 2010; Niyongere et al., 2018). Moreover, several of the secreted factors identified in this chapter have previously been described in AML and MDS,

including CXCL10, CCL3, CCL17, IL18 and CXCL12, (Kornblau et al., 2010; Feng et al., 2011; Olsnes et al., 2006; Kalinkovich et al., 2006; Zhang et al., 2003b). When taken together, these findings indicated that secreted factors derived from leukemic cells may play an important role in disease progression and outcome.

Using the hydrodynamic injection model, the over-expression of *Ccl6* and *Flt3l in vivo* caused a significant increase in the frequency of myeloid progenitor cells, but did not alter the frequency of erythroid progenitors, mature myeloid, lymphoid or erythroid cell types (figures 5.3.1.a and 5.3.2.b). In contrast to recent reports, the over-expression of *Ccl3* and *Tnfsf12* did not negatively impact erythropoiesis, despite both being considered important drivers of anemia (Wang et al., 2016, Felli et al., 2005). The finding that *Flt3l* and *Ccl6* over-expression caused significant GMP and pGM expansion implied that these molecules were likely responsible for the immunophenotypic changes to myeloid progenitor frequency observed during leukemic development (see Chapter 3, figure 3.3.2.a). Indeed, the administration of recombinant FLT3L *in vivo* has previously been demonstrated to expand GMPs, as well as mobilize BM cells into the periphery and spleen of mice (Karsunky et al., 2003; Brasel et al., 1996; Robinson et al., 2000; Robinson et al., 2003). Immature LSK cell types were not analysed after over-expression during this study, however it is likely that upstream LMPP/MPP4 cell populations were responsible for the FLT3L-mediated expansion of myeloid progenitors. Although negative controls were used during the hydrodynamic over-expression assays described in this chapter (empty pCMV-entry vector), the level of protein expression after injection (*i.e.* a positive control) was not measured. In the majority of cases, over-expression did not lead to any observable immunophenotypic effects. However, it is currently not known whether this was due to a genuine lack of effect, insufficient exposure time, or

because the protein of interest was not correctly expressed. This therefore presents as a technical limitation which is currently being addressed by measuring serum protein concentration using enzyme-linked immunosorbent assays (ELISA).

CCL6 has not been widely studied for its role in hematopoiesis, but has been demonstrated to act as a chemoattractant molecule for macrophages, CD11b+ myeloid cells, B and T lymphocytes (Hara et al., 1995; Hogaboam et al., 1999; Coelho et al., 2007). Moreover, the expression of CCL6 has been documented in a number of inflammatory and tissue remodelling conditions (Steinhauser et al., 2000; LaFleur et al., 2004; Núñez et al., 2010), but is yet to be discussed in the context of hematological disorders. In addition to being transcriptionally expressed, CCL6 was also present at the protein level in BM serum samples from leukemic mice, becoming increasingly expressed after 3 weeks, but subsiding again by week 4 (figures 5.3.4.a and 5.3.4.b). Interestingly, the time point at which this protein was most highly expressed correlated with the expansion of endogenous GMPs (see Chapter 3, figure 3.3.2.a), as well as the emergence of CD11b+ myeloid blasts (see Chapter 3, figures 3.2.c and 3.2.d).

MMP9 over-expression was also detected in the BM serum of leukemic mice at week 3, and followed a similar pattern of expression to CCL6. Transcriptionally, *Mmp9* was expressed by blasts cells, but was largely absent in LICs (figure 5.3.4.c). MMP9 is a zinc-dependent endopeptidase responsible for both physiological and pathophysiological tissue remodelling processes. During AML, blast cell surface expression of MMP9 has been demonstrated to be inversely correlated with patient risk, presenting itself as a novel marker for disease prognosis (Schmohl et al., 2016; Kuittinen et al., 1999). In contrast to this, inhibition of cell-surface expressed MMP9 reduces the invasiveness of patient-derived leukemic cells (Paupert et al., 2008). Of

note, IL-18, a secreted factor also expressed by AML blasts, is able to promote the expression of MMP9 and subsequently enhance the aggressiveness of leukemic cells (Zhang et al., 2004b; Zhang et al., 2003b). Collectively, these findings suggested that both MMP9 and IL-18 may have played important roles in leukemogenesis, unrelated to the direct interference of normal hematopoiesis.

Transcriptionally, the receptors *Ccr1* and *Flt3* were both expressed by LICs and blasts throughout leukemic development (figure 5.4.a). However, over-expression of *Flt3l* and *Ccl6* did not accelerate leukemogenesis, as was initially hypothesised, and therefore autocrine signalling via these molecules was ruled out. These findings were in contrast to reports demonstrating an autocrine role for FLT3L during AML leukemogenesis (Zheng et al., 2004). CCL6 on the other hand has been shown to play an anti-leukemic role, whose expression offers immunomodulatory protection during CML, probably through the recruitment of immune cell types to the BM (Nardi et al., 2009). Given that FLT3L over-expression caused significant myeloid expansion, it is feasible that the BM niches normally utilised by LICs became over-occupied. However, analysis of the BM and spleen burden beyond 33 days revealed that regardless of treatment group, all mice experienced comparable disease penetrance. This suggested that *Flt3l* may not have slowed disease onset, but instead temporarily prevented the movement of leukemic cells from the BM into the periphery.

Pharmacological inhibition of the receptors CCR1 and FLT3 was hypothesised to extend remission following chemotherapy. Indeed, CCR1 inhibition has previously been demonstrated to play an important role in chronic lymphocytic leukemic cell survival (van Attekum et al., 2017), and also reduces the adhesion of multiple myeloma cells to osteoclasts, leading to decreased malignant cell

proliferation and cell survival (Vallet et al., 2007). To evaluate this, an AML relapse model was created by treating leukemia-transplanted mice with a single, 5 day cycle of combined cytarabine and doxorubicin. Cytarabine is an antimetabolite agent that interferes with DNA synthesis and stalls cell replication in S phase (van Pelt et al., 2005). Doxorubicin on the other hand intercalates with DNA and prevents topoisomerase II from relaxing supercoiled genomic structures prior to replication (Pommier et al., 2010). Therefore, cells that rapidly divide (*i.e.* leukemic cells) are impacted significantly by the presence of these molecules. After 38 days post-transplantation, chemotherapy treated mice began showing signs of peripheral blood engraftment, which eventually resulted in relapse after 44-48 days. Chemotherapy-treated mice were given a combination of J113863 and Quizartinib for 3 days. J113863 is a potent inhibitor of CCR1 that has previously been demonstrated to ameliorate murine collagen-induced arthritis via the inhibition of inflammatory cell recruitment (Amat et al., 2006) and has been explored for neoplastic and inflammatory hyperalgesia (Llorián-Salvador et al., 2016; Pevida et al., 2012). Quizartinib, also known as AC220, is a selective, small molecule tyrosine kinase inhibitor that is both efficacious and tolerable in tumour xenograft models (Chao et al., 2009). The use of this inhibitor for the therapeutic treatment of AML has been demonstrated to dramatically enhance the survival of FLT3-internal tandem repeat positive AML patients post-relapse, and has formerly been evaluated in phase 2 and 3 clinical trials (Hills et al., 2015). Although additive treatment with these inhibitors marginally decreased peripheral blood engraftment at day 43 post-transplantation (figure 5.5.2.b), this was insufficient to increase the overall survival. Despite the doses, administration routes and vehicle formulas used during this report were taken from published sources, independent pharmacokinetic studies were not carried out

to investigate freely available inhibitor concentrations. Moreover, different inhibitors of the same class were also not assessed due to time limitations. Therefore, it would be necessary to carry out these studies prior to concluding a lack of effect.

Sinusoidal and arteriolar vascular subsets were differentially perturbed during leukemia, both immunophenotypically and transcriptionally (see chapter 3, figure 3.5.d; see chapter 4, figure 4.4.4.e). Leukemia-derived secreted factors were investigated for their ability to mimic the niche immunophenotype observed during AML. Unfortunately however, *in vivo* over-expression did not parallel the AML niche composition (figures 5.3.3.a and 5.3.3.b), indicating that the effects of these factors was confined to the hematopoietic progenitor compartment. Alternatively, the lack of niche remodelling may also be due to the short incubation period used. Extension of this may allow for these secreted factors to remodel niche cells, however that is yet to be investigated.

Collectively, the data presented in this chapter demonstrated that leukemic populations aberrantly expressed several pro-inflammatory secreted factors, two of which were responsible for the expansion of myeloid progenitors. However, inhibiting the primary receptor interactions of these molecules did not attenuate leukemic progression, nor did over-expression enhance leukemic engraftment.

5.7. Conclusions

1. **The transcriptional processes enriched within LICs and blasts during AML were investigated**

Using differential gene expression analysis and Metacore, the transcriptional processes enriched in LICs and blasts during leukemic development were evaluated. This led to the discovery that both LICs and blasts were highly transcriptionally active and expressed numerous process networks related to cell cycle, adhesion and protein synthesis. Furthermore, LICs and blasts consistently enriched for inflammatory processes, which suggested that these cells likely expressed aberrant levels of pro-inflammatory secreted factors throughout disease development.

2. **Leukemic cells expressed a plethora of pro-inflammatory receptors, cytokines and chemokines**

Pathway enrichment analysis revealed that both LICs and blasts upregulated the cytokine-cytokine receptor interaction pathway. Upon closer inspection, leukemic cells differentially expressed numerous pro-inflammatory secreted factors, including *Ccl6* and *Flt3l*. CCL6 was also expressed at the protein level, and at a time point where endogenous GMPs were immunophenotypically expanded during leukemic development.

3. **The *in vivo* over-expression of leukemia derived secreted factors at steady state was investigated**

Leukemic-cell derived secreted factors were over-expressed in wild type mice in order to study the impact on progenitor, mature and niche cell frequencies. The over-expression of *Ccl6* and *Flt3l* in wildtype mice resulted in the expansion of pGM and

GMP myeloid progenitor populations. These findings therefore suggested that the myeloid expansive immunophenotype observed during this model of leukemia was likely caused by the expression of these molecules.

4. **The autocrine signaling capacity of FLT3L and CCL6 was assessed**

Over-expression of *Flt3l* in wildtype mice prior to the transplantation of leukemic cells temporarily slowed the peripheral blood engraftment of malignant cells. This likely occurred due to insufficient space within the niche as a result of an over-expanded committed myeloid progenitor population. If true, this would have implied that LICs and GMPs occupied similar niches within the BM.

5. **FLT3 and CCR1 inhibition was investigated for its effectiveness in delaying relapse**

The effectiveness of inhibiting CCR1 and FLT3 on prolonging remission during a relapse model of AML was investigated. There was a minor reduction in peripheral engraftment, however after 48 days, mice experienced similar levels of tumour engraftment, which suggested that this is not a viable therapeutic target for treating AML.

Chapter 6

Investigating the relationship between leukemia and the aged BM niche

6.1. Introduction and aims

The incidence rate of AML increases significantly with age (Juliusson et al., 2009), and is accompanied by a five year survival rate after treatment of only 10%, compared to 40% in young adults (Menzin et al., 2002; Alibhai et al., 2009). This translates into a mortality rate of 70% for patients aged 65 or older that receive chemotherapy (Meyers et al., 2013). Poor response to traditional treatment options in elderly patients is often attributed to a higher mutational load, adverse cytogenetics, and a lower tolerance to high-dose chemotherapy. However, when compared to patients that are younger, have an equivalent cytogenic risk and also receive comparable treatments, elderly patients still experience lower overall median survival (Appelbaum et al., 2006). This therefore suggests that mechanisms unrelated to those intrinsic to leukemogenesis, contribute towards the increased risk of AML during ageing.

The transplantation of young HSCs into aged congenic mice yields normal long-term myeloid and B cell reconstitution, suggesting that cell intrinsic mechanisms are highly deterministic of lineage potential (Rossi et al., 2005; Beerman et al., 2010; Sudo et al., 2000; Kim et al., 2003; Gekas and Graf, 2013). However, it has also been demonstrated that there are a higher frequency of committed myeloid progenitors during ageing, an effect which cannot be recapitulated after transplantation into a young setting (Rossi et al., 2005). Whilst these findings are consistent with changes to the BM environment, there is very little currently known about how niche populations change on a gene expression level during ageing, and whether this subsequently impacts HSPC functionality. Moreover, there is now a growing body of evidence implicating niche-related signalling as being important for mediating MDS and AML onset (Raaijmakers et al., 2010; Dong et al., 2016; Arranz et al., 2014;

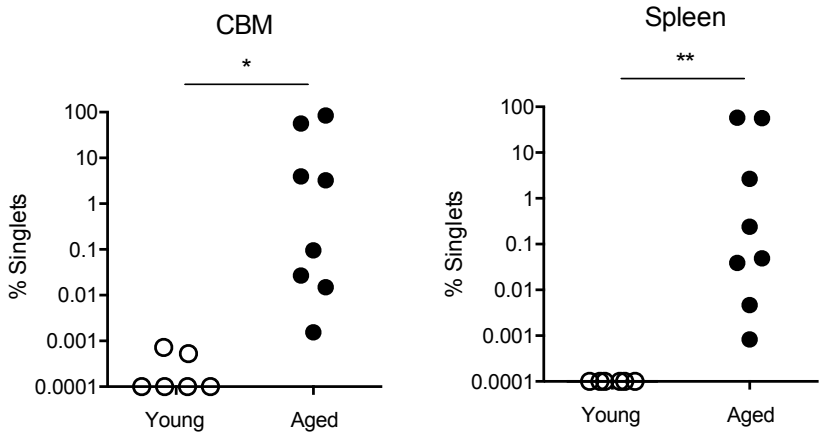
Balderman et al., 2016; Colmone et al., 2008). When considered together, these findings propose that age-related changes to the hematopoietic BM niche may be sufficient to support the development of myeloid malignancies. In order to understand the relationship between leukemia, the BM niche and ageing, the following aims were proposed:

1. Investigate the kinetics of leukemic development after transplantation into non-irradiated aged mice.
2. Immunophenotypically and transcriptionally profile BM niche populations from young and aged mice.
3. Elucidate global gene expression changes shared by individual BM niche populations during ageing.
4. Investigate the effects of inhibiting candidate molecules that may enhance leukemic susceptibility during ageing.

6.2. Investigating the ability of leukemic cells to engraft in aged mice

A cohort of non-irradiated young (~2 months) and aged (~22-24 months) female mice were transplanted with 25,000 KIT+ mutant *Cebpa* K/L LICs. After 4 weeks, BM and spleen leukemic cell engraftment was investigated. As seen in figure 6.2.a, aged mice showed a marked, yet highly variable level of leukemic engraftment as a percentage of live singlets in the BM (16.5±31% vs. 0.0003±0.0003%, $p \leq 0.05$) and spleen (13±25% vs. 0.0001±0%, $p \leq 0.01$) when compared to young controls. These findings therefore suggested that the aged microenvironment was capable of supporting leukemogenesis, whereas the young was not.

6.2.a



Investigating the ability of leukemic cells to engraft in aged mice

6.2.a. Engraftment of CD45.2 leukemic cells as % of singlets in the BM and spleen after 4 weeks post-transplantation. Non-irradiated aged (~22-24 months) and young (~2-3 months) female mice were transplanted with 25,000 KIT+ LICs. A Mann-Whitney test was used to determine statistical significance, comparing aged mice to young (*$p \leq 0.05$, **$p \leq 0.01$). N=6-8 from two independent experiments.

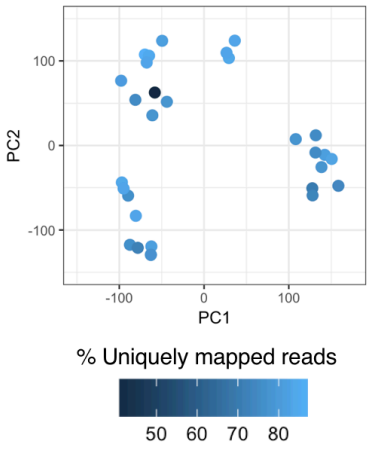
6.3. Bulk RNA-seq of the CBM and BL niche cells during ageing

Having established that ageing was sufficient to support leukemogenesis, it was next hypothesised that this was driven by changes to the BM niche. LepR+ PV cells, OBs, PαS MSCs, CBM VECs and BL VECs were FACS isolated from aged (~22-24 months) and young (~2 months) mice using the immunophenotypic definitions described earlier (see Chapter 3, figures 3.5.a and 3.5.b). Samples were prepared for bulk RNA-seq using the SMART-seq2 protocol (see Materials and methods, section 2.1.7), after which a series of computational analyses were carried out in order to delineate the major molecular events that occurred in these cell populations during ageing.

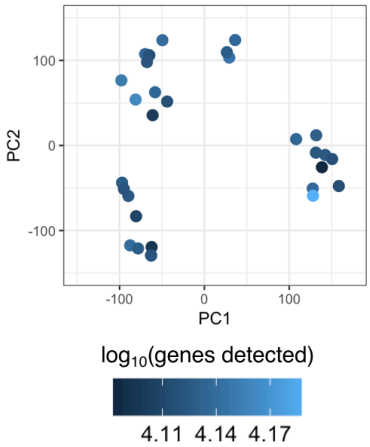
6.3.1. Data quality check

Prior to analysis, sequenced aged niche samples were validated for read mapping percentage, library size and total number of genes detected per sample. Library size and total number of genes detected are displayed as $\log_{10}$ values. As seen in figure 6.3.1.a, all sequenced niche samples aligned to the mm9 reference genome with approximately 40-85% mapping efficiency. The library sizes and number of uniquely detected genes for each sample was consistent (figures 6.3.1.b and 6.3.1.c) and therefore no samples were excluded on this basis.

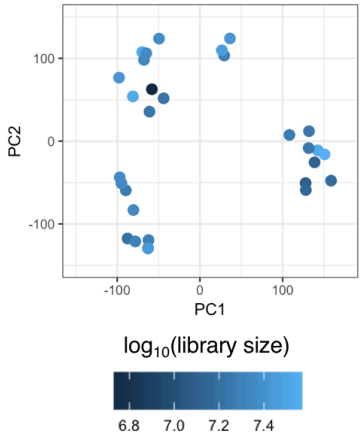
6.3.1.a



6.3.1.b



6.3.1.c



Data quality check

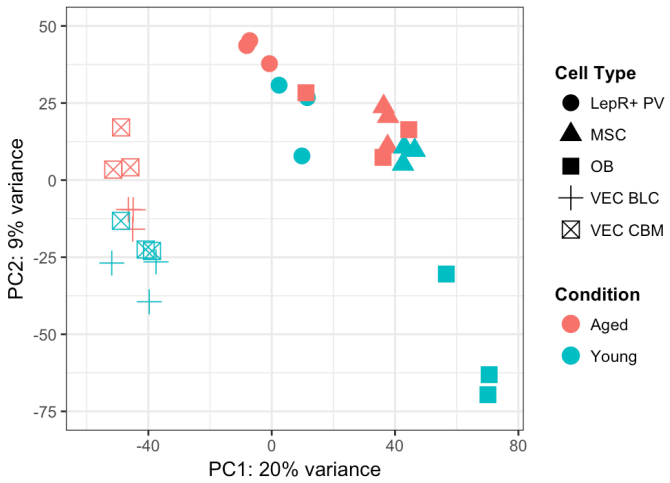
6.3.1.a. Percentage of mapped reads per leukemic cell sample. **6.3.1.b.** Log_{10} number of genes detected per leukemic cell sample. **6.3.1.c.** Log_{10} library size per leukemic cell sample.

6.3.2. PCA of aged and young niche cell populations

To further evaluate the quality of the sequenced samples, PCA was carried out on the top 500 variable genes from all aged niche cell types (figure 6.3.2.a). VECs and

mesenchymal cells (i.e. PαS MSCs, LepR+ PV cells and OBs) clustered separately along PC1, whereas PC2 appeared to define whether cells were from young or aged mice. Interestingly, aged mature OBs clustered in closer proximity to immature PαS MSCs, whereas young OBs appeared to be transcriptionally distinct, clustering separately. Furthermore, variance between CBM VECs from young and aged mice appeared greater than that of BL VECs, suggesting that these cells were transcriptionally different during ageing.

6.3.2.a



PCA of aged and young niche cell populations

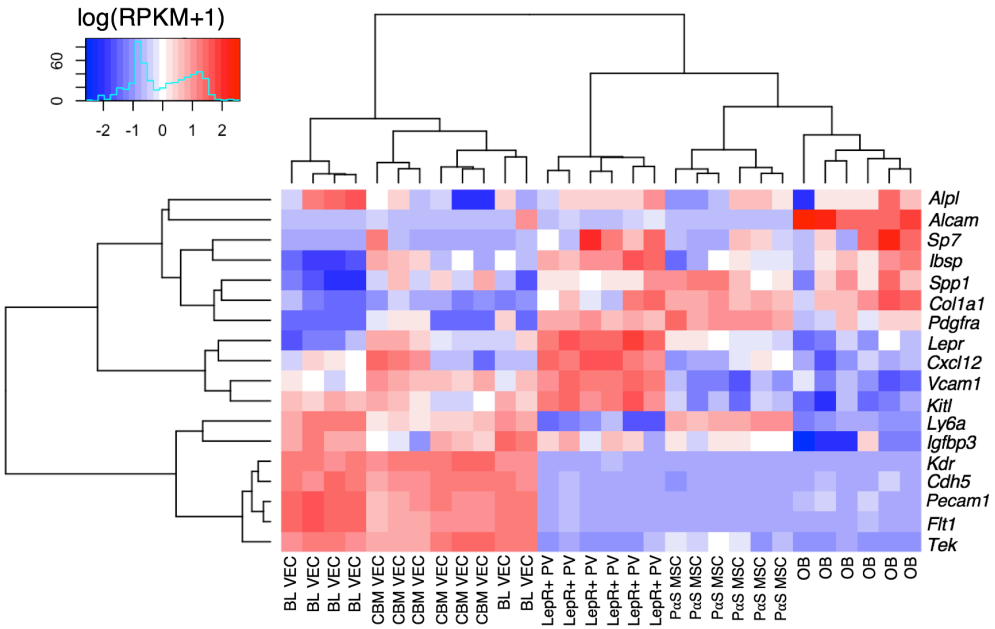
6.3.2.a. PCA constructed based on the top 500 variable genes from young and aged BM niche populations.

6.3.3. Heatmap of known niche cell markers

A heatmap was generated that clustered aged BM niche populations based on the expression of known niche genes using Wards method and Euclidean distance. As seen in figure 6.3.3.a, VECs clustered together based on their expression of the known VEC genes *Pecam1*, *Kdr*, *Cdh5*, *Flt1* and *Tek*. LepR+ PV cells, on the other

hand, clustered based on their expression of the LepR+ PV cell associated genes *Lepr*, *Cxcl12*, *Vcam1* and *Kitl* (Ding et al., 2012; Ding and Morrison, 2013), but also shared expression of *Pdgfra* with PαS MSCs. Unlike LepR+ PV cells, PαS MSCs also expressed *Ly6a*, a marker associated with *in vitro* and *in vivo* MSC multipotency (Morikawa et al., 2009). Lastly, OBs clustered together based on their expression of known OB genes *Alcam*, *Col1a1*, *Sp7* and *Ibsp* (Nakamura et al., 2010; Huang et al., 2007). This analysis demonstrated that the transcriptional profiles of cell types analysed represented the cell types isolated by FACS.

6.3.3.a



Heatmap of known niche cell markers

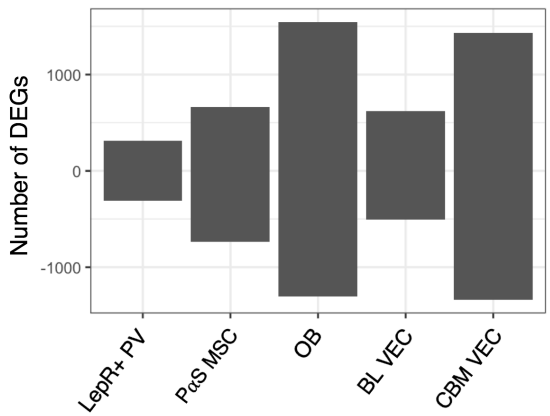
6.3.3.a. Heatmap of CBM and BL niche cell types clustered against known niche gene markers. Expression values are scaled, log(RPKM+1).

6.3.4. Differential gene expression analysis of aged BM niche populations

Having assessed samples using PCA, as well as for their expression of known genes, the number of up- and down-DEGs present in each of the niche populations during ageing was next determined. DESeq2 was used to compare niche populations isolated from aged (~22-24 months) mice to young (~2 months) mice.

The number of up- and down-DEGs with an adjusted $p \leq 0.05$ varied significantly between cell types (figure 6.3.4.a). CBM VECs and OBs exhibited several thousand transcriptional changes, whereas LepR+ PV cells displayed only hundreds. This suggested that during ageing, the majority of transcriptional changes occurred within only certain cell types, and did not appear to depend on whether a cell type was from the BL or CBM niche.

6.3.4.a



Differential gene expression analysis of aged niche populations

6.3.4.a. Number of up- and down-regulated DEGs with an adjusted $p \leq 0.05$ from LepR+ PV cells, PαS MSCs, OBs, BL VECs and CBM VECs. DEGs were determined using DESeq2.

6.3.5. Shared process network enrichment analysis of aged niche populations

Using Metacore, process networks that were consistently enriched across all CBM and BL niche populations during ageing were investigated. DEGs with an adjusted $p \leq 0.05$ from each niche cell type were imported into Metacore. Process networks shown have a $p \leq 0.05$ and FDR$\leq$0.05. The process networks that enriched multiple times across different cell populations were determined, and are illustrated in table 6.3.5.a.

Based on this analysis, all five niche cells consistently enriched for processes associated with bone remodelling and ossification, integrin mediated cell adhesion and cytoskeletal rearrangement. Process networks shared by at least four niche cells included TGF-β signalling, blood vessel morphogenesis, cell adhesion and neutrophil activation. The widespread enrichment of IL-6 signalling was consistent with findings demonstrating that IL-6 production is a common feature during ageing, and is primarily expressed by skeletal muscle tissue (Wei et al., 1992; Weigert et al., 2005). Processes such as cell adhesion and cell cycle continued to be enriched by at least two or three niche populations. The enrichment of inflammatory processes was also in agreement with the widely believed “inflamm-ageing” phenomenon, which proposes low-levels of unresolved chronic inflammation during ageing (Franceschi et al., 2000).

6.3.5.a

Number of niche populations sharing network	*Enriched process networks*
5	Cell adhesion_Integrin-mediated cell-matrix adhesion
	Development_Neurogenesis_Axonal guidance
	Development_Ossification and bone remodelling
4	Cell adhesion_Attractive and repulsive receptors
	Cell adhesion_Integrin priming
	Cell adhesion_Platelet aggregation
	Cell adhesion_Platelet-endothelium-leucocyte interactions
	Cytoskeleton_Actin filaments
	Cytoskeleton_Regulation of cytoskeleton rearrangement
	Development_Blood vessel morphogenesis
	Development_EMT_Regulation of epithelial-to-mesenchymal transition
	Development_Regulation of angiogenesis
	Immune response_Phagosome in antigen presentation
	Inflammation_Neutrophil activation
	Proliferation_Positive regulation cell proliferation
	Reproduction_Feeding and Neurohormone signalling
	Reproduction_FSH-beta signalling pathway
	Signal Transduction_TGF-beta, GDF and Activin signalling
3	Cell adhesion_Amyloid proteins
	Cell adhesion_Cell junctions
	Cell adhesion_Leucocyte chemotaxis
	Cell cycle_G1-S Growth factor regulation
	Cell cycle_G1-S Interleukin regulation
	Cell cycle_G2-M
	Immune response_Antigen presentation
	Immune response_BCR pathway
	Immune response_IL-5 signalling
	Immune response_Th17-derived cytokines
	Inflammation_IL-6 signalling
	Inflammation_Protein C signalling
	Proteolysis_Proteolysis in cell cycle and apoptosis
	Reproduction_Progesterone signalling
	Translation_Regulation of initiation
2	Apoptosis_Anti-apoptosis mediated by external signals via NF-kB
	Cell adhesion_Cadherins
	Cell adhesion_Cell-matrix interactions

Cell cycle_Meiosis
Cell cycle_Mitosis
Cell cycle_S phase
Cytoskeleton_Intermediate filaments
Development_Cartilage development
Development_ERK5 in cell proliferation and neuronal survival
Development_Hemopoiesis, Erythropoietin pathway
Immune response_Phagocytosis
Immune response_TCR signalling
Inflammation_Amphoterin signalling
Proliferation_Negative regulation of cell proliferation
Protein folding_Folding in normal condition
Protein folding_Response to unfolded proteins
Proteolysis_Ubiquitin-proteasomal proteolysis
Signal transduction_Androgen receptor nuclear signalling
Signal transduction_Androgen receptor signalling cross-talk
Signal Transduction_Cholecystokinin signalling
Signal transduction_ERBB-family signalling
Signal transduction_ESR1-membrane pathway
Signal transduction_ESR1-nuclear pathway
Signal transduction_Leptin signalling
Signal transduction_WNT signalling
Transcription_mRNA processing

Shared process network enrichment analysis of aged niche populations

6.3.5.a. Process networks shared by 2 or more niche populations during ageing as determined by Metacore. DEGs with an adjusted $p \leq 0.05$ were used as input. All process networks shown have a $p \leq 0.05$ and FDR$\leq$0.05.

6.3.6. Aged and leukemic CBM VECs were transcriptionally and immunophenotypically alike

During ageing, CBM VECs displayed a high number of up- and down-DEGs (~3000) when compared to other aged niche populations (figure 6.3.4.a). Given that CBM VECs exhibited significant immunophenotypic and transcriptional changes during leukemia, it was hypothesised that aged CBM VECs shared overlapping

transcriptional features with leukemic VECs, making them comparably supportive of leukemogenesis.

To evaluate this, the immunophenotypic frequency of BL and CBM VECs during ageing was assessed. As seen in figure 6.3.6.a, the frequency of CBM VECs as a percentage of live singlets during age was decreased when compared to young controls (0.053±0.016% vs. 0.013±0.007%, $p \leq 0.01$), whereas BL VECs were not (0.48±0.13% vs. 0.64±0.2%, $p > 0.05$). The age-dependent decrease in CBM VEC frequency paralleled the observations made during leukemia (see Chapter 3, figure 3.5.d).

Transcriptionally enriched process networks shared by both CBM VECs during leukemia and ageing were assessed. Illustrated in table 6.3.6.b are the enriched process networks shared by CBM VECs at weeks 2, 3 and 4 of leukemic development, and aged CBM VECs. This analysis was generated by overlaying process networks identified in section 6.3.5.a of this chapter with those analysed in section 4.3.5.a of Chapter 4. Displayed are the shared process networks, the time point at which they appeared during leukemic development, and the *p*-value/FDR values associated with each network. All output process networks had a $p \leq 0.05$ and FDR$\leq$0.05. Based on this analysis, CBM VECs during ageing shared numerous process networks with those identified during leukemia, including cell adhesion, blood vessel morphogenesis and inflammation. The majority of shared networks occurred at the week 3 time point of leukemic development, which coincided with the major immunophenotypic, functional and transcriptional changes to HSPCs and the niche.

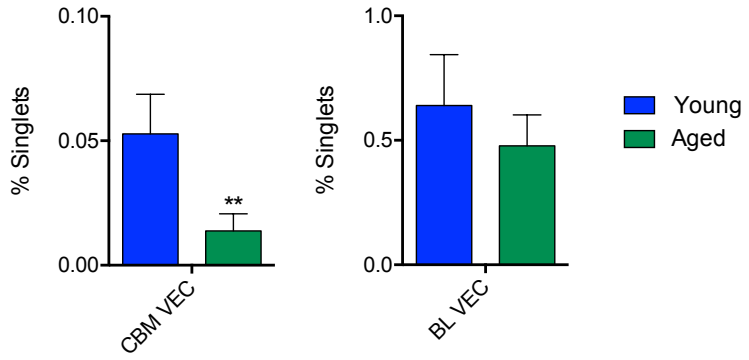
Having observed shared enriched process networks, DEGs with an adjusted $p \leq 0.05$ from CBM VECs exposed to leukemia for 2, 3 and 4 weeks were compared

to DEGs with an adjusted $p \leq 0.05$ from CBM VECs during ageing. Using a hypergeometric statistical test, it was demonstrated that CBM VEC DEGs at week 3 of leukemic development shared a highly significant gene expression profile ($p < 0.0001$) with aged CBM VECs, consisting of 97 up- and 185 down-DEGs (figure 6.3.6.c). Closer inspection of shared down-DEGs revealed a reduced expression of *Mrc1* (figure 6.3.6.d). This gene was exclusively expressed by sinusoidal VECs in young mice at steady state (see Chapter 4, figure 4.4.5.b). Moreover, there was a significant increase in the expression of CBM VEC-derived *Cxcl12* and *Kitl* during ageing (figure 6.3.6.d). These genes are normally expressed by arteriolar VECs at steady state (Xu et al., 2018; see Chapter 4, figure 4.4.5.a), and was a population of VECs that were expanded in frequency during leukemia (see Chapter 3, figure 3.5.c). The expression of *Cxcl12* and *Kitl* by a population of VECs that do not normally express these factors indicated that during ageing, VEC sub-populations underwent significant transcriptional changes.

Based on these findings, it was further hypothesised that the loss and gain of genes experienced during ageing was driven by vascular remodelling of *Vcam1* positive and negative VECs. This was evaluated by measuring the enrichment score of genes shared by both CBM VECs after 3 weeks of leukemia and ageing in *Vcam1* positive and *Vcam1* negative VEC clusters at steady state. Shared up-regulated genes were enriched in *Vcam1* negative VECs, whereas shared down-regulated genes were enriched in *Vcam1* positive VECs (figures 6.3.6.e). Collectively, these findings suggested that the genes shared by VECs during ageing and leukemia were enriched in a subset of VECs that were also significantly depleted during leukemia. Furthermore, the over-expression of *Cxcl12* and *Kitl* by CBM VECs suggested that

the expansion or loss of certain vascular subsets during ageing may have led to the over-expression of factors important for leukemic-cell engraftment.

6.3.6.a



6.3.6.b

Time Point	*Overlapping Process Network*	*Leukemia p-value*	*Leukemia FDR*	*Aged p-value*	*Aged FDR*
Week 2	Development_Blood vessel morphogenesis	0.0011	0.0348	0.0000	0.0000
	Signal transduction_WNT signalling	0.0015	0.0348	0.0006	0.0030
Week 3	Cell adhesion_Cell-matrix interactions	0.0024	0.0338	0.0060	0.0225
	Cell adhesion_Integrin priming	0.0048	0.0398	0.0041	0.0176
	Cell adhesion_Integrin-mediated cell-matrix adhesion	0.0014	0.0276	0.0000	0.0000
	Cell adhesion_Leucocyte chemotaxis	0.0030	0.0338	0.0027	0.0125
	Cell adhesion_Platelet aggregation	0.0030	0.0338	0.0093	0.0320
	Cell adhesion_Platelet-endothelium-leucocyte interactions	0.0000	0.0000	0.0000	0.0001
	Cytoskeleton_Actin filaments	0.0010	0.0220	0.0001	0.0007
	Cytoskeleton_Intermediate filaments	0.0057	0.0453	0.0055	0.0211
	Cytoskeleton_Regulation of cytoskeleton rearrangement	0.0036	0.0381	0.0000	0.0000
	Development_Blood vessel morphogenesis	0.0017	0.0293	0.0000	0.0000

	Development_EMT_Regulation of epithelial-to-mesenchymal transition	0.0006	0.0155	0.0000	0.0000
	Development_Regulation of angiogenesis	0.0048	0.0398	0.0000	0.0000
	Immune response_Phagocytosis	0.0000	0.0001	0.0000	0.0000
	Inflammation_IL-6 signalling	0.0042	0.0398	0.0005	0.0028
	Proliferation_Positive regulation cell proliferation	0.0005	0.0149	0.0000	0.0002
	Reproduction_Feeding and Neurohormone signalling	0.0002	0.0079	0.0000	0.0000
	Signal Transduction_TGF-beta, GDF and Activin signalling	0.0022	0.0338	0.0000	0.0000
Week 4	Cell adhesion_Platelet-endothelium-leucocyte interactions	0.0014	0.0498	0.0000	0.0001
	Development_Blood vessel morphogenesis	0.0026	0.0498	0.0000	0.0000
	Development_EMT_Regulation of epithelial-to-mesenchymal transition	0.0006	0.0498	0.0000	0.0000
	Development_Regulation of angiogenesis	0.0022	0.0498	0.0000	0.0000
	Proliferation_Positive regulation cell proliferation	0.0021	0.0498	0.0000	0.0002
	Signal Transduction_TGF-beta, GDF and Activin signalling	0.0025	0.0498	0.0000	0.0000

Aged and leukemic CBM VECs were transcriptionally and immunophenotypically alike

6.3.6.a. Immunophenotypic frequency of CBM and BL VECs from young and aged mice as a % of live singlets. A two-tailed unpaired *t*-test was used to determine significance (**$p \leq 0.01$). Mean±SD, N=4 from one experiment. **6.3.6.b.** Process networks shared between CBM VECs during leukemia at weeks 2, 3 and 4 and aged CBM VECs. Analysis was completed using Metacore and DEGs with an adjusted $p \leq 0.05$. Process networks shown have a $p \leq 0.05$ and FDR≤0.05. *P*-values and FDR values from both leukemic and aged CBM VECs are shown.

6.3.6.c

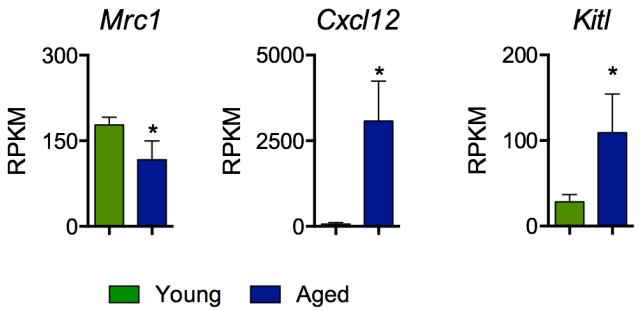


Comparison	*p*-value	Representation factor (Rf)
Age vs W2 AML up	7.272e-05	3.5
Age vs W3 AML up	1.364e-25	3.3
Age vs W4 AML up	3.986e-06	3.2
Age vs W2 AML down	0.213	0
Age vs W3 AML down	9.186e-105	6.7
Age vs W4 AML down	0.291	1.3

Aged and leukemic CBM VECs were transcriptionally and immunophenotypically alike

6.3.6.c. Overlap of up- and down-DEGs from CBM VECs during ageing and after 2, 3 and 4 weeks of leukemic development. DEGs with an adjusted $p \leq 0.05$ were used as input. A hypergeometric statistical test was used to determine significance of overlapping genes (*$p<0.0001$, Rf>1).

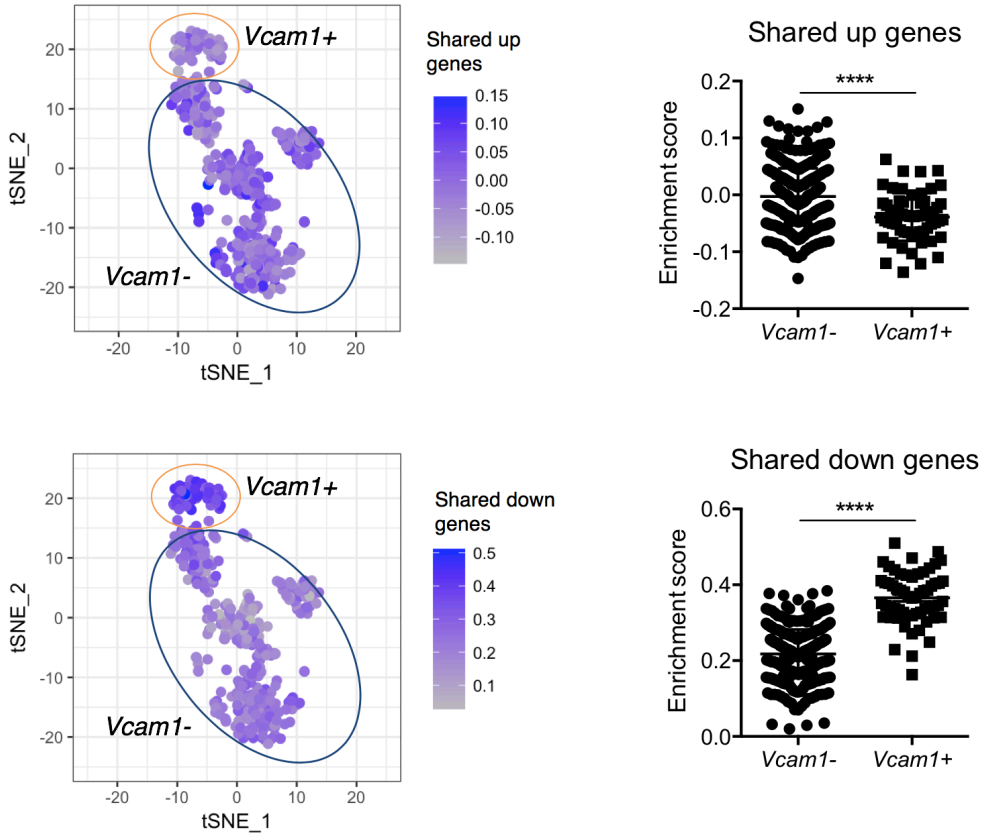
6.3.6.d



Aged and leukemic CBM VECs were transcriptionally and immunophenotypically alike

6.3.6.d. RPKM expression values for *Mrc1*, *Cxcl12* and *Kitl* in aged CBM VECs. Significance determined using DESeq2 by comparing aged niche populations to young (*adjusted $p \leq 0.05$). Mean±SD, N=4 from one experiment.

6.3.6.e



Aged and leukemic CBM VECs were transcriptionally and immunophenotypically alike

6.3.6.e. Enrichment score of shared up- and down- regulated genes from CBM VECs during week 3 of leukemia and ageing. Score is plotted against *Vcam1* negative and *Vcam1* positive VECs from young mice. A Mann-Whitney test was used to determine significance (****$p \leq 0.0001$).

6.3.7. OBs were immunophenotypically and transcriptionally perturbed during ageing

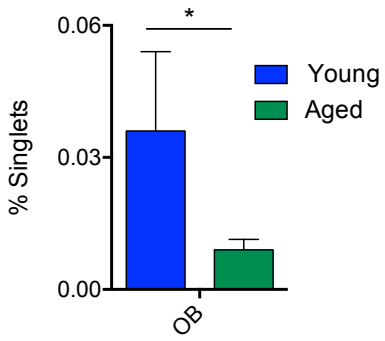
Bone remodelling and ossification processes were highly enriched across all niche populations during ageing (figure 6.3.5.a). In line with this, OBs were significantly depleted in frequency as a percentage of live singlets during ageing when compared to young (0.009±0.002 vs. 0.036±0.02, $p \leq 0.05$; figure 6.3.7.a), and also clustered by PCA in proximity to MSCs (figure 6.3.2.a). The expression of genes previously reported as being important for osteogenesis were investigated in aged OBs. This included *Bglap*, *Spp1*, *Bmp7*, *Omd*, *Ibsp*, *Notch2*, *Runx2* and *Dlx5* (Aubin, 1998; Morinobu et al., 2003; Chen and Webster, 2009). There was a statistically significant down-regulation of all of these genes in aged OBs, to levels that were comparable to PαS MSCs (figure 6.3.7.b). Interestingly, this also occurred despite OBs expressing normal levels of *Alcam* (14.4±7.5 RPKM vs. 7.4±2.5 RPKM, adjusted $p>0.05$). Taken together, these findings suggested that mature OBs, whilst capable of appearing immunophenotypically normal (*i.e.* isolable by FACS based on ALCAM expression), lose their osteogenic gene expression profile.

PαS MSCs have both adipogenic and osteogenic potential (Morikawa et al., 2009), therefore, the enrichment of genes related to adipogenesis in young and aged PαS MSCs was investigated. This analysis revealed that during ageing, PαS MSCs became mildly enriched for an adipogenic gene signature ($p<0.1$, FDR<0.25; figure 6.3.7.c), which included the statistically significant over-expression of several pro-adipogenic genes including *Pparg*, *Aldh2*, *Adipoq* and *Agt* (Massiéra et al., 2001; Yu et al., 2016; Lefterova et al., 2014; Hu et al., 1996). Moreover, two important osteogenic genes, *Spp1* and *Col1a1,* were significantly down regulated (figure

6.3.7.d). Taken together, these findings implied that PαS MSCs were less primed towards OB production, yet appeared able to generate adipocytes.

Using GSEA, the entire Molecular Signatures Database (v5.2) was run against ranked OB DEGs with an adjusted $p \leq 0.05$. This analysis revealed that, in addition to losing their osteogenic gene expression profile, aged OBs also became highly enriched for signatures related to leukocyte chemotaxis, myeloid leukocyte migration and granulocyte migration (figure 6.3.7.e). Closer inspection of GSEA leading edge genes revealed that aged OBs over-expressed a number of cell surface receptors and secreted molecules including *Ccl6*, *Tgfb1*, *Ccr1*, *Vegfb*, *Icam2*, *Ccr2*, and *Csf3r* (figures 6.3.7.f and 6.3.7.g).

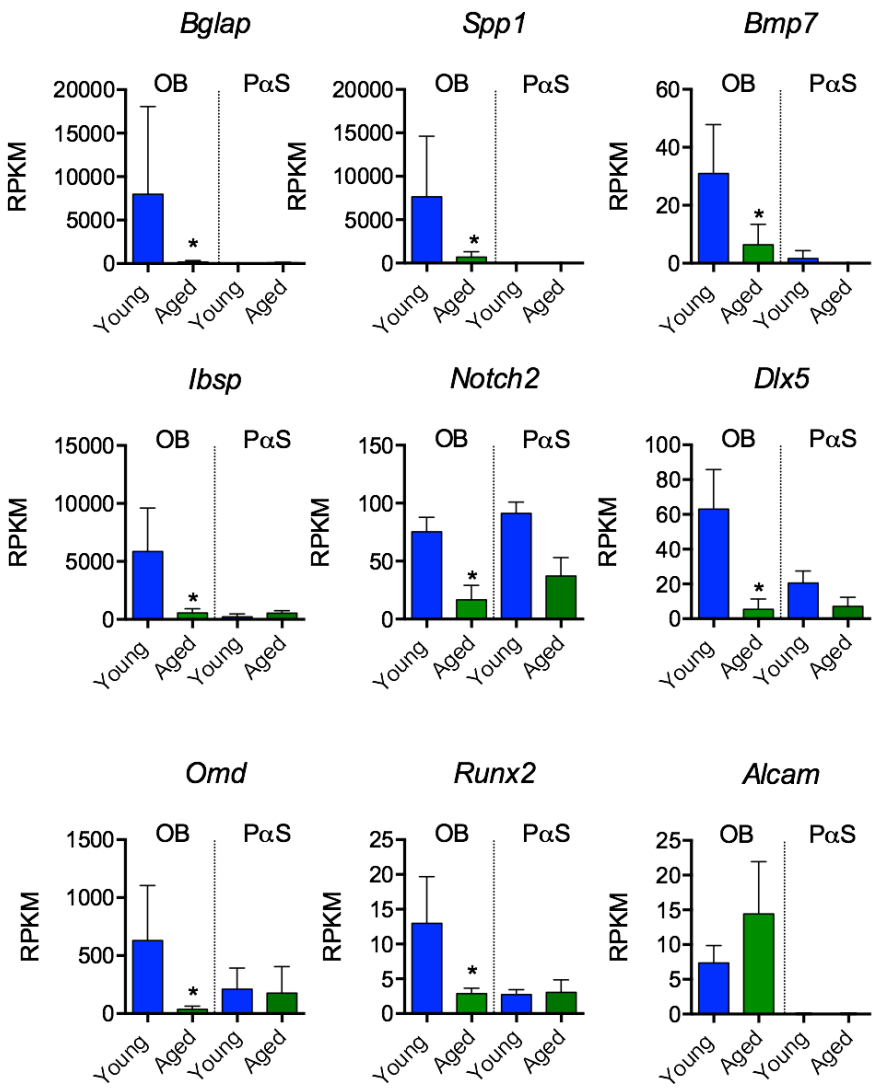
6.3.7.a



OBs were immunophenotypically and transcriptionally perturbed during ageing

6.3.7.a. Immunophenotypic frequency of mature OBs as a % of live singlets in young (~2 months) and aged (~22-24 months) mice. A two-tailed unpaired *t*-test was used to determine statistical significance (*$p \leq 0.05$). Mean±SD, N=4 from one experiment.

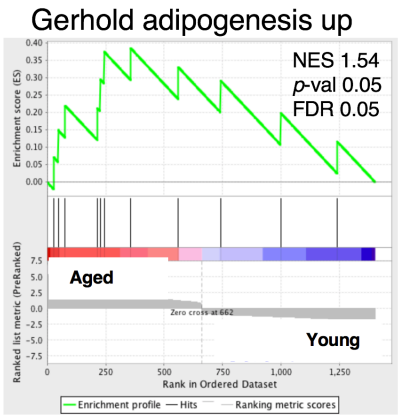
6.3.7.b

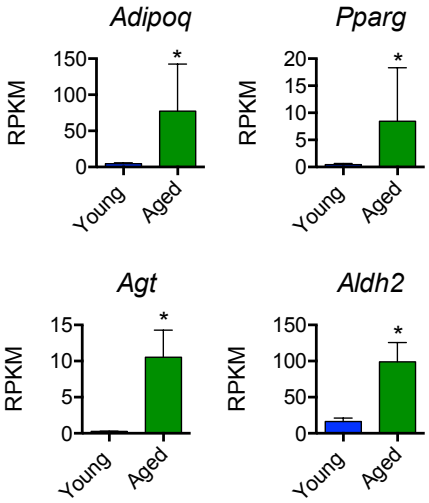


OBs were immunophenotypically and transcriptionally perturbed during ageing

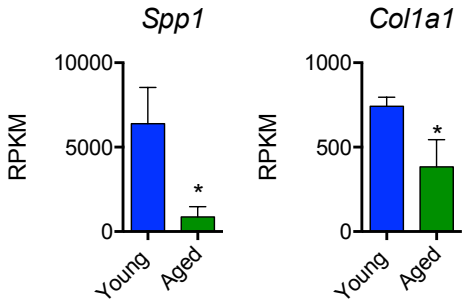
6.3.7.b. RPKM expression values for genes related to osteogenesis in young and aged OBs and PαS MSCs. Statistical significance determined using DESeq2, comparing young niche cells to aged (*adjusted $p \leq 0.05$). Mean±SD, N=3 from one experiment.

6.3.7.c





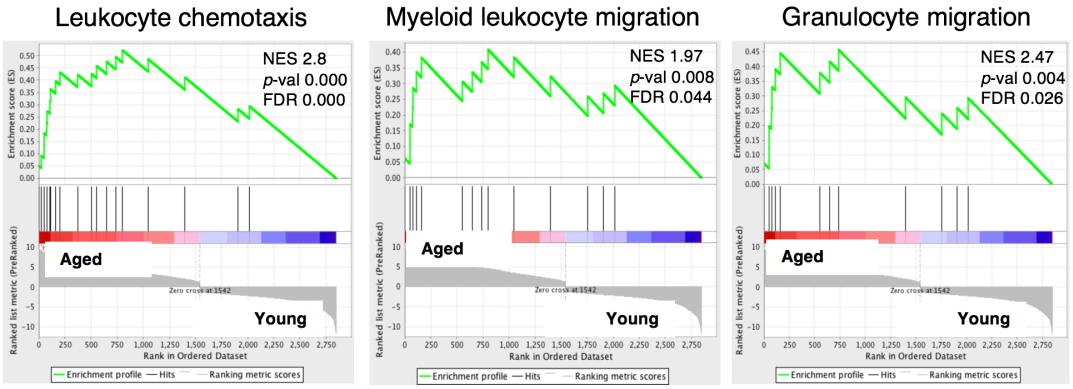
6.3.7.d



OBs were immunophenotypically and transcriptionally perturbed during ageing

6.3.7.c. GSEA using the Gerhold adipogenesis up- gene signature comparing young and aged PαS MSCs. DEGs with an adjusted $p \leq 0.05$ were used as input. RPKM expression values for GSEA leading edge genes are to the right. GSEA significance was considered where $p \leq 0.05$ and FDR≤0.25. **6.3.7.d.** RPKM expression values for osteogenic genes in PαS MSCs from young and aged mice. Significance determined using DESeq2, comparing young and aged mice (*adjusted $p \leq 0.05$). Mean±SD, N=3 from one experiment.

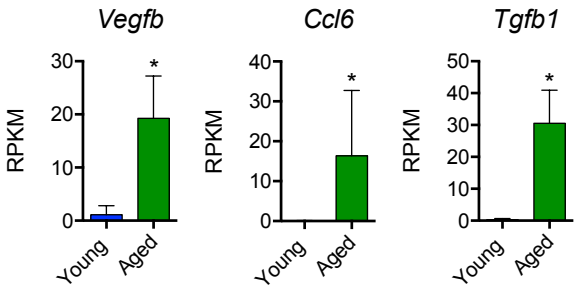
6.3.7.e



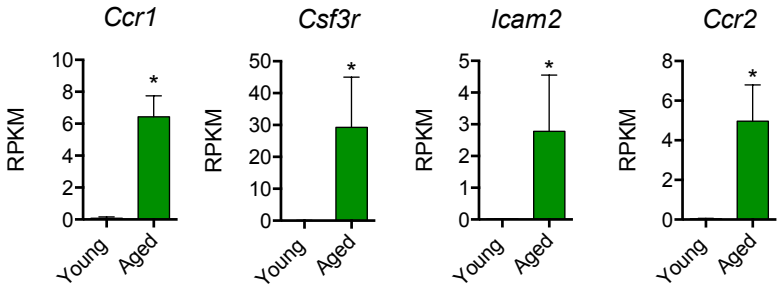
OBs were immunophenotypically and transcriptionally perturbed during ageing

6.3.7.e. GSEA using ranked DEGs with an adjusted $p \leq 0.05$ as input. Leukocyte chemotaxis, granulocyte migration and myeloid leukocyte migration gene sets were highly enriched in OBs during ageing. All gene sets shown are significant with a $p \leq 0.05$ and FDR$\leq$0.25.

6.3.7.f



6.3.7.g



OBs were immunophenotypically and transcriptionally perturbed during ageing

6.3.7.f. RPKM expression values for secreted factor genes in young and aged mice.

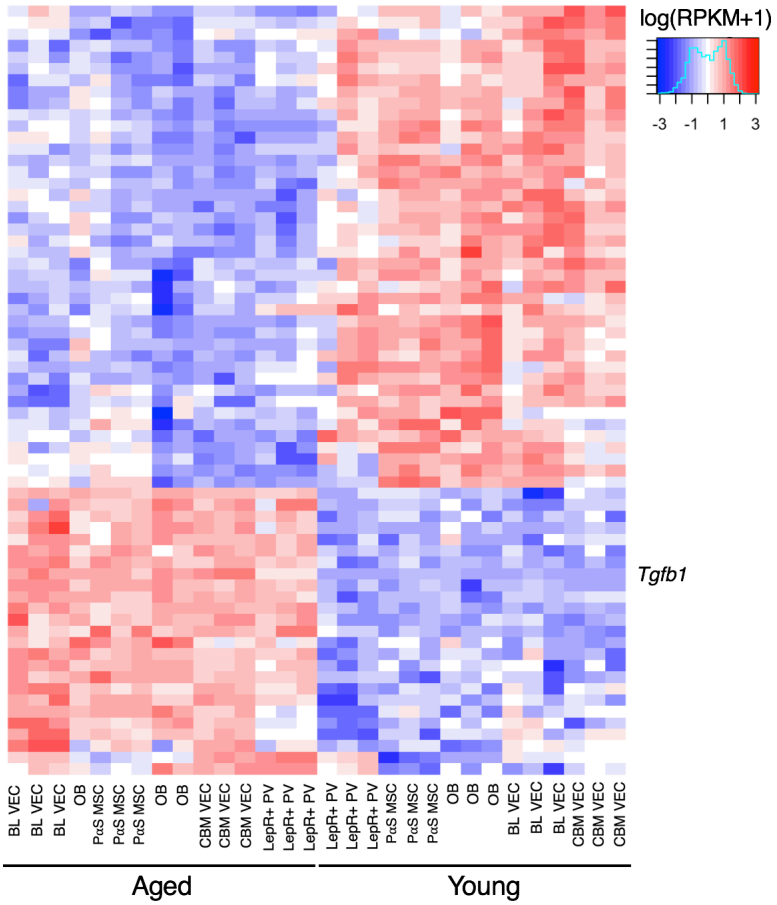
6.3.7.g. RPKM expression values for cell surface expressed genes in young and aged mice. All genes were statistically significant, determined using DESeq2 by comparing young to aged mice (*adjusted $p \leq 0.05$). Mean±SD, N=3 from one experiment.

6.3.8. Aged niche cells expressed a common gene signature

Upon comparing DEGs (adjusted $p \leq 0.05$) from aged niche populations, a common gene signature was uncovered which was comprised of 25 shared up- and 43 shared down-DEGs (figure 6.3.8.a). Closer inspection of these genes revealed the consistent, and statistically significant over-expression of *Tgfb1,* which unlike other important niche factors, was the only ubiquitously over-expressed secreted factor present in all cell types during ageing (figure 6.3.8.b). TGF-β1 process networks were also enriched in four out of five niche populations during ageing (figure 6.3.5.a), in addition to *Tgfbr1* and *Tgfbr2* both being expressed by all niche populations (figure 6.3.8.c).

Having demonstrated at the beginning of this chapter that the process of ageing was sufficient to enable the engraftment of leukemic cells (figure 6.2.a) and in light of the results discussed above, it was hypothesised that the expression of TGF-β1 by the niche played an important role in supporting leukemogenesis. Indeed, *Tgfbr1* was expressed by both LICs and blast cells during leukemic development (figure 6.3.8.d), and CBM VECs from leukemic mice also began differentially expressing *Tgfb2* after 3 and 4 weeks (figure 6.3.8.e).

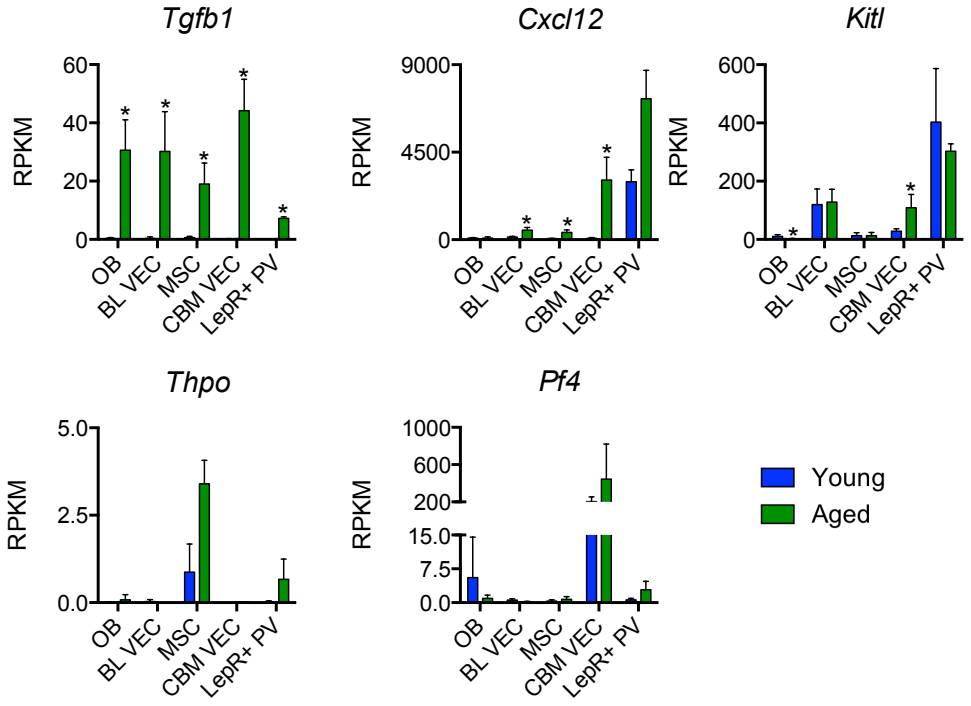
6.3.8.a



Aged niche cells expressed a common gene signature

6.3.8.a. Heatmap depicting DEGs with an adjusted $p \leq 0.05$ shared amongst all niche populations including CBM VECs, BL VECs, OBs, PαS MSCs and LepR+ PV cells. Expression values are shown as log(RPKM+1).

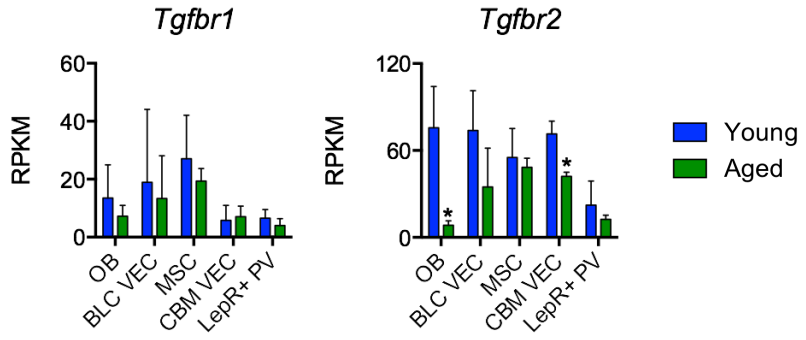
6.3.8.b



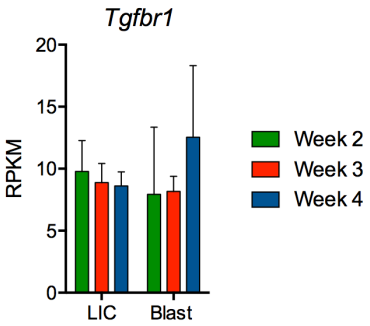
Aged niche cells expressed a common gene signature

6.3.8.b. RPKM expression values for the niche secreted factors *Tgfb1*, *Cxcl12*, *Kitl*, *Thpo* and *Pf4* amongst all niche cell types from young and aged mice (*adjusted $p \leq 0.05$, determined using DESeq2 by comparing aged niche cells to young). Mean±SD, N=3 from one experiment.

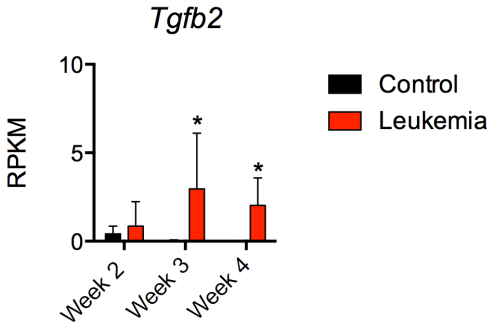
6.3.8.c



6.3.8.d



6.3.8.e



Aged niche cells expressed a common gene signature

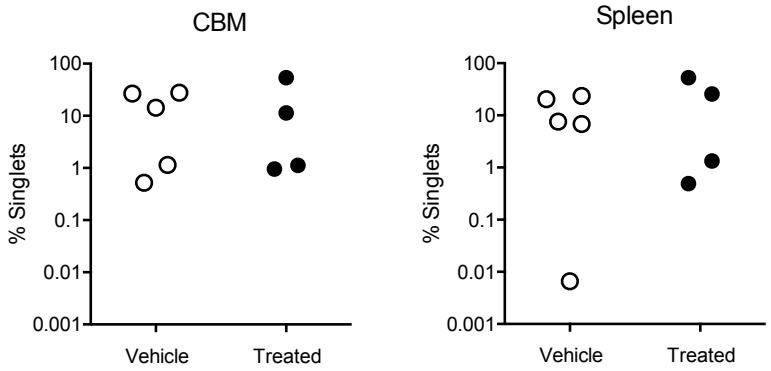
6.3.8.c. RPKM expression values for *Tgfbr1* and *Tgfbr2* in all niche cell types studied. **6.3.8.d.** RPKM expression of *Tgfbr1* in LICs and blasts at weeks 2, 3 and 4 post-leukemia transplantation. **6.3.8.e.** RPKM expression values for *Tgfb2* in CBM VECs during leukemic development at weeks 2, 3 and 4. (*adjusted $p \leq 0.05$ as determined using DESeq2). Mean±SD, N=3 from one experiment.

6.3.9. Inhibiting TGF-β receptor 1 in leukemia transplanted aged mice

Having established that TGF-β1 was over-expressed by all aged niche population, the inhibition of this molecule's primary receptor during leukemic transplantation was next assessed. To achieve this, a cohort of aged (~22-24 month) CD45.1 female mice were pre-treated for 14 days with either vehicle or a single daily dose (30mg/kg) of the potent TGF-β receptor 1 inhibitor, SB525334 (Grygielko et al., 2005). All mice were injected with 25,000 CD45.2 KIT+ LICs on the 10th day of treatment. After 21 days post-transplantation, mice were euthanised and analysed.

Figure 6.3.9.a depicts the BM and spleen engraftment of CD45.2 leukemic cells as a percentage of singlets. Based on these findings, TGF-β receptor 1 inhibition during ageing did not reduce the engraftment of leukemic cells when compared to vehicle treated mice in either the BM (14±13.2 vs. 16.9±23.2, p>0.05) or spleen (11.7±14 vs. 20±25, p>0.05).

6.3.9.a



Inhibiting TGF-β receptor 1 in leukemia transplanted aged mice

6.3.9.a. Leukemic cell engraftment after 21 days as a % of live singlets in the BM and spleen of aged female CD45.1. Mice were treated daily for 14 days with either vehicle or the TGF-β receptor 1 pharmacological inhibitor, SB525334 (30mg/kg). N=4-5 from two experiments. A Mann-Whitney test was used to determine statistical significance, comparing aged mice to young.

6.4. scRNA-seq of unfractionated non-hematopoietic aged BM cells

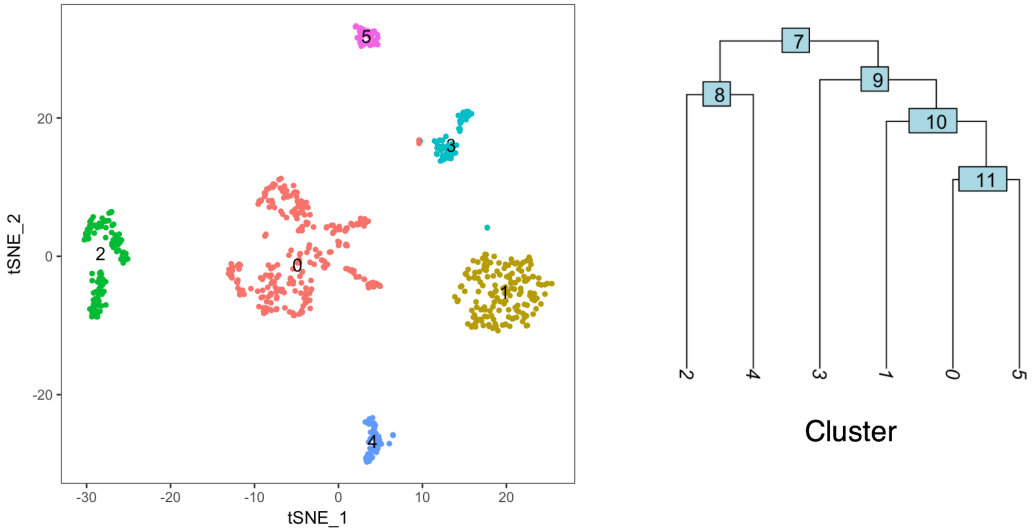
Very little is currently known with regards to the heterogeneity of the BM niche during ageing. Therefore, 5300 CD45- TER119- 7AAD- BL and 5300 CBM niche cells were isolated by FACS from aged mice (~22-24 month), and used for droplet based scRNA-seq. Following processing, 4051 unfractionated niche cells were sequenced, of which 704 remained after computational filtering (see Materials and methods, section 2.3.2). On average, cells expressed 2130 genes and 6248 UMIs each. These data were used to understand niche cell heterogeneity in the context of ageing, and to also evaluate whether BM niche populations become transcriptionally perturbed.

6.4.1. Niche cell heterogeneity during ageing

As seen in figure 6.4.1.a, there were 6 transcriptionally distinct non-hematopoietic populations present in the BM of aged mice. Differential gene expression analysis using a negative binomial statistical test was carried out to identify cluster-specific gene markers.

The top DEGs with an adjusted $p \leq 0.05$ and LogFC$\geq$0.25 for each cluster are displayed as a heatmap in figure 6.4.1.b. As was also the case in young niche, LepR+ PV cells, PαS MSCs and VECs could be prospectively identified by the markers *Lepr*, *Pdgfra* and *Pecam1*, respectively (figure 6.4.1.c). In contrast to the young niche, the total number of aged non-hematopoietic clusters was significantly less in comparison. Cluster 5 expressed high levels of *Des,* a gene largely present in muscle tissue (Lazarides et al., 1976; Weng et al., 2002). Despite efforts to filter hematopoietic cell types from this analysis, clusters 2 and 4 were labelled by *Cd79a*, *Vpreb3*, *S100a8* and *S100a9*, genes commonly found in B and myeloid cell populations (Mason et al., 1991; Pinkus and Pinkus, 1991; Rammes et al., 1997). Hematopoietic identity was confirmed using phylogenetic clustering, which showed that clusters 2 and 4 shared a close transcriptional relationship, but were separated at node 7 from other cell populations (figure 6.4.1.a, right panel).

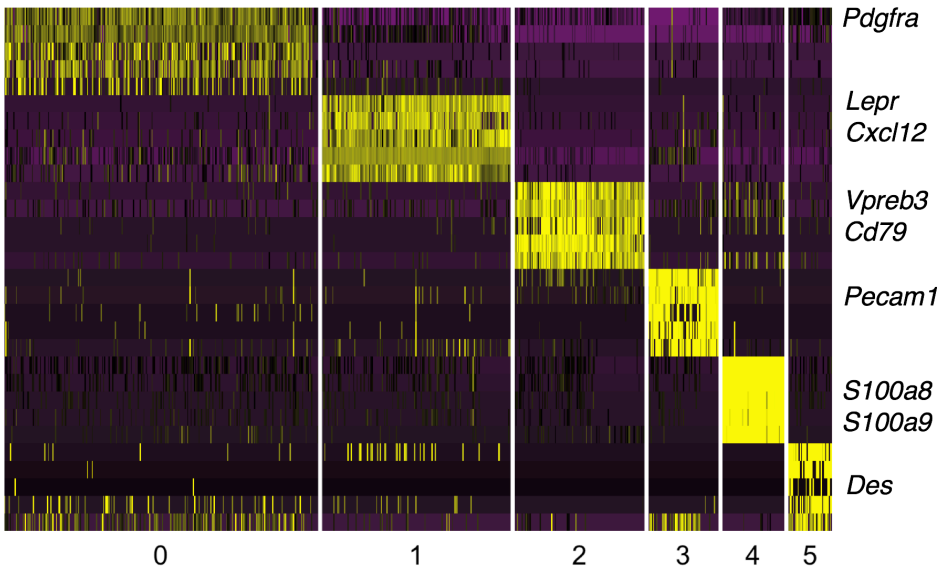
6.4.1.a



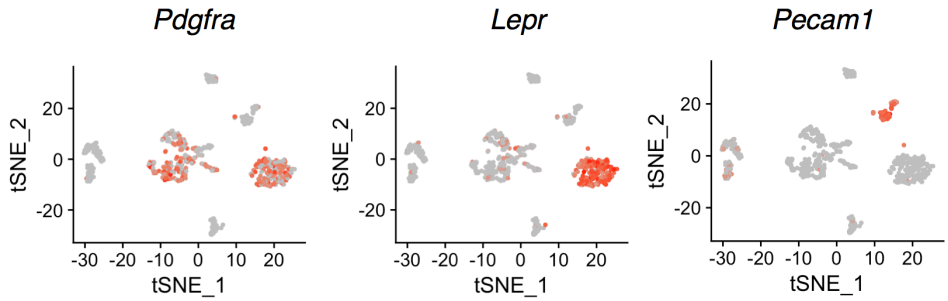
Niche cell heterogeneity during ageing

6.4.1.a. tSNE plot displaying 703 filtered, non-hematopoietic BL and CBM cell populations isolated from aged (~22-24 months) mice. Phylogenetic tree constructed in PCA space and ordered by cluster.

6.4.1.b



6.4.1.c



Niche cell heterogeneity during ageing

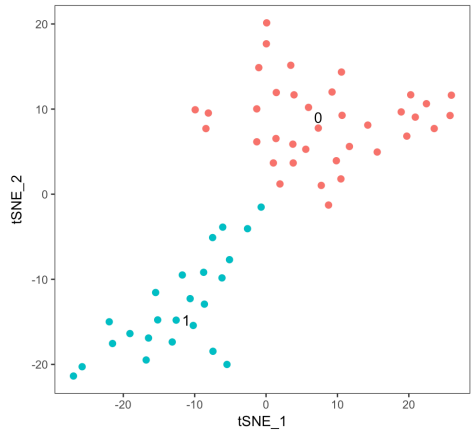
6.4.1.b. Heatmap of top DEGs from clusters 0-5 in aged non-hematopoietic niche cells. Differential gene expression was carried out using a negative binomial statistical test where genes shown have an adjusted $p \leq 0.05$ and LogFC$\geq$0.25. **6.4.1.c.** Expression of *Pdgfra*, *Lepr* and *Pecam1*, markers of PαS MSCs, LepR+ PV cells and VECs, respectively.

6.4.2. Vascular endothelial cell heterogeneity during ageing

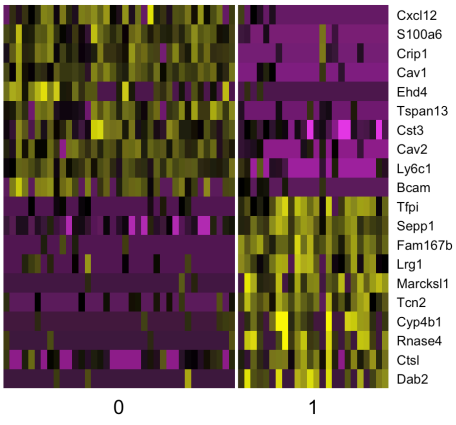
Having extensively analysed young BM VECs in chapter 4, VECs were next analysed at the single cell level in aged mice. There were significantly fewer VECs present during ageing when compared to young controls, evidenced both immunophenotypically (figure 6.3.6.a) and transcriptionally (figure 6.4.1.c). After isolating *Pecam1* expressing cells from the total single cell dataset (see Materials and methods, section 2.3.2), two transcriptionally distinct clusters were observed (figure 6.4.2.a). Differential gene expression analysis using a negative binomial statistical test revealed that aged VEC clusters could be distinguished by a number markers highlighted in figure 6.4.2.b. For example, cluster 0 expressed *Cxcl12* whereas cluster 1 expressed *Tfpi* (figures 6.4.2.b and 6.4.2.c).

Using the SEC and AEC gene sets described by Xu et al., (2018), the assumed anatomical location of aged VECs was investigated. As observed in figure 6.4.2.d, cluster 0 enriched for arteriolar genes whereas cluster 1 enriched for sinusoidal genes. CBM and BL fractions were isolated and processed separately before being computationally merged. This was therefore used to confirm the assumed AEC and SEC identity as evidenced in figure 6.4.2.e. These findings demonstrated that the majority of assumed AECs were originally isolated from the BL or endosteal fraction, whereas SECs were isolated from the CBM or sinusoidal fraction.

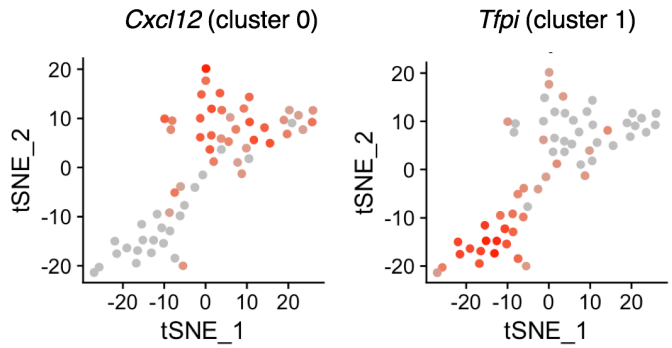
6.4.2.a



6.4.2.b



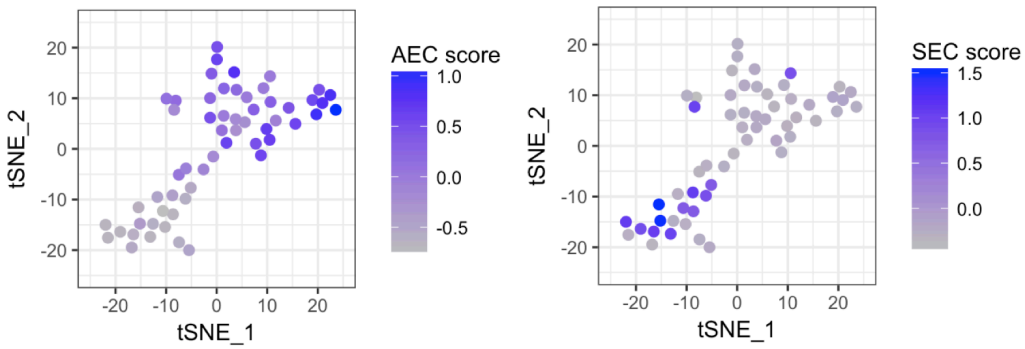
6.4.2.c



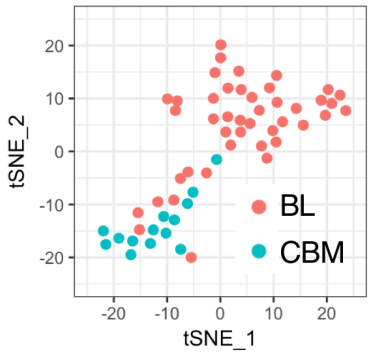
Vascular endothelial cell heterogeneity during ageing

6.4.2.a. tSNE plot of VECs from aged mice. Two transcriptionally distinct sub-populations of VECs were identified. **6.4.2.b.** Heatmap of top 10 DEGs from clusters 0 and 1 in aged VECs. DEGs were calculated using a negative binomial statistical test (adjusted $p \leq 0.05$, LogFC$\geq$0.25). **6.4.2.c.** Cluster specific expression of *Cxcl12* and *Tfpi* in aged CBM VECs.

6.4.2.d



6.4.2.e



Vascular endothelial cell heterogeneity during ageing

6.4.2.d. Expression of AEC and SEC genes in aged VECs. **6.4.2.e.** Original cellular location of VECs prior to computational merging.

6.4.3. *Vcam1* did not identify a discrete sub-population of VECs during ageing

In chapter 4, it was demonstrated that *Vcam1* expression could both transcriptionally, and immunophenotypically, distinguish a subset of VECs that during leukemia became perturbed (see Chapter 4, figure 4.4.2.c). Given that aged VEC cluster 1 differentially expressed *Cxcl12*, a marker that was exclusively expressed by young *Vcam1* negative VECs, the transcriptional relationship between young and aged VEC clusters was next investigated. Young *Vcam1* positive and negative VEC DEGs (adjusted $p \leq 0.05$, LogFC$\geq$0.25), were compared to DEGs (adjusted $p \leq 0.05$, LogFC$\geq$0.25) from aged VEC clusters 0 and 1. This analysis revealed that aged VEC

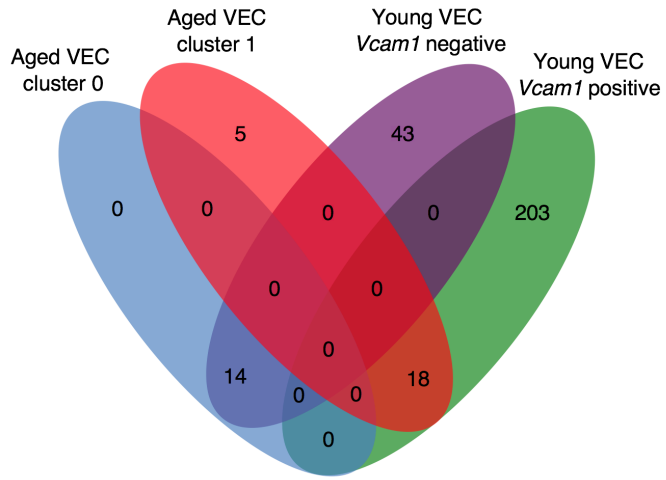
cluster 0 shared a significant number of genes expressed by young *Vcam1* negative VECs, whereas aged VEC cluster 1 shared numerous genes with young *Vcam1* positive VECs (figure 6.4.3.a). Cluster relationships were further evaluated from young and aged mice by performing a Pearson correlation coefficient analysis. Similarly to young mice, aged VEC cluster 0, which represented an equivalent *Vcam1* negative cluster, positively correlated ($R>0$, $p<0.01$) with DEGs from VECs after exposure to leukemia for 3 weeks (figure 6.4.3.b). The opposite was true of aged VEC cluster 1 ($R<0$, $p<0.01$), which appeared to express genes that were downregulated in VECs during leukemia. Taken together, these findings suggested that VEC clusters during ageing retained the same correlative relationship as those present in young mice and during leukemia. Interestingly, *Vcam1* was not differentially expressed by aged VEC cluster 1, despite this sub-population having shared a significant transcriptional relationship with young *Vcam1* expressing VECs (figure 6.4.3.c). This suggested that despite the presence of a *Vcam1* positive-like cluster during ageing, the expression of *Vcam1* itself was not sufficient to prospectively isolate these cells transcriptionally.

Using a recently described computational alignment strategy that leverages canonical correlation analysis (Butler and Satija, 2017; see Materials and methods, section 2.3.2.10), young and aged VECs were aligned within the same dimensional space to determine if there was a loss of certain vascular subsets during ageing (figure 6.4.3.d). From this analysis, it was demonstrated that aged VECs aligned to those from young mice, but appeared to lack a well-defined *Vcam1* expressing cluster (figure 6.4.3.e). Moreover, cells that did express *Vcam1* during ageing appeared not to be confined to any single grouping of cells, and were instead randomly distributed. This again suggested that, despite the cluster being present

and transcriptionally comparable to the young setting, *Vcam1* expression was largely absent. In contrast, the expression of *Cxcl12* and *Kitl* in aged VECs appeared correlated with the equivalent cluster of young *Vcam1* negative cells (figure 6.4.3.f). This suggested that this cluster of cells retained similar transcriptional and dimensional properties even after being aged, whereas *Vcam1* was no longer able to label sinusoidal VECs.

In conclusion, these data indicated that during ageing, there was a lack of *Vcam1* expression despite the presence of a transcriptionally equivalent cluster. Furthermore, there was retention of *Vcam1* negative VECs during ageing which, similarly to young mice, expressed the important niche factors *Cxcl12* and *Kitl*.

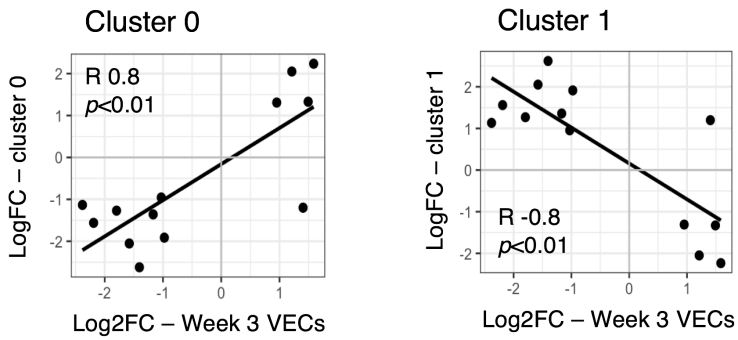
6.4.3.a



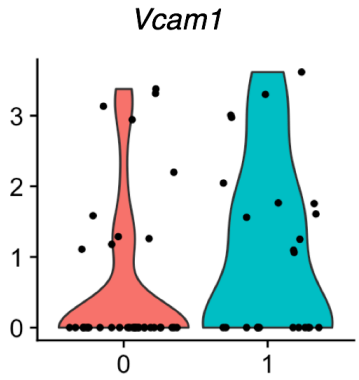
***Vcam1* did not identify a discrete sub-population of VECs during ageing**

6.4.3.a. DEGs (adjusted $p \leq 0.05$, LogFC≥ 0.25) from aged clusters 0 and 1, compared to DEGs (adjusted $p \leq 0.05$, LogFC≥ 0.25) from young *Vcam1* positive and negative clusters.

6.4.3.b



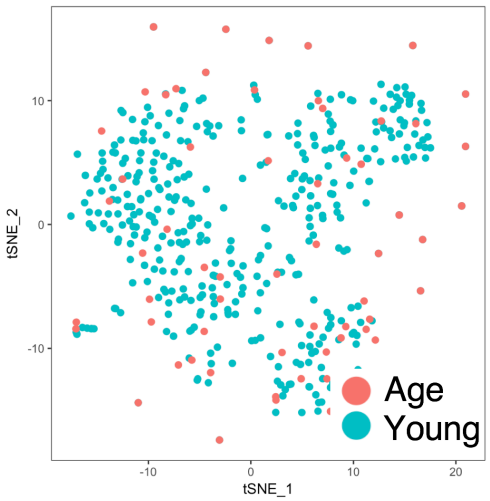
6.4.3.c



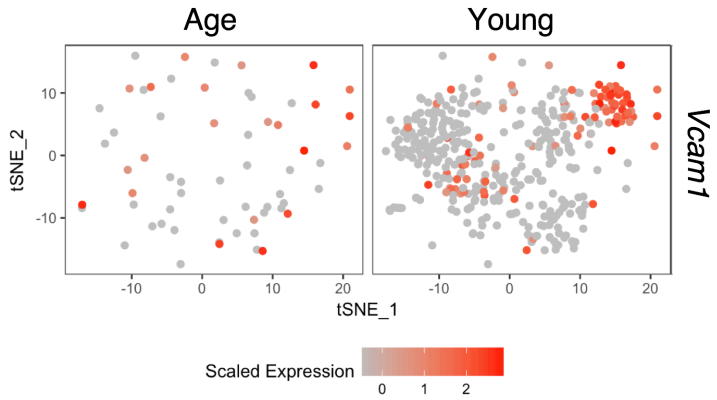
***Vcam1* did not identify a discrete sub-population of VECs during ageing**

6.4.3.b. Correlation analysis comparing DEGs with an adjusted $p \leq 0.05$ and LogFC$\geq$0.25 from aged VEC clusters 0 and 1 against up- and down- DEGs with an adjusted $p \leq 0.05$ expressed by VECs at week 3 post-transplantation. Pearson correlation coefficient R and *p*-values are displayed for each plot. **6.4.3.c.** Normalised expression values for *Vcam1* in aged VEC clusters 0 and 1.

6.4.3.d



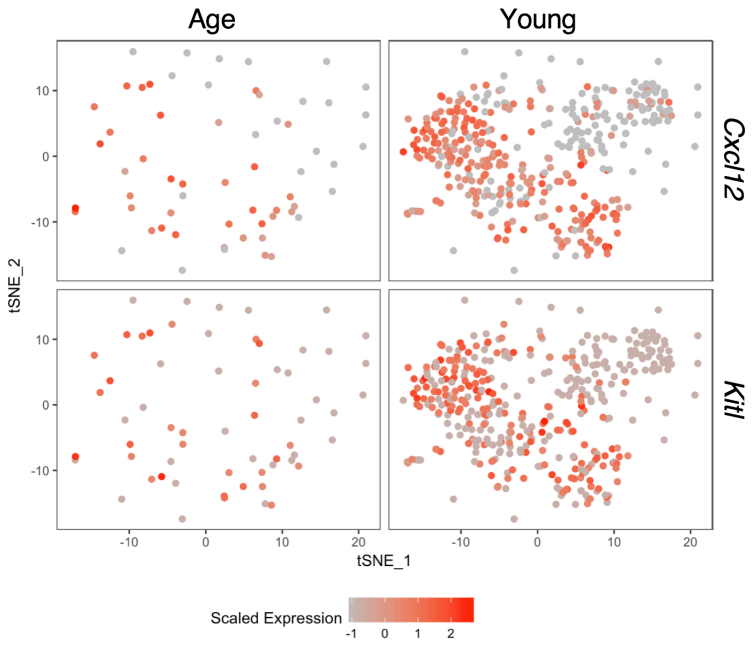
6.4.3.e



***Vcam1* did not identify a discrete sub-population of VECs during ageing**

6.4.3.d. Canonical correlation analysis of VECs from young and aged mice. **6.4.3.e.** Scaled expression values for *Vcam1* in young and aged aligned VEC datasets.

6.4.3.f



***Vcam1* did not identify a discrete sub-population of VECs during ageing**

6.4.3.f. Scaled UMI expression values for *Cxcl12* and *Kitl* in young and aged VECs after canonical correlation analysis and alignment.

6.5. Summary and discussion

The transplantation of leukemic cells into non-irradiated aged female mice resulted in the engraftment of AML, an effect that was not observed in young controls (figure 6.2.a). This strongly indicated that age-related microenvironmental conditioning was sufficient to support leukemogenesis, without prior myeloablation. Indeed, this is consistent with findings suggesting that the aged niche is responsible for both promoting HSPC mono-clonality, as well as enhancing pre-leukemic stem cell and myeloid blast frequency after transplantation (Vas et al., 2012a; Vas et al., 2012b). When considered together, these findings implicate both intrinsic and extrinsic mechanisms as being responsible for mediating leukemic predisposition during ageing, and was something clearly evidenced during this study.

In addition to being immunophenotypically reduced in frequency (figure 6.3.6.a), aged CBM VECs also displayed the greatest number of DEGs when compared to other cell types in the niche (figure 6.3.4.a). A comparison of aged and leukemic CBM VECs revealed a high number of shared process networks (table 6.3.6.b), suggesting that the aged niche possessed the key molecular characteristics of an AML-conditioned microenvironment. The relevance of these shared networks in the context of leukemic predisposition is yet to be concluded, however the enrichment of processes such as cellular adhesion implied that vasculature during ageing may be an important homing site for LICs. Indeed, it has formerly been demonstrated that leukemic cell adhesion to endothelial cells is sufficient to shield leukemic cells from chemotherapy, which eventually contributes towards disease relapse (Pezeshkian et al., 2013).

A comparison of DEGs from aged and leukemic VECs revealed a shared list of up- and down-DEGs (figure 6.3.6.c). An integrated analysis of these shared genes using the scRNA-seq dataset described in chapter 4 revealed that the expression of shared up-DEGs was confined to *Vcam1* negative VECs, whereas shared down-DEGs were predominantly expressed by *Vcam1* positive VECs (figure 6.3.6.e). Immunophenotypically, *Vcam1* negative VECs, also formerly identified as sinusoidal (CBM) endothelial cells, were reduced in frequency, whereas the opposite was true for *Vcam1* negative, or arteriolar endothelial cells (see Chapter 4, figures 4.4.3.a and 4.4.4.e). Moreover, scRNA-seq revealed that aged VEC clusters appeared to molecularly resemble *Vcam1* positive and negative clusters found in young (figure 6.4.3.a). However, unlike the young setting, *Vcam1* could not be used to demarcate a specific aged endothelial subset. Canonical correction analysis revealed that the equivalent *Vcam1* negative cluster during ageing could be defined by its expression

of *Cxcl12* and *Kitl*, whereas *Vcam1* positive VECs did not appear to overlap to the same extent with those found in young mice. The similarities that existed between leukemic and aged CBM VECs therefore suggested that during ageing, VECs may play a crucial role in the observed support of leukemogenesis.

During ageing, a significant over-expression of CBM VEC derived *Cxcl12* and *Kitl* was observed. The CXCL12-CXCR4 axis is an important chemotactic mechanism utilised by both normal and malignant hematopoietic cells which, upon being genetically deleted from VECs, results in attenuated tumour growth (Pitt et al., 2015). This suggested that endothelial-specific expression of CXCL12 may have been sufficient to sustain leukemic cell engraftment, and therefore the over-expression of this molecule during ageing may also infer an enhanced capacity to support leukemogenesis. This is further complemented by findings that suggest the disruption of CXCR4 signalling ameliorates the homing of leukemic blasts, which are normally located in CXCL12 expressing regions of the BM (Sipkins et al., 2005). Given that the LIC used during this present study is KIT positive (see Chapter 3, figure 3.2.b), it would be unsurprising to find that initial engraftment of these cells relied on interactions with KITL. Indeed, the targeting of KIT has formerly been shown to cause AML cell death, suggesting that a lack of this molecular interaction is detrimental for leukemic cell function (Heo et al., 2017). Taken together, the overexpression of *Cxcl12* and *Kitl* by BM endothelial cells during ageing may play an important functional role in AML engraftment.

Aged OBs expressed several pro-inflammatory secreted factors and cell surface receptors during ageing (figures 6.3.7.f and 6.3.7.g). This included *Ccl6*, a factor that was identified earlier as being aberrantly expressed by leukemic cells, and whose over-expression was sufficient to disrupt normal hematopoiesis (see Chapter

5, figure 5.3.1.a). CCR1, the primary receptor for CCL6, has formerly been shown to be an important component in leukemic cell survival (van Attekum et al., 2017), and was also over-expressed by OBs during ageing. Furthermore, OBs differentially expressed *Csf3r*, the gene encoding for G-CSFR. A number of studies have shown that young OBs do not express this receptor, but are indirectly suppressed after G-CSF treatment, possibly via macrophages or sympathetic activation (Semerad et al., 2005; Katayama et al., 2006; Christopher et al., 2011; Winkler et al., 2010; Lucas et al., 2012). The expression of this receptor therefore may indicate an alternative role during ageing. Indeed, G-CSFR has formerly been demonstrated to play an important role in maintaining the frequency of myeloid cells after competitive transplantation (Richards et al., 2003), suggesting that its expression on hematopoietic cells is crucial for maintaining balanced hematopoiesis. Moreover, G-CSF given during induction chemotherapy leads to an increase in both disease free and 5-year survival rates, suggesting a paradoxical yet important role for the G-CSFR-G-CSF axis in both normal and malignant hematopoiesis (Löwenberg et al., 2003).

Aged OBs were immunophenotypically reduced in frequency (figure 6.3.7.a), a finding that was in agreement with previous studies investigating the impact of age on trabecular thickness (Lips et al., 1978). OBs also appeared to transcriptionally resemble immature mesenchymal cell types, whilst retaining a normal cellular immunophenotype. This was first evidenced in figure 6.3.2.a, whereby it was demonstrated that aged OBs clustered in proximity to immature mesenchymal cell types. Additional analysis revealed that despite expressing normal levels of *Alcam*, a mature OB marker (Nakamura et al., 2010), these cells down-regulated a number of important osteogenic factors normally present in young mice (figure 6.3.7.b). This was further validated by the observation that PαS MSCs, a multipotent cell type,

became enriched for an adipogenic gene signature and began over-expressing *Pparg*, *Aldh2* and *Adipoq* (figures 6.3.7.c and 6.3.7.d). The expression of PPARγ by aged MSCs has previously been demonstrated to promote adipogenesis at the expense of osteogenesis (Moerman et al., 2004). Moreover, age-related adipogenesis leads to the aberrant RANKL expression, a factor responsible for promoting osteoclastogenesis (Takeshita et al., 2014). Therefore, adipogenic skewing of PαS MSCs may explain the significant reduction in OBs that was observed during ageing, and also the reversion of these cell types to an immature state.

Remodelling of OBs, as well as direct genetic perturbation of osteolineage cells, is both a predisposing factor in MDS and can be beneficial for malignant cell survival (Krevvata et al., 2014; Raajimakers et al., 2010). MDS patient derived MSCs exhibit perturbed differentiation potential, resulting in the over-expression of numerous niche factors required for malignant cell expansion (Medyouf et al., 2014). It is therefore possible that age-dependent remodelling of OBs was responsible for the production of pro-inflammatory cell surface receptors and secreted factors observed during this study. The promotion of adipogenesis at the expense of osteogenesis may have also created permissive niches for leukemic-cell engraftment during ageing. Indeed, there is a positive correlative relationship between obesity and leukemia incidence (Larsson and Wolk, 2008; Orgel et al., 2014). Furthermore, adipocytes have been demonstrated to create a pro-tumoral microenvironment for leukemic blasts (Shafat et al., 2017). However, an opposing role for these cell types also exists, whereby the promotion of adipogenesis rescues normal hematopoietic function whilst repressing AML growth (Boyd et al., 2017). Additionally, leukemia-

induced changes to adipocyte morphology have been shown to play an important role in determining AML prognosis (Lu et al., 2018).

Despite previous studies having demonstrated that TGF-β1 can both maintain HSC quiescence and determine lineage commitment (Challen et al., 2010; Fortunel et al., 2000; Chabanon et al., 2008), the link between TGF-β1 expression and malignant hematopoiesis during ageing has not yet been established. A number of studies have explored aberrant TGF-β1 signalling within the brain as well as its roles in hypothalamic inflammation and stroke (Doyle et al., 2010; Yan et al., 2014), yet very little is known about this molecule's expression elsewhere, and what effect this may have on surrounding tissues. During this present study, *Tgfb1* was consistently over-expressed by all niche cells during ageing (figures 6.3.8.a and 6.3.8.b). Furthermore, leukemic cells expressed high levels of *Tgfbr1* throughout the course of leukemic development (figure 6.3.8.d), and also conditioned CBM VECs to express *Tgfb2* (figure 6.3.8.e). These findings therefore suggested that the up-regulation of TGF-β1 may have played an important role in either supporting the engraftment of leukemic cells, or maintaining their growth and survival during ageing. Indeed, it has previously been demonstrated that the TGF-β-FOXO signalling axis is critical for maintaining CML LICs (Naka et al., 2010). Based on this, the inhibition of TGF-β receptor 1 during leukemic engraftment in aged mice was investigated using a potent pharmacological agent. Unfortunately however, prolonged inhibition did not reduce leukemic engraftment, implying that TGF-β1 was unlikely to be important for processes related to leukemic cell engraftment and/or cell survival during ageing.

6.6. Conclusions

1. **Established that ageing was sufficient to support leukemogenesis**

Non-irradiated aged female mice developed leukemia after transplantation, whereas young controls did not. This indicated that the ageing microenvironment provided the necessary factors required for leukemic cell survival.

2. **Consistently enriched process networks from aged niche populations were investigated**

Using differential gene expression analysis and Metacore, there was a consistent enrichment of numerous process networks amongst niche cell types during ageing. This included cell adhesion, inflammatory, and signal transduction pathways.

3. **The transcriptional similarities between leukemic and aged CBM VECs were evaluated**

A direct comparison of process networks and DEGs from aged and leukemic CBM VECs revealed that there was a significant overlap. This suggested that the aged niche possessed the key molecular characteristics of an AML-conditioned microenvironment.

4. **Changes in OB frequency and gene expression profile during ageing were assessed**

Aged OBs were immunophenotypically reduced in frequency and transcriptionally resembled mesenchymal cell types. Moreover, OBs during ageing represented a major source of pro-inflammatory and cell surface receptors.

5. **Niche cell heterogeneity was assessed and compared to the young setting**

The composition of aged niche cells was evaluated by scRNA-seq, revealing that vascular heterogeneity is confined to two sub-populations, as opposed to the five observed in young mice. Furthermore, in contrast to the young setting, aged VECs could not be discriminated via their expression of *Vcam1*, yet both sub-populations expressed genes that resembled those found in young mice. Taken together, this suggested that during ageing, *Vcam1* could no longer be used as a marker to distinguish sinusoidal from arteriolar VECs.

Chapter 7

Final discussion

7.1. Key findings

The key findings from this study were as follows:

1. Erythroid progenitors were immunophenotypically and functionally perturbed at the earliest stages of leukemic development, and was an effect also detectable in hierarchically immature *Gata1*-EGFP+ pGMs. pGMs were also transcriptionally affected the most after only 2 weeks of leukemogenesis.
2. Endogenous GMPs expanded in frequency during AML, and was a phenomenon caused by the over-expression of leukemia-derived FLT3L and CCL6. However, the over-expression of these factors was not beneficial for leukemogenesis, nor did the combined inhibition of CCR1 and FLT3 after chemotherapy improve overall survival.
3. Long-term HSC functionality remained normal once removed from the leukemic BM environment. This was in line with the maintained frequency of HSCs and MPP populations, despite leukemic burden exceeding 50% of the BM.
4. VCAM1^{hi} expressing sinusoidal (CBM) VECs were significantly reduced in frequency as a result of leukemic development. *Cxcl12* and *Kitl*-expressing arteriolar VECs, on the other hand, expanded in frequency.
5. Ageing was sufficient to support leukemogenesis, and was also associated with significant changes to BM niche, including the reprogramming of OBs and VECs.

7.2. Final discussion

Endogenous HSCs and MPPs remained unperturbed both immunophenotypically and transcriptionally during the first 3 weeks of leukemic development. These

findings were in line with previous work (Miraki-Moud et al., 2013) and were also validated functionally within this report. Committed erythroid progenitor populations on the other hand showed signs of immediate immunophenotypic impairment at even the earliest time point measured. This was also despite remaining transcriptionally normal, and enriching for very few process networks. At an equivalent time point, early pGM myeloid progenitors exhibited a high number of transcriptional changes, yet lacked observable immunophenotypic differences. *Gata1* expression defines a functionally distinct pGM progenitor population that has the capacity to produce erythrocytes, and exists hierarchically upstream of committed erythroid pCFUE and CFUE progenitors (Drissen et al., 2016). During leukemia, the proportion of *Gata1*-EGFP+ pGMs were decreased, which both coincided with the observed erythroid phenotype, and also explained the restricted transcriptional activity of pGMs at week 2. When taken together, these findings suggested that early changes in erythroid output during leukemia were likely due to the molecular disruption of *Gata1*-EGFP expressing myeloid progenitors.

Endogenous GMPs at the mid-stage of leukemic development were expanded immunophenotypically almost two-fold in frequency compared to non-transplanted controls. This finding was in direct contrast to the sustained decrease of endogenous myeloerythroid progenitors observed by Boyd et al., (2017) and Miraki-Moud et al., (2013). Transcriptionally, pro-inflammatory process networks were enriched consistently amongst HSCs, MPPs and progenitors during AML. After assessing the gene expression profiles of LICs and blasts, it was later discovered that leukemic populations were a major source of pro-inflammatory secreted factors. Using the hydrodynamic injection technique, the individual over-expression of two leukemia-derived secreted factors, *Ccl6* and *Flt3l*, resulted in a comparable

immunophenotypic expansion of GMPs. However, the inhibition of CCR1 and FLT3, the corresponding receptors for CCL6 and FLT3L, resulted in limited anti-leukemic capacity, despite both being expressed by both LICs and blasts. Moreover, the over-expression of *Flt3l* and *Ccl6* was insufficient to promote LIC engraftment, despite causing a temporary impairment in peripheral engraftment. This therefore ruled out an autocrine signalling role for these molecules, instead suggesting that their sole purpose was to stimulate endogenous myelopoiesis.

BL and CBM niche cells were investigated immunophenotypically and transcriptionally during leukemic development. Of note, BL VECs, PαS MSCs and OBs were increased in frequency, whereas sinusoidal CBM VECs declined. Bulk RNA-seq of CBM VECs revealed a consistent enrichment of adhesive, chemotactic and pro-inflammatory process networks, which upon closer inspection consisted of numerous secreted factors and cell surface receptors. These findings therefore suggested that VECs were actively remodelled during leukemic development, and were conditioned to upregulate factors that may have been pivotal for disrupting hematopoiesis or supporting leukemogenesis. One such molecule was *Tnf*, whose aberrant expression has been proposed to impair erythropoiesis and perturb HSC functionality during MDS (Mead et al., 2017; Mei et al., 2018).

Previous attempts at resolving BM vascular heterogeneity have relied almost exclusively on imaging and bulk RNA-seq approaches (Kopp et al., 2009; Chi et al., 2003; Xu et al., 2018). During this study, VEC heterogeneity was measured at the single cell level, resulting in the identification of five discrete sub-populations, one of which could be labelled by *Vcam1*. By flow cytometry, the majority of VCAM1^{hi} expressing VECs were found in the CBM niche, suggesting that this marker was capable of prospectively labelling sinusoidal (CBM) VECs. Indeed, the proportion of

VCAM1^{hi} CBM VECs decreased significantly during leukemia, mirroring the immunophenotypic findings made regarding CBM VECs and leukemic development earlier on. Closer inspection of *Vcam1* negative endothelium (also known as BL or arteriolar VECs) revealed that the majority of endothelial-derived *Kitl* and *Cxcl12* was confined to this sub-population.

The transplantation of LICs into non-irradiated aged mice resulted in the onset of leukemia, and was an effect not recapitulated in young controls. This finding was followed by the hypothesis that changes in the BM niche during ageing were sufficient to support leukemogenesis. To address this question, five niche populations from the BL and CBM niche compartments of young and aged mice were transcriptionally profiled. In doing so, it was demonstrated that there were significant and globally enriched changes to gene expression. Of note, aged CBM VECs exhibited an immunophenotype comparable to what was observed during leukemia, yet BL VECs did not. On a gene expression level, aged CBM VECs also shared numerous process networks and DEGs with those found in CBM VECs during leukemia, in addition to the overexpression of *Cxcl12* and *Kitl*. Lastly, DEGs that were both upregulated in CBM VECs during ageing and leukemia, were also predominantly found in BL (arteriole) VECs, whereas shared down-regulated genes were largely expressed in CBM (sinusoidal) VECs. These findings suggested that the major molecular changes that existed during ageing, paralleled those that occurred as a result of leukemic conditioning.

Aged OBs clustered by PCA in proximity to MSCs and also down-regulated mature osteogenic genes. However, these cells also expressed comparable levels of *Alcam*, enabling them to resemble mature OBs by FACS. PαS MSCs became enriched for an adipogenic gene signature and simultaneously down-regulated

several genes important for osteogenesis. Taken together, these findings suggested that during ageing, MSCs became transcriptionally primed to generate adipocytes at the expense of osteocytes. Furthermore, we also observed that OBs became a source of pro-inflammatory secreted factors and chemotactic cell surface receptors, which were similar to those expressed by leukemic cells and leukemia-conditioned niche cells.

Using differential gene expression analysis, *Tgfb1* was consistently over-expressed by all niche populations studied during ageing, which also coincided with a consistent enrichment of TGF-β1-related process network. Based on this, it was postulated that the aberrant expression of *Tgfb1* by the niche played a supportive leukemogenic role during ageing. This was supported by the observation that leukemic cells transcriptionally expressed *Tgfbr1* and also appeared to induce CBM VEC-derived expression of *Tgfb2*. However, prolonged inhibition of TGF-β receptor 1 using an orally available pharmacological agent in aged mice did not attenuate leukemic engraftment, therefore suggesting that this molecule's aberrant expression during ageing did not play a role in promoting leukemic susceptibility.

Lastly, scRNA-seq was used to investigate the unfractionated niche composition during ageing. From this analysis, VECs appeared to cluster into two distinct subsets, defined transcriptionally as either arterioles or sinusoids based on work completed by Xu et al., (2018). Much like in the young setting, each subset expressed distinct gene expression profiles. However, *Vcam1* in aged VECs did not appear to demarcate a distinct subset of vasculature, nor did the equivalent population overlay with young VECs. Taken together, this suggested that an equivalent *Vcam1* expressing VEC population was likely missing during ageing, however this is yet to be shown by flow cytometry. When considered together, the

aged microenvironment shared a number of immunophenotypic and transcriptional parities with what was observed during leukemia. However, it is yet to be established whether this corresponds to leukemogenic support.

In contrast to former studies investigating the disruption of hematopoiesis during AML (Miraki-Moud et al., 2013; Boyd et al., 2017), the findings reported here have attempted to address with higher specificity how endogenous HSPC and BM niche populations become perturbed immunophenotypically, functionally and transcriptionally during leukemic development and ageing. In doing, this study has provided a comprehensive and novel understanding of how functioning BM cell types respond, and change as a consequence of hematopoietic malignancy.

7.3. Technical limitations

7.3.1. Murine AML transplantation model

Despite having demonstrated that the transplantation of *Cebpa* mutant LICs resulted in a clinically comparable AML, the model used in this study required the use of sub-lethal irradiation in order to achieve a biologically reproducible disease. Although the effects of irradiation were controlled for between transplanted and non-transplanted mice, there was a significant impairment in LT-HSC engraftment following transplantation (see Chapter 3, figure 3.4.2.a). Total body irradiation of HSCs has formerly been demonstrated to cause defects in donor chimerism, which persists even after increasing donor cell number and serial transplantation (Chua et al., 2012). To overcome this, it would be necessary to clonally select LICs that can engraft to the same extent as those found within an irradiated setting. This however represents a technical limitation that has not yet been resolved.

7.3.2. RNA-sequencing

This study extensively relied on RNA-seq to elucidate how distinct cell populations changed in response to leukemic development and ageing. Although measuring the abundance of RNA can be used as an accurate proxy for inferring protein expression, the presence of RNA alone does not guarantee a functional end product. This was evident in chapter 5 whereby *Flt3l* was detected transcriptionally within LICs and blasts, but not in the BM serum of leukemic mice (see Chapter 5, figures 5.3.a and 5.4.3.a). To overcome this, it would be necessary to either measure RNA by an additional means (i.e. qRT-PCR), or evaluate protein expression either by FACS or using an ELISA.

7.3.3. Hydrodynamic injections

Hydrodynamic injections were used in chapter 5 to model the over-expression of leukemia derived secreted factors. In these experiments, a negative control (empty pCMV6-Entry vector) was used, but the quantity of protein expression after injection was not measured (*i.e.* a positive control). In the majority of cases, over-expression did not lead to any observable immunophenotypic effects, however we do not currently know whether this was due to a genuine lack of effect, or because protein expression was unsuccessful after injection. To determine this, it would be necessary to quantify serum protein expression levels using an ELISA assay, or by mass spectrometry. Serum samples were collected from each hydrodynamically injected mouse after euthanising, and therefore this can be achieved post-hoc if necessary.

7.3.4. Pharmacological inhibitors

Several pharmacological inhibitors were utilised throughout chapters 5 and 6, however pharmacokinetic studies were not carried out to determine bioavailable inhibitor concentrations after dosing. To improve on these experiments, it would be necessary to carry out these studies in the future in order to optimise dosing schedules and delivery routes.

7.4. Future directions

7.4.1. Delineating the molecular drivers of impaired erythropoiesis during leukemia

During this study, the drivers of anemia were not extensively investigated despite the discovery of several previously published leukemia-derived anti-erythropoietic candidates such as *Ccl3* (Wang et al., 2016) and *Tnfsf12* (Felli et al., 2005). Although the over-expression of these candidates during steady state was explored, there was no discernible impact on erythropoiesis. Indeed, terminally differentiated erythrocytes can persist for >40 days, thus a short over-expression period of just 3 days (as was used during these studies) may not have been sufficient to impair erythropoiesis. The prolonged over-expression of these factors therefore represents a potential avenue for follow up studies. For example, kinetic analysis of peripheral HGB levels and BM erythroid progenitor frequency could be explored after extended over-expression of *Ccl3* and *Tnfsf12*. Moreover, the inhibition of these molecules may be explored during leukemic development to measure their effectiveness in promoting leukemogenesis.

To test the hypothesis regarding the immunophenotypic disruption of *Gata1*-EGFP expressing pGMs, it would be necessary to transcriptionally profile these two distinct cell populations separately, as well as perform *in vitro* functional assays. From

this, it would be possible to understand on a gene expression level which pGM population is affected during leukemic development, and indeed whether these cells were responsible for the eventual onset of anemia observed.

7.4.2. Establishing the functional impact of enhanced myelopoiesis during leukemia

Despite having observed that leukemia-derived secreted factors caused a significant increase in myeloid progenitor frequencies, the functional consequences of this effect have not yet been studied. Therefore, in order to fully evaluate the consequences of myeloid progenitor expansion, it would be necessary to conduct *in vitro* functional assays on FACS isolated LK progenitors after exposure to either FLT3L or CCL6.

7.4.3. Imaging studies

The immunophenotypic and gene expression profiles of BM niche populations during AML were extensively discussed throughout this study. Furthermore, it has been demonstrated that only specific progenitor populations were perturbed in frequency during leukemic development, not HSCs nor MPPs. Taken together, these findings suggested that leukemic populations during this model occupied highly specific niches within the BM. To explore this further, we are currently developing a fluorescently labelled LIC, whose anatomical localisation after transplantation will be assessed using transgenic mouse models. In doing so, this would enable us to evaluate which niche populations are occupied by leukemic cells, as well as observe changes to cellular composition as a function of time.

Bibliography

Acar, M., Kocherlakota, K., Murphy, M., Peyer, J., Oguro, H., Inra, C., Jaiyeola, C., Zhao, Z., Luby-Phelps, K. and Morrison, S. (2015). Deep imaging of bone marrow shows non-dividing stem cells are mainly perisinusoidal. *Nature*, 526(7571), pp.126-130.

Adolfsson, J., Borge, O., Bryder, D., Theilgaard-Mönch, K., Åstrand-Grundström, I., Sitnicka, E., Sasaki, Y. and Jacobsen, S. (2001). Upregulation of Flt3 Expression within the Bone Marrow Lin−Sca1+c-kit+ Stem Cell Compartment Is Accompanied by Loss of Self-Renewal Capacity. *Immunity*, 15(4), pp.659-669.

Adolfsson, J., Månsson, R., Buza-Vidas, N., Hultquist, A., Liuba, K., Jensen, C., Bryder, D., Yang, L., Borge, O., Thoren, L., Anderson, K., Sitnicka, E., Sasaki, Y., Sigvardsson, M. and Jacobsen, S. (2005). Identification of Flt3+ Lympho-Myeloid Stem Cells Lacking Erythro-Megakaryocytic Potential. *Cell*, 121(2), pp.295-306.

Akashi, K., Traver, D., Miyamoto, T. and Weissman, I. (2000). A clonogenic common myeloid progenitor that gives rise to all myeloid lineages. *Nature*, 404(6774), pp.193-197.

Akbar, A. and Fletcher, J. (2005). Memory T cell homeostasis and senescence during aging. *Current Opinion in Immunology*, 17(5), pp.480-485.

Alibhai, S., Leach, M., Minden, M. and Brandwein, J. (2009). Outcomes and quality of care in acute myeloid leukemia over 40 years. *Cancer*, 115(13), pp.2903-2911.

Amat, M., Benjamim, C., Williams, L., Prats, N., Terricabras, E., Beleta, J., Kunkel, S. and Godessart, N. (2006). Pharmacological blockade of CCR1 ameliorates murine arthritis and alters cytokine networksin vivo. *British Journal of Pharmacology*, 149(6), pp.666-675.

Ambrosi, T., Scialdone, A., Graja, A., Gohlke, S., Jank, A., Bocian, C., Woelk, L., Fan, H., Logan, D., Schürmann, A., Saraiva, L. and Schulz, T. (2017). Adipocyte Accumulation in the Bone Marrow during Obesity and Aging Impairs Stem Cell-Based Hematopoietic and Bone Regeneration. *Cell Stem Cell*, 20(6), pp.771-784.e6.

Andrews, S. (2010). FastQC: a quality control tool for high throughput sequence data. Available online at: http://www.bioinformatics.babraham.ac.uk/projects/fastqc

Appelbaum, F., Gundacker, H., Head, D., Slovak, M., Willman, C., Godwin, J., Anderson, J. and Petersdorf, S. (2006). Age and acute myeloid leukemia. *Blood*, 107(9), pp.3481-3485.

Arinobu, Y., Mizuno, S., Chong, Y., Shigematsu, H., Iino, T., Iwasaki, H., Graf, T., Mayfield, R., Chan, S., Kastner, P. and Akashi, K. (2007). Reciprocal Activation of GATA-1 and PU.1 Marks Initial Specification of Hematopoietic Stem Cells into Myeloerythroid and Myelolymphoid Lineages. *Cell Stem Cell*, 1(4), pp.416-427.

Arranz, L., Sánchez-Aguilera, A., Martín-Pérez, D., Isern, J., Langa, X., Tzankov, A., Lundberg, P., Muntión, S., Tzeng, Y., Lai, D., Schwaller, J., Skoda, R. and Méndez-Ferrer, S. (2014). Neuropathy of haematopoietic stem cell niche is essential for myeloproliferative neoplasms. *Nature*, 512(7512), pp.78-81.

Asada, N., Kunisaki, Y., Pierce, H., Wang, Z., Fernandez, N., Birbrair, A., Ma'ayan, A. and Frenette, P. (2017). Differential cytokine contributions of perivascular haematopoietic stem cell niches. *Nature Cell Biology*, 19(3), pp.214-223.

Aubin, J. (1998). Bone stem cells. *Journal of Cellular Biochemistry*, 72(S30-31), pp.73-82.

Balderman, S., Li, A., Hoffman, C., Frisch, B., Goodman, A., LaMere, M., Georger, M., Evans, A., Liesveld, J., Becker, M. and Calvi, L. (2016). Targeting of the bone marrow microenvironment improves outcome in a murine model of myelodysplastic syndrome. *Blood*, 127(5), pp.616-625.

Becker, A., Mcculloch, E. and Till, J. (1963). Cytological demonstration of the clonal nature of spleen colonies derived from transplanted mouse marrow cells. *Nature*, 197, pp.452-454.

Beerman, I., Bhattacharya, D., Zandi, S., Sigvardsson, M., Weissman, I., Bryder, D. and Rossi, D. (2010). Functionally distinct hematopoietic stem cells modulate hematopoietic lineage potential during aging by a mechanism of clonal expansion. *Proceedings of the National Academy of Sciences*, 107(12), pp.5465-5470.

Bereshchenko, O., Mancini, E., Moore, S., Bilbao, D., Månsson, R., Luc, S., Grover, A., Jacobsen, S., Bryder, D. and Nerlov, C. (2009). Hematopoietic Stem Cell Expansion Precedes the Generation of Committed Myeloid Leukemia-Initiating Cells in C/EBPα Mutant AML. *Cancer Cell*, 16(5), pp.390-400.

Berliner, N. (2013). Anemia in the elderly. *Trans Am Clin Climatol Assoc*, 124, pp.230-237.

Bianco, P., Robey, P. and Simmons, P. (2008). Mesenchymal Stem Cells: Revisiting History, Concepts, and Assays. *Cell Stem Cell*, 2(4), pp.313-319.

Binato, R., de Almeida Oliveira, N., Du Rocher, B. and Abdelhay, E. (2015). The molecular signature of AML mesenchymal stromal cells reveals candidate genes related to the leukemogenic process. *Cancer Letters*, 369(1), pp.134-143.

Bloomfield, C., Lawrence, D., Byrd, J., Carroll, A., Pettenati, M., Tantravahi, R., Patil, S., Davey, F., Berg, D., Schiffer, C., Arthur, D. and Mayer, R. (1998). Frequency of Prolonged Remission Duration after High-Dose Cytarabine Intensification in Acute Myeloid Leukemia Varies by Cytogenetic Subtype. *Cancer Research*, 58, pp.4173-4179.

Bowman, R., Busque, L. and Levine, R. (2018). Clonal Hematopoiesis and Evolution to Hematopoietic Malignancies. *Cell Stem Cell*, 22(2), pp. 157-170.

Boyd, A., Reid, J., Salci, K., Aslostovar, L., Benoit, Y., Shapovalova, Z., Nakanishi, M., Porras, D., Almakadi, M., Campbell, C., Jackson, M., Ross, C., Foley, R., Leber, B., Allan, D., Sabloff, M., Xenocostas, A., Collins, T. and Bhatia, M. (2017). Acute myeloid leukaemia disrupts endogenous myelo-erythropoiesis by compromising the adipocyte bone marrow niche. *Nature Cell Biology*, 19(11), pp.1336-1347.

Brandau, O., Meindl, A., Fässler, R. and Aszódi, A. (2001). A novel gene,tendin, is strongly expressed in tendons and ligaments and shows high homology with chondromodulin-I. *Developmental Dynamics*, 221(1), pp.72-80.

Brasel, K., McKenna, H., Morrissey, P., Charrier, K., Morris, A., Lee, C., Williams, D. and Lyman, S. (1996). Hematologic effects of flt3 ligand in vivo in mice. *Blood*, 88(6), pp.2004-2012.

Broxmeyer, H., Jacobsen, N., Kurland, J., Mendelsohn, N. and Moore, M. (1978). In Vitro Suppression of Normal Granulocytic Stem Cells by Inhibitory Activity Derived From Human Leukemia Cells. *JNCI: Journal of the National Cancer Institute*, 60(3), pp.497-511.

Bruns, I., Lucas, D., Pinho, S., Ahmed, J., Lambert, M., Kunisaki, Y., Scheiermann, C., Schiff, L., Poncz, M., Bergman, A. and Frenette, P. (2014). Megakaryocytes regulate hematopoietic stem cell quiescence through CXCL4 secretion. *Nature Medicine*, 20(11), pp.1315-1320.

Burnett, A., Wetzler, M. and Löwenberg, B. (2011). Therapeutic Advances in Acute Myeloid Leukemia. *Journal of Clinical Oncology*, 29(5), pp.487-494.

Busch, K., Klapproth, K., Barile, M., Flossdorf, M., Holland-Letz, T., Schlenner, S., Reth, M., Höfer, T. and Rodewald, H. (2015). Fundamental properties of unperturbed haematopoiesis from stem cells in vivo. *Nature*, 518(7540), pp.542-546.

Butler, A. and Satija, R. (2017). Integrated analysis of single cell transcriptomic data across conditions, technologies, and species. *bioRxiv*.

Butler, J., Nolan, D., Vertes, E., Varnum-Finney, B., Kobayashi, H., Hooper, A., Seandel, M., Shido, K., White, I., Kobayashi, M., Witte, L., May, C., Shawber, C., Kimura, Y., Kitajewski, J., Rosenwaks, Z., Bernstein, I. and Rafii, S. (2010). Endothelial Cells Are Essential for the Self-Renewal and Repopulation of Notch-Dependent Hematopoietic Stem Cells. *Cell Stem Cell*, 6(3), pp.251-264.

Calvi, L., Adams, G., Weibrecht, K., Weber, J., Olson, D., Knight, M., Martin, R., Schipani, E., Divieti, P., Bringhurst, F., Milner, L., Kronenberg, H. and Scadden, D. (2003). Osteoblastic cells regulate the haematopoietic stem cell niche. *Nature*, 425(6960), pp.841-846.

Carrelha, J., Meng, Y., Kettyle, L., Luis, T., Norfo, R., Alcolea, V., Boukarabila, H., Grasso, F., Gambardella, A., Grover, A., Högstrand, K., Lord, A., Sanjuan-Pla, A., Woll, P., Nerlov, C. and Jacobsen, S. (2018). Hierarchically related lineage-restricted fates of multipotent haematopoietic stem cells. *Nature*, 554(7690), pp.106-111.

Chabanon, A., Desterke, C., Rodenburger, E., Clay, D., Guerton, B., Boutin, L., Bennaceur-Griscelli, A., Pierre-Louis, O., Uzan, G., Abecassis, L., Bourgeade, M., Lataillade, J. and Le Bousse-Kerdilès, M. (2008). A Cross-Talk Between Stromal Cell-Derived Factor-1 and Transforming Growth Factor-β Controls the Quiescence/Cycling Switch of CD34+Progenitors Through FoxO3 and Mammalian Target of Rapamycin. *Stem Cells*, 26(12), pp.3150-3161.

Challen, G., Boles, N., Chambers, S. and Goodell, M. (2010). Distinct Hematopoietic Stem Cell Subtypes Are Differentially Regulated by TGF-β1. *Cell Stem Cell*, 6(3), pp.265-278.

Chao, Q., Sprankle, K., Grotzfeld, R., Lai, A., Carter, T., Velasco, A., Gunawardane, R., Cramer, M., Gardner, M., James, J., Zarrinkar, P., Patel, H. and Bhagwat, S. (2009). Identification ofN-(5-tert-Butyl-isoxazol-3-yl)-N′-{4-[7-(2-morpholin-4-yl-ethoxy)imidazo[2,1-b][1,3]benzothiazol-2-yl]phenyl}urea Dihydrochloride (AC220), a Uniquely Potent, Selective, and Efficacious FMS-Like Tyrosine Kinase-3 (FLT3) Inhibitor. *Journal of Medicinal Chemistry*, 52(23), pp.7808-7816.

Chao, R., Gong, X., Wang, L., Wang, P. and Wang, Y. (2015). CD71high population represents primitive erythroblasts derived from mouse embryonic stem cells. *Stem Cell Research*, 14(1), pp.30-38.

Chen, J., Miyanishi, M., Wang, S., Yamazaki, S., Sinha, R., Kao, K., Seita, J., Sahoo, D., Nakauchi, H. and Weissman, I. (2016). Hoxb5 marks long-term haematopoietic stem cells and reveals a homogenous perivascular niche. *Nature*, 530(7589), pp.223-227.

Chen, K., Liu, J., Heck, S., Chasis, J., An, X. and Mohandas, N. (2009). Resolving the distinct stages in erythroid differentiation based on dynamic changes in membrane protein expression during erythropoiesis. *Proceedings of the National Academy of Sciences*, 106(41), pp.17413-17418.

Chen, Y. and Webster, T. (2009). Increased osteoblast functions in the presence of BMP-7 short peptides for nanostructured biomaterial applications. *Journal of Biomedical Materials Research Part A*, 91(1), pp.296-304.

Cheng, T., Rodrigues, N., Shen, H., Yang, Y., Dombkowski, D., Sykes, M. and Scadden, D. (2000). Hematopoietic Stem Cell Quiescence Maintained by p21cip1/waf1. *Science*, 287(5459), pp.1804-1808.

Cheshier, S., Morrison, S., Liao, X. and Weissman, I. (1999). In vivo proliferation and cell cycle kinetics of long-term self-renewing hematopoietic stem cells. *Proceedings of the National Academy of Sciences*, 96(6), pp.3120-3125.

Chi, J., Chang, H., Haraldsen, G., Jahnsen, F., Troyanskaya, O., Chang, D., Wang, Z., Rockson, S., van de Rijn, M., Botstein, D. and Brown, P. (2003). Endothelial cell diversity revealed by global expression profiling. *Proceedings of the National Academy of Sciences*, 100(19), pp.10623-10628.

Christensen, J. and Weissman, I. (2001). Flk-2 is a marker in hematopoietic stem cell differentiation: A simple method to isolate long-term stem cells. *Proceedings of the National Academy of Sciences*, 98(25), pp.14541-14546.

Christopher, M., Rao, M., Liu, F., Woloszynek, J. and Link, D. (2011). Expression of the G-CSF receptor in monocytic cells is sufficient to mediate hematopoietic progenitor mobilization by G-CSF in mice. *The Journal of Experimental Medicine*, 208(2), pp.251-260.

Chua, H., Plett, P., Sampson, C., Joshi, M., Tabbey, R., Katz, B., MacVittie, T. and Orschell, C. (2012). Long-Term Hematopoietic Stem Cell Damage in a Murine Model of the Hematopoietic Syndrome of the Acute Radiation Syndrome. *Health Physics*, 103(4), pp.356-366.

Coelho, A., Schaller, M., Benjamim, C., Orlofsky, A., Hogaboam, C. and Kunkel, S. (2007). The Chemokine CCL6 Promotes Innate Immunity via Immune Cell Activation and Recruitment. *The Journal of Immunology*, 179(8), pp.5474-5482.

Colmone, A., Amorim, M., Pontier, A., Wang, S., Jablonski, E. and Sipkins, D. (2008). Leukemic Cells Create Bone Marrow Niches That Disrupt the Behavior of Normal Hematopoietic Progenitor Cells. *Science*, 322(5909), pp.1861-1865.

Conboy, I., Conboy, M., Wagers, A., Girma, E., Weissman, I. and Rando, T. (2005). Rejuvenation of aged progenitor cells by exposure to a young systemic environment. *Nature*, 433(7027), pp.760-764.

Cornelissen, J., van Putten, W., Verdonck, L., Theobald, M., Jacky, E., Daenen, S., van Marwijk Kooy, M., Wijermans, P., Schouten, H., Huijgens, P., van der Lelie, H., Fey, M., Ferrant, A., Maertens, J., Gratwohl, A. and Lowenberg, B. (2007). Results of a HOVON/SAKK donor versus no-donor analysis of myeloablative HLA-identical sibling stem cell transplantation in first remission acute myeloid leukemia in young and middle-aged adults: benefits for whom?. *Blood*, 109(9), pp.3658-3666.

Cozzio, A., Passegué, É., Ayton, P., Karsunky, H., Cleary, M. and Weissman, I. (2003). Similar MLL-associated leukemias arising from self-renewing stem cells and short-lived myeloid progenitors. *Genes & Development*, 17(24), pp.3029-3035.

Dai, M., Heinrich, M., Broxmeyer, H. and Lu, L. (2000). Enhancing effects of co-transduction of both human erythropoietin receptor and c-kit cDNAs into hematopoietic stem/progenitor cells from cord blood on proliferation and differentiation of erythroid progenitors. *Cytokines Cell Mol Ther*, 6(1), pp.1-8.

De Kouchkovsky, I. and Abdul-Hay, M. (2016). Acute myeloid leukemia: a comprehensive review and 2016 update. *Blood Cancer Journal*, 6(7), pp.441-441.

Di, Y. (2015). Single-gene negative binomial regression models for RNA-Seq data with higher-order asymptotic inference. *Statistics and Its Interface*, 8(4), pp.405-418.

Dick, J. (2008). Stem cell concepts renew cancer research. *Blood*, 112(13), pp.4793-4807.

Ding, L. and Morrison, S. (2013). Haematopoietic stem cells and early lymphoid progenitors occupy distinct bone marrow niches. *Nature*, 495(7440), pp.231-235.

Ding, L., Saunders, T., Enikolopov, G. and Morrison, S. (2012). Endothelial and perivascular cells maintain haematopoietic stem cells. *Nature*, 481(7382), pp.457-462.

Dobin, A., Davis, C., Schlesinger, F., Drenkow, J., Zaleski, C., Jha, S., Batut, P., Chaisson, M. and Gingeras, T. (2013). STAR: ultrafast universal RNA-seq aligner. *Bioinformatics* , 29(1), pp.15-21.

Döhner, H., Estey, E., Amadori, S., Appelbaum, F., Buchner, T., Burnett, A., Dombret, H., Fenaux, P., Grimwade, D., Larson, R., Lo-Coco, F., Naoe, T., Niederwieser, D., Ossenkoppele, G., Sanz, M., Sierra, J., Tallman, M., Lowenberg, B. and Bloomfield, C.

(2010). Diagnosis and management of acute myeloid leukemia in adults: recommendations from an international expert panel, on behalf of the European LeukemiaNet. *Blood*, 115(3), pp.453-474.

Dong, L., Yu, W., Zheng, H., Loh, M., Bunting, S., Pauly, M., Huang, G., Zhou, M., Broxmeyer, H., Scadden, D. and Qu, C. (2016). Leukaemogenic effects of Ptpn11 activating mutations in the stem cell microenvironment. *Nature*, 539(7628), pp.304-308.

Doyle, K., Cekanaviciute, E., Mamer, L. and Buckwalter, M. (2010). TGFβ signaling in the brain increases with aging and signals to astrocytes and innate immune cells in the weeks after stroke. *Journal of Neuroinflammation*, 7(1), p.62.

Draghici, S., Khatri, P., Tarca, A., Amin, K., Done, A., Voichita, C., Georgescu, C. and Romero, R. (2007). A systems biology approach for pathway level analysis. *Genome Research*, 17(10), pp.1537-1545.

Drissen, R., Buza-Vidas, N., Woll, P., Thongjuea, S., Gambardella, A., Giustacchini, A., Mancini, E., Zriwil, A., Lutteropp, M., Grover, A., Mead, A., Sitnicka, E., Jacobsen, S. and Nerlov, C. (2016). Distinct myeloid progenitor–differentiation pathways identified through single-cell RNA sequencing. *Nature Immunology*, 17(6), pp.666-676.

Duarte, D., Hawkins, E., Akinduro, O., Ang, H., De Filippo, K., Kong, I., Haltalli, M., Ruivo, N., Straszkowski, L., Vervoort, S., McLean, C., Weber, T., Khorshed, R., Pirillo, C., Wei, A., Ramasamy, S., Kusumbe, A., Duffy, K., Adams, R., Purton, L., Carlin, L. and Lo Celso, C. (2018). Inhibition of Endosteal Vascular Niche Remodeling Rescues Hematopoietic Stem Cell Loss in AML. *Cell Stem Cell*, 22(1), pp.64-77.

Dudek, A., Nesmelova, I., Mayo, K., Verfaillie, C., Pitchford, S. and Slungaard, A. (2003). Platelet factor 4 promotes adhesion of hematopoietic progenitor cells and binds IL-8: novel mechanisms for modulation of hematopoiesis. *Blood*, 101(12), pp.4687-4694.

Dykstra, B., Kent, D., Bowie, M., McCaffrey, L., Hamilton, M., Lyons, K., Lee, S., Brinkman, R. and Eaves, C. (2007). Long-Term Propagation of Distinct Hematopoietic Differentiation Programs In Vivo. *Cell Stem Cell*, 1(2), pp.218-229.

Dykstra, B., Olthof, S., Schreuder, J., Ritsema, M. and de Haan, G. (2011). Clonal analysis reveals multiple functional defects of aged murine hematopoietic stem cells. *The Journal of Experimental Medicine*, 208(13), pp.2691-2703.

Ema, H., Takano, H., Sudo, K. and Nakauchi, N. (2000). In Vitro Self-Renewal Division of Hematopoietic Stem Cells. *Journal of Experimental Medicine*, 192(9), pp.1285-1288.

Ergen, A., Boles, N. and Goodell, M. (2012). Rantes/Ccl5 influences hematopoietic stem cell subtypes and causes myeloid skewing. *Blood*, 119(11), pp.2500-2509.

Estey, E. and Döhner, H. (2006). Acute myeloid leukaemia. *The Lancet*, 368(9550), pp.1894-1907.

Ewels, P., Magnusson, M., Lundin, S. and Käller, M. (2016). MultiQC: summarize analysis results for multiple tools and samples in a single report. *Bioinformatics*, 32(19), pp.3047-3048.

Fathman, J., Fernhoff, N., Seita, J., Chao, C., Scarfone, V., Weissman, I. and Inlay, M. (2018). Upregulation of CD11A on Hematopoietic Stem Cells Denotes the Loss of Long-Term Reconstitution Potential. *Cell Stem Cell*, 3(5), pp.707-715.

Federzoni, E., Humbert, M., Torbett, B., Behre, G., Fey, M. and Tschan, M. (2014). CEBPA-dependent HK3 and KLF5 expression in primary AML and during AML differentiation. *Scientific Reports*, 4(1). pp.1-7.

Felli, N., Pedini, F., Zeuner, A., Petrucci, E., Testa, U., Conticello, C., Biffoni, M., Di Cataldo, A., Winkles, J., Peschle, C. and De Maria, R. (2005). Multiple Members of the TNF Superfamily Contribute to IFN-Mediated Inhibition of Erythropoiesis. *The Journal of Immunology*, 175(3), pp.1464-1472.

Feng, X., Scheinberg, P., Wu, C., Samsel, L., Nunez, O., Prince, C., Ganetzky, R., McCoy, J., Maciejewski, J. and Young, N. (2011). Cytokine signature profiles in acquired aplastic anemia and myelodysplastic syndromes. *Haematologica*, 96(4), pp.602-606.

Ford, C., Hamerton, J., Barnes, D. and Loutit, J. (1956). Cytological Identification of Radiation-Chimæras. *Nature*, 177, pp.452–454.

Fortunel, N., Hatzfeld, J., Kisselev, S., Monier, M., Ducos, K., Cardoso, A., Batard, P. and Hatzfeld, A. (2000). Release from Quiescence of Primitive Human Hematopoietic Stem/Progenitor Cells by Blocking Their Cell-Surface TGF-β Type II Receptor in a Short-Term In Vitro Assay. Stem Cells, 18(2), pp.102-111.

Franceschi, C., Bonafè, M., Valensin, S., Olivieri, F., De Luca, M., Ottaviani, E. and De Benedictis, G. (2000). Inflamm-aging. An evolutionary perspective on immunosenescence. Ann N Y Acad Sci, 908, pp.244-254.

Frasca, D., Landin, A., Riley, R. and Blomberg, B. (2008). Mechanisms for Decreased Function of B Cells in Aged Mice and Humans. The Journal of Immunology, 180(5), pp.2741-2746.

Friedenstein, A., Chailakhjan, R. and Lalykina, K. (1970). The development of fibroblast colonies in monolayer cultures of guinea-pig bone marrow and spleen cells. *Cell Tissue Kinet*, 3(4), pp.393-403.

Friedman, A. (2007). Transcriptional control of granulocyte and monocyte development. *Oncogene*, 26(47), pp.6816-6828.

Gekas, C. and Graf, T. (2013). CD41 expression marks myeloid-biased adult hematopoietic stem cells and increases with age. *Blood*, 121(22), pp.4463-4472.

Giladi, A., Paul, F., Herzog, Y., Lubling, Y., Weiner, A., Yofe, I., Jaitin, D., Cabezas-Wallscheid, N., Dress, R., Ginhoux, F., Trumpp, A., Tanay, A. and Amit, I. (2018). Single-cell

characterization of haematopoietic progenitors and their trajectories in homeostasis and perturbed haematopoiesis. *Nature Cell Biology*, 20(7), pp.836-846.

Gilliland, D. and Griffin, J. (2002). The roles of FLT3 in hematopoiesis and leukemia. *Blood*, 100(5), pp.1532-1542.

Goardon, N., Marchi, E., Atzberger, A., Quek, L., Schuh, A., Soneji, S., Woll, P., Mead, A., Alford, K., Rout, R., Chaudhury, S., Gilkes, A., Knapper, S., Beldjord, K., Begum, S., Rose, S., Geddes, N., Griffiths, M., Standen, G., Sternberg, A., Cavenagh, J., Hunter, H., Bowen, D., Killick, S., Robinson, L., Price, A., Macintyre, E., Virgo, P., Burnett, A., Craddock, C., Enver, T., Jacobsen, S., Porcher, C. and Vyas, P. (2011). Coexistence of LMPP-like and GMP-like Leukemia Stem Cells in Acute Myeloid Leukemia. *Cancer Cell*, 19(1), pp.138-152.

Goncalves, K., Silberstein, L., Li, S., Severe, N., Hu, M., Yang, H., Scadden, D. and Hu, G. (2016). Angiogenin Promotes Hematopoietic Regeneration by Dichotomously Regulating Quiescence of Stem and Progenitor Cells. *Cell*, 166(4), pp.894-906.

Gong, J. (1978). Endosteal marrow: a rich source of hematopoietic stem cells. *Science*, 199(4336), pp.1443-1445.

Goodell, M., Brose, K., Paradis, G., Conner, A. and Mulligan, R. (1996). Isolation and functional properties of murine hematopoietic stem cells that are replicating in vivo. *Journal of Experimental Medicine*, 183(4), pp.1797-1806.

Greenbaum, A., Hsu, Y., Day, R., Schuettpelz, L., Christopher, M., Borgerding, J., Nagasawa, T. and Link, D. (2013). CXCL12 in early mesenchymal progenitors is required for haematopoietic stem-cell maintenance. *Nature*, 495(7440), pp.227-230.

Grimwade, D., Hills, R., Moorman, A., Walker, H., Chatters, S., Goldstone, A., Wheatley, K., Harrison, C. and Burnett, A. (2010). Refinement of cytogenetic classification in acute myeloid leukemia: determination of prognostic significance of rare recurring chromosomal abnormalities among 5876 younger adult patients treated in the United Kingdom Medical Research Council trials. *Blood*, 116(3), pp.354-365.

Grygielko, E., Martin, W., Tweed, C., Thornton, P., Harling, J., Brooks, D. and Laping, N. (2005). Inhibition of Gene Markers of Fibrosis with a Novel Inhibitor of Transforming Growth Factor- Type I Receptor Kinase in Puromycin-Induced Nephritis. Journal of Pharmacology and Experimental Therapeutics, 313(3), pp.943-951.

Hamamura, K., Matsuda, H., Takeuchi, Y., Habu, S., Yagita, H. and Okumura, K. (1996). A critical role of VLA-4 in erythropoiesis in vivo. *Blood*, 87(6), pp.2513-2517.

Hanoun, M., Maryanovich, M., Arnal-Estapé, A. and Frenette, P. (2015). Neural Regulation of Hematopoiesis, Inflammation, and Cancer. *Neuron*, 86(2), pp.360-373.

Hanoun, M., Zhang, D., Mizoguchi, T., Pinho, S., Pierce, H., Kunisaki, Y., Lacombe, J., Armstrong, S., Dührsen, U. and Frenette, P. (2014). Acute Myelogenous Leukemia-Induced Sympathetic Neuropathy Promotes Malignancy in an Altered Hematopoietic Stem Cell Niche. *Cell Stem Cell*, 15(3), pp.365-375.

Hara, T., Bacon, K., Cho, L., Yoshimura, A., Morikawa, Y., Copeland, N., Gilbert, D., Jenkins, N., Schall, T. and Miyajima, A. (1995). Molecular cloning and functional characterization of a novel member of the C-C chemokine family. *Journal of Immunology*, 155(11), pp.5352-5358.

Harrison, D. and Astle, C. (1982). Loss of stem cell repopulating ability upon transplantation. Effects of donor age, cell number, and transplantation procedure. *J Exp Med*, 156(6), pp.1767–1779.

Hasemann, M., Lauridsen, F., Waage, J., Jakobsen, J., Frank, A., Schuster, M., Rapin, N., Bagger, F., Hoppe, P., Schroeder, T. and Porse, B. (2014). C/EBPα Is Required for Long-Term Self-Renewal and Lineage Priming of Hematopoietic Stem Cells and for the Maintenance of Epigenetic Configurations in Multipotent Progenitors. *PLoS Genetics*, 10(1), p.e1004079.

Haylock, D., Williams, B., Johnston, H., Liu, M., Rutherford, K., Whitty, G., Simmons, P., Bertoncello, I. and Nilsson, S. (2007). Hemopoietic Stem Cells with Higher Hemopoietic Potential Reside at the Bone Marrow Endosteum. *Stem Cells*, 25(4), pp.1062-1069.

Heath, V., Suh, H., Holman, M., Renn, K., Gooya, J., Parkin, S., Klarmann, K., Ortiz, M., Johnson, P. and Keller, J. (2004). C/EBP deficiency results in hyperproliferation of hematopoietic progenitor cells and disrupts macrophage development in vitro and in vivo. *Blood*, 104(6), pp.1639-1647.

Heazlewood, S., Neaves, R., Williams, B., Haylock, D., Adams, T. and Nilsson, S. (2013). Megakaryocytes co-localise with hemopoietic stem cells and release cytokines that up-regulate stem cell proliferation. *Stem Cell Research*, 11(2), pp.782-792.

Heo, S., Noh, E., Kim, J., Jeong, Y., Jo, J., Choi, Y., Koh, S., Baek, J., Min, Y. and Kim, H. (2017). Targeting c-KIT (CD117) by dasatinib and radotinib promotes acute myeloid leukemia cell death. *Scientific Reports*, 7(1).

Hérault, A., Binnewies, M., Leong, S., Calero-Nieto, F., Zhang, S., Kang, Y., Wang, X., Pietras, E., Chu, S., Barry-Holson, K., Armstrong, S., Göttgens, B. and Passegué, E. (2017). Myeloid progenitor cluster formation drives emergency and leukaemic myelopoiesis. *Nature*, 544(7648), pp.53-58.

Hills, R., Gammon, G., Trone, D. and Burnett, A. (2015). Quizartinib Significantly Improves Overall Survival in FLT3-ITD Positive AML Patients Relapsed after Stem Cell Transplantation or after Failure of Salvage Chemotherapy: A Comparison with Historical AML Database (UK NCRI data). *Blood*, 126, p.2557.

Hoellenriegel, J., Zboralski, D., Maasch, C., Rosin, N., Wierda, W., Keating, M., Kruschinski, A. and Burger, J. (2014). The Spiegelmer NOX-A12, a novel CXCL12 inhibitor, interferes with chronic lymphocytic leukemia cell motility and causes chemosensitization. *Blood*, 123(7), pp.1032-1039.

Hogaboam, C., Gallinat, C., Taub, D., Strieter, R., Kunkel, S. and Lukacs, N. (1999). Immunomodulatory Role of C10 Chemokine in a Murine Model of Allergic Bronchopulmonary Aspergillosis. *Journal of Immunology*, 162(10), pp.6071-6079.

Holtschke, T., Löhler, J., Kanno, Y., Fehr, T., Giese, N., Rosenbauer, F., Lou, J., Knobeloch, K., Gabriele, L., Waring, J., Bachmann, M., Zinkernagel, R., Morse, H., Ozato, K. and Horak, I. (1996). Immunodeficiency and Chronic Myelogenous Leukemia-like Syndrome in Mice with a Targeted Mutation of the ICSBP Gene. *Cell*, 87(2), pp.307-317.

Holyoake, T., Freshney, M., McNair, L., Parker, A., McKay, P., Steward, W., Fitzsimons, E., Graham, G. and Pragnell, I. (1996). Ex Vivo Expansion With Stem Cell Factor and Interleukin-11 Augments Both Short-Term Recovery Posttransplant and the Ability to Serially Transplant Marrow. *Blood*, 87(11), pp.4589-4595.

Hooper, A., Butler, J., Nolan, D., Kranz, A., Iida, K., Kobayashi, M., Kopp, H., Shido, K., Petit, I., Yanger, K., James, D., Witte, L., Zhu, Z., Wu, Y., Pytowski, B., Rosenwaks, Z., Mittal, V., Sato, T. and Rafii, S. (2009). Engraftment and Reconstitution of Hematopoiesis Is Dependent on VEGFR2-Mediated Regeneration of Sinusoidal Endothelial Cells. *Cell Stem Cell*, 4(3), pp.263-274.

Horwitz, E., Le Blanc, K., Dominici, M., Mueller, I., Slaper-Cortenbach, I., Marini, F., Deans, R., Krause, D. and Keating, A. (2005). Clarification of the nomenclature for MSC: The International Society for Cellular Therapy position statement. *Cytotherapy*, 7(5), pp.393-395.

Hsieh, Y., Jiang, E., Pham, J., Kim, H., Abdel-Azim, H., Khazal, S., Bug, G., Spohn, G., Bonig, H. and Kim, Y. (2013). VLA4 Blockade In Acute Myeloid Leukemia. *Blood*, 122, p.3944.

Hu, E., Liang, P. and Spiegelman, B. (1996). AdipoQ Is a Novel Adipose-specific Gene Dysregulated in Obesity. *Journal of Biological Chemistry*, 271(18), pp.10697-10703.

Huang, W., Yang, S., Shao, J. and Li, W. (2007). Signaling and transcriptional regulation in osteoblast commitment and differentiation. *Front Biosci*, 12, pp.3068-3092.

Ilicic, T., Kim, J., Kolodziejczyk, A., Bagger, F., McCarthy, D., Marioni, J. and Teichmann, S. (2016). Classification of low quality cells from single-cell RNA-seq data. *Genome Biology*, 17(1).

Itkin, T., Gur-Cohen, S., Spencer, J., Schajnovitz, A., Ramasamy, S., Kusumbe, A., Ledergor, G., Jung, Y., Milo, I., Poulos, M., Kalinkovich, A., Ludin, A., Golan, K., Khatib, E., Kumari, A., Kollet, O., Shakhar, G., Butler, J., Rafii, S., Adams, R., Scadden, D., Lin, C. and Lapidot, T. (2016). Distinct bone marrow blood vessels differentially regulate haematopoiesis. *Nature*, 532(7599), pp.323-328.

Jacamo, R., Chen, Y., Wang, Z., Ma, W., Zhang, M., Spaeth, E., Wang, Y., Battula, V., Mak, P., Schallmoser, K., Ruvolo, P., Schober, W., Shpall, E., Nguyen, M., Strunk, D., Bueso-Ramos, C., Konoplev, S., Davis, R., Konopleva, M. and Andreeff, M. (2014). Reciprocal leukemia-stroma VCAM-1/VLA-4-dependent activation of NF- B mediates chemoresistance. *Blood*, 123(17), pp.2691-2702.

Jacobson, L., Simmons, E., Marks, E. and Eldredge, J. (1951). Recovery from Radiation Injury. *Science*, 113(2940), pp.510-511.

Jaitin, D., Kenigsberg, E., Keren-Shaul, H., Elefant, N., Paul, F., Zaretsky, I., Mildner, A., Cohen, N., Jung, S., Tanay, A. and Amit, I. (2014). Massively Parallel Single-Cell RNA-Seq for Marker-Free Decomposition of Tissues into Cell Types. *Science*, 343(6172), pp.776-779.

Jiang, Y., Bonig, H., Ulyanova, T., Chang, K. and Papayannopoulou, T. (2009). On the adaptation of endosteal stem cell niche function in response to stress. *Blood*, 114(18), pp.3773-3782.

Jin, L., Hope, K., Zhai, Q., Smadja-Joffe, F. and Dick, J. (2006). Targeting of CD44 eradicates human acute myeloid leukemic stem cells. *Nature Medicine*, 12(10), pp.1167-1174.

Juarez, J., Bradstock, K., Gottlieb, D. and Bendall, L. (2003). Effects of inhibitors of the chemokine receptor CXCR4 on acute lymphoblastic leukemia cells in vitro. *Leukemia*, 17(7), pp.1294-1300.

Juliusson, G., Antunovic, P., Derolf, A., Lehmann, S., Mollgard, L., Stockelberg, D., Tidefelt, U., Wahlin, A. and Hoglund, M. (2009). Age and acute myeloid leukemia: real world data on decision to treat and outcomes from the Swedish Acute Leukemia Registry. *Blood*, 113(18), pp.4179-4187.

Junt, T., Schulze, H., Chen, Z., Massberg, S., Goerge, T., Krueger, A., Wagner, D., Graf, T., Italiano, J., Shivdasani, R. and von Andrian, U. (2007). Dynamic Visualization of Thrombopoiesis Within Bone Marrow. *Science*, 317(5845), pp.1767-1770.

Justesen, J., Stenderup, K., Ebbesen, E., Mosekilde, L., Steiniche, T. and Kassem, M. (2001). *Biogerontology*, 2(3), pp.165-171.

Kanahisa, M., Goto S. (2000). KEGG: kyoto encyclopedia of genes and genomes. *Nucleic Acids Research*. 28, pp.27-30.

Kalinkovich, A., Tavor, S., Avigdor, A., Kahn, J., Brill, A., Petit, I., Goichberg, P., Tesio, M., Netzer, N., Naparstek, E., Hardan, I., Nagler, A., Resnick, I., Tsimanis, A. and Lapidot, T. (2006). Functional CXCR4-Expressing Microparticles and SDF-1 Correlate with Circulating Acute Myelogenous Leukemia Cells. *Cancer Research*, 66(22), pp.11013-11020.

Karamitros, D., Stoilova, B., Aboukhalil, Z., Hamey, F., Reinisch, A., Samitsch, M., Quek, L., Otto, G., Repapi, E., Doondeea, J., Usukhbayar, B., Calvo, J., Taylor, S., Goardon, N., Six, E., Pflumio, F., Porcher, C., Majeti, R., Göttgens, B. and Vyas, P. (2017). Single-cell analysis reveals the continuum of human lympho-myeloid progenitor cells. *Nature Immunology*, 19(1), pp.85-97.

Karsunky, H., Inlay, M., Serwold, T., Bhattacharya, D. and Weissman, I. (2008). Flk2+ common lymphoid progenitors possess equivalent differentiation potential for the B and T lineages. *Blood*, 111(12), pp.5562-5570.

Karsunky, H., Merad, M., Cozzio, A., Weissman, I. and Manz, M. (2003). Flt3 Ligand Regulates Dendritic Cell Development from Flt3+Lymphoid and Myeloid-committed Progenitors to Flt3+Dendritic Cells In Vivo. *The Journal of Experimental Medicine*, 198(2), pp.305-313.

Katayama, Y., Battista, M., Kao, W., Hidalgo, A., Peired, A., Thomas, S. and Frenette, P. (2006). Signals from the Sympathetic Nervous System Regulate Hematopoietic Stem Cell Egress from Bone Marrow. *Cell*, 124(2), pp.407-421.

Kelly, L. and Gilliland, D. (2002). Genetics of Myeloid Leukemias. *Annual Review of Genomics and Human Genetics*, 3(1), pp.179-198.

Kennedy, D. and Knight, K. (2015). Inhibition of B Lymphopoiesis by Adipocytes and IL-1–Producing Myeloid-Derived Suppressor Cells. *The Journal of Immunology*, 195(6), pp.2666-2674.

Khatri, P., Draghici, S., Tarca, A., Hassan, S. and Romero, R. (2007). A System Biology Approach for the Steady-State Analysis of Gene Signaling Networks. *Lecture Notes in Computer Science*, pp.32-41.

Kiel, M., Acar, M., Radice, G. and Morrison, S. (2009). Hematopoietic Stem Cells Do Not Depend on N-Cadherin to Regulate Their Maintenance. *Cell Stem Cell*, 4(2), pp.170-179.

Kiel, M., He, S., Ashkenazi, R., Gentry, S., Teta, M., Kushner, J., Jackson, T. and Morrison, S. (2007). Haematopoietic stem cells do not asymmetrically segregate chromosomes or retain BrdU. *Nature*, 449(7159), pp.238-242.

Kiel, M., Yilmaz, Ö., Iwashita, T., Yilmaz, O., Terhorst, C. and Morrison, S. (2005). SLAM Family Receptors Distinguish Hematopoietic Stem and Progenitor Cells and Reveal Endothelial Niches for Stem Cells. *Cell*, 121(7), pp.1109-1121.

Kim, M. and Ahituv, N. (2013). The Hydrodynamic Tail Vein Assay as a Tool for the Study of Liver Promoters and Enhancers. *Methods in Molecular Biology*, pp.279-289.

Kim, M., Moon, H. and Spangrude, G. (2003). Major Age-Related Changes Of Mouse Hematopoietic Stem/Progenitor Cells. *Annals of the New York Academy of Sciences*, 996(1), pp.195-208.

Kim, Y., Koo, B., Jeong, H., Yoon, M., Song, R., Shin, J., Jeong, D., Kim, S. and Kong, Y. (2008). Defective Notch activation in microenvironment leads to myeloproliferative disease. *Blood*, 112(12), pp.4628-4638.

Kirstetter, P., Schuster, M., Bereshchenko, O., Moore, S., Dvinge, H., Kurz, E., Theilgaard-Mönch, K., Månsson, R., Pedersen, T., Pabst, T., Schrock, E., Porse, B., Jacobsen, S., Bertone, P., Tenen, D. and Nerlov, C. (2008). Modeling of C/EBPα Mutant Acute Myeloid Leukemia Reveals a Common Expression Signature of Committed Myeloid Leukemia-Initiating Cells. *Cancer Cell*, 13(4), pp.299-310.

Klein, A., Mazutis, L., Akartuna, I., Tallapragada, N., Veres, A., Li, V., Peshkin, L., Weitz, D. and Kirschner, M. (2015). Droplet Barcoding for Single-Cell Transcriptomics Applied to Embryonic Stem Cells. *Cell*, 161(5), pp.1187-1201.

Kobayashi, H., Butler, J., O'Donnell, R., Kobayashi, M., Ding, B., Bonner, B., Chiu, V., Nolan, D., Shido, K., Benjamin, L. and Rafii, S. (2010). Angiocrine factors from Akt-activated

endothelial cells balance self-renewal and differentiation of haematopoietic stem cells. *Nature Cell Biology*, 12(11), pp.1046-1056.

Kode, A., Manavalan, J., Mosialou, I., Bhagat, G., Rathinam, C., Luo, N., Khiabanian, H., Lee, A., Murty, V., Friedman, R., Brum, A., Park, D., Galili, N., Mukherjee, S., Teruya-Feldstein, J., Raza, A., Rabadan, R., Berman, E. and Kousteni, S. (2014). Leukaemogenesis induced by an activating β-catenin mutation in osteoblasts. *Nature*, 506(7487), pp.240-244.

Kondo, M., Weissman, I. and Akashi, K. (1997). Identification of Clonogenic Common Lymphoid Progenitors in Mouse Bone Marrow. *Cell*, 91(5), pp.661-672.

Kopp, H., Hooper, A., Avecilla, S. and Rafii, S. (2009). Functional Heterogeneity of the Bone Marrow Vascular Niche. *Annals of the New York Academy of Sciences*, 1176(1), pp.47-54.

Kornblau, S., McCue, D., Singh, N., Chen, W., Estrov, Z. and Coombes, K. (2010). Recurrent expression signatures of cytokines and chemokines are present and are independently prognostic in acute myelogenous leukemia and myelodysplasia. *Blood*, 116(20), pp.4251-4261.

Kowalczyk, M., Tirosh, I., Heckl, D., Rao, T., Dixit, A., Haas, B., Schneider, R., Wagers, A., Ebert, B. and Regev, A. (2015). Single-cell RNA-seq reveals changes in cell cycle and differentiation programs upon aging of hematopoietic stem cells. *Genome Research*, 25(12), pp.1860-1872.

Krause, D., Lazarides, K., von Andrian, U. and Van Etten, R. (2006). Requirement for CD44 in homing and engraftment of BCR-ABL–expressing leukemic stem cells. *Nature Medicine*, 12(10), pp.1175-1180.

Kreso, A. and Dick, J. (2014). Evolution of the Cancer Stem Cell Model. *Cell Stem Cell*, 14(3), pp.275-291.

Krevvata, M., Silva, B., Manavalan, J., Galan-Diez, M., Kode, A., Matthews, B., Park, D., Zhang, C., Galili, N., Nickolas, T., Dempster, D., Dougall, W., Teruya-Feldstein, J., Economides, A., Kalajzic, I., Raza, A., Berman, E., Mukherjee, S., Bhagat, G. and Kousteni, S. (2014). Inhibition of leukemia cell engraftment and disease progression in mice by osteoblasts. *Blood*, 124(18), pp.2834-2846.

Krivtsov, A., Figueroa, M., Sinha, A., Stubbs, M., Feng, Z., Valk, P., Delwel, R., Döhner, K., Bullinger, L., Kung, A., Melnick, A. and Armstrong, S. (2013). Cell of origin determines clinically relevant subtypes of MLL-rearranged AML. *Leukemia*, 27(4), pp.852-860.

Krueger, F. (2012). TrimGalore! Available online at: http://www.bioinformatics.babraham.ac.uk/projects/trim_galore

Kuittinen, O., Savolainen, E., Koistinen, P. and Turpeenniemi-Hujanen, T. (1999). Gelatinase A and B (MMP-2, MMP-9) in leukaemia MMP-2 may indicate a good prognosis in AML. *Anticancer Research*, 19(5), pp.4395-4400.

Kumar, B., Garcia, M., Weng, L., Jung, X., Murakami, J., Hu, X., McDonald, T., Lin, A., Kumar, A., DiGiusto, D., Stein, A., Pullarkat, V., Hui, S., Carlesso, N., Kuo, Y., Bhatia, R., Marcucci, G. and Chen, C. (2018). Acute myeloid leukemia transforms the bone marrow niche into a leukemia-permissive microenvironment through exosome secretion. *Leukemia*, 32(3), pp.575-587.

Kunisaki, Y., Bruns, I., Scheiermann, C., Ahmed, J., Pinho, S., Zhang, D., Mizoguchi, T., Wei, Q., Lucas, D., Ito, K., Mar, J., Bergman, A. and Frenette, P. (2013). Arteriolar niches maintain haematopoietic stem cell quiescence. *Nature*, 502(7473), pp.637-643.

Kuranda, K., Vargaftig, J., de la Rochere, P., Dosquet, C., Charron, D., Bardin, F., Tonnelle, C., Bonnet, D. and Goodhardt, M. (2011). Age-related changes in human hematopoietic stem/progenitor cells. *Aging Cell*, 10(3), pp.542-546.

Kuribayashi, W., Takizawa, K., Sugata, K., Kuramitsu, M., Momose, H., Sasaki, E., Hiradate, Y., Furuhata, K., Asada, Y., Iwama, A., Matsuoka, M., Mizukami, T. and Hamaguchi, I. (2016). Impact of the SCF signaling pathway on leukemia stem cell-mediated ATL initiation and progression in an HBZ transgenic mouse model. *Oncotarget*, 7(32).

Kusumbe, A., Ramasamy, S. and Adams, R. (2014). Coupling of angiogenesis and osteogenesis by a specific vessel subtype in bone. *Nature*, 507(7492), pp.323-328.

Kusumbe, A., Ramasamy, S., Itkin, T., Mäe, M., Langen, U., Betsholtz, C., Lapidot, T. and Adams, R. (2016). Age-dependent modulation of vascular niches for haematopoietic stem cells. *Nature*, 532(7599), pp.380-384.

Kwon, H., Johnson, T. and Tomarev, S. (2013). Myocilin Stimulates Osteogenic Differentiation of Mesenchymal Stem Cells through Mitogen-activated Protein Kinase Signaling. *Journal of Biological Chemistry*, 288(23), pp.16882-16894.

LaFleur, A., Lukacs, N., Kunkel, S. and Matsukawa, A. (2004). Role of CC chemokine CCL6/C10 as a monocyte chemoattractant in a murine acute peritonitis. *Mediators of Inflammation*, 13(5), pp.349-355.

Lambertsen, R. and Weiss, L. (1984). A model of intramedullary hematopoietic microenvironments based on stereologic study of the distribution of endocloned marrow colonies. *Blood*, 63, pp.287-297.

Larsson, S. and Wolk, A. (2008). Overweight and obesity and incidence of leukemia: A meta-analysis of cohort studies. *International Journal of Cancer*, 122(6), pp.1418-1421.

Layani-Bazar, A., Skornick, I., Berrebi, A., Pauker, M., Noy, E., Silberman, A., Albeck, M., Longo, D., Kalechman, Y. and Sredni, B. (2014). Redox Modulation of Adjacent Thiols in VLA-4 by AS101 Converts Myeloid Leukemia Cells from a Drug-Resistant to Drug-Sensitive State. *Cancer Research*, 74(11), pp.3092-3103.

Lazarides, E. and Hubbard, B. (1976). Immunological characterization of the subunit of the 100 A filaments from muscle cells. *Proceedings of the National Academy of Science USA. 1976 Dec;73(12):4344-8.*, 73(12), pp.4344-4348.

Lefterova, M., Haakonsson, A., Lazar, M. and Mandrup, S. (2014). PPARγ and the global map of adipogenesis and beyond. *Trends in Endocrinology & Metabolism*, 25(6), pp.293-302.

Leroy, H., Roumier, C., Huyghe, P., Biggio, V., Fenaux, P. and Preudhomme, C. (2005). CEBPA point mutations in hematological malignancies. *Leukemia*, 19(3), pp.329-334.

Li, J. (2011). Quiescence regulators for hematopoietic stem cell. *Experimental Hematology*, 39(5), pp.511-520.

Liao, Y., Smyth, G. and Shi, W. (2014). featureCounts: an efficient general purpose program for assigning sequence reads to genomic features. *Bioinformatics*, 30(7), pp.923-930.

Lim, M., Pang, Y., Ma, S., Hao, S., Shi, H., Zheng, Y., Hua, C., Gu, X., Yang, F., Yuan, W. and Cheng, T. (2016). Altered mesenchymal niche cells impede generation of normal hematopoietic progenitor cells in leukemic bone marrow. *Leukemia*, 30(1), pp.154-162.

Lips, P., Courpron, P. and Meunier, P. (1978). Mean wall thickness of trabecular bone packets in the human iliac crest: changes with age. *Calcif Tissue Res*, (1), pp.13-17.

Llorián-Salvador, M., González-Rodríguez, S., Lastra, A., Fernández-García, M., Hidalgo, A., Menéndez, L. and Baamonde, A. (2016). Involvement of CC Chemokine Receptor 1 and CCL3 in Acute and Chronic Inflammatory Pain in Mice. *Basic & Clinical Pharmacology & Toxicology*, 119(1), pp.32-40.

Lo Celso, C., Fleming, H., Wu, J., Zhao, C., Miake-Lye, S., Fujisaki, J., Côté, D., Rowe, D., Lin, C. and Scadden, D. (2009). Live-animal tracking of individual haematopoietic stem/progenitor cells in their niche. *Nature*, 457(7225), pp.92-96.

Lord, B., Testa, N. and Hendy, J. (1975). The relative spatial distributions of CFUs and CFUc in the normal mouse femur. *Blood*, 46, pp.65-72.

Love, M., Huber, W. and Anders, S. (2014). Moderated estimation of fold change and dispersion for RNA-seq data with DESeq2. *Genome Biology*, 15(12).

Löwenberg, B., van Putten, W., Theobald, M., Gmür, J., Verdonck, L., Sonneveld, P., Fey, M., Schouten, H., de Greef, G., Ferrant, A., Kovacsovics, T., Gratwohl, A., Daenen, S., Huijgens, P. and Boogaerts, M. (2003). Effect of Priming with Granulocyte Colony-Stimulating Factor on the Outcome of Chemotherapy for Acute Myeloid Leukemia. *New England Journal of Medicine*, 349(8), pp.743-752.

Lu, W., Weng, W., Zhu, Q., Zhai, Y., Wan, Y., Liu, H., Yang, S., Yu, Y., Wei, Y. and Shi, J. (2018). Small bone marrow adipocytes predict poor prognosis in acute myeloid leukemia. *Haematologica*, 103(1), pp.e21-e24.

Lucas, D., Bruns, I., Battista, M., Mendez-Ferrer, S., Magnon, C., Kunisaki, Y. and Frenette, P. (2012). Norepinephrine reuptake inhibition promotes mobilization in mice: potential impact to rescue low stem cell yields. *Blood*, 119(17), pp.3962-3965.

Ma, O., Hong, S., Guo, H., Ghiaur, G. and Friedman, A. (2014). Granulopoiesis Requires Increased C/EBPα Compared to Monopoiesis, Correlated with Elevated Cebpa in Immature G-CSF Receptor versus M-CSF Receptor Expressing Cells. *PLoS ONE*, 9(4), p.e95784.

Macanas-Pirard, P., Quezada, T., Navarrete, L., Broekhuizen, R., Leisewitz, A., Nervi, B. and Ramírez, P. (2017). The CCL2/CCR2 Axis Affects Transmigration and Proliferation but Not Resistance to Chemotherapy of Acute Myeloid Leukemia Cells. *PLOS ONE*, 12(1), p.e0168888.

Macosko, E., Basu, A., Satija, R., Nemesh, J., Shekhar, K., Goldman, M., Tirosh, I., Bialas, A., Kamitaki, N., Martersteck, E., Trombetta, J., Weitz, D., Sanes, J., Shalek, A., Regev, A. and McCarroll, S. (2015). Highly Parallel Genome-wide Expression Profiling of Individual Cells Using Nanoliter Droplets. *Cell*, 161(5), pp.1202-1214.

Maffei, R., Bulgarelli, J., Fiorcari, S., Martinelli, S., Castelli, I., Valenti, V., Rossi, D., Bonacorsi, G., Zucchini, P., Potenza, L., Vallisa, D., Gattei, V., Poeta, G., Forconi, F., Gaidano, G., Narni, F., Luppi, M. and Marasca, R. (2014). Endothelin-1 Promotes Survival and Chemoresistance in Chronic Lymphocytic Leukemia B Cells through ETA Receptor. *PLoS ONE*, 9(6), p.e98818.

Mason, D., Cordell, J., Tse, A., van Dongen, J., van Noesel, C., Micklem, K., Pulford, K., Valensi, F., Comans-Bitter, W., Borst, J. and Gatter, K. (1991). The IgM-associated protein mb-1 as a marker of normal and neoplastic B cells. *Journal of Immunology*, 147(11), pp.2474-2482.

Massiéra, F., Seydoux, J., Geloen, A., Quignard-Boulange, A., Turban, S., Saint-Marc, P., Fukamizu, A., Negrel, R., Ailhaud, G. and Teboul, M. (2001). Angiotensinogen-Deficient Mice Exhibit Impairment of Diet-Induced Weight Gain with Alteration in Adipose Tissue Development and Increased Locomotor Activity. *Endocrinology*, 142(12), pp.5220-5225.

Mcculloch, E., Siminovitch, L. and Till, J. (1964). Till Spleen-colony formation in anemic mice of genotype WW. *Science*, 144, pp.844-846.

Mead, A., Neo, W., Barkas, N., Matsuoka, S., Giustacchini, A., Facchini, R., Thongjuea, S., Jamieson, L., Booth, C., Fordham, N., Di Genua, C., Atkinson, D., Chowdhury, O., Repapi, E., Gray, N., Kharazi, S., Clark, S., Bouriez, T., Woll, P., Suda, T., Nerlov, C. and Jacobsen, S. (2017). Niche-mediated depletion of the normal hematopoietic stem cell reservoir by Flt3-ITD–induced myeloproliferation. *The Journal of Experimental Medicine*, 214(7), pp.2005-2021.

Medyouf, H., Mossner, M., Jann, J., Nolte, F., Raffel, S., Herrmann, C., Lier, A., Eisen, C., Nowak, V., Zens, B., Müdder, K., Klein, C., Obländer, J., Fey, S., Vogler, J., Fabarius, A., Riedl, E., Roehl, H., Kohlmann, A., Staller, M., Haferlach, C., Müller, N., John, T., Platzbecker, U., Metzgeroth, G., Hofmann, W., Trumpp, A. and Nowak, D. (2014). Myelodysplastic Cells in Patients Reprogram Mesenchymal Stromal Cells to Establish a Transplantable Stem Cell Niche Disease Unit. *Cell Stem Cell*, 14(6), pp.824-837.

Mei, Y., Zhao, B., Basiorka, A., Yang, J., Cao, L., Zhang, J., List, A. and Ji, P. (2018). Age-related inflammatory bone marrow microenvironment induces ineffective erythropoiesis mimicking del(5q) MDS. *Leukemia*, 32(4), pp.1023-1033.

Méndez-Ferrer, S., Lucas, D., Battista, M. and Frenette, P. (2008). Haematopoietic stem cell release is regulated by circadian oscillations. *Nature*, 452(7186), pp.442-447.

Méndez-Ferrer, S., Michurina, T., Ferraro, F., Mazloom, A., MacArthur, B., Lira, S., Scadden, D., Ma'ayan, A., Enikolopov, G. and Frenette, P. (2010). Mesenchymal and haematopoietic stem cells form a unique bone marrow niche. *Nature*, 466(7308), pp.829-834.

Menzin, J., Lang, K., Earle, C., Kerney, D. and Mallick, R. (2002). The Outcomes and Costs of Acute Myeloid Leukemia Among the Elderly. *Archives of Internal Medicine*, 162(14), p.1597.

Metacalf, D. (1986). The molecular biology and functions of the granulocyte-macrophage colony-stimulating factors. *Blood*, 67(257-267).

Meyers, J., Yu, Y., Kaye, J. and Davis, K. (2013). Medicare Fee-for-Service Enrollees with Primary Acute Myeloid Leukemia: An Analysis of Treatment Patterns, Survival, and Healthcare Resource Utilization and Costs. *Applied Health Economics and Health Policy*, 11(3), pp.275-286.

Miller, A., Marmor, J., Page,, P., Russell, J. and Robinson, S. (1976). Unregulated growth of murine leukemic cells and suppression of normal granulocyte growth in diffusion chamber cultures. *Blood*, 47, pp.737-745.

Miraki-Moud, F., Anjos-Afonso, F., Hodby, K., Griessinger, E., Rosignoli, G., Lillington, D., Jia, L., Davies, J., Cavenagh, J., Smith, M., Oakervee, H., Agrawal, S., Gribben, J., Bonnet, D. and Taussig, D. (2013). Acute myeloid leukemia does not deplete normal hematopoietic stem cells but induces cytopenias by impeding their differentiation. *Proceedings of the National Academy of Sciences*, 110(33), pp.13576-13581.

Moerman, E., Teng, K., Lipschitz, D. and Lecka-Czernik, B. (2004). Aging activates adipogenic and suppresses osteogenic programs in mesenchymal marrow stroma/stem cells: the role of PPAR-γ2 transcription factor and TGF-β/BMP signaling pathways. *Aging Cell*, 3(6), pp.379-389.

Mohrin, M., Bourke, E., Alexander, D., Warr, M., Barry-Holson, K., Le Beau, M., Morrison, C. and Passegué, E. (2010). Hematopoietic Stem Cell Quiescence Promotes Error-Prone DNA Repair and Mutagenesis. *Cell Stem Cell*, 7(2), pp.174-185.

Moore, M. (2005). Converging pathways in leukemogenesis and stem cell self-renewal. *Experimental Hematology*, 33(7), pp.719-737.

Morikawa, S., Mabuchi, Y., Kubota, Y., Nagai, Y., Niibe, K., Hiratsu, E., Suzuki, S., Miyauchi-Hara, C., Nagoshi, N., Sunabori, T., Shimmura, S., Miyawaki, A., Nakagawa, T., Suda, T., Okano, H. and Matsuzaki, Y. (2009). Prospective identification, isolation, and systemic transplantation of multipotent mesenchymal stem cells in murine bone marrow. *The Journal of Experimental Medicine*, 206(11), pp.2483-2496.

Morinobu, M., Ishijima, M., Rittling, S., Tsuji, K., Yamamoto, H., Nifuji, A., Denhardt, D. and Noda, M. (2003). Osteopontin Expression in Osteoblasts and Osteocytes During Bone

Formation Under Mechanical Stress in the Calvarial Suture In Vivo. *Journal of Bone and Mineral Research*, 18(9), pp.1706-1715.

Morrison, S. and Weissman, I. (1994). The long-term repopulating subset of hematopoietic stem cells is deterministic and isolatable by phenotype. *Immunity*, 1(8), pp.661-673.

Morrison, S., Wandycz, A., Akashi, K., Globerson, A. and Weissman, I. (1996). The aging of hematopoietic stem cells. *Nature Medicine*, 2(9), pp.1011-1016.

Müller-Sieburg, C., Cho, R., Thoman, M., Adkins, B. and Sieburg, H. (2002). Deterministic regulation of hematopoietic stem cell self-renewal and differentiation. *Blood*, 100, pp.1302-1309.

Nagai, Y., Garrett, K., Ohta, S., Bahrun, U., Kouro, T., Akira, S., Takatsu, K. and Kincade, P. (2006). Toll-like Receptors on Hematopoietic Progenitor Cells Stimulate Innate Immune System Replenishment. *Immunity*, 24(6), pp.801-812.

Nagasawa, T., Hirota, S., Tachibana, K., Takakura, N., Nishikawa, S., Kitamura, Y., Yoshida, N., Kikutani, H. and Kishimoto, T. (1996). Defects of B-cell lymphopoiesis and bone-marrow myelopoiesis in mice lacking the CXC chemokine PBSF/SDF-1. *Nature*, 382(6592), pp.635-638.

Nagasawa, T., Kikutani, H. and Kishimoto, T. (1994). Molecular cloning and structure of a pre-B-cell growth-stimulating factor. *Proceedings of the National Academy of Sciences*, 91(6), pp.2305-2309.

Naka, K., Hoshii, T., Muraguchi, T., Tadokoro, Y., Ooshio, T., Kondo, Y., Nakao, S., Motoyama, N. and Hirao, A. (2010). TGF-β–FOXO signalling maintains leukaemia-initiating cells in chronic myeloid leukaemia. *Nature*, 463(7281), pp.676-680.

Nakamura, Y., Arai, F., Iwasaki, H., Hosokawa, K., Kobayashi, I., Gomei, Y., Matsumoto, Y., Yoshihara, H. and Suda, T. (2010). Isolation and characterization of endosteal niche cell populations that regulate hematopoietic stem cells. *Blood*, 116(9), pp.1422-1432.

Nakamura-Ishizu, A., Takubo, K., Kobayashi, H., Suzuki-Inoue, K. and Suda, T. (2015). CLEC-2 in megakaryocytes is critical for maintenance of hematopoietic stem cells in the bone marrow. *The Journal of Experimental Medicine*, 212(12), pp.2133-2146.

Nakorn, T., Miyamoto, T. and Weissman, I. (2003). Characterization of mouse clonogenic megakaryocyte progenitors. *Proceedings of the National Academy of Sciences*, 100(1), pp.205-210.

Nardi, V., Naveiras, O., Azam, M. and Daley, G. (2009). ICSBP-mediated immune protection against BCR-ABL-induced leukemia requires the CCL6 and CCL9 chemokines. *Blood*, 113(16), pp.3813-3820.

Naveiras, O., Nardi, V., Wenzel, P., Hauschka, P., Fahey, F. and Daley, G. (2009). Bone-marrow adipocytes as negative regulators of the haematopoietic microenvironment. *Nature*, 460(7252), pp.259-263.

Nerlov, C. (2004). C/EBPα mutations in acute myeloid leukaemias. *Nature Reviews Cancer*, 4(5), pp.394-400.

Nerlov, C. (2007). The C/EBP family of transcription factors: a paradigm for interaction between gene expression and proliferation control. *Trends in Cell Biology*, 17(7), pp.318-324.

Nervi, B., Ramirez, P., Rettig, M., Uy, G., Holt, M., Ritchey, J., Prior, J., Piwnica-Worms, D., Bridger, G., Ley, T. and DiPersio, J. (2008). Chemosensitization of acute myeloid leukemia (AML) following mobilization by the CXCR4 antagonist AMD3100. *Blood*, 113(24), pp.6206-6214.

Nestorowa, S., Hamey, F., Pijuan Sala, B., Diamanti, E., Shepherd, M., Laurenti, E., Wilson, N., Kent, D. and Gottgens, B. (2016). A single-cell resolution map of mouse hematopoietic stem and progenitor cell differentiation. *Blood*, 128(8), pp.e20-e31.

Nilsson, S., Johnston, H. and Coverdale, J. (2001). Spatial localization of transplanted hemopoietic stem cells: inferences for the localization of stem cell niches. *Blood*, 97(8), pp.2293-2299.

Nilsson, S., Johnston, H., Whitty, G., Williams, B., Webb, R., Denhardt, D., Bertoncello, I., Bendall, L., Simmons, P. and Haylock, D. (2005). Osteopontin, a key component of the hematopoietic stem cell niche and regulator of primitive hematopoietic progenitor cells. *Blood*, 106(4), pp.1232-1239.

Niyongere, S., Lucas, N., Zhou, J., Sansil, S., Pomicter, A., Balasis, M., Robinson, J., Kroeger, J., Zhang, Q., Zhao, Y., Ball, M., Komrokji, R., List, A., Deininger, M., Fridley, B., Santini, V., Solary, E. and Padron, E. (2018). Heterogeneous expression of cytokines accounts for clinical diversity and refines prognostication in CMML. *Leukemia*.

Núñez, V., Alameda, D., Rico, D., Mota, R., Gonzalo, P., Cedenilla, M., Fischer, T., Bosca, L., Glass, C., Arroyo, A. and Ricote, M. (2010). Retinoid X receptor controls innate inflammatory responses through the up-regulation of chemokine expression. *Proceedings of the National Academy of Sciences*, 107(23), pp.10626-10631.

Ogawa, M., Yonemura, Y. and Ku, H. (1997). In vitro expansion of hematopoietic stem cells. *Stem Cells*, 15(S2), pp.7-12.

Oguro, H., Ding, L. and Morrison, S. (2013). SLAM Family Markers Resolve Functionally Distinct Subpopulations of Hematopoietic Stem Cells and Multipotent Progenitors. *Cell Stem Cell*, 13(1), pp.102-116.

Okada, S., Nakauchi, H., Nagayoshi, K., Nishikawa, S., Nishikawa, S., Miura, Y. and Suda, T. (1991). Enrichment and characterization of murine hematopoietic stem cells that express c-kit molecule. *Blood*, 78, pp.1706-1712.

Oldberg, A., Franzen, A. and Heinegard, D. (1986). Cloning and sequence analysis of rat bone sialoprotein (osteopontin) cDNA reveals an Arg-Gly-Asp cell-binding sequence. *Proceedings of the National Academy of Sciences*, 83(23), pp.8819-8823.

Olsnes, A., Motorin, D., Ryningen, A., Zaritskey, A. and Bruserud, Ø. (2006). T lymphocyte chemotactic chemokines in acute myelogenous leukemia (AML): local release by native human AML blasts and systemic levels of CXCL10 (IP-10), CCL5 (RANTES) and CCL17 (TARC). *Cancer Immunology, Immunotherapy*, 55(7), pp.830-840.

Olsson, A., Venkatasubramanian, M., Chaudhri, V., Aronow, B., Salomonis, N., Singh, H. and Grimes, H. (2016). Single-cell analysis of mixed-lineage states leading to a binary cell fate choice. *Nature*, 537(7622), pp.698-702.

Omatsu, Y., Sugiyama, T., Kohara, H., Kondoh, G., Fujii, N., Kohno, K. and Nagasawa, T. (2010). The Essential Functions of Adipo-osteogenic Progenitors as the Hematopoietic Stem and Progenitor Cell Niche. *Immunity*, 33(3), pp.387-399.

Orgel, E., Tucci, J., Alhushki, W., Malvar, J., Sposto, R., Fu, C., Freyer, D., Abdel-Azim, H. and Mittelman, S. (2014). Obesity is associated with residual leukemia following induction therapy for childhood B-precursor acute lymphoblastic leukemia. *Blood*, 124(26), pp.3932-3938.

Orkin, S. and Zon, L. (2008). Hematopoiesis: An Evolving Paradigm for Stem Cell Biology. *Cell*, 132(4), pp.631-644.

Osawa, M., Hanada, K., Hamada, H. and Nakauchi, H. (1996). Long-Term Lymphohematopoietic Reconstitution by a Single CD34-Low/Negative Hematopoietic Stem Cell. *Science*, 273(5272), pp.242-245.

Ossenkoppele, G., Stussi, G., Maertens, J., van Montfort, K., Biemond, B., Breems, D., Ferrant, A., Graux, C., de Greef, G., Halkes, C., Hoogendoorn, M., Hollestein, R., Jongen-Lavrencic, M., Levin, M., van de Loosdrecht, A., van Marwijk Kooij, M., van Norden, Y., Pabst, T., Schouten, H., Vellenga, E., Verhoef, G., de Weerdt, O., Wijermans, P., Passweg, J. and Lowenberg, B. (2012). Addition of bevacizumab to chemotherapy in acute myeloid leukemia at older age: a randomized phase 2 trial of the Dutch-Belgian Cooperative Trial Group for Hemato-Oncology (HOVON) and the Swiss Group for Clinical Cancer Research (SAKK). *Blood*, 120(24), pp.4706-4711.

Ott, M., Bober, E., Lyons, G., Arnold, H. and Buckingham, M. (1991). Early expression of the myogenic regulatory gene, myf-5, in precursor cells of skeletal muscle in the mouse embryo. *Development*, 111(4), pp.1097-1107.

Pabst, T., Mueller, B., Zhang, P., Radomska, H., Narravula, S., Schnittger, S., Behre, G., Hiddemann, W. and Tenen, D. (2001). Dominant-negative mutations of CEBPA, encoding CCAAT/enhancer binding protein-α (C/EBPα), in acute myeloid leukemia. *Nature Genetics*, 27(3), pp.263-270.

Pang, W., Price, E., Sahoo, D., Beerman, I., Maloney, W., Rossi, D., Schrier, S. and Weissman, I. (2011). Human bone marrow hematopoietic stem cells are increased in frequency and myeloid-biased with age. *Proceedings of the National Academy of Sciences*, 108(50), pp.20012-20017.

Papaemmanuil, E., Gerstung, M., Bullinger, L., Gaidzik, V., Paschka, P., Roberts, N., Potter, N., Heuser, M., Thol, F., Bolli, N., Gundem, G., Van Loo, P., Martincorena, I., Ganly, P.,

Mudie, L., McLaren, S., O'Meara, S., Raine, K., Jones, D., Teague, J., Butler, A., Greaves, M., Ganser, A., Döhner, K., Schlenk, R., Döhner, H. and Campbell, P. (2016). Genomic Classification and Prognosis in Acute Myeloid Leukemia. *New England Journal of Medicine*, 374(23), pp.2209-2221.

Passaro, D., Di Tullio, A., Abarrategi, A., Rouault-Pierre, K., Foster, K., Ariza-McNaughton, L., Montaner, B., Chakravarty, P., Bhaw, L., Diana, G., Lassailly, F., Gribben, J. and Bonnet, D. (2017). Increased Vascular Permeability in the Bone Marrow Microenvironment Contributes to Disease Progression and Drug Response in Acute Myeloid Leukemia. *Cancer Cell*, 32(3), pp.324-341.e6.

Patel, J., Gönen, M., Figueroa, M., Fernandez, H., Sun, Z., Racevskis, J., Van Vlierberghe, P., Dolgalev, I., Thomas, S., Aminova, O., Huberman, K., Cheng, J., Viale, A., Socci, N., Heguy, A., Cherry, A., Vance, G., Higgins, R., Ketterling, R., Gallagher, R., Litzow, M., van den Brink, M., Lazarus, H., Rowe, J., Luger, S., Ferrando, A., Paietta, E., Tallman, M., Melnick, A., Abdel-Wahab, O. and Levine, R. (2012). Prognostic Relevance of Integrated Genetic Profiling in Acute Myeloid Leukemia. *New England Journal of Medicine*, 366(12), pp.1079-1089.

Paul, F., Arkin, Y., Giladi, A., Jaitin, D., Kenigsberg, E., Keren-Shaul, H., Winter, D., Lara-Astiaso, D., Gury, M., Weiner, A., David, E., Cohen, N., Lauridsen, F., Haas, S., Schlitzer, A., Mildner, A., Ginhoux, F., Jung, S., Trumpp, A., Porse, B., Tanay, A. and Amit, I. (2015). Transcriptional Heterogeneity and Lineage Commitment in Myeloid Progenitors. *Cell*, 163(7), pp.1663-1677.

Paupert, J., Mansat-De Mas, V., Demur, C., Salles, B. and Muller, C. (2008). Cell-surface MMP-9 regulates the invasive capacity of leukemia blast cells with monocytic features. *Cell Cycle*, 7(8), pp.1047-1053.

Pei, W., Feyerabend, T., Rössler, J., Wang, X., Postrach, D., Busch, K., Rode, I., Klapproth, K., Dietlein, N., Quedenau, C., Chen, W., Sauer, S., Wolf, S., Höfer, T. and Rodewald, H. (2017). Polylox barcoding reveals haematopoietic stem cell fates realized in vivo. *Nature*, 548(7668), pp.456-460.

Pevida, M., González-Rodríguez, S., Lastra, A., Hidalgo, A., Menéndez, L. and Baamonde, A. (2012). CCL2 released at tumoral level contributes to the hyperalgesia evoked by intratibial inoculation of NCTC 2472 but not B16-F10 cells in mice. *Naunyn-Schmiedeberg's Archives of Pharmacology*, 385(11), pp.1053-1061.

Pezeshkian, B., Donnelly, C., Tamburo, K., Geddes, T. and Madlambayan, G. (2013). Leukemia Mediated Endothelial Cell Activation Modulates Leukemia Cell Susceptibility to Chemotherapy through a Positive Feedback Loop Mechanism. *PLoS ONE*, 8(4), p.e60823.

Picelli, S., Björklund, Å., Faridani, O., Sagasser, S., Winberg, G. and Sandberg, R. (2013). Smart-seq2 for sensitive full-length transcriptome profiling in single cells. *Nature Methods*, 10(11), pp.1096-1098.

Picelli, S., Faridani, O., Björklund, Å., Winberg, G., Sagasser, S. and Sandberg, R. (2014). Full-length RNA-seq from single cells using Smart-seq2. *Nature Protocols*, 9(1), pp.171-181.

Pietras, E., Reynaud, D., Kang, Y., Carlin, D., Calero-Nieto, F., Leavitt, A., Stuart, J., Göttgens, B. and Passegué, E. (2015). Functionally Distinct Subsets of Lineage-Biased Multipotent Progenitors Control Blood Production in Normal and Regenerative Conditions. *Cell Stem Cell*, 17(1), pp.35-46.

Pinho, S., Lacombe, J., Hanoun, M., Mizoguchi, T., Bruns, I., Kunisaki, Y. and Frenette, P. (2013). PDGFRα and CD51 mark human Nestin+sphere-forming mesenchymal stem cells capable of hematopoietic progenitor cell expansion. *The Journal of Experimental Medicine*, 210(7), pp.1351-1367.

Pinkus, G. and Pinkus, J. (1991). Myeloperoxidase: a specific marker for myeloid cells in paraffin sections. *Mod Pathol*, 4(6), pp.733-741.

Pitt, L., Tikhonova, A., Hu, H., Trimarchi, T., King, B., Gong, Y., Sanchez-Martin, M., Tsirigos, A., Littman, D., Ferrando, A., Morrison, S., Fooksman, D., Aifantis, I. and Schwab, S. (2015). CXCL12-Producing Vascular Endothelial Niches Control Acute T Cell Leukemia Maintenance. *Cancer Cell*, 27(6), pp.755-768.

Pittenger, M., Mackay, A., Beck, S., Jaiswal, R., Douglas, R., Mosca, J., Moorman, M., Simonetti, D., Craig, S. and Markshak, D. (1999). Multilineage Potential of Adult Human Mesenchymal Stem Cells. *Science*, 284(5411), pp.143-147.

Plowden, J., Renshaw-Hoelscher, M., Engleman, C., Katz, J. and Sambhara, S. (2004). Innate immunity in aging: impact on macrophage function. *Aging Cell*, 3(4), pp.161-167.

Pommier, Y., Leo, E., Zhang, H. and Marchand, C. (2010). DNA Topoisomerases and Their Poisoning by Anticancer and Antibacterial Drugs. *Chemistry & Biology*, 17(5), pp.421-433.

Poulos, M., Guo, P., Kofler, N., Pinho, S., Gutkin, M., Tikhonova, A., Aifantis, I., Frenette, P., Kitajewski, J., Rafii, S. and Butler, J. (2013). Endothelial Jagged-1 Is Necessary for Homeostatic and Regenerative Hematopoiesis. *Cell Reports*, 4(5), pp.1022-1034.

Pronk, C., Rossi, D., Månsson, R., Attema, J., Norddahl, G., Chan, C., Sigvardsson, M., Weissman, I. and Bryder, D. (2007). Elucidation of the Phenotypic, Functional, and Molecular Topography of a Myeloerythroid Progenitor Cell Hierarchy. *Cell Stem Cell*, 1(4), pp.428-442.

Raaijmakers, M., Mukherjee, S., Guo, S., Zhang, S., Kobayashi, T., Schoonmaker, J., Ebert, B., Al-Shahrour, F., Hasserjian, R., Scadden, E., Aung, Z., Matza, M., Merkenschlager, M., Lin, C., Rommens, J. and Scadden, D. (2010). Bone progenitor dysfunction induces myelodysplasia and secondary leukaemia. *Nature*, 464(7290), pp.852-857.

Rammes, A., Roth, J., Goebeler, M., Klempt, M., Hartmann, M. and Sorg, C. (1997). Myeloid-related protein (MRP) 8 and MRP14, calcium-binding proteins of the S100 family, are secreted by activated monocytes via a novel, tubulin-dependent pathway. *J Biol Chem*, 272(14), pp.9496-9502.

Rauch, P., Ellegast, J., Widmer, C., Fritsch, K., Goede, J., Valk, P., Lowenberg, B., Takizawa, H. and Manz, M. (2016). MPL expression on AML blasts predicts peripheral blood neutropenia and thrombocytopenia. *Blood*, 128(18), pp.2253-2257.

Richards, M., Liu, F., Iwasaki, H., Akashi, K. and Link, D. (2003). Pivotal role of granulocyte colony-stimulating factor in the development of progenitors in the common myeloid pathway. *Blood*, 102(10), pp.3562-3568.

Rieger, M., Hoppe, P., Smejkal, B., Eitelhuber, A. and Schroeder, T. (2009). Hematopoietic Cytokines Can Instruct Lineage Choice. *Science*, 325(5937), pp.217-218.

Robinson, M., McCarthy, D. and Smyth, G. (2010). edgeR: a Bioconductor package for differential expression analysis of digital gene expression data. *Bioinformatics*, 26(1), pp.139-140.

Robinson, S., Chavez, J., Pisarev, V., Mosley, R., Rosenthal, G., Blonder, J. and Talmadge, J. (2003). Delivery of Flt3 ligand (Flt3L) using a poloxamer-based formulation increases biological activity in mice. *Bone Marrow Transplantation*, 31(5), pp.361-369.

Robinson, S., Mosley, R., Parajuli, P., Pisarev, V., Sublet, J., Ulrich, A. and Talmadge, J. (2000). Comparison of the hematopoietic activity of flt-3 ligand and granulocyte-macrophage colony-stimulating factor acting alone or in combination. *J Hematother Stem Cell Res*, 9(5), pp.711-720.

Rodriguez-Fraticelli, A., Wolock, S., Weinreb, C., Panero, R., Patel, S., Jankovic, M., Sun, J., Calogero, R., Klein, A. and Camargo, F. (2018). Clonal analysis of lineage fate in native haematopoiesis. *Nature*, 553(7687), pp.212-216.

Röllig, C., Bornhäuser, M., Thiede, C., Taube, F., Kramer, M., Mohr, B., Aulitzky, W., Bodenstein, H., Tischler, H., Stuhlmann, R., Schuler, U., Stölzel, F., von Bonin, M., Wandt, H., Schäfer-Eckart, K., Schaich, M. and Ehninger, G. (2011). Long-Term Prognosis of Acute Myeloid Leukemia According to the New Genetic Risk Classification of the European LeukemiaNet Recommendations: Evaluation of the Proposed Reporting System. *Journal of Clinical Oncology*, 29(20), pp.2758-2765.

Rossi, D., Bryder, D., Zahn, J., Ahlenius, H., Sonu, R., Wagers, A. and Weissman, I. (2005). Cell intrinsic alterations underlie hematopoietic stem cell aging. *Proceedings of the National Academy of Sciences*, 102(26), pp.9194-9199.

Rupec, R., Jundt, F., Rebholz, B., Eckelt, B., Weindl, G., Herzinger, T., Flaig, M., Moosmann, S., Plewig, G., Dörken, B., Förster, I., Huss, R. and Pfeffer, K. (2005). Stroma-Mediated Dysregulation of Myelopoiesis in Mice Lacking IκBα. *Immunity*, 22(4), pp.479-491.

Saito, Y., Kitamura, H., Hijikata, A., Tomizawa-Murasawa, M., Tanaka, S., Takagi, S., Uchida, N., Suzuki, N., Sone, A., Najima, Y., Ozawa, H., Wake, A., Taniguchi, S., Shultz, L., Ohara, O. and Ishikawa, F. (2010). Identification of Therapeutic Targets for Quiescent, Chemotherapy-Resistant Human Leukemia Stem Cells. *Science Translational Medicine*, 2(17), pp.17ra9-17ra9.

Sanjuan-Pla, A., Macaulay, I., Jensen, C., Woll, P., Luis, T., Mead, A., Moore, S., Carella, C., Matsuoka, S., Jones, T., Chowdhury, O., Stenson, L., Lutteropp, M., Green, J., Facchini, R., Boukarabila, H., Grover, A., Gambardella, A., Thongjuea, S., Carrelha, J., Tarrant, P., Atkinson, D., Clark, S., Nerlov, C. and Jacobsen, S. (2013). Platelet-biased stem cells reside at the apex of the haematopoietic stem-cell hierarchy. *Nature*, 502(7470), pp.232-236.

Satija, R., Farrell, J., Gennert, D., Schier, A. and Regev, A. (2015). Spatial reconstruction of single-cell gene expression data. *Nature Biotechnology*, 33(5), pp.495-502.

Sawai, C., Babovic, S., Upadhaya, S., Knapp, D., Lavin, Y., Lau, C., Goloborodko, A., Feng, J., Fujisaki, J., Ding, L., Mirny, L., Merad, M., Eaves, C. and Reizis, B. (2016). Hematopoietic Stem Cells Are the Major Source of Multilineage Hematopoiesis in Adult Animals. *Immunity*, 45(3), pp.597-609.

Schmidt, T., Masouleh, B., Loges, S., Cauwenberghs, S., Fraisl, P., Maes, C., Jonckx, B., De Keersmaecker, K., Kleppe, M., Tjwa, M., Schenk, T., Vinckier, S., Fragoso, R., De Mol, M., Beel, K., Dias, S., Verfaillie, C., Clark, R., Brümmendorf, T., Vandenberghe, P., Rafii, S., Holyoake, T., Hochhaus, A., Cools, J., Karin, M., Carmeliet, G., Dewerchin, M. and Carmeliet, P. (2011). Loss or Inhibition of Stromal-Derived PlGF Prolongs Survival of Mice with Imatinib-Resistant Bcr-Abl1+ Leukemia. *Cancer Cell*, 19(6), pp.740-753.

Schmohl, J., Santovito, D., Guenther, T., Sutanto, W., Kroell, T., Salih, H., Pitsch, T., Egea, V., Weber, C., Schmetzer, H. and Ries, C. (2016). Expression of surface-associated 82kDa-proMMP-9 in primary acute leukemia blast cells inversely correlates with patients' risk. *Experimental Hematology*, 44(5), pp.358-362.e5.

Schofield, R. (1978). The relationship between the spleen colony-forming cell and the haemopoietic stem cell. *Blood Cells*, 4, pp.7-25.

Semerad, C., Christopher, M., Liu, F., Short, B., Simmons, P., Winkler, I., Levesque, J., Chappel, J., Ross, F. and Link, D. (2005). G-CSF potently inhibits osteoblast activity and CXCL12 mRNA expression in the bone marrow. *Blood*, 106(9), pp.3020-3027.

Shafat, M., Oellerich, T., Mohr, S., Robinson, S., Edwards, D., Marlein, C., Piddock, R., Fenech, M., Zaitseva, L., Abdul-Aziz, A., Turner, J., Watkins, J., Lawes, M., Bowles, K. and Rushworth, S. (2017). Leukemic blasts program bone marrow adipocytes to generate a protumoral microenvironment. *Blood*, 129(10), pp.1320-1332.

Shah, A., Andersson, T., Rachet, B., Björkholm, M. and Lambert, P. (2013). Survival and cure of acute myeloid leukaemia in England, 1971-2006: a population-based study. *British Journal of Haematology*, 162(4), pp.509-516.

Shen, Y., Zhu, Y., Fan, X., Shi, J., Wang, Q., Yan, X., Gu, Z., Wang, Y., Chen, B., Jiang, C., Yan, H., Chen, F., Chen, H., Chen, Z., Jin, J. and Chen, S. (2011). Gene mutation patterns and their prognostic impact in a cohort of 1185 patients with acute myeloid leukemia. *Blood*, 118(20), pp.5593-5603.

Shirasawa, T., Ohnishi, K., Hagiwara, S., Shigemoto, K., Takebe, Y., Rajewsky, K. and Takemori, T. (1993). A novel gene product associated with mu chains in immature B cells. *EMBO J*, 12(5), pp.1827-1834.

Shukunami, C. and Hiraki, Y. (2001). Role of cartilage-derived anti-angiogenic factor, chondromodulin-I, during endochondral bone formation. *Osteoarthritis and Cartilage*, 9, pp.S91-S101.

Signer, R., Magee, J., Salic, A. and Morrison, S. (2014). Haematopoietic stem cells require a highly regulated protein synthesis rate. *Nature*, 509(7498), pp.49-54.

Signer, R., Montecino-Rodriguez, E., Witte, O., McLaughlin, J. and Dorshkind, K. (2007). Age-related defects in B lymphopoiesis underlie the myeloid dominance of adult leukemia. *Blood*, 110(6), pp.1831-1839.

Silberstein, L., Goncalves, K., Kharchenko, P., Turcotte, R., Kfoury, Y., Mercier, F., Baryawno, N., Severe, N., Bachand, J., Spencer, J., Papazian, A., Lee, D., Chitteti, B., Srour, E., Hoggatt, J., Tate, T., Lo Celso, C., Ono, N., Nutt, S., Heino, J., Sipilä, K., Shioda, T., Osawa, M., Lin, C., Hu, G. and Scadden, D. (2016). Proximity-Based Differential Single-Cell Analysis of the Niche to Identify Stem/Progenitor Cell Regulators. *Cell Stem Cell*, 19(4), pp.530-543.

Siminovitch, L., Till, J. and Mcculloch, E. (1964). Decline in colony-forming ability of marrow cells subjected to serial transplantation into irradiated mice. *J Cell Physiol*, 64, pp.23-31.

Singh, L., Brennan, T., Russell, E., Kim, J., Chen, Q., Brad Johnson, F. and Pignolo, R. (2016). Aging alters bone-fat reciprocity by shifting in vivo mesenchymal precursor cell fate towards an adipogenic lineage. *Bone*, 85, pp.29-36.

Sipkins, D., Wei, X., Wu, J., Runnels, J., Côté, D., Means, T., Luster, A., Scadden, D. and Lin, C. (2005). In vivo imaging of specialized bone marrow endothelial microdomains for tumour engraftment. *Nature*, 435(7044), pp.969-973.

Snaddon, J., Smith, M., Neat, M., Cambal-Parrales, M., Dixon-McIver, A., Arch, R., Amess, J., Rohatiner, A., Lister, T. and Fitzgibbon, J. (2003). Mutations of CEBPA in acute myeloid leukemia FAB types M1 and M2. *Genes, Chromosomes and Cancer*, 37(1), pp.72-78.

Socolovsky, M., Nam, H., Fleming, M., Haase, V., Brugnara, C. and Lodish, H. (2001). Ineffective erythropoiesis in Stat5a-/-5b-/- mice due to decreased survival of early erythroblasts. *Blood*, 98(12), pp.3261-3273.

Spangrude, G., Heimfeld, S. and Weissman, I. (1988). Purification and characterization of mouse hematopoietic stem cells. *Science*, 241(4861), pp.58-62.

Spencer, J., Ferraro, F., Roussakis, E., Klein, A., Wu, J., Runnels, J., Zaher, W., Mortensen, L., Alt, C., Turcotte, R., Yusuf, R., Côté, D., Vinogradov, S., Scadden, D. and Lin, C. (2014). Direct measurement of local oxygen concentration in the bone marrow of live animals. *Nature*, 508(7495), pp.269-273.

Steinhauser, M., Hogaboam, C., Matsukawa, A., Lukacs, N., Strieter, R. and Kunkel, S. (2000). Chemokine C10 Promotes Disease Resolution and Survival in an Experimental Model of Bacterial Sepsis. *Infection and Immunity*, 68(11), pp.6108-6114.

Stier, S., Ko, Y., Forkert, R., Lutz, C., Neuhaus, T., Grünewald, E., Cheng, T., Dombkowski, D., Calvi, L., Rittling, S. and Scadden, D. (2005). Osteopontin is a hematopoietic stem cell niche component that negatively regulates stem cell pool size. *The Journal of Experimental Medicine*, 201(11), pp.1781-1791.

Subramanian, A., Tamayo, P., Mootha, V., Mukherjee, S., Ebert, B., Gillette, M., Paulovich, A., Pomeroy, S., Golub, T., Lander, E. and Mesirov, J. (2005). Gene set enrichment analysis: A knowledge-based approach for interpreting genome-wide expression profiles. *Proceedings of the National Academy of Sciences*, 102(43), pp.15545-15550.

Sudo, K., Ema, H., Morita, Y. and Nakauchi, H. (2000). Age-Associated Characteristics of Murine Hematopoietic Stem Cells. *The Journal of Experimental Medicine*, 192(9), pp.1273-1280.

Sugiyama, T., Kohara, H., Noda, M. and Nagasawa, T. (2006). Maintenance of the Hematopoietic Stem Cell Pool by CXCL12-CXCR4 Chemokine Signaling in Bone Marrow Stromal Cell Niches. *Immunity*, 25(6), pp.977-988.

Sun, J., Ramos, A., Chapman, B., Johnnidis, J., Le, L., Ho, Y., Klein, A., Hofmann, O. and Camargo, F. (2014). Clonal dynamics of native haematopoiesis. *Nature*, 514(7522), pp.322-327.

Takeshita, S., Fumoto, T., Naoe, Y. and Ikeda, K. (2014). Age-related Marrow Adipogenesis Is Linked to Increased Expression of RANKL. *Journal of Biological Chemistry*, 289(24), pp.16699-16710.

Tarca, A., Draghici, S., Khatri, P., Hassan, S., Mittal, P., Kim, J., Kim, C., Kusanovic, J. and Romero, R. (2009). A novel signaling pathway impact analysis. *Bioinformatics*, 25(1), pp.75-82.

Taussig, D., Miraki-Moud, F., Anjos-Afonso, F., Pearce, D., Allen, K., Ridler, C., Lillington, D., Oakervee, H., Cavenagh, J., Agrawal, S., Lister, T., Gribben, J. and Bonnet, D. (2008). Anti-CD38 antibody-mediated clearance of human repopulating cells masks the heterogeneity of leukemia-initiating cells. *Blood*, 112(3), pp.568-575.

Till, J., Mcculloch, E. and Siminovitch, L. (1964a). A stochastic model of stem cell proliferation based on the growth of spleen colony-forming cells. *Proc Natl Acad Sci USA*, 51, pp.29-36.

Till, J., Mcculloch, E. and Siminovitch, L. (1964b). Isolation of variant cell lines during serial transplantation of hematopoietic cells derived from fetal liver. *J Natl Cancer Inst*, 33, pp.707-720.

Tokoyoda, K., Egawa, T., Sugiyama, T., Choi, B. and Nagasawa, T. (2004). Cellular Niches Controlling B Lymphocyte Behavior within Bone Marrow during Development. *Immunity*, 20(6), pp.707-718.

Uchida, N., Weissman, I. (1992). Searching for hematopoietic stem cells: evidence that Thy-1.1lo Lin- Sca-1+ cells are the only stem cells in C57BL/Ka-Thy-1.1 bone marrow. *Journal of Experimental Medicine*, 175(1), pp.175-184.

Vallet, S., Raje, N., Ishitsuka, K., Hideshima, T., Podar, K., Chhetri, S., Pozzi, S., Breitkreutz, I., Kiziltepe, T., Yasui, H., Ocio, E., Shiraishi, N., Jin, J., Okawa, Y., Ikeda, H., Mukherjee, S., Vaghela, N., Cirstea, D., Ladetto, M., Boccadoro, M. and Anderson, K. (2007). MLN3897, a novel CCR1 inhibitor, impairs osteoclastogenesis and inhibits the interaction of multiple myeloma cells and osteoclasts. *Blood*, 110(10), pp.3744-3752.

van Attekum, M., Terpstra, S., Slinger, E., von Lindern, M., Moerland, P., Jongejan, A., Kater, A. and Eldering, E. (2017). Macrophages confer survival signals via CCR1-dependent translational MCL-1 induction in chronic lymphocytic leukemia. *Oncogene*, 36(26), pp.3651-3660.

van Pelt, K., de Haan, G., Vellenga, E. and Daenen, S. (2005). Administration of low-dose cytarabine results in immediate S-phase arrest and subsequent activation of cell cycling in murine stem cells. *Experimental Hematology*, 33(2), pp.226-231.

Vas, V., Senger, K., Dörr, K., Niebel, A. and Geiger, H. (2012a). Aging of the Microenvironment Influences Clonality in Hematopoiesis. *PLoS ONE*, 7(8), p.e42080.

Vas, V., Wandhoff, C., Dörr, K., Niebel, A. and Geiger, H. (2012b). Contribution of an Aged Microenvironment to Aging-Associated Myeloproliferative Disease. *PLoS ONE*, 7(2), p.e31523.

Visnjic, D., Kalajzic, Z., Rowe, D., Katavic, V., Lorenzo, J. and Aguila, H. (2004). Hematopoiesis is severely altered in mice with an induced osteoblast deficiency. *Blood*, 103(9), pp.3258-3264.

Walkley, C., Olsen, G., Dworkin, S., Fabb, S., Swann, J., McArthur, G., Westmoreland, S., Chambon, P., Scadden, D. and Purton, L. (2007a). A Microenvironment-Induced Myeloproliferative Syndrome Caused by Retinoic Acid Receptor γ Deficiency. *Cell*, 129(6), pp.1097-1110.

Walkley, C., Shea, J., Sims, N., Purton, L. and Orkin, S. (2007b). Rb Regulates Interactions between Hematopoietic Stem Cells and Their Bone Marrow Microenvironment. *Cell*, 129(6), pp.1081-1095.

Walter, R., Alonzo, T., Gerbing, R., Ho, P., Smith, F., Raimondi, S., Hirsch, B., Gamis, A., Franklin, J., Hurwitz, C., Loken, M. and Meshinchi, S. (2010). High Expression of the Very Late Antigen-4 Integrin Independently Predicts Reduced Risk of Relapse and Improved Outcome in Pediatric Acute Myeloid Leukemia: A Report From the Children's Oncology Group. *Journal of Clinical Oncology*, 28(17), pp.2831-2838.

Wang, L., Zhang, H., Rodriguez, S., Cao, L., Parish, J., Mumaw, C., Zollman, A., Kamoka, M., Mu, J., Chen, D., Srour, E., Chitteti, B., HogenEsch, H., Tu, X., Bellido, T., Boswell, H., Manshouri, T., Verstovsek, S., Yoder, M., Kapur, R., Cardoso, A. and Carlesso, N. (2014). Notch-Dependent Repression of miR-155 in the Bone Marrow Niche Regulates Hematopoiesis in an NF-κB-Dependent Manner. *Cell Stem Cell*, 15(1), pp.51-65.

Wang, X., Prakash, S., Lu, M., Tripodi, J., Ye, F., Najfeld, V., Li, Y., Schwartz, M., Weinberg, R., Roda, P., Orazi, A. and Hoffman, R. (2012). Spleens of myelofibrosis patients contain malignant hematopoietic stem cells. *Journal of Clinical Investigation*, 122(11), pp.3888-3899.

Wang, Y., Gao, A., Zhao, H., Lu, P., Cheng, H., Dong, F., Gong, Y., Ma, S., Zheng, Y., Zhang, H., Zhang, Y., Xu, J., Zhu, X., Yuan, W., Zhang, X., Hao, S. and Cheng, T. (2016). Leukemia cell infiltration causes defective erythropoiesis partially through MIP-1α/CCL3. *Leukemia*, 30(9), pp.1897-1908.

Wei, J., Xu, H., Davies, J. and Hemmings, G. (1992). Increase of plasma IL-6 concentration with age in healthy subjects. *Life Sci.*, 51(25), pp.1953-1956.

Weigert, C., Hennige, A., Brodbeck, K., Häring, H. and Schleicher, E. (2005). Interleukin-6 acts as insulin sensitizer on glycogen synthesis in human skeletal muscle cells by phosphorylation of Ser473 of Akt. *American Journal of Physiology-Endocrinology and Metabolism*, 289(2), pp.E251-E257.

Weisberg, E., Azab, A., Manley, P., Kung, A., Christie, A., Bronson, R., Ghobrial, I. and Griffin, J. (2012). Inhibition of CXCR4 in CML cells disrupts their interaction with the bone marrow microenvironment and sensitizes them to nilotinib. *Leukemia*, 26(5), pp.985-990.

Welch, J., Ley, T., Link, D., Miller, C., Larson, D., Koboldt, D., Wartman, L., Lamprecht, T., Liu, F., Xia, J., Kandoth, C., Fulton, R., McLellan, M., Dooling, D., Wallis, J., Chen, K., Harris, C., Schmidt, H., Kalicki-Veizer, J., Lu, C., Zhang, Q., Lin, L., O'Laughlin, M., McMichael, J., Delehaunty, K., Fulton, L., Magrini, V., McGrath, S., Demeter, R., Vickery, T., Hundal, J., Cook, L., Swift, G., Reed, J., Alldredge, P., Wylie, T., Walker, J., Watson, M., Heath, S., Shannon, W., Varghese, N., Nagarajan, R., Payton, J., Baty, J., Kulkarni, S., Klco, J., Tomasson, M., Westervelt, P., Walter, M., Graubert, T., DiPersio, J., Ding, L., Mardis, E. and Wilson, R. (2012). The Origin and Evolution of Mutations in Acute Myeloid Leukemia. *Cell*, 150(2), pp.264-278.

Weng, L., Smits, P., Wauters, J. and Merregaert, J. (2002). Molecular Cloning and Characterization of Human Chondrolectin, a Novel Type I Transmembrane Protein Homologous to C-Type Lectins. *Genomics*, 80(1), pp.62-70.

Wilson, A., Laurenti, E., Oser, G., van der Wath, R., Blanco-Bose, W., Jaworski, M., Offner, S., Dunant, C., Eshkind, L., Bockamp, E., Lió, P., MacDonald, H. and Trumpp, A. (2008). Hematopoietic Stem Cells Reversibly Switch from Dormancy to Self-Renewal during Homeostasis and Repair. *Cell*, 135(6), pp.1118-1129.

Winkler, I., Barbier, V., Nowlan, B., Jacobsen, R., Forristal, C., Patton, J., Magnani, J. and Lévesque, J. (2012). Vascular niche E-selectin regulates hematopoietic stem cell dormancy, self renewal and chemoresistance. *Nature Medicine*, 18(11), pp.1651-1657.

Winkler, I., Sims, N., Pettit, A., Barbier, V., Nowlan, B., Helwani, F., Poulton, I., van Rooijen, N., Alexander, K., Raggatt, L. and Levesque, J. (2010). Bone marrow macrophages maintain hematopoietic stem cell (HSC) niches and their depletion mobilizes HSCs. *Blood*, 116(23), pp.4815-4828.

Wölfler, A., Danen-van Oorschot, A., Haanstra, J., Valkhof, M., Bodner, C., Vroegindeweij, E., van Strien, P., Novak, A., Cupedo, T. and Touw, I. (2010). Lineage-instructive function of C/EBP in multipotent hematopoietic cells and early thymic progenitors. *Blood*, 116(20), pp.4116-4125.

Wu, W., Sun, H., Chen, H., Liang, J., Yu, X., Wu, C., Wang, Z. and Zheng, L. (2014). Circulating hematopoietic stem and progenitor cells are myeloid-biased in cancer patients. *Proceedings of the National Academy of Sciences*, 111(11), pp.4221-4226.

Xu, C., Gao, X., Wei, Q., Nakahara, F., Zimmerman, S., Mar, J. and Frenette, P. (2018). Stem cell factor is selectively secreted by arterial endothelial cells in bone marrow. *Nature Communications*, 9(1).

Yamashita, T., Ohneda, O., Sakiyama, A., Iwata, F., Ohneda, K. and Fujii-Kuriyama, Y. (2008). The microenvironment for erythropoiesis is regulated by HIF-2 through VCAM-1 in endothelial cells. *Blood*, 112(4), pp.1482-1492.

Yamazaki, S., Ema, H., Karlsson, G., Yamaguchi, T., Miyoshi, H., Shioda, S., Taketo, M., Karlsson, S., Iwama, A. and Nakauchi, H. (2011). Nonmyelinating Schwann Cells Maintain Hematopoietic Stem Cell Hibernation in the Bone Marrow Niche. *Cell*, 147(5), pp.1146-1158.

Yan, J., Zhang, H., Yin, Y., Li, J., Tang, Y., Purkayastha, S., Li, L. and Cai, D. (2014). Obesity- and aging-induced excess of central transforming growth factor-β potentiates diabetic development via an RNA stress response. *Nature Medicine*, 20(9), pp.1001-1008.

Yates, J., Wallace, H., Ellison, R. and Holland, J. (1973). Cytosine arabinoside (NSC-63878) and daunorubicin (NSC-83142) therapy in acute nonlymphocytic leukemia. *Cancer Chemother Rep*, 57(4), pp.485-488.

Yoshihara, H., Arai, F., Hosokawa, K., Hagiwara, T., Takubo, K., Nakamura, Y., Gomei, Y., Iwasaki, H., Matsuoka, S., Miyamoto, K., Miyazaki, H., Takahashi, T. and Suda, T. (2007). Thrombopoietin/MPL Signaling Regulates Hematopoietic Stem Cell Quiescence and Interaction with the Osteoblastic Niche. *Cell Stem Cell*, 1(6), pp.685-697.

Yu, Y., Liao, P., Guo, C., Chen, C., Mochly-Rosen, D. and Chuang, L. (2016). PKC-ALDH2 Pathway Plays a Novel Role in Adipocyte Differentiation. *PLOS ONE*, 11(8), p.e0161993.

Zambetti, N., Ping, Z., Chen, S., Kenswil, K., Mylona, M., Sanders, M., Hoogenboezem, R., Bindels, E., Adisty, M., Van Strien, P., van der Leije, C., Westers, T., Cremers, E., Milanese, C., Mastroberardino, P., van Leeuwen, J., van der Eerden, B., Touw, I., Kuijpers, T., Kanaar, R., van de Loosdrecht, A., Vogl, T. and Raaijmakers, M. (2016). Mesenchymal Inflammation Drives Genotoxic Stress in Hematopoietic Stem Cells and Predicts Disease Evolution in Human Pre-leukemia. *Cell Stem Cell*, 19(5), pp.613-627.

Zeng, Z., Xi Shi, Y., Samudio, I., Wang, R., Ling, X., Frolova, O., Levis, M., Rubin, J., Negrin, R., Estey, E., Konoplev, S., Andreeff, M. and Konopleva, M. (2009). Targeting the leukemia microenvironment by CXCR4 inhibition overcomes resistance to kinase inhibitors and chemotherapy in AML. *Blood*, 113(24), pp.6215-6224.

Zhang, B., Ho, Y., Huang, Q., Maeda, T., Lin, A., Lee, S., Hair, A., Holyoake, T., Huettner, C. and Bhatia, R. (2012). Altered Microenvironmental Regulation of Leukemic and Normal Stem Cells in Chronic Myelogenous Leukemia. *Cancer Cell*, 21(4), pp.577-592.

Zhang, B., Ma, X., Zheng, G., Li, G., Rao, Q. and Wu, K. (2003b). Expression of IL-18 and its receptor in human leukemia cells. *Leukemia Research*, 27(9), pp.813-822.

Zhang, B., Wu, K., Cao, Z., Rao, Q., Ma, X., Zheng, G. and Li, G. (2004b). IL-18 increases invasiveness of HL-60 myeloid leukemia cells: up-regulation of matrix metalloproteinases-9 (MMP-9) expression. *Leukemia Research*, 28(1), pp.91-95.

Zhang, D., Zhang, P., Wang, N., Hetherington, C., Darlington, G. and Tenen, D. (1997). Absence of granulocyte colony-stimulating factor signaling and neutrophil development in CCAAT enhancer binding protein -deficient mice. *Proceedings of the National Academy of Sciences*, 94(2), pp.569-574.

Zhang, G., Budker, V. and Wolff, J. (1999). High Levels of Foreign Gene Expression in Hepatocytes after Tail Vein Injections of Naked Plasmid DNA. *Human Gene Therapy*, 10(10), pp.1735-1737.

Zhang, J., Niu, C., Ye, L., Huang, H., He, X., Tong, W., Ross, J., Haug, J., Johnson, T., Feng, J., Harris, S., Wiedemann, L., Mishina, Y. and Li, L. (2003a). Identification of the haematopoietic stem cell niche and control of the niche size. *Nature*, 425(6960), pp.836-841.

Zhang, P., Iwasaki-Arai, J., Iwasaki, H., Fenyus, M., Dayaram, T., Owens, B., Shigematsu, H., Levantini, E., Huettner, C., Lekstrom-Himes, J., Akashi, K. and Tenen, D. (2004a). Enhancement of Hematopoietic Stem Cell Repopulating Capacity and Self-Renewal in the Absence of the Transcription Factor C/EBPα. *Immunity*, 21(6), pp.853-863.

Zhao, M., Perry, J., Marshall, H., Venkatraman, A., Qian, P., He, X., Ahamed, J. and Li, L. (2014). Megakaryocytes maintain homeostatic quiescence and promote post-injury regeneration of hematopoietic stem cells. *Nature Medicine*, 20(11), pp.1321-1326.

Zheng, G., Terry, J., Belgrader, P., Ryvkin, P., Bent, Z., Wilson, R., Ziraldo, S., Wheeler, T., McDermott, G., Zhu, J., Gregory, M., Shuga, J., Montesclaros, L., Underwood, J., Masquelier, D., Nishimura, S., Schnall-Levin, M., Wyatt, P., Hindson, C., Bharadwaj, R., Wong, A., Ness, K., Beppu, L., Deeg, H., McFarland, C., Loeb, K., Valente, W., Ericson, N., Stevens, E., Radich, J., Mikkelsen, T., Hindson, B. and Bielas, J. (2017). Massively parallel digital transcriptional profiling of single cells. *Nature Communications*, 8, p.14049.

Zheng, R., Levis, M., Piloto, O., Brown, P., Baldwin, B., Gorin, N., Beran, M., Zhu, Z., Ludwig, D., Hicklin, D., Witte, L., Li, Y. and Small, D. (2004). FLT3 ligand causes autocrine signaling in acute myeloid leukemia cells. *Blood*, 103(1), pp.267-274.

Zhou, B., Yu, H., Yue, R., Zhao, Z., Rios, J., Naveiras, O. and Morrison, S. (2017). Bone marrow adipocytes promote the regeneration of stem cells and haematopoiesis by secreting SCF. *Nature Cell Biology*, 19(8), pp.891-903.

Zhou, B., Yue, R., Murphy, M., Peyer, J. and Morrison, S. (2014). Leptin-Receptor-Expressing Mesenchymal Stromal Cells Represent the Main Source of Bone Formed by Adult Bone Marrow. *Cell Stem Cell*, 15(2), pp.154-168.

Zhu, J., Garrett, R., Jung, Y., Zhang, Y., Kim, N., Wang, J., Joe, G., Hexner, E., Choi, Y., Taichman, R. and Emerson, S. (2007). Osteoblasts support B-lymphocyte commitment and differentiation from hematopoietic stem cells. *Blood*, 109(9), pp.3706-3712.

Zhu, R., Wu, M., Li, Z., Zhang, Y. and Liu, K. (2012). Hematopoietic recovery following chemotherapy is improved by BADGE-induced inhibition of adipogenesis. *International Journal of Hematology*, 97(1), pp.58-72.

Zuber, J., Radtke, I., Pardee, T., Zhao, Z., Rappaport, A., Luo, W., McCurrach, M., Yang, M., Dolan, M., Kogan, S., Downing, J. and Lowe, S. (2009). Mouse models of human AML accurately predict chemotherapy response. *Genes & Development*, 23(7), pp.877-889.